



TECHNISCHE  
UNIVERSITÄT  
WIEN  
Vienna | Austria



**Dissertation**

# **Development of High-Performance Thermoplastic Composite Laminates: The Role of Interfacial Adhesion**

carried out for the purpose of obtaining the degree of Doctor technicae (Dr. techn.), submitted at  
TU Wien, Faculty of Mechanical and Industrial Engineering, by

**Dipl.-Ing. Peter Kiss, BSc**

Mat.Nr.: 00805805

under the supervision of

**Ao.Univ.Prof. Dipl.-Ing. Dr.mont. Vasiliki-Maria Archodoulaki**

**Institute of Materials Science and Technology, E308**

reviewed by

.....  
FH-Prof. h.c. Mag. Dr. Wolfgang Stadlbauer

Research Center Wels

Stelzhamerstraße 23, 4600 Wels

.....  
Univ.-Prof. Dipl.-Ing. Dr. Christian Paulik

Institute for Chemical Technology

of Organic Materials

Altenberger Straße 69, 4040 Linz

This work was cofinanced by State Government of Upper Austria and the European Regional Development Fund within the framework of the EFRE-IWB 2020 programme for the project “ProFVK - Industrielle Produktionsprozesse für die Verarbeitung von FaserVerbundKunststoffen und zur Herstellung von Leichtbaustrukturen”



I confirm, that going to press of this thesis needs the confirmation of the examination committee.

### *Affidavit*

I declare in lieu of oath, that I wrote this thesis and performed the associated research myself, using only literature cited in this volume. If text passages from sources are used literally, they are marked as such.

I confirm that this work is original and has not been submitted elsewhere for any examination, nor is it currently under consideration for a thesis elsewhere.

I acknowledge that the submitted work will be checked electronically-technically using suitable and state-of-the-art means (plagiarism detection software). On the one hand, this ensures that the submitted work was prepared according to the high-quality standards within the applicable rules to ensure good scientific practice "Code of Conduct" at the TU Wien. On the other hand, a comparison with other student theses avoids violations of my personal copyright.

Vienna, February, 2023



*Signature*

# Acknowledgements

As an external doctoral student, I was enrolled at the TU-Wien and employed at the University of Applied Sciences Upper Austria - Wels in a cooperative doctoral programme during the past three, very educational and exciting years. I had the honour to be mentored by Ao.Univ.Prof. Dipl.-Ing. Dr.mont. Vasiliki-Maria Archodoulaki on the part of the TU-Wien and FH-Prof. h.c. Mag. Dr. Wolfgang Stadlbauer on the part of the FH-Wels.

Above all, I would like to express my sincerest gratitude to my doctoral supervisor Ao.Univ.Prof. Dipl.-Ing. Dr.mont. Vasiliki-Maria Archodoulaki for accepting me as one of her doctoral students. I would like to acknowledge her excellent guidance throughout my scientific investigations and for her extraordinarily fast proofreading whenever a new manuscript was due for journal submission.

Likewise, I thank my FH-supervisor FH-Prof. h.c. Mag. Dr. Wolfgang Stadlbauer wholeheartedly that he saw the potential of a materials scientist in me and for hiring me as his assistant. Working together with him was one of the most joyful and successful times of my life. By the end of 2022, he will go into his well-deserved retirement, and I thereby wish him a wonderful and peaceful time with his family.

Special thanks go to Univ.-Prof. Dipl.-Ing. Dr. Christian Paulik, who agreed to be a reviewer for my doctoral thesis.

I thank the entire team of TCKT GmbH located in Wels, for their excellent cooperativeness throughout my studies and for always welcoming me warmly at their institution. I especially thank them for letting me use their infrastructure to conduct much of my experimental work. Special thanks go to Dr. Christoph Burgstaller, the managing director of the TCKT, for his excellent advice and commentary on my research manuscripts.

I also thank the FH-staff, David Grininger and Ing. Markus Gillich for teaching me to operate the SEM, Judith El-Miligi for managing materials purchasing as well as my

office colleagues Manuel Längauer, MSc and Stefan Augl, MSc for many entertaining conversations.

I would also like to thank several industrial contacts for supplying many special raw materials for my work. One of my most important contacts throughout the years was Thorsten Ommer, R&D manager at Gividi Fabrics S.r.l located in Italy, who answered many questions of mine regarding the technology of glass fibre weaving and the finishing process. Without the supply of Gividi Fabrics' materials, there would have been a large missing link throughout my experimental work.

Finally, I would like to express my deepest gratitude to my family and close friends for supporting me throughout the past years.

In engineering, interfacial adhesion is both an incredibly important, yet remarkably complex topic that is still characterised by many unknowns. Over the past years, I have puzzled countless times on interfacial phenomena within the composite materials I have developed. In the end of my doctoral journey, Wolfgang Pauli's quote described my situation spot-on:

*"God made the bulk; surfaces were invented by the devil."*

- Wolfgang Pauli -

# Table of Contents

<b>Acknowledgements</b> .....	II
<b>Table of Contents</b> .....	IV
<b>English Abstract</b> .....	VI
<b>Deutsche Kurzfassung</b> .....	VIII
<b>List of Figures</b> .....	X
<b>List of Tables</b> .....	XV
<b>List of Abbreviations and Symbols</b> .....	XVI
<b>1 Introduction and motivation</b> .....	1
<b>1.1 Motivation and aim of the work</b> .....	3
<b>2 Fibre, matrix, and interface in composite systems</b> .....	5
<b>2.1 Fibres</b> .....	6
<b>2.1.1 Fibre architectures and terminology</b> .....	7
<b>2.2 Matrices</b> .....	11
<b>2.3 Interfacial adhesion</b> .....	13
<b>2.3.1 Wetting</b> .....	14
<b>2.3.2 The unknowns about covalent bond formation of thermoplastic matrices</b> .....	16
<b>2.3.3 Methods to distinguish good interfacial adhesion from poor interfacial adhesion</b> ..	17
<b>3 Fibre sizings - “the secret sauce”</b> .....	21
<b>3.1 Glass fibre sizing and finishing technology</b> .....	21
<b>3.1.1 Textile sizings and finishes for glass fibre yarns</b> .....	22
<b>3.1.2 Direct sizings for glass fibre rovings</b> .....	24
<b>3.1.3 Glass fibre adhesion promoters</b> .....	26
<b>3.1.4 Polymeric film formers in glass fibre direct sizings</b> .....	29
<b>3.1.5 Auxiliary agents in glass fibre direct sizings</b> .....	31
<b>3.1.6 Glass fibre direct sizings vs finishes</b> .....	33
<b>3.2 Carbon fibre sizings</b> .....	34
<b>3.2.1 Continuous carbon fibres in the thermoplastic process</b> .....	36
<b>4 TPCL manufacturing processes</b> .....	37
<b>4.1 Matrix forms and pressing processes</b> .....	37
<b>4.1.1 Discontinuous (static) pressing</b> .....	38
<b>4.1.2 Semi-continuous (intermittent) pressing</b> .....	39
<b>4.1.3 Continuous (double belt) pressing</b> .....	41
<b>4.1.4 Direct melt processing</b> .....	42
<b>4.1.5 Polymer powder processing</b> .....	42

4.1.6 Polymer film processing.....	44
4.1.7 Polymer fibre (commingling) processing.....	44
4.2 TPCL recycling.....	45
5 Materials and methods.....	47
5.1 Woven fabrics .....	47
5.1.1 Thermoplastic matrices.....	48
5.1.2 Thermoset matrix .....	50
5.1.3 Industrial reference materials .....	50
5.1.4 Cast film extrusion .....	51
5.2 Methods .....	52
5.2.1 TPCL manufacture.....	52
5.2.2 GF-epoxy and CF-epoxy laminate manufacture .....	55
5.2.3 Analytical methods - specimen preparation, conditioning and mechanical testing	55
5.2.4 Microscopical analyses .....	57
6 Results and discussion .....	58
6.1 GF-PP laminates (Publication I) .....	58
6.1.1 GF-PP laminates unpublished results .....	62
6.2 GF-PA6 laminates (Publication III).....	66
6.2.1 GF-PA6 laminates unpublished results .....	68
6.3 GF-PPS laminates (Publication III).....	70
6.4 CF-PA6, CF-PPS and CF-PEEK laminates (Publication IV) .....	73
6.5 TPCL recycling (Publication II).....	79
6.6 Summary of TPCL investigations .....	82
7 Conclusion .....	84
List of References.....	87
Original Publications.....	98
Curriculum Vitae.....	148

## English Abstract

Thermoplastic composites with continuous fibre reinforcements are undoubtedly the next generation of lightweight high-performance materials. Thermoplastic matrices offer the much-required property of simple recyclability and unprecedented material performance - if engineered sufficiently well. Since the thermoplastic composite manufacturing process is a relatively new field of expertise, a lot of knowledge gaps still need to be filled. Especially with regard to material performance optimisation by means of fibre and/or matrix interfacial modification.

Within this study, multiple material combinations including standard-, engineering- and high-performance thermoplastics have been combined with fibrous reinforcements based on woven glass (GF) - and carbon fibre (CF) fabrics via hot compression moulding.

In the case of GF reinforcements, surface treatments containing adhesion promoters were employed for fibre-matrix compatibilisation with polypropylene (PP), polyamide 6 (PA6) and polyphenylene sulphide (PPS). Among the adhesion promoters tested,  $\gamma$ -aminopropyltriethoxysilane (A-1100) and chromium (III) methacrylate complex (Volan<sup>®</sup> A) were identified as key candidates, yielding exceptional material performance. Due to its non-polar nature, PP required additional modification with a coupling agent. For this matter, PP was modified with maleic anhydride grafted PP (MAH-g-PP). Within a concentration range of 0.04-0.06% MAH, the strength characteristics of the GF-PP composite could be harnessed maximally, close to 400 MPa at a fibre volume fraction of 50%. In the case of PA6 and PPS, neat (unmodified) matrices sufficed for optimal interfacial bonding and laminate properties. GF-PA6 laminates resulted in flexural strengths in the region of 500 MPa and fibre volume fractions of 47%, whereas the best performing GF-PPS laminates offered flexural strengths beyond 700 MPa at fibre volume fractions of 56%. The determined multicompatibility of the adhesion promoters A-1100 and Volan<sup>®</sup> A with thermoplastics was deemed a promising outlook for material developments in this area.

The approach taken for CF compatibilisation with thermoplastics was fundamentally different to GF-thermoplastics compatibilisation. Commercially available CF reinforcements are almost always coated with epoxy-based formulations that are generally incompatible with thermoplastics. Therefore, methods were investigated to remove the incompatible epoxy coating and expose the pristine carbon surface. Due to coating removal at 400 °C it was inferred that additional functional groups were introduced to the carbon surface, providing interfacial compatibility with thermoplastics. In fact, epoxy coating removal was so successful in

promoting interfacial adhesion, that subsequently moulded CF-PA6, CF-polycarbonate (PC), CF-PPS and CF-polyetheretherketone (PEEK) laminates offered material performance close to that of automotive and aerospace grade reference materials. At fibre volume fractions of 44-46% CF-PA6, CF-PC, CF-PPS and CF-PEEK laminates offered 600 MPa, 720 MPa, 830 MPa and 845 MPa flexural strength, respectively. Besides wetting, mechanical keying (interlocking) was determined as an important mechanism for interfacial adhesion by SEM analyses. The observations provide valuable insights for CF composite material development.

Finally, the recyclability of thermoplastic composites was investigated by the example of GF-PP and CF-PA6 laminates. Two recycling approaches were found highly promising. Shredded composite material was co-moulded as a core layer between two continuous fibre skins, replacing 50% of the materials volume by recyclate. The flexural and impact properties were largely unaffected by this measure and offered similar performance than their virgin material counterparts. Another idea was investigated by directly reshaping thermoformed parts into flat blanks for reuse. Likewise, the mechanical properties of the reshaped flat blanks were maintained. Both ideas present viable methods and potential solutions to either bring alternative products to the market, or reduce rejected parts.



# Deutsche Kurzfassung

Thermoplastische Composite Lamine weisen neben ihrer hervorragenden Recyclingfähigkeit ein außerordentlich interessantes Performancespektrum auf, um mit herkömmlichen duroplastischen Composites oder metallischen Werkstoffen zu konkurrieren. Da die Materialentwicklung in diesem Bereich größtenteils durch Großkonzerne angetrieben wird und hinter verschlossenen Türen stattfindet, besteht für universitäre Forscher wenig Möglichkeit einen Blick hinter die Kulissen zu werfen. Insbesondere unterliegt das Wissen über Fasermodifizierungen zur Verbesserung der Grenzflächenhaftung derartiger Materialien besonderer Geheimhaltung.

Da das Eigenschaftsspektrum von gewebebasierten thermoplastischen Composites auf Basis von Glasfaser (GF)- und Carbonfaserverstärkung (CF) bislang noch nicht systematisch erforscht wurde, bietet diese Forschungsarbeit einen praxisorientierten Einblick in die Composite Materialentwicklung.

GF-basierte Lamine wurden in Kombination mit Polypropylen (PP), Polyamid 6 (PA6) und Polyphenylsulfid (PPS) Matrices im Heißpressverfahren hergestellt. Innerhalb der Faser-Matrix Kompatibilitätsstudien wurden  $\gamma$ -Aminopropyltriethoxysilan (A-1100) und Chrom (III) Methacrylat (Volan<sup>®</sup> A) als äußerst potente Haftvermittler für die zuvor genannten Matrices ausfindig gemacht. PP wurde zusätzlich mit einem Matrixseitigem Haftvermittler auf Basis von Maleinsäureanhydrid gepropftem PP (MAH-g-PP) modifiziert. Innerhalb einer Konzentration von 0.04-0.06% MAH wurden bei GF-PP Laminaten Biegefestigkeiten von 400 MPa verzeichnet. Hingegen, mussten PA6 und PPS Matrices nicht weiter modifiziert werden. Die Homopolymere wiesen eine außerordentlich hohe Affinität zu den Faserseitig aufgetragenen Haftvermittlern auf. Die ermittelten Biegefestigkeiten von GF-PA6 Laminaten mit einem Faservolumengehalt von 47% betragen 500 MPa; bei GF-PPS wurden über 700 MPa bei einem Faservolumengehalt von 56% ermittelt. Die Kenntnis der hohen Kompatibilität bestimmter Haftvermittler mit bestimmten Thermoplasten ist eine wichtige Grundlage für künftige GF Materialentwicklungen.

CF-basierte Lamine wurden in Kombination mit PA6, Polycarbonat (PC), PPS und Polyetheretherketon (PEEK) hergestellt. Besonderes Augenmerk wurde dabei auf eine optimierte Grenzflächenhaftung zwischen CF und Thermoplastmatrix gelegt. Da kommerzielle CF Gewebe beinahe ausschließlich für Epoxidharzanwendungen mit Epoxidharz basierenden Schichten ausgerüstet werden, wurde ein erfolgsversprechender Ansatz mittels thermischer Entschlichtung und Oxidation der CF Gewebe gefunden. Mittels entschlichteter CF Gewebe

wurde eine hervorragende Benetzbarkeit durch die thermoplastischen Matrizes erreicht und dadurch Lamineigenschaften auf höchstem Industrieniveau verzeichnet.

Zuletzt wurde das Thema des Laminatrecyclings näher beleuchtet. Durch einen innovativen Ansatz wurde Schreddergut als Kernschicht zwischen zwei dünnen Laminatdecklagen eingebracht und heißverpresst. Derartige „Micro-sandwiches“ mit 50% recyclingmaterial wiesen Biege- und Schlageigenschaften auf dem Niveau von Neumaterialien auf. Eine weitere vielversprechende Idee um die Wiederaufschmelzbarkeit der thermoplastischen Matrix auszunutzen, wurde mittels Rückverformung von Thermogeformten Bauteilen verfolgt. Die Rückverformung von Bauteilen zu wiederverwendbarer Plattenware mit dem gleichzeitigen Erhalt der mechanischen Eigenschaften wurde als äußerst vielversprechende Methode für die industrielle Produktion bewertet.

Zusammenfassend, wurden thermoplastische Composite Lamine mit einem breiten Anwendungsfeld erforscht und Maßnahmen präsentiert, um die höchsten mechanischen Eigenschaften von Neuware sowie Abfallprodukten zu generieren.

# List of Figures

- Fig. 1** Constituents of a composite (cross sectional view). The matrix, the fibre, the fibre-matrix interface and a transition zone called the interphase..... 5
- Fig. 2** Left to right: E-glass fibre yarn 300 Tex, E-glass fibre roving 1200 Tex, E-glass fibre roving 2400 Tex. Yarn bobbin is unwound by external pull, roving bobbins by internal pull. . 7
- Fig. 3** 3K high tenacity (HT) carbon fibre tow (left) and 50K HT carbon fibre tow (right). Both bobbins are unwound by external pull..... 8
- Fig. 4** Most common weave patterns of fabrics used in composite applications. .... 9
- Fig. 5** Glass yarn fabric 50” (Gividi Fabrics VR48 2/2 twill) based on 68 x 3 Tex yarns with an areal weight of 290 g/m<sup>2</sup> and thread count of 7/cm. .... 9
- Fig. 6** Glass roving fabric 50” (Gividi Fabrics ST600TU 2/2 twill) based on 1200 Tex rovings with an areal weight of 600 g/m<sup>2</sup> and thread count of 2.5/cm..... 10
- Fig. 7** Carbon fibre fabric 50” (ECC - Engineered Cramer Composites Style 452 2/2 twill) based on 3K - 200 Tex tows with an areal weight of 200 g/m<sup>2</sup> and thread count of 5/cm..... 10
- Fig. 8** Some key thermoplastics utilised in automotive and aerospace grade composites. .... 13
- Fig. 9** Mechanisms contributing to the overall adhesion in composites [12,30,50,75]..... 14
- Fig. 10** Comparison between poor and good adhesion in CF composite samples. Interfacial debonding (left): bare fibres. Cohesive matrix failure and straight fibre fracture surfaces (right): fibres are completely covered by adherent matrix (adapted from [25])..... 19
- Fig. 11** Top-view of failed glass fibre TPCL specimen due to micro-buckling on the compression side during a 3-point flexural test (failure in longitudinal fibre direction). .... 20
- Fig. 12** E-Glass fibre yarn and roving manufacturing process (adapted from [33,34,103]). Note that either yarn or roving is produced depending on the configuration of the melting furnace and design of the bushings (diameter and number of orifices)..... 22
- Fig. 13** Processing scheme (top view) for the production of finished glass yarn fabrics including warping, slashing, weaving, heat cleaning and finishing (adapted from [106])..... 23
- Fig. 14** Processing scheme for producing woven glass roving fabrics. .... 24
- Fig. 15** Glass fibre surface of heat-cleaned glass yarn (top) and A-1100 aminosilane finished glass yarn (bottom). Both samples were derived from woven fabrics. .... 25
- Fig. 16** Surface of direct sized PP-compatible roving. Sample was derived from a bobbin. .... 25
- Fig. 17** Adhesion promoters for glass fibres (adapted from [12,28,29,108,109])..... 26

<b>Fig. 18</b> Proposed mechanism of glass fibre surface silanization. An aqueous solution of silane is prepared. The silanes undergo hydrolysis to form silanols, which in turn polymerise into siloxanes and subsequently condense with the glass fibre surface upon drying (adapted from [12,28,29,108]).	27
<b>Fig. 19</b> Hydrolysis and condensation of the glass fibre adhesion promoter Volan A (adapted from [22,28,109]).	28
<b>Fig. 20</b> Aminosilane network formed on glass fibre surface by protonated aminogroups, hydrogen bonding and covalent interactions (adapted from [92,111,112]).	29
<b>Fig. 21</b> Scheme of an interpenetrating network (IPN) formed between a glass fibre direct sizing and a polymer matrix. The adhesion promoter (silane) is deposited closest to the glass surface. Note, the scheme is not to scale.	30
<b>Fig. 22</b> Possible interaction of silanized GF-surface with reactive film former type (MAH-g-PP) for PP compatibilization (adapted from [108]).	31
<b>Fig. 23</b> Carbon fibre (HT-type) production process from a PAN-copolymer based precursor: oxidation of the PAN-precursor, carbonisation in inert gas furnaces, electrochemical surface treatment (activation), sizing application and winding (adapted from [31]).	35
<b>Fig. 24</b> Functional groups on an electrochemically oxidised (activated) carbon fibre surface (adapted from [140–142]).	35
<b>Fig. 25</b> Polymer matrix forms for TPCL production provided as direct melt, polymer powder, polymer film or polymer fibre.	37
<b>Fig. 26</b> Press configurations for processing TPCL including static pressing, intermittent pressing, or continuous pressing.	38
<b>Fig. 27</b> Cetex <sup>®</sup> TPCL consolidated on static presses. CF-PPS fabric TC1100 (large panel background 500 · 500 mm <sup>2</sup> ); TPCL from bottom left to top right: CF-LMPAEK UD, CF-PEI fabric, CF-PPS UD, CF-PPS fabric, CF-PEI UD, GF-PEI fabric, GF-PPS fabric. Samples kindly provided by Toray Advanced Composites.	39
<b>Fig. 28</b> Step pattern arising from semi-continuous pressing of a 50” wide Tepex <sup>®</sup> 202 CF-PA6 TPCL produced by Bond Laminates GmbH.	40
<b>Fig. 29</b> CF-polymer powder-semipreg (top left, top right and bottom left), and compression moulded laminate therefrom (bottom right).	43
<b>Fig. 30</b> Commingled GF-PP roving (left) and commingled GF-PP roving fabric (right).	44
<b>Fig. 31</b> Recycling route for TPCL via shredding and compression moulding.	45
<b>Fig. 32</b> Processing scheme of TPCL manufacture via film stacking and hot compression moulding.	52
<b>Fig. 33</b> Static heating and cooling presses utilised in the experiments.	53

<b>Fig. 34</b> Vacuum assisted infusion of carbon fibre fabrics with epoxy resin. Resin inlet (left), resin outlet to vacuum pump (right) and infusion lines. Dry CF stack is covered by a peel ply, flow media and the vacuum bagging film (secured by sealant tape).....	55
<b>Fig. 35</b> Standardised composite test specimens for $2 \pm 0.2$ mm thick laminates. The inner dimension represents the support span or gage length, respectively. All dimensions are given in millimetres.....	56
<b>Fig. 36</b> Flexural strength vs. active MAH content (Polybond 3000) in HK060AE (PP matrix). Fabrics used: FK144 (Volan A chromium complex GF finish) and StarRov 490 (PP-compatible GF direct sizing). ( <b>Publication I</b> [22]).....	59
<b>Fig. 37</b> Flexural strength of in-house moulded TPCL vs different fabrics and industrial reference TPCL. ( <b>Publication I</b> [22]). .....	60
<b>Fig. 38</b> Flexural properties of aminosilane finished fabrics in GF-PP TPCL. ( <b>Publication I</b> [22]). .....	61
<b>Fig. 39</b> FK144 Volan A chromium complex finished glass yarn fabric laminate, impregnated with strips of natural coloured PP HK060AE films with different MAH coupling agent concentrations. The change in hue indicates improved wettability or coupling between MAH and the Volan A chromium complex finish.....	62
<b>Fig. 40</b> Required amount of carbon black masterbatch to make GF-PP TPCL visually more appealing.....	63
<b>Fig. 41</b> Comparison of industrial reference TPCL Tepex dynalite 104 (left) overlapped with in-house developed GF-PP TPCL with 2.0 wt% carbon black masterbatch (right background). .....	63
<b>Fig. 42.</b> Flexural strengths of different MAH-g-PP coupling agent additives in GF-PP TPCL at an active MAH concentration of 0.04%. .....	65
<b>Fig. 43</b> Flexural strengths of different MAH-g-PP coupling agent additives in GF-PP TPCL at an active MAH concentration of 0.10% .....	65
<b>Fig. 44</b> Flexural properties of GF-PA6 TPCL prepared from differently modified glass fibre fabrics and neat PA6 matrix. GF-PA6 specimens were tested in conditioned state (23 °C, 50% relative humidity, 14 days duration of conditioning). ( <b>Publication III</b> [24]).....	66
<b>Fig. 45</b> Cross-section of compression moulded 8-ply GF-PA6 TPCL with A-1100 finish. The microstructure of the laminate appeared fully impregnated and void-free. ( <b>Publication III</b> [24]) .....	67
<b>Fig. 46</b> Different specimen failure mechanisms of flexural tested GF-PA6 TPCL. Failure mechanisms changing from compressive micro-buckling to mixed compressive-tensile failure depending on the adhesion promoter and quality of interfacial adhesion (adapted from [24]). .....	68
<b>Fig. 47</b> Flexural properties of GF-PA6 TPCL modified with coupling agent EBA-g-MAH. .	69

<b>Fig. 48</b> Charpy impact properties of GF-PA6 TPCL modified with coupling agent EBA-g-MAH.....	69
<b>Fig. 49</b> Flexural properties of GF-PPS TPCL prepared from differently modified glass fibre fabrics and neat PPS matrix. ( <b>Publication III</b> [24]) .....	70
<b>Fig. 50</b> GF-PPS TPCL cross-sections indicating good impregnation of both desized (left) and FK144 Volan A chromium finished (right) materials. ( <b>Publication III</b> [24]).....	71
<b>Fig. 51</b> Flexural tested GF-PPS TPCL based on FK144 Volan A chromium complex finish. The test specimens evinced tensile fracture only without compressive micro-buckling. ( <b>Publication III</b> [24]).....	72
<b>Fig. 52</b> SEM images of fractured GF-PPS TPCL. Left: Desized GF-PPS laminate with interfacial debonding and no adherent PPS matrix on the glass fibre. Right: GF-PPS laminate with FK144 Volan A chromium complex finish exhibiting cohesive failure and a fully adhered layer of PPS matrix on the glass fibre. ( <b>Publication III</b> [24]) .....	72
<b>Fig. 53</b> Decomposition behaviour of EP-sizing measured by thermogravimetric analysis. A decomposition onset of the EP-sizing at roughly 250 °C was observed. ( <b>Publication IV</b> [25]) .....	73
<b>Fig. 54</b> CF-fabric desizing by means of infrared irradiation (IR-desizing) at 380-400 °C. ( <b>Publication IV</b> [25]).....	74
<b>Fig. 55</b> SEM images of EP-sized (top) and IR-desized (bottom) carbon fibre reinforcement. Note, the IR-desized fibres appeared completely free from sizing residues after heating to 400 °C in air atmosphere. ( <b>Publication IV</b> [25]).....	74
<b>Fig. 56</b> MTGA analysis of an IR-desized carbon fibre fabric indicating full removal of the sizing due to the low LOI measured. ( <b>Publication IV</b> [25]) .....	75
<b>Fig. 57</b> Flexural properties of in-house moulded CF TPCL vs. industrial reference CF TPCL. ( <b>Publication IV</b> [25]).....	75
<b>Fig. 58</b> Flexural properties of CF-EP and CF-PC laminates.....	77
<b>Fig. 59</b> Charpy impact strengths of CF-EP and CF-PC laminates.....	77
<b>Fig. 60</b> SEM image of fractured CF-EP (EP-sized) laminate. The sample shows good wetting of the carbon fibre with the epoxy resin and brittle fracture behaviour of the matrix.....	78
<b>Fig. 61</b> SEM image of fractured CF-EP (desized) laminate. The sample shows good wetting of the carbon fibre with the epoxy resin and brittle fracture behaviour of the matrix.....	79
<b>Fig. 62</b> SEM image of fractured CF-PC (desized) laminate. The sample shows good wetting of the carbon fibre with polycarbonate and ductile fracture behaviour of the matrix. ....	79
<b>Fig. 63</b> Flexural properties of recycled TPCL. Left: recycled GF-PP TPCL, right: recycled CF-PA6 TPCL. ....	80

---

<b>Fig. 64</b> SEM micrographs of polished specimen cross-sections. Left: recycled TP-SMC panels, right: recycled sandwich panels with shredded material core and continuous fibre skins. ....	80
<b>Fig. 65</b> Direct recycling of TPCL by reverse thermoforming. A complexly shaped part is reshaped into its initial flat geometry by means of heat and tension. ....	81
<b>Fig. 66</b> Performance range of in-house developed woven TPCL with bidirectional ply layup vs. aerospace grade aluminium alloys. ....	82
<b>Fig. 67</b> Impact performance of in-house developed woven TPCL with bidirectional ply layup vs. aerospace grade aluminium alloys. ....	83

# List of Tables

<b>Table 1</b> Comparison between dry E-glass and HT-type carbon fibres [1,31,35]. .....	6
<b>Table 2</b> Bond energy comparison [94,95] .....	17
<b>Table 3</b> Generic composition of a water-based glass roving direct sizing [33,119].....	32
<b>Table 4</b> Compatibility chart of pressing processes and fibre-matrix intermediate forms for dry woven fabrics.....	45
<b>Table 5</b> Dry glass fibre fabrics used in the experiments. ( <b>Publications I and III</b> ) .....	47
<b>Table 6</b> Dry carbon fibre fabric used in the experiments. ( <b>Publication IV</b> ).....	48
<b>Table 7</b> Thermoplastic matrices used in the experiments. ( <b>Publications I, III and IV</b> ).....	48
<b>Table 8</b> Additives used for PP homopolymer modification. ( <b>Publication I</b> ).....	49
<b>Table 9</b> Additives used for PA6 homopolymer modification. (used in unpublished results)..	49
<b>Table 10</b> Thermoset epoxy matrix used for carbon fibre resin infusion. (used in unpublished results) .....	50
<b>Table 11</b> Industrial GF and CF reference materials. (0,90) represents one fabric ply. ( <b>Publications I-IV</b> ) .....	50
<b>Table 12</b> Aerospace grade aluminium alloy reference materials. (used in unpublished results) .....	51
<b>Table 13</b> Drying and processing conditions for cast film extrusion ( <b>Publications I and III</b> )	51
<b>Table 14</b> Overview of investigated TPCL fibre-matrix combinations. ....	52
<b>Table 15</b> Processing conditions of thermoplastic matrices during TPCL manufacture.....	55
<b>Table 16</b> Blend formulations of MAH-g-PP and PP HK060AE homopolymer. Additives sorted according to fluidity.....	64
<b>Table 17</b> Blend formulations of EBA-g-MAH and PA6 Ultramid® B3W homopolymer.....	68



# List of Abbreviations and Symbols

CF .....	Carbon Fibre
GF .....	Glass Fibre
LFT-D .....	Direct Long Fibre Thermoplastics
LFT-G .....	Long Fibre Thermoplastics Granules
MAH .....	Maleic anhydride
MTGA .....	Macro Thermogravimetric Analysis
PA6 .....	Polyamide 6
PC .....	Polycarbonate
PP .....	Polypropylene
PPS .....	Polyphenylene Sulfide
PAEK .....	Polyaryletherketone
PEEK .....	Polyetheretherketone
SEM .....	Scanning electron microscopy
GPa .....	Gigapascal
MPa .....	Megapascal
$T_g$ .....	glass transition temperature
$T_m$ .....	melting temperature
$v_f$ .....	Fibre volume fraction
$\rho$ .....	Density

# 1 Introduction and motivation

Composites are a macroscopic construct of two or more microscopically distinct materials exhibiting properties and characteristics that differ from those of their individual components. One component represents the continuous phase called the matrix, whereas the other component represents a reinforcement of particulate or fibrous origin dispersed evenly within the matrix. Compared to particulates, fibrous reinforcements have lengths much greater than their cross-sectional dimensions. Consequently, their aspect ratio, which is the relation of length to the diameter is especially high. The size and abundance of flaws have great influence on the failure probability of materials. In a fibre, a flaw cannot exceed the fibre diameter. For this reason, thin fibres exhibit an extraordinary reinforcing effect over bulk materials [1].

In nature, materials have evolved over an enormous period of time and combined to form highly efficient, load-adapted structures. In essence, fibrous composites with hierarchical structures are omnipresent in biological matter including: cortical bone composed of mineralised collagen nanofibrils [2], wood made of lignocellulosic fibres [3], feathers made of  $\beta$ -keratin fibrils [4], or arthropod cuticle (exoskeletons) composed of helicoidally arranged chitin fibres [5,6], just to name a few. It is truly remarkable that nature arranges such extremely complex structures through biosynthesis and self-assembly, all under ambient conditions. Until now, it has not been possible to synthesise hierarchical nano-composite structures with the precision found in nature. Nonetheless, the general concept of using composite materials for structural lightweight design continues to be intensively researched, since the potential of this technology is far from being exhausted. Following nature's example, many concepts are recreated through so-called "biomimicry" in vast areas of modern mechanical engineering to solve technological problems [7]. For instance, the use of lightweight honeycomb sandwich-structured composites has been state-of-the-art for decades in aerospace engineering. Here, the load-bearing components of aircraft structures are composed of two thin fibrous skins separated by a lightweight core, much like the structure of bird wings or flat bone [8].

Modern high-performance composites are mainly constructed from man-made continuous fibres embedded within synthetic polymer matrices. This combination offers enormous lightweighting potential at high specific strengths and stiffnesses. Especially laminar composite structures composed of several reinforcing plies (lamina) are considered for high-performance applications. Consequently, the use of composite laminates is an exciting prospect throughout mechanical engineering despite many challenges that arise in material development, part design, manufacturing methods, processing stability and waste treatment.

Due to the rising awareness of environmental impacts from greenhouse gas emissions, interest is growing in lightweight materials and lightweighting concepts. Transportation is a particularly important sector where weight reduction leads to considerable fuel or energy savings over the lifespan of vehicles. In the continuous fibre-reinforced composites market, thermoset based polymer matrices such as epoxy resins have gained great acceptance in high-performance applications. Once available exclusively to the aerospace and defence industries in the 1950s and 1960s, these carbon- and glass fibre-reinforced epoxy composites have made inroads in many application fields and products to date [1]. Boat hulls, wind turbine blades, pipes and rebar in civil engineering, automotive components, and recreational products (tennis rackets, skis, hockey sticks, bike frames) have been increasingly constructed from thermoset composites in the last few decades [1]. However, what has kept composites from achieving a more profound breakthrough in commercial applications is their overall higher cost compared to metallic components made of steel or aluminium alloys. Additionally, a circular economy mindset (including the European Green Deal [9]) has emerged in recent years that, rightfully, puts an emphasis on the recyclability of materials. Recycling methods for cured thermoset polymers are extremely cumbersome due to their covalently crosslinked structures, and to this day most of the composite waste material is sent to landfills [10,11]. As far as recyclability is concerned, thermoset polymers are clearly outshined by their thermoplastic (thermosoftening) counterparts which can be remelted and remoulded multiple times [10]. Therefore, thermoplastic composites are envisioned as viable candidates to partially replace thermoset composites in the long-term.

Thermoplastics have a long tradition of being used for short fibre-reinforced injection moulding compounds [12], or more recently as long fibre-reinforced thermoplastic compounds (LFT-D or LFT-G) [13–15]. Conversely, the technology of continuous fibre-reinforced thermoplastics is still maturing. The very high melt viscosities of thermoplastics complicate fibre wet-out, rendering the industrial scale production of thermoplastic composite laminates (TPCL) technologically difficult. The production of such TPCL, frequently termed “organo sheets” requires compression moulding techniques with lengthy impregnation times. Furthermore, adhesion between the fibres and the relatively inert thermoplastic polymers is often insufficient for many fibre-matrix combinations and largely unexplored, unoptimized or unpublished due to proprietary reasons. An arbitrarily chosen fibre reinforcement and polymer type cannot be expected to perform to the highest standards. Parameters including polymer viscosity, polymer modification, fibre surface treatment, the manufacturing process itself and the processing conditions all need to be factored in for optimal material performance. Especially the fibre surface treatment plays a pivotal role in determining the processability and mechanical properties of the final composite. The reinforcement is only capable of strengthening the matrix sufficiently if strong adhesion persists between the two phases. Extensive work has been reported in literature in conjunction with fibre surface treatments, however, with a predominant focus on thermosets instead of thermoplastics.

The production of high-performance TPCL on large scales is a complex and capital-intensive process. As of yet, such production processes are only practiced well by a handful of specialty manufacturers including Bond-Laminates GmbH a subsidiary of the High Performance Materials (HPM) business unit at LANXESS [16], Toray Advanced Composites [17], Teijin Limited [18] or Mitsubishi Chemical Advanced Materials Plastic Composites [19]. These companies have introduced a range of high-performance TPCL to the market in the past two decades which lead so a slow but steady acceptance of these materials in several industries. The potential of TPCL is put to full use in subsequent high-volume manufacturing methods including stamp forming or thermoforming in combination with back injection moulding [20,21]. Short takt times of 1-2 minutes per part with high reproducibility promise a bright future for this class of materials.

While the aforementioned companies have been successful in developing and optimising their materials over many years, material formulations have been hidden behind a veil of secrecy. Little work has been published in literature focussing on high-performance TPCL development.

### 1.1 Motivation and aim of the work

This work came into existence at the FH-Wels in the research project “ProFVK” due to a material shortage of TPCL in early 2019. The standard material for thermoforming experiments was Tepex<sup>®</sup> dynalite by Bond-Laminates GmbH. In early 2019 the remaining material stock of thin Tepex sheets (0.5-1.0 mm thickness) of the FH-Wels was almost depleted. Unexpectedly, Bond-Laminates GmbH had estimated a delivery time of 7-8 months for a reorder, which would have temporarily halted all thermoforming trials. To continue the thermoforming research work, in-house development of thermoplastic composite laminates commenced on existing flat platen hydraulic hot presses. Driven by the fascination of these materials, a considerable expenditure of experimentation was necessary in order to fabricate TPCL of industrial-quality in-house.

The optimisation of interfacial adhesion and its direct effects on macroscopic composite properties has not been investigated systematically yet. Ultimately, such a task requires a multidisciplinary approach involving fibre science, polymer chemistry, formulation chemistry, processing science and materials testing. To this end, the aim of the work is to develop automotive and aerospace grade thermoplastic composite laminates in a practice-oriented and industry-relevant manner. Specifically, engineering-relevant thermoplastic matrices and fibre reinforcements are targeted with a broad application spectrum. Aimed at the cheaper end and high-volume combinations, glass fibre-reinforced polypropylene (GF-PP) and glass fibre-reinforced polyamide 6 (GF-PA6) are investigated.

High-end fibre-matrix combinations include glass fibre-reinforced polyphenylene sulfide (GF-PPS), carbon fibre-reinforced polyamide 6 (CF-PA6), carbon fibre-reinforced polycarbonate (CF-PC), carbon fibre-reinforced polyphenylene sulfide (CF-PPS) and carbon fibre-reinforced polyetheretherketone (CF-PEEK).

The in-house developed materials are benchmarked against industrial references. Moreover, comparisons are made to glass and carbon fibre-reinforced epoxy (GF-EP, CF-EP) and aerospace grade aluminium alloys (AW-2024 T6 and AW-7075 T6) which some of the thermoplastic composite materials intend to substitute.

Finally, the general recyclability of TPCL is investigated by several innovative ideas, which shall highlight the advantages of this composite material class.

**Publication I:** Dedicated to GF-PP laminate development

[22] Kiss P, Stadlbauer W, Burgstaller C, Archodoulaki V-M. Development of high-performance glass fibre-polypropylene composite laminates: Effect of fibre sizing type and coupling agent concentration on mechanical properties. *Compos Part A Appl Sci Manuf* 2020;138:106056. doi:10.1016/j.compositesa.2020.106056.

**Publication II:** Recycling of GF-PP and CF-PA6 laminates

[23] Kiss P, Stadlbauer W, Burgstaller C, Stadler H, Fehringer S, Haeuserer F, et al. In-house recycling of carbon- and glass fibre-reinforced thermoplastic composite laminate waste into high-performance sheet materials. *Compos Part A Appl Sci Manuf* 2020;139:106110. doi:10.1016/j.compositesa.2020.106110.

**Publication III:** Dedicated to GF-PA6 and GF-PPS laminate development

[24] Kiss P, Schoefer J, Stadlbauer W, Burgstaller C, Archodoulaki V-M. An experimental study of glass fibre roving sizings and yarn finishes in high-performance GF-PA6 and GF-PPS composite laminates. *Compos Part B Eng* 2021;204:108487. doi:10.1016/j.compositesb.2020.108487.

**Publication IV:** Dedicated to CF-PA6, CF-PPS, CF-PEEK laminate development

[25] Kiss P, Glinz J, Stadlbauer W, Burgstaller C, Archodoulaki V-M. The effect of thermally desized carbon fibre reinforcement on the flexural and impact properties of PA6, PPS and PEEK composite laminates: A comparative study. *Compos Part B Eng* 2021:108844. doi:10.1016/j.compositesb.2021.108844.

Unpublished data for comparisons: Mechanical values of CF-PC, CF-EP and aerospace grade aluminium alloys

## 2 Fibre, matrix, and interface in composite systems

Fibrous composites technically consist of three constituents. The fibres, the matrix, and the interface/interphase.

- The reinforcing fibres convey stiffness, strength, and fatigue strength to the material.
- The matrix governs many important roles such as fixing the fibres in a desired geometric position, transmitting stress by shear forces to the fibres, transferring stresses from fibre to fibre, supporting the fibres in compression, redistributing load in the event of fibre failure, protecting the fibres from abrasion, protecting the fibres from the operating environment (gaseous and liquid media), and determining the service temperature of the composite [1].

All the important traits of the fibres and the matrix may only be harnessed if the fibre and the matrix are sufficiently adhered to each other. Therefore, the third constituent of a composite is the region of interactions between the fibre and the matrix.

- The two-dimensional area of contact between the fibre and matrix (or fibre coating and matrix) is called the interface [26–28]. Physicochemical interactions at the solid-liquid interface determine the wettability of the system during composite fabrication. Intimate contact generated by good wetting is a prerequisite for possible chemical bond formation and several other adhesion mechanisms between fibres and the matrix. In micromechanical analyses it is frequently observed that the properties from the bulk matrix to the fibre change gradually in a roughly 100-300 nm thick three-dimensional region which is called the interphase, as illustrated in Fig. 1 [26,29–31].

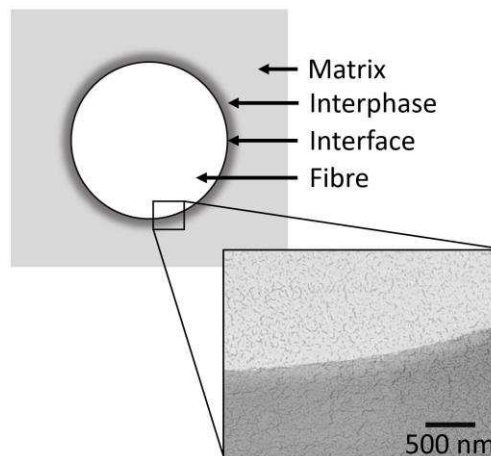


**Fig. 1** Constituents of a composite (cross sectional view). The matrix, the fibre, the fibre-matrix interface and a transition zone called the interphase.

The consideration of an interphase is especially important for fibres which are equipped with a thin surface coating (called a sizing or finish, as will be discussed). The complex interactions at the interface and within the interphase, alongside other factors including the fibre content, fibre orientation and void content, determine the final macroscopic properties of the composite material.

## 2.1 Fibres

For technical applications a wide range of reinforcing fibres are available, all of which differ in price, density and performance [1]. The demand for low-cost and high-performance fibres with consistent quality is apparent. Natural fibres are very cost-effective and a sustainable material source for composite applications [32]. However, variations in fibre quality and in turn inconsistent mechanical performance, long growth periods (seasonality), moisture absorption, microbial attack, low thermal stability and unpleasant odour emissions currently strongly limit the applicability of natural fibres in advanced composites [32]. Therefore, the advanced composites sector is mainly comprised of man-made fibres including glass and carbon fibres which guarantee consistent material quality at an almost unlimited shelf-life.

According to Thomason [33,34] E-glass fibres remain the workhorse reinforcement in the global composites industry with over 95% market share. The rest is divided between other types of glass fibres (S-glass, ECR-glass, M-glass), carbon fibres and aramid fibres. E-glass, which was initially developed for electrical applications due to its extraordinary electrical insulation properties (hence the term “E” [29]) is considered a general-purpose reinforcement today. Nevertheless, due to the myriad of fibre coating preparations available, research is still needed to find the optimal performance in glass fibre composites. The cost and performance characteristics of E-glass and carbon fibres are compared in Table 1. Carbon fibre reinforcements are ten to twenty times the cost per kilo compared to E-glass. Yet, carbon fibre usage is growing in popularity due to the unrivalled mechanical properties at their given density.

**Table 1** Comparison between dry E-glass and HT-type carbon fibres [1,31,35].

	dry E-glass fibre roving	dry carbon fibre tow HT-type (high tenacity)
Composition	Aluminium borosilicate	> 95% Carbon
Density [g/cm <sup>3</sup> ]	2.5-2.6	1.7-1.8
Tensile modulus [GPa]	70	240
Tensile strength [MPa]	2500-3500	4000
Elongation at break [%]	< 5	< 2
Cost [€/kg]	0.5-2	20-50

### 2.1.1 Fibre architectures and terminology

Dry glass and carbon fibre reinforcements come in various forms (architectures) ranging from continuous fibre products to discontinuous fibre products. High-performance parts are made primarily from continuous fibre reinforcement, whereas parts with less stringent performance requirements may be constructed from discontinuous fibre reinforcement. The most common products made from continuous fibres include unidirectional reinforcement, non-crimp fabrics, woven fabrics, braided fabrics, and knitted fabrics. Products made from discontinuous fibres originate from continuous fibre precursors and include fabrics from staple yarns, mats, nonwovens and chopped fibres [1]. It should be noted that the following literature review focuses strictly on continuous strand types. The terminology used to classify continuous fibre strands varies to some extent between the glass- and carbon fibre industry.

The terminology used in the glass fibre industry is strongly related to the textile (garment) industry. Continuous glass fibres (filaments) are formed by drawing molten glass through heated bushings at very high speeds of over 20 m/s [33,34]. Depending on the diameter and number of orifices within the bushings, glass is drawn into fine strands (yarn) or thick strands (roving) as displayed in Fig. 2. The unit of measure for glass fibre strands is linear density, defined as the mass in grams per kilometre (Tex: g/km). Consequently, a glass fibre strand with 1200 Tex weighs 1.2 grams per metre. A further classification within glass fibre strands is made by the fibre diameter. Glass yarn refers to strands with filaments typically under 14 microns in diameter and linear densities  $\leq 300$  Tex. Glass roving refers to strands with filaments typically over 13 microns in diameter and linear densities of 300-4800 Tex [12,22]. Yarns have a protective twist [36] of up to 20-40 twists per metre to ensure strand integrity and reduce friction during subsequent handling operations, whereas rovings come untwisted.



**Fig. 2** Left to right: E-glass fibre yarn 300 Tex, E-glass fibre roving 1200 Tex, E-glass fibre roving 2400 Tex. Yarn bobbin is unwound by external pull, roving bobbins by internal pull.



High strength type carbon fibres are derived from stabilisation and carbonisation of PAN (polyacrylonitrile)-copolymer precursors. Typical PAN comonomers are itaconic acid, methacrylic acid, methyl acrylate or methyl methacrylate [1,31,37–39]. The terminology used to classify carbon fibre strands is different to glass fibres. Carbon fibre strands are usually referred to as “tow” instead of yarn or roving. The number of individual filaments per tow is given in “K” which is an abbreviated symbol referring to “thousand”. For instance, a 3K tow contains 3000 individual 7 micron carbon filaments. 3K (200 Tex) tows are typically employed for weaving, whereas heavy tows such as 50K are mainly used for unidirectional (UD) tape production. Carbon fibre tows are generally supplied in untwisted form. A comparison between a 3K tow and 50K tow is given in Fig. 3.



**Fig. 3** 3K high tenacity (HT) carbon fibre tow (left) and 50K HT carbon fibre tow (right). Both bobbins are unwound by external pull.

As mentioned, continuous fibre strands are frequently interlaced by weaving on looms, creating fabrics with superior handling characteristics compared to unidirectional (UD) reinforcement. In a woven fabric, the “warp” refers to the lengthwise running strands, whereas the “weft” refers to strands running perpendicularly to the warp strands [40]. The most common weave patterns used in automotive and aerospace applications are the plain weave, 2/2 twill weave, 5-harness satin weave and the 8-harness satin weave as portrayed in Fig. 4.

The weave patterns affect the drapeability (how well the fabrics conform to complex geometries without wrinkling) and fibre crimp (strong undulation of strands affect composite properties adversely) [1,31]. “Looser” weaves such as twill weaves and satin weaves are easily distorted and well suited for compound curves, whereas plain weaves are very stable and suited mostly for planar parts.

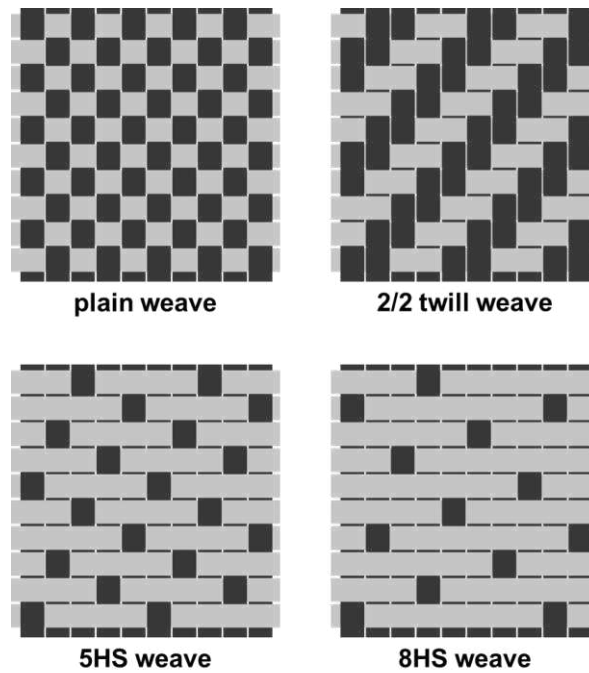


**Fig. 4** Most common weave patterns of fabrics used in composite applications.

For the construction of fabrics, low Tex glass yarns are frequently twisted (plied) together to form thicker yarn assemblies, sometimes called threads. An example is given in Fig. 5 of a delicate fabric constructed from 68 x 3 Tex yarn (three individual 68 Tex yarns were twisted together per thread). The architecture of the fibre reinforcement, its linear density, spreading width of the strands and thread count (strands per unit length, or thr./cm) determine the areal weight of the product, given in  $\text{g/m}^2$  (or gsm) and its thickness. One of the heaviest 2/2 twill yarn fabrics available on the market is produced by Hexcel from 136 x 3 Tex yarns resulting in a fabric areal weight of  $600 \text{ g/m}^2$  and thread count of 7.35/cm (style HexForce<sup>®</sup> 01083).



**Fig. 5** Glass yarn fabric 50'' (Gividi Fabrics VR48 2/2 twill) based on 68 x 3 Tex yarns with an areal weight of  $290 \text{ g/m}^2$  and thread count of 7/cm.

Glass rovings are available in two types, as either assembled (multi-end) rovings gathered together from several lower Tex rovings without twist, or as direct (single-end) rovings. Direct rovings have the advantage of more uniform fibre tension compared to assembled rovings. Yet, both types are utilised in weaving processes. Glass roving fabrics, as depicted in Fig. 6 are generally considered as heavy reinforcement where only a low number of plies is required to build up thick laminates rapidly. Due to the coarse weave, the surface coverage (weave density) within roving fabrics is worse compared to yarn fabrics. In a laminate this results in matrix-rich regions where the rovings intersect. The use of woven rovings in TPCL was made popular by Bond-Laminates GmbH [16] in an effort to reduce cost and simplify production.

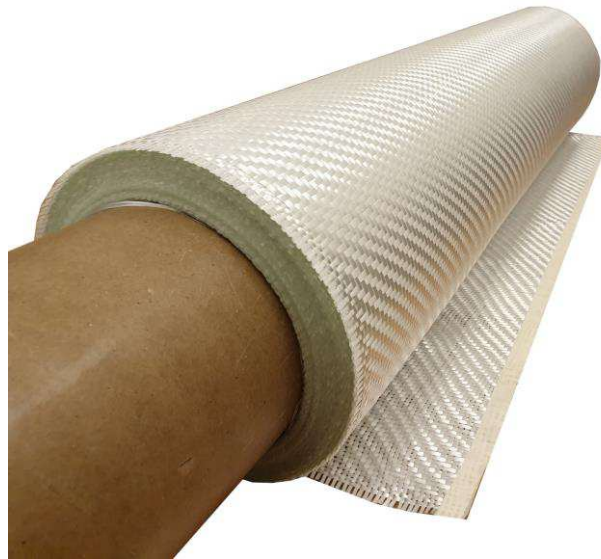


**Fig. 6** Glass roving fabric 50'' (Gividi Fabrics ST600TU 2/2 twill) based on 1200 Tex rovings with an areal weight of  $600 \text{ g/m}^2$  and thread count of 2.5/cm.

In the case of carbon fibre fabrics, the most commonly available types are 3K carbon fibre fabrics as shown in Fig. 7.



**Fig. 7** Carbon fibre fabric 50'' (ECC - Engineered Cramer Composites Style 452 2/2 twill) based on 3K - 200 Tex tows with an areal weight of  $200 \text{ g/m}^2$  and thread count of 5/cm.

## 2.2 Matrices

Virtually any polymer is suitable to be reinforced by fibres. However, specific properties make various types of polymers technologically more relevant for advanced composite applications over others. Elastomers (natural, synthetic and silicone rubbers) for instance, are not considered for constructing structural composite panels due to their extremely low rigidity. Generally, for structural applications in the aerospace and automotive sector, thermoset and thermoplastic polymers come into question. The most important factors are matrix price, price-to-performance, and overall composite material price. Since the matrix determines the required processing parameters and machinery (temperature, pressure, auxiliary equipment etc.), the part manufacturing cost is equally important. However, in certain areas ultimate lightweight performance may be favoured over more cost-effective solutions (aerospace, motorsports, professional sports equipment). In these fields the use of special matrices is nothing out of the ordinary which may include bismaleimide resins, polyimide resins, cyanate ester resins or benzoxazine resins [12]. However, the focus shall be on thermoplastics, especially homopolymers which consist of identical repeat units (monomers). Thermoplastics are inherently recyclable, non-toxic when processed, corrosion resistant, weldable and thermoformable.

Polyolefins belong to the class of standard thermoplastics. These polymers are highly non-polar and need to be modified in order to bond sufficiently to fibres [22]. Especially polypropylene (PP) is used extensively in automotive composites for various reasons. It has a melting temperature of around 165 °C, which makes processing highly economical. Moreover, PP is a very forgiving material e.g., in thermoforming, short temperature spikes over 230 °C do not degrade the material considerably. The excellent chemical resistance, together with a continuous usage temperature range of below -20 °C to 70 °C suffices for many applications [16]. PP is typically used above its glass transition temperature ( $T_g$ : -20 °C) and progressively softens as it is heated further above room temperature. Composite materials usually benefit from well bonded matrices which are in a rigid “glassy” state (below  $T_g$ ) during service. Composites subjected to bending or compression above the  $T_g$  of the matrix tend to micro-buckle, giving rise to premature failure of the material [23,41]. This is due to a fibre destabilisation effect of a softened matrix which cannot support the fibres in compression sufficiently [42]. To this end, theoretically calculated composite properties cannot be achieved with PP matrices at room temperature. Nevertheless, the cost effectiveness of PP (unmodified roughly 1 €/kg) and its versatility still make it one of the most used matrices in thermoplastic composites.

It is frequently preferred to use other thermoplastics with higher glass transition temperatures, whereby the matrices remain in a rigid state over a greater usage temperature range. Polyamide 6 (PA6) is an engineering thermoplastic with a melting temperature of 220 °C and used due to its good price-to-performance characteristics (roughly 2 €/kg). It has a  $T_g$  of around

60 °C and is suited for many demanding applications. Polyamides are inherently polar polymers and therefore do not necessarily require matrix modification as polyolefins do [24]. However, a problem that exists with PA6 is its tendency to absorb moisture from its surroundings. Unreinforced PA6 absorbs up to 10 wt% moisture [43]. This moisture absorption can be counteracted by the addition of reinforcements, whereby reinforced PA6 types show a matrix moisture uptake of 2-5 wt% depending on the fibre content [44]. Generally, moisture within the matrix acts as a plasticiser and lowers its elastic modulus [45]. As such, the problem with micro-buckling is also existent in PA6 composites [22]. Other parameters with PA6 matrices that need to be factored in are the sensitivity to oxidation at processing temperatures and an average chemical resistance. Due to these disadvantages, PA6 composites are used mainly in automotive applications rather than aerospace applications [16].

Polyphenylene sulfide (PPS) is the entry-level high-performance thermoplastic with a melting temperature of around 280 °C and a price of roughly 20 €/kg (aerospace grade). Despite its aromatic backbone it displays a  $T_g$  of only 90 °C. PPS is inherently flame retardant, exceptionally resistant to chemical attack and shows negligible moisture absorption. As such, it is frequently employed in aerospace composite structures [24,46]. Very little is known about the requirements for achieving good fibre-matrix adhesion in PPS composites since PPS is known to be very difficult to bond due to its chemical inertness.

The top-of-the-line thermoplastics are formed by the group of polyaryletherketones (PAEK) with typical prices of over 60 €/kg. Each type of PAEK differs in its melting temperature and glass transition temperature. Polyetheretherketone PEEK is possibly the best-known of the PAEK family and qualified for many structural applications in aerospace composites due to its exceptional mechanical performance, low flammability, and good chemical resistance. The main challenges with PAEK lie within the required processing temperatures of up to 380-400 °C. PEEK has a melting temperature of 343 °C and a  $T_g$  of 143 °C. In recent years polyetherketoneketone (PEKK) has attracted attention due to its slightly lower melting temperature of 337 °C and a  $T_g$  of 160 °C. However, another interesting alternative has emerged with a recently engineered low-melt PEEK copolymer by Victrex plc termed LMPAEEK [47,48]. LMPAEEK has identical mechanical properties compared to PEEK at a similar processing temperature range of PPS. LMPAEEK has a melting temperature of 305 °C and a  $T_g$  of 147 °C [47]. Unfortunately, the LMPAEEK material VICTREX AE™ 250 is currently limited to aerospace and industrial aerospace research facilities.

It is apparent that all the thermoplastics described so far were semi-crystalline types. Among advanced thermoplastic composites, amorphous thermoplastics are also represented, however, to a much lesser extent. Compared to semi-crystalline thermoplastics, amorphous thermoplastics exhibit inferior chemical and solvent resistance. The two most important candidates among amorphous thermoplastic matrices are possibly polycarbonates (PC) and polyetherimides (PEI).

PC impresses with an exceptional surface quality and high transparency at moderate cost (2-4 €/kg). Unreinforced PC is one of the toughest plastics and utilised in impact critical applications. However, these positive traits do not necessarily translate to composites, which always impart brittleness to the structure. PC has a  $T_g$  of 150 °C and is processed between 260-300 °C.

PEI is an expensive thermoplastic (over 20 €/kg) with excellent flame retardancy, low moisture absorption and moderate chemical and solvent resistance. It is used predominantly in aircraft interior composites [49]. Due to its excellent bondability it is easily painted. In certain applications this is desirable since natural PEI types have an amber colour. PEI has one of the highest glass transition temperatures of thermoplastics ( $T_g$ : 220 °C) and a processing temperature range between 320-360 °C.

The chemical structures of the mentioned thermoplastics are outlined in Fig. 8.

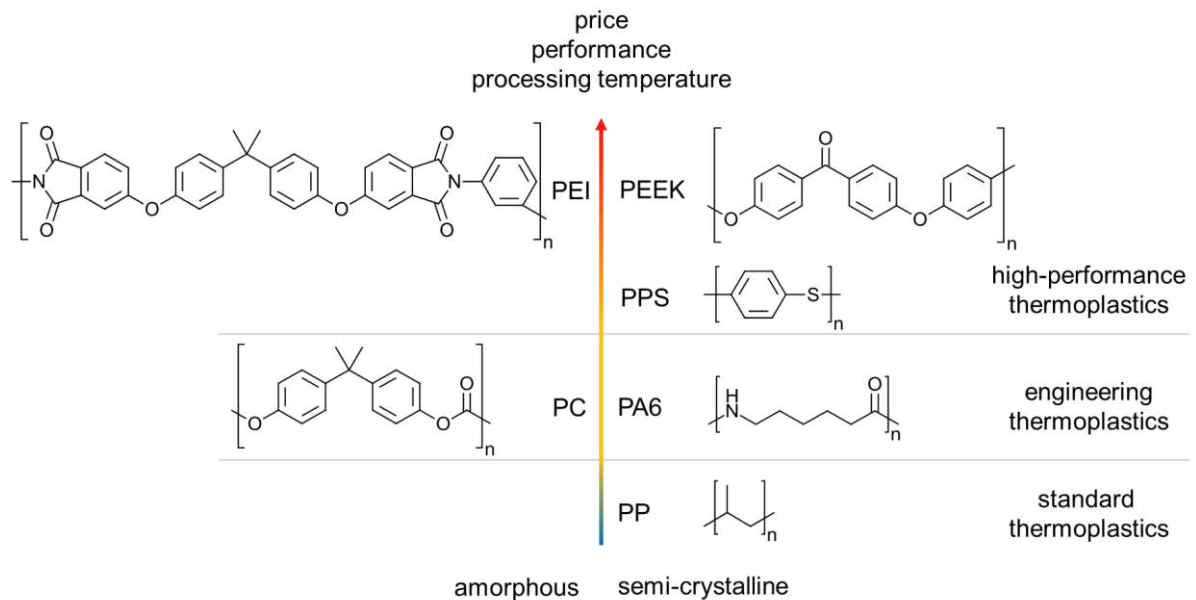


**Fig. 8** Some key thermoplastics utilised in automotive and aerospace grade composites.

### 2.3 Interfacial adhesion

The level of adhesion between the fibres and the matrix affects the macroscopic strength properties of a composite considerably, not only in the transverse fibre direction (perpendicular to the fibres) but also in the longitudinal direction (parallel to the fibres) [50]. In contrast, the elastic modulus is relatively insensitive to the level of adhesion, given that the composite is sufficiently impregnated [50].

The surface chemistries of fibres are vastly different compared to those of the organic polymer matrices. Hence, fibre surfaces require specific modification to promote interfacial compatibility with a specific matrix. Without some form of fibre surface treatment, many matrices would only loosely enclose the fibres with interfacial defects being present (entrapped

air) [51]. In such a case the fibres would not contribute much to strengthen the matrix. In order to improve interfacial adhesion, glass fibre surfaces are coated with active chemicals called adhesion promoters, while carbon fibre surfaces are activated by electrochemical oxidation [34,52–54].

Several theories have been proposed to explain how fibre surface treatments and interfacial coatings improve composite performance. However, the complex nature of interactions on the nanoscale led to no conclusive or unified adhesion theory thus far. Multiple mechanisms have been discovered and suspected to jointly contribute to the adhesion between fibres and matrices, including: adsorption and wetting [55–59], interdiffusion and entanglement [30,60,61], acid-base interactions [62–65], covalent bonding [63,66–69], radial compression at the interface due to shrinkage [70–72] mechanical interlocking and interface friction [62,70,73,74]. Some of these adhesion mechanisms are illustrated in Fig. 9.

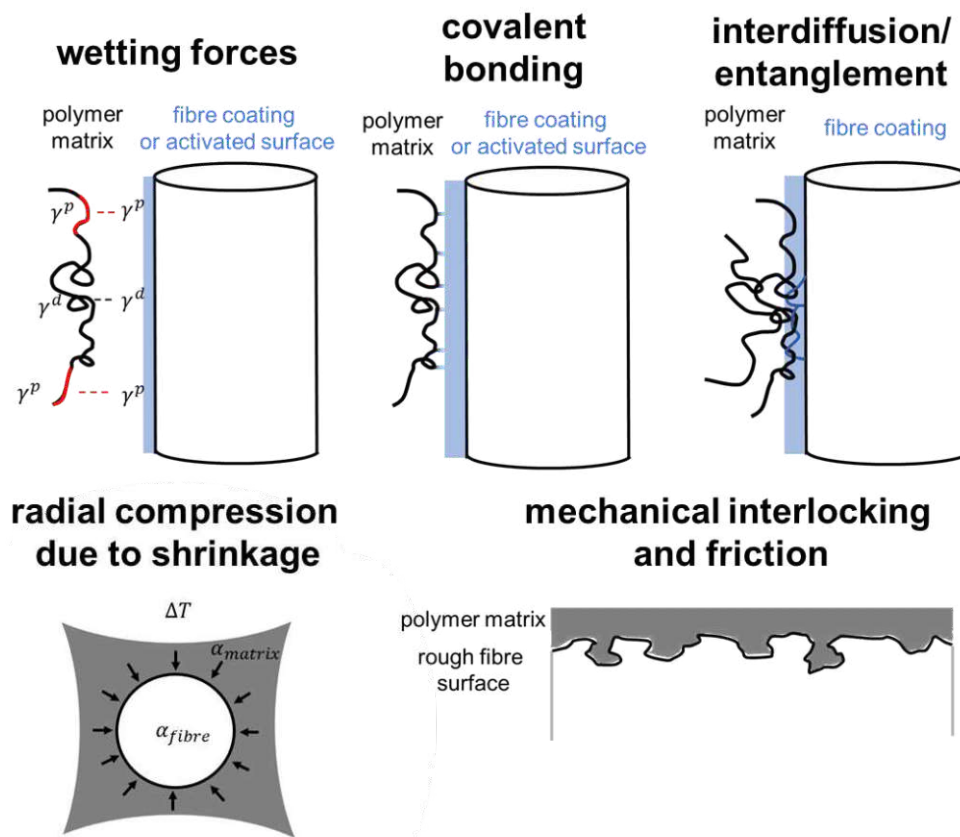


**Fig. 9** Mechanisms contributing to the overall adhesion in composites [12,30,50,75].

### 2.3.1 Wetting

Wetting plays an important role during composite manufacture and it is generally accepted that wetting forces exerted between fibres and matrices are contributing to the overall adhesion in the final composite system [59,69].

Wettability is investigated by contact angle measurement between solids and liquids. The experiments usually generate a good estimation of interfacial compatibility (physicochemical affinity via polar and dispersive interactions). A low contact angle ( $< 20\text{-}30^\circ$ ) is desirable for proper wetting and occurs when the surface free energy of the solid (given in  $\text{mJ}/\text{m}^2$  or also  $\text{mN}/\text{m}$ ) is equal or higher than the surface tension of the liquid (given in  $\text{mN}/\text{m}$ ) [63]. If this condition is fulfilled, then in composite applications a molten thermoplastic matrix should theoretically follow all imperfections of the fibre surface while displacing the trapped air [76].

In practice, wettability is determined relatively easily by depositing liquid droplets (sessile drop method) on a flat solid substrate and measuring the contact angle via optical methods. To determine the surface free energy of a solid according to the Owens, Wendt, Rabel and Kaelble method (OWRK) [77], at least two liquids with known polar ( $\gamma_p$ ) and dispersive ( $\gamma_d$ ) components are required - at least one of the liquids must have a polar component of  $> 0$ . Test liquids such as water, n-hexane or diiodomethane with known surface tensions and corresponding polar and dispersive components are used most frequently [57].

When the solid substrate has the form of fibres, contact angle measurement becomes considerably more complex and specialty equipment is required. The direct measurement of contact angles on yarns, rovings, tows or fabrics via the sessile drop method leads to erroneous results due to influences of surface texture and capillary action between adjacent fibres [78]. Therefore, it is desirable to determine the surface free energy of fibres by single fibre wetting experiments according to the Wilhelmy technique [55,70,76]. High-precision force tensiometers with micro balances and video analysis are required. The forces exerted by test liquids (typically in a region of  $0.0002\text{-}0.0010$  mN) on the wetted perimeter of the single fibre, together with the contact angle are related to the surface free energy of the fibre [78].

A direct measurement of the fibre wettability with molten thermoplastics would be ideal but is complicated by the fact that the exact surface tension of thermoplastic melts is usually unknown and very difficult to measure. Instead, in many publications the surface free energies of solid thermoplastics and fibres are evaluated separately via test liquids at room temperature and compared to each other [55]. According to Pisanova [63] and Duchoslav [79], the approach of comparing contact angle data between solid thermoplastics and fibres does not provide reliable information. This was validated by Roe, who measured the surface tension of molten thermoplastics via the pendant drop method [80]. The surface tension of thermoplastics is significantly lower in the molten state, as when extrapolated to room temperature where the thermoplastic is a solid. However, even the readings via the pendant drop method of molten thermoplastics are associated with many potential errors, being both time- and temperature dependant [57].

According to Pisanova [63] the contact angles of many molten thermoplastics on reinforcing fibres lie within a range of  $20\text{-}30^\circ$  (good wettability), since the surface free energies of surface



treated carbon fibres and coated glass fibres are generally higher than the surface tension of the molten thermoplastics. However, wetting tests refer to surface free energies only, and the fact that molten thermoplastics are extremely viscous and require several minutes to flow and reach their equilibrium contact angles [57,81] is frequently omitted. As such, an estimation of interfacial compatibility carried out solely by wetting experiments could lead to several misconceptions which may not apply to real-world conditions during thermoplastic composite processing.

To give an idea of the challenges involved in wetting fibrous reinforcements with molten thermoplastics, Cattanaach [82] gave a great example: *“To make 10 cm<sup>3</sup> of a totally wetted fibrous composite containing 50% by volume of fine (10 μm) fibres it is necessary to spread 5 cm<sup>3</sup> of resin over 2 m<sup>2</sup> of surface area. In the case of thermosets, it can be considered equivalent to spreading a sticky liqueur over the surface of a dining table but in the case of thermoplastics, the sticky liqueur is replaced by a material equivalent to chewing gum that has to be spread over the same area.”*

Summarising, it is generally accepted that good wettability of a fibre surface with a matrix is a prerequisite for intimate contact. However, wetting alone does not guarantee permanent adhesion. Other adhesion mechanisms including entanglement, interlocking, radial compression, and covalent bonding are not considered in wetting experiments. Mäder [77] concluded that fibre wetting tests can by no means be used to predict final composite properties, but are nonetheless useful to roughly estimate compatibility.

### 2.3.2 The unknowns about covalent bond formation of thermoplastic matrices

Most fibre surface modifications are designed with thermoset compatibility in mind. Many thermoset resins are initially low viscosity liquids at room temperature that are polymerised (cured) “in situ” by the addition of a hardeners or catalysts during composite manufacture. Specific functional groups present on the fibre surfaces are thought to be incorporated by covalent bonding into the thermoset networks [28,30,52,59,69,83,84]. As observed by Plueddemann, glass fibres with vinyl-functionalities which were impregnated by an unsaturated polyester (UP) resin matrix gave much higher laminate strengths when compared to laminates with different glass fibre surface functionalities. This was indirect evidence that the vinyl-functionalities must have co-reacted with the UP resin during the curing process [30].

Thermoplastics are already fully polymerised when processed (there are some exceptions such as anionic PA and liquid methyl methacrylate resins [85,86]). Apart from potential reactive end-groups, the backbone of thermoplastic homopolymers provide few, or no interaction sites for covalent bonding. Therefore, covalent bonding of thermoplastics with fibre surfaces is usually not thought to be among their prime mechanism of adhesion [34,83], unless the

thermoplastics contain reactive additives [22]. The interactions of most thermoplastics are thought to be of physical and mechanical nature (non-covalent interactions, interlocking and entanglement) [30,52,87,88]. Nevertheless, many surface treatment methods which tend to work well for bonding thermosets do also work with thermoplastics [30]. Multiple studies therefore suggest that covalent bonding is involved in some form in the fibre-matrix adhesion of thermoplastics [89–91]. Other scientific work has proposed that dispersive interactions only would suffice to exceed the cohesive strengths of many matrices if the reinforcement is wetted fully [30,59,69,84]. It remains difficult to resolve the question about covalent bond formation because of the ambiguity in the experimental evidence [92].

Despite many contradictions found in literature regarding fibre-matrix adhesion mechanisms of thermoplastics, one cannot ignore the fact that well-engineered thermoplastic composites (especially with high-temperature thermoplastics) are able to display mechanical properties on the level, or even beyond high-performance thermoset composites [24,25,93]. Naturally, this raises the question whether non-covalent interactions from wetting could compensate covalent bonding. Viewed from a nanometre perspective, this consideration is unsatisfactory when taking into account typical bond strength values given in Table 2. A thermoplastic matrix which is supposedly adhered only non-covalently to a fibre should give much lower composite mechanical properties compared to a covalently bonded thermoset matrix. But this is not what is observed in practice when testing the materials [22,24,25,93].

**Table 2** Bond energy comparison [94,95]

Interaction type	Bond strengths [kJ/mol]
Covalent bond	~300-800
Hydrogen bond	~10-40
Dipole-dipole forces	~10
van der Waals forces	~1-4

By judging typical bond strengths only, other micro- and macromechanical effects are not considered such as interlocking, friction, polymer entanglement and radial compression due to shrinkage, which altogether may contribute largely to the overall composite properties.

### 2.3.3 Methods to distinguish good interfacial adhesion from poor interfacial adhesion

The exact level of adhesion is difficult to quantify in a composite material. However, two approaches can be taken to establish the general quality of interfacial adhesion.

- Direct methods: include the manipulation of individual fibres embedded in a matrix, or fibres covered with a droplet of matrix. Micromechanical single fibre tests include single fibre pull-out, fragmentation, microbond or indentation and lend themselves for an assessment of the interfacial shear strength (IFSS) [12,50]. IFSS reflects the load transfer efficiency between the fibre and the matrix and is sensitive to changes in fibre-matrix adhesion [12,50,96]. Unfortunately, single fibre tests show considerable data scatter, rely extraordinarily on specimen preparation and correct microscopic measurement of the fibre diameters and embedded lengths [50]. While the obtained data often provides valuable information on fibre-matrix adhesion, it is not possible to relate the measured IFSS to macroscopic composite properties [50]. Moreover, single fibre tests and specimen preparation techniques are not standardised. Single fibre tests have been employed most frequently in academic research and have failed to spark industrial interest thus far [97].
- Indirect methods: are based on testing interface-sensitive properties of macroscopic composite samples which include compression, flexural or shear properties [12]. Vice versa, the obtained test results cannot be used to predict the IFSS and are purely qualitative for ranking fibre-matrix adhesion between different sets of samples. Special care must be taken in order to preserve continuity between the sets of samples (same processing conditions and sample geometries). ASTM- and ISO-standards are available for these test methods which specify test specimen geometries and testing conditions.

A practice-oriented approach for composite material development may be followed by selecting any of the indirect test methods, accompanied by fracture analysis and fractography [12,87]. In industrial practice indirect methods are generally favoured over direct methods for both carbon fibre [98] and glass fibre [99–101] thermoplastic composite material development. A common approach taken, is by modifying fibres or matrices, followed by compounding, injection moulding into test specimens and subsequent mechanical testing [99–101]. Higher tensile or flexural strengths of these short fibre composites are indicative of better fibre-matrix compatibility and adhesion [102]. Thus, the effectivity of fibre surface treatments or adaptations in coating formulations can be assessed relatively conveniently.

Similar rules apply to continuous fibre-reinforced laminates. Composite laminates with poor fibre-matrix adhesion are identified by very low laminate strengths and interfacial debonding. Interfacial debonding manifests itself in clean fibre surfaces where the matrix has been cleanly peeled away from. Likewise, a high amount of fibre pull-out, which leaves behind clean matrix channels indicates poor adhesion in continuous fibre-reinforced composites [24]. Composites with good fibre-matrix adhesion are characterised by high laminate strengths, sudden brittle failure, and adherent matrix residues on fractured fibres as outlined in Fig.10. Ideally, the entire surfaces of the fibres are covered in matrix residues indicating that the adhesive strength at the interface or within the interphase exceeded the cohesive strength of the matrix [28,30]. In

general, it is advisable to inspect  $90^\circ$  fracture surfaces (areas which have failed in transverse tension), since the transverse properties are extremely sensitive to interfacial adhesion [12,87]. This approach is also applicable to laminates with bidirectional (woven) reinforcements which have been fractured in flexural or tensile tests [12].

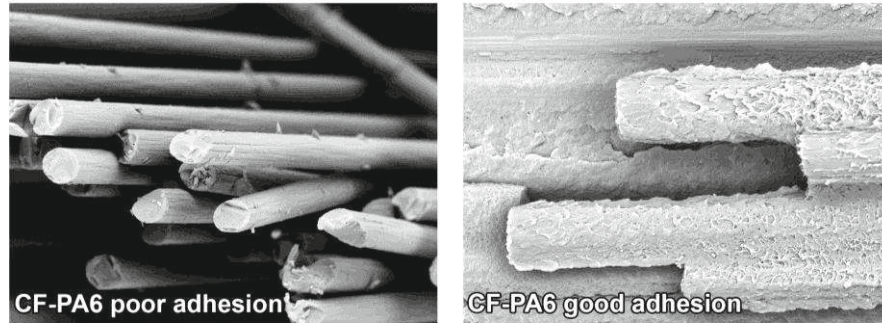


**Fig. 10** Comparison between poor and good adhesion in CF composite samples. Interfacial debonding (left): bare fibres. Cohesive matrix failure and straight fibre fracture surfaces (right): fibres are completely covered by adherent matrix (adapted from [25]).

Some fractured samples may exhibit areas of mixed adhesion quality, where some fibres appear well bonded, while others appear poorly bonded. In such a case, it is difficult to assess the adhesion quality purely from the fractographic analysis. The corresponding mechanical properties and specimen failure mechanisms should give a deeper understanding of possible problems during material production (e.g., inadequate processing conditions, incomplete wet-out, a partly incompatible fibre coating, problems with moisture, inhomogeneous compounding of reactive polymer additives, or possible contaminants).

The 3-point flexural test is a sound method to evaluate the quality of interfacial adhesion in a practice-oriented way [56]. If sets of samples are prepared equally (high degree of impregnation, processing- and conditioning history), those with poor adhesion will fail due to micro-buckling on the compression side. While some argue that the interpretation of flexural test trends in terms of microscale adhesion is a step too far, Kiss et al. found evidence that the phenomenon of micro-buckling in the longitudinal fibre direction is clearly linked to fibre-matrix adhesion effects of tested specimens (**Publication III**) [24]. Micro-buckled regions are often detectable by the naked eye or under a microscope. The effect of micro-buckling in polymer composites tested below  $T_g$  arises due to premature debonding mechanisms or micro-cracking and an associated loss of lateral support of the fibres by the matrix. In poorly bonded fibre-matrix combinations the fibres undergo buckling in groups when compressed beyond a relatively low load threshold as shown in Fig. 11. Micro-buckling frequently propagates along the laminate surface (away from the loading nose) or surface near plies until the entire composite specimen fails in compression. Flexural test specimens with good interfacial adhesion, on the other hand, will fail in a combined compression-tension mode, where the severity of micro-buckled regions is indicative of the quality of adhesion [24]. Flexural test

specimens with very high adhesion are characterised by fracture on the tension side only and catastrophic brittle (explosive) failure. Failure on the tension side only is relatively rare in glass fibre-reinforced composites and more common in carbon fibre composites [24,25]. An overly brittle composite displays high static strength but also a high susceptibility to delamination from impacts. For specific applications, some material combinations require a balance of properties and a certain control of interfaces/interphases.

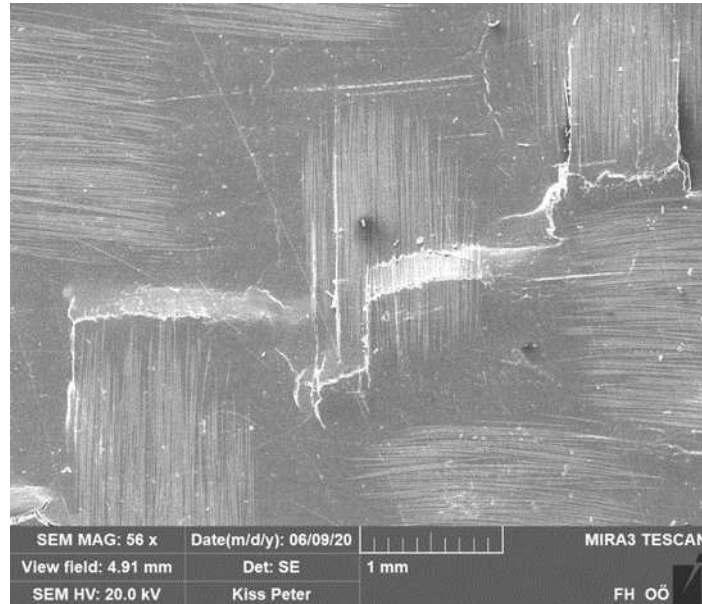


**Fig. 11** Top-view of failed glass fibre TPCL specimen due to micro-buckling on the compression side during a 3-point flexural test (failure in longitudinal fibre direction).

Compression tests would lend themselves equally well (or even better) for an assessment of fibre-matrix adhesion related effects. However, there is a limitation with many TPCL of bonding grip tabs and strain gauges to specimens that are both required for correct load introduction and strain reading, respectively. End-loading of specimens requires extreme parallelism of the prepared samples to avoid localised end-load crushing. Another way of load introduction may be realised by means of hydraulic clamping fixtures via shear-load. However, here there a risk of lateral crushing due to extremely high clamping forces.

Irrespective of the fibres and matrices used, interfacial adhesion and associated characterisation methods are a very controversial topic as demonstrated by the literature review so far. It is outside the scope of this work to present every single adhesion theory in much greater detail. Instead, the idea is rather to give an understanding of the way in which glass fibre manufacturers, glass fabric weavers and carbon fibre manufacturers treat their materials in order to facilitate fibre-matrix adhesion in the following section.

## 3 Fibre sizings - “the secret sauce”

Nearly all types of man-made fibres are coated with a chemical surface treatment formulation during their manufacture. These thin interfacial coatings are referred to as a fibre “size” or “sizing” in the art [34]. Sizings are responsible for protecting the fibres from abrasion and breakage during handling operations while assuring good strand integrity. In the case of glass fibres, adhesion promoters are required to maximise the reinforcing effect of the fibres in a composite. The formulation of glass fibre sizings is therefore very complex and inherently different to carbon fibre sizings, as will be explained.

### 3.1 Glass fibre sizing and finishing technology

As mentioned previously, molten glass is pulled from bushings into thin fibres at very high speeds of over 20 m/s and immediately sprayed by a fine mist of water [33]. Before the individual fibres are gathered into a strand, a water-based organic sizing is applied by a kiss-roll applicator. Once the fibres have passed the applicator roll and picked up the sizing, they are wound into so called forming packages (cakes, spools or bobbins) and subsequently dried in ovens to drive off residual water [34,40]. The processing speeds involved during glass fibre melt drawing place enormous demands on the formulations of sizings. Ideally, the fibres are coated uniformly by the sizing at the given processing speeds to guarantee optimal protection and performance of the product. However, effects such as sizing sling-off due to the processing speeds and associated centrifugal forces, or sizing migration during drying can affect the performance of a product negatively [33]. The exact formulations of sizings are highly proprietary since the effectiveness of the sizing in processability or adhesion promotion is the main factor which differentiates the products of competing glass fibre manufacturers.

The sizing composition generally depends on whether glass filaments are gathered into a yarn or roving as schematically depicted in Fig 12. As such, glass fibre sizings may be divided into two main categories - textile sizings for yarn and direct sizings for roving. Glass fibre finishes represent a third important type of fibre coating and are applied only to woven yarn products in a multi-stage treatment process. In the following section, these three types of glass fibre coatings shall be explained in more detail. For scientific investigations it is of importance to know which type of coating had been applied to the fibres.

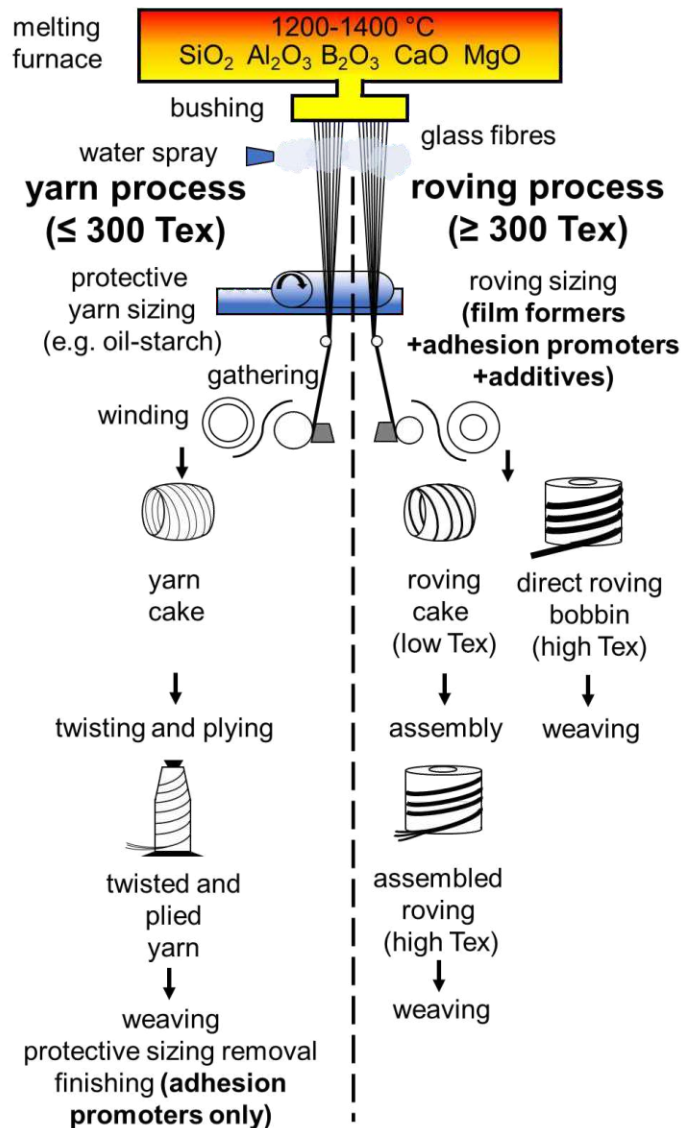


**Fig. 12** E-Glass fibre yarn and roving manufacturing process (adapted from [33,34,103]). Note that either yarn or roving is produced depending on the configuration of the melting furnace and design of the bushings (diameter and number of orifices).

### 3.1.1 Textile sizings and finishes for glass fibre yarns

- Textile sizings for yarns: These sizings are applied to yarns immediately after fibre formation and are considered as temporary coatings. Textile sizings serve the sole purpose of protecting the glass yarns from abrasion during subsequent textile operations (twisting, plying, weaving) and require removal thereafter, followed by finishing [33]. Generally, textile sizings are based on aqueous starch-oil and/or polyvinyl alcohol (PVA) mixtures, which lubricate the yarns and are well suitable for subsequent heat cleaning.

As outlined in Fig. 13, the warp yarns must go through additional preparation steps before they are ready to be woven into fabrics. Depending on the fabric style and width, the desired number of warp yarns are pulled from a creel and wound in parallel onto a beam by the weaver (this

process is called warping or beaming). If the creel holds fewer yarns than are required for weaving, then multiple section beams will be made. Subsequently, the warp yarns are coated in a slasher with a secondary sizing which is also based on an aqueous starch-oil and/or PVA formulation for additional protection (the application of a secondary warp size is called slashing) [40,104,105]. The slashed warp yarns are wound onto a single loom beam and fed into the loom. The weft yarns, on the other hand, do not require to be slashed since they do not have to withstand the abrasive forces which are encountered by the warp yarns from the moving parts of the loom [40]. After high-speed weaving, the yarn fabrics are in the so called “loomstate”. At this point, the textile sizing is still present on the fibres and would strongly inhibit subsequent matrix bonding in structural composites. Therefore, the textile sizing must be completely removed from the loomstate fabrics. This is realised most frequently by thermal treatment (heat cleaning/desizing) at up to 350-400 °C in large batch ovens [12,22]. The heat cleaned glass yarn fabrics turn from brown (caramelized) to white and undergo a final coating process called “finishing” in order to functionalise the glass fibre surface.

- Finishes for yarn fabrics: A “finish” is applied exclusively to heat cleaned glass yarn fabrics by the weaver. The heat cleaned yarn fabrics are fully immersed in a finish bath which contains an aqueous dilution of chemically pure adhesion promoters or blends thereof [12]. After drying, the finish is responsible for facilitating adhesion between the glass yarn fabric and specific polymer matrices. Finishes are typically applied at 0.1-0.2 wt% by weight of the glass. Technically, a finish is not to be confused with a sizing.

### Yarn fabric finishing process

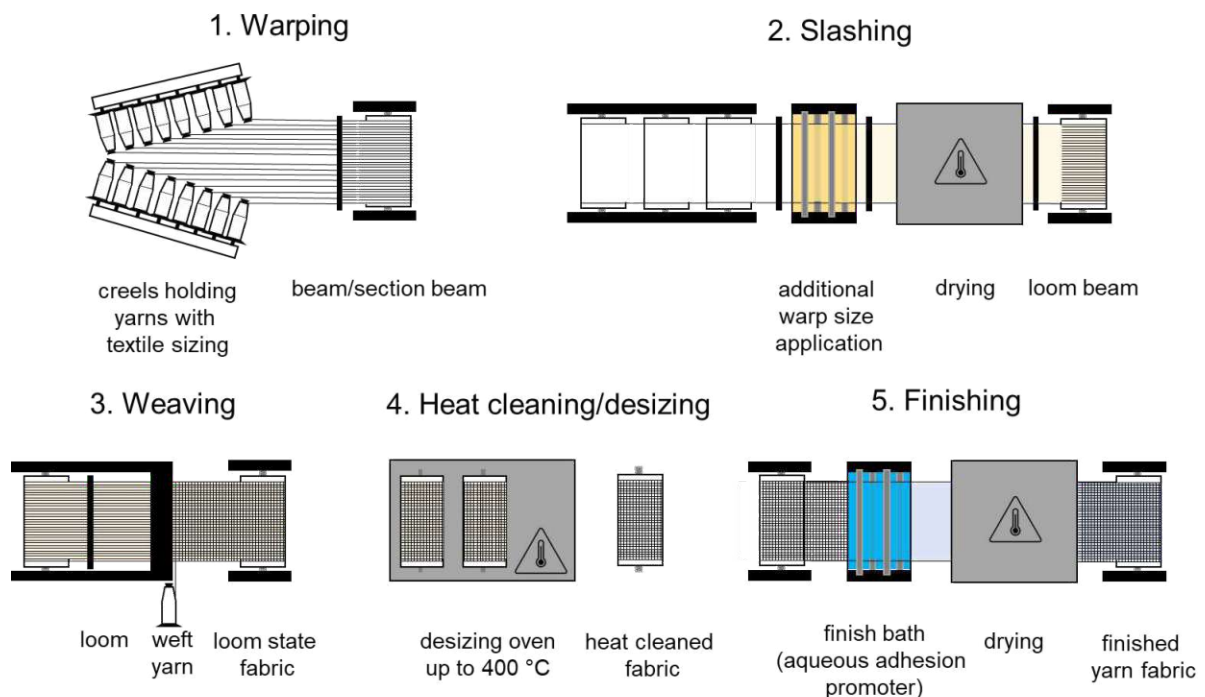


**Fig. 13** Processing scheme (top view) for the production of finished glass yarn fabrics including warping, slashing, weaving, heat cleaning and finishing (adapted from [106]).



### 3.1.2 Direct sizings for glass fibre rovings

- Direct sizings for rovings: Direct sizings are mainly applied to rovings during melt drawing by the glass fibre manufacturer and are permanent coatings (no sizing removal is required). These sizings are an “all-in-one formulation” made up of ingredients including polymeric film formers, silane adhesion promoters, surfactants, antistatics, lubricants and many more. Depending on their formulation, direct sizings are compatible with specific matrices and constitute a compromise between processability and adhesion performance. Depending on the application (weaving, chopping, pultrusion etc.), direct sizings are applied at specific amounts in a range of 0.5-2.0 wt% by weight of the glass [33]. Direct rovings or assembled rovings can be used immediately for reinforcement or weaving after their production as shown in Fig. 14 and are therefore highly economical products.

Weaving rovings is less labour intensive compared to weaving yarns since the thick strands are directly fed from creels into a loom. No construction of a loom beam is required. Due to the slower weaving process and higher sizing content, rovings are also experiencing less mechanical friction compared to yarns. Therefore, a secondary sizing for warp protection is not required. Since the overall weaving of rovings is a less laborious process, woven roving is significantly lower cost compared to finished yarn fabrics.

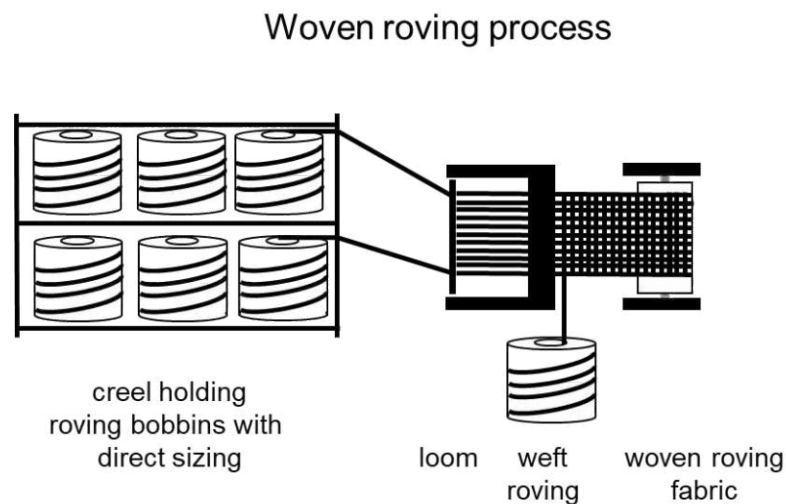


**Fig. 14** Processing scheme for producing woven glass roving fabrics.

Fig. 15 shall point out the general difference between a heat cleaned glass yarn sample (before finishing) and a silane finished glass yarn sample. It is identifiable that the heat cleaned glass fibres are extremely smooth on the microscale, whereas the silane finished fibres have a somewhat striated appearance of the coating. These rough looking channels originate from areas where adjacent fibres were in contact and the finish accumulated, most possibly due to capillary action during drying. Apart from these accumulations which are obviously composed of pure adhesion promoter, the rest of the glass surface should theoretically also be covered in

a thin silane film. The thickness of this silane film could be in the order of a few tens of nanometres. However, this is not deducible from the images. Since finishes usually do not contain surfactants it is also possible that certain areas of the fibre surface are only covered partially by the adhesion promoter [60].

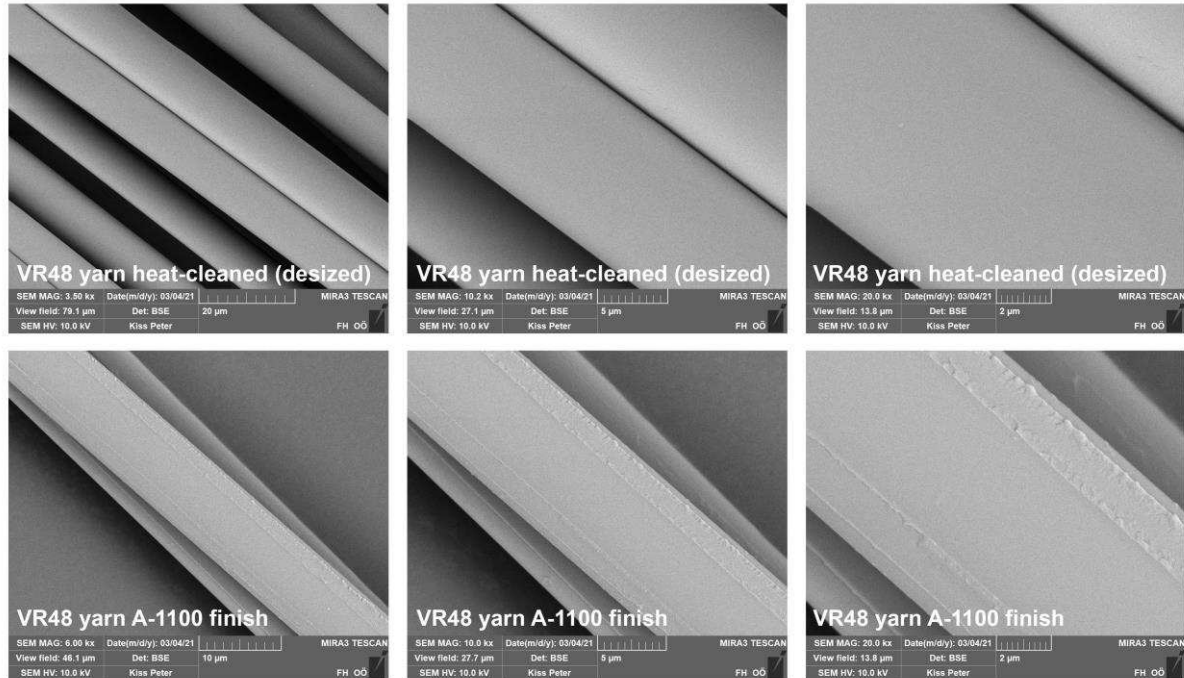


**Fig. 15** Glass fibre surface of heat-cleaned glass yarn (top) and A-1100 aminosilane finished glass yarn (bottom). Both samples were derived from woven fabrics.

In comparison, the surface morphology of a PP-compatible direct sized glass roving is presented in Fig. 16. It can be immediately seen that the amount of coating applied is much greater compared to a finish. The coating also appears to be distributed non-uniformly across the surface, despite the assumption that surfactants were utilised in the sizing. Sizing accumulation between neighbouring fibres is also visible in this direct sized sample.

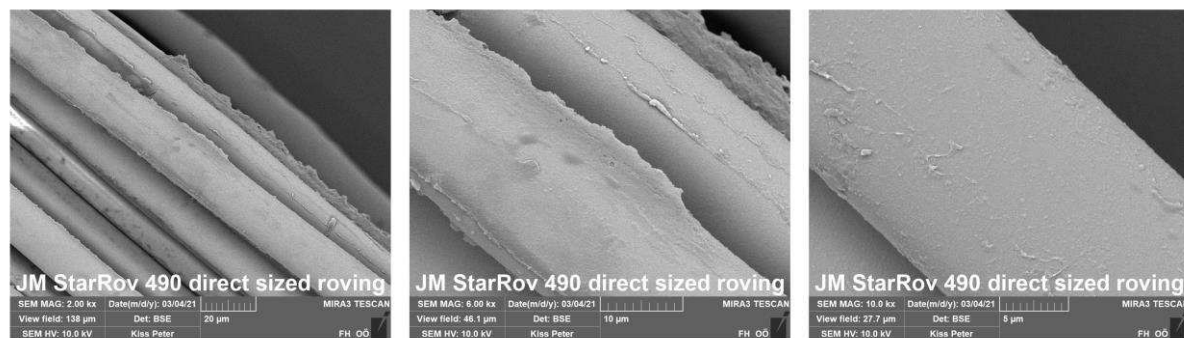


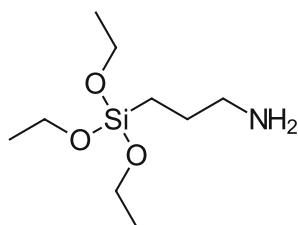
**Fig. 16** Surface of direct sized PP-compatible roving. Sample was derived from a bobbin.

The observed partial coverage of the glass fibre surfaces indicates that industrial finishes and sizings still have some room for improvement in coating uniformity. However, capillary effects are difficult to overcome in closely packed fibre bundles.

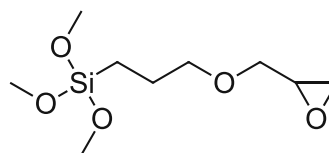
### 3.1.3 Glass fibre adhesion promoters

According to Thomason [33] many glass fibre coatings were developed essentially by a trial and error approach. Certain substances were found to bond matrices to the glass fibres exceptionally well. Even though the fundamental science of how the substances interact with matrices is still not fully understood today [33], these so called adhesion promoters are the most important ingredient in both glass roving sizings and glass yarn fabric finishes. These substances are of such high importance for adhesion, that in practice, glass fibre coatings are never formulated without adhesion promoters for structural composite applications.

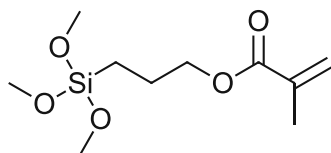
As their name suggests, adhesion promoters constitute a chemical or physical link between two incompatible materials, such as the inorganic glass fibre and the organic matrix [107]. The most widely used group of adhesion promoters are organosilanes. In Fig. 17 some common adhesion promoters are depicted, alongside a “non-silane” adhesion promoter termed Volan<sup>®</sup> A.



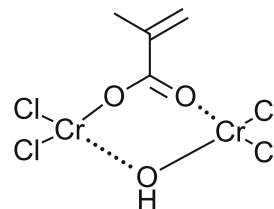
(3-Aminopropyl)triethoxysilane (A-1100)



(3-Glycidoxypropyl)trimethoxysilane (Z-6040)



(3-Methacryloxypropyl)trimethoxysilane (Z-6030)



Cr(III)-methacrylate (Volan A)

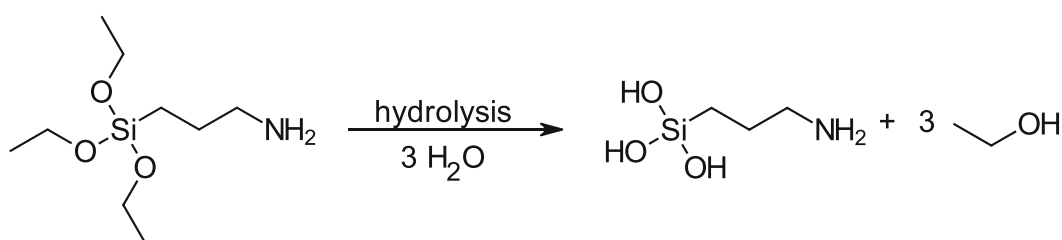
**Fig. 17** Adhesion promoters for glass fibres (adapted from [12,28,29,108,109]).

The very first glass fibre adhesion promoter Volan A was developed by DuPont in the 1950s [12,30,109]. It is a complex of two trivalent chromium compounds linked by coordinate valences and a methacrylic group [109]. While there are other non-silane adhesion promoters including titanates, aluminates and zirconates [29,30], Volan A is the only non-silane adhesion promoter to have reached commercial importance [30]. Due to its aerospace certification it is still used today in aviation as a standard finish for glass yarn fabrics [110] and currently produced by Zaclon LLC. Volan A is easily identified by the blueish-green tint imparted to clear resin laminates [30].

Ongoing development in adhesion promoter chemistry introduced the group of organosilanes. Organosilanes, more precisely trialkoxysilanes, have in common that they possess a central silicon atom with three hydrolysable methoxy or ethoxy substituents and a fourth

organofunctional substituent [107]. The chemical functionalities may include amino, epoxy, methacrylic, vinyl, thiol and many more. Depending on the functional group, structure of the silane, concentration, or blends of different silanes, a certain affinity to a polymeric matrix or matrices (multi-compatibility) is generated.

The characteristic feature of these adhesion promoters (trialkoxysilanes and Volan A) is that they can be hydrolysed in aqueous solution as can be seen in Fig.18. Under the right conditions (pH range 3-6), trialkoxysilanes are converted by acid catalysed hydrolysis into silanols within several minutes [30]. The silanols condense into siloxanes and are deposited on the glass fibre surface. The glass fibre surface is thought to be composed mostly of hydroxyl groups which potentially interact with the siloxanes during drying by covalent bonding or hydrogen bonding [28,30,109]. Moreover, several metal ions or metal hydroxides contained in the glass composition could also play a role in binding specific adhesion promoters [111,112]. Some trialkoxysilanes have ethoxy substituents, while others are methoxy based. Methoxy groups hydrolyse at a faster rate compared to ethoxy groups (more hydrophobic) [30,113]. This effect can be exploited during coating preparation to have a certain control over the rate of self-condensation.



(3-Aminopropyl)triethoxysilane (A-1100)

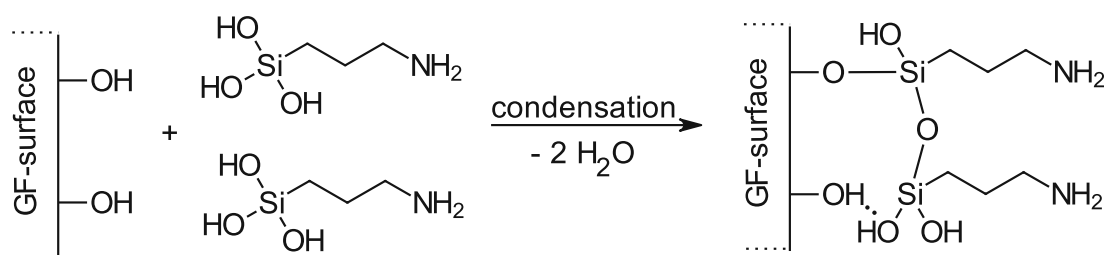


**Fig. 18** Proposed mechanism of glass fibre surface silanization. An aqueous solution of silane is prepared. The silanes undergo hydrolysis to form silanols, which in turn polymerise into siloxanes and subsequently condense with the glass fibre surface upon drying (adapted from [12,28,29,108]).

The hydrolysis of Volan A, shown in Fig. 19 is almost analogous to silane hydrolysis. Chromium chloride is partly hydrolysed in aqueous solution under the formation of hydrochloric acid. The solution needs to be neutralised to a pH of 6 in order to displace more of the chloride by hydroxyl groups [109]. Subsequently, the chromium complexes begin the process of olation (self-condensation) and condensation with the glass fibre surface [109].

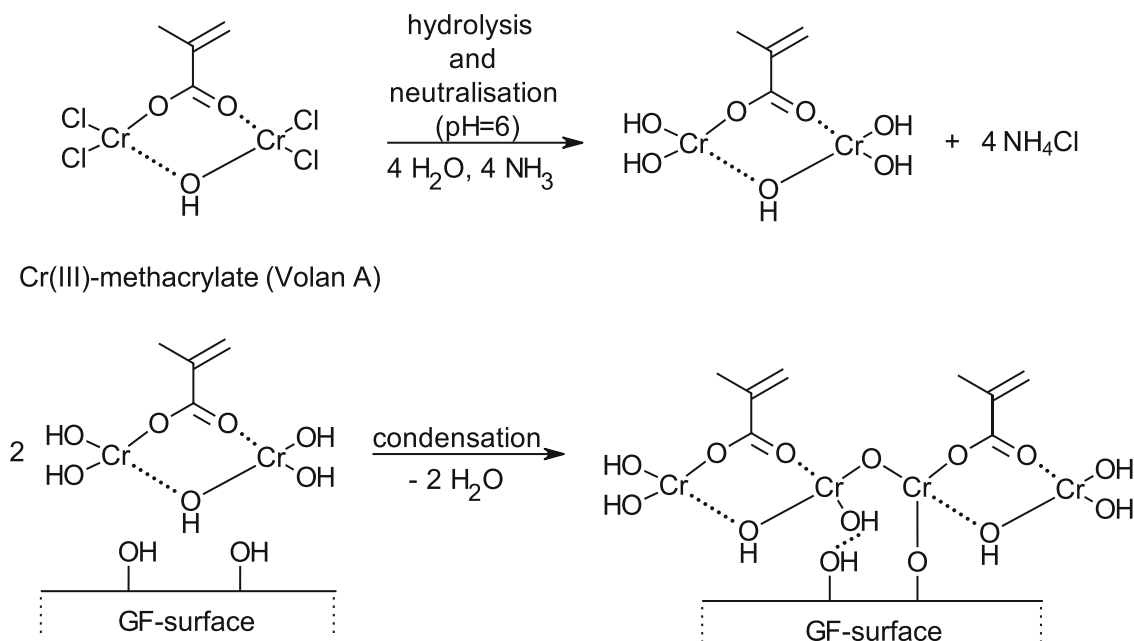


**Fig. 19** Hydrolysis and condensation of the glass fibre adhesion promoter Volan A (adapted from [22,28,109]).

Despite the fact that Volan A is the oldest adhesion promoter for glass fibres, it seems that it has been rarely tested in combination with thermoplastics. Only recently, have Kiss et al. (**Publication I and III**) reported exceptional compatibility of Volan A with polypropylene, polyamide and polyphenylene sulfide [22,24]. Due to its excellent high-temperature resistance it is also thought to function as an excellent adhesion promoter for other high-temperature thermoplastics including polyetherimide [114] and possibly polyetheretherketone.

It should be mentioned that the reactions shown so far represent an oversimplification of the actual situation. Undoubtedly, adhesion promoters do not create a perfect monolayer on the fibre surface. It is more likely that multi-layered networks are formed [30,111,115] as depicted in Fig. 20. Closest to the fibre a strongly chemisorbed crosslinked silane layer is suspected, followed by a loosely chemisorbed layer and a non-crosslinked physisorbed layer composed of silane oligomers [112]. The situation becomes even more complex with direct sizings, where several sizing ingredients potentially interact with the adhesion promoter networks.

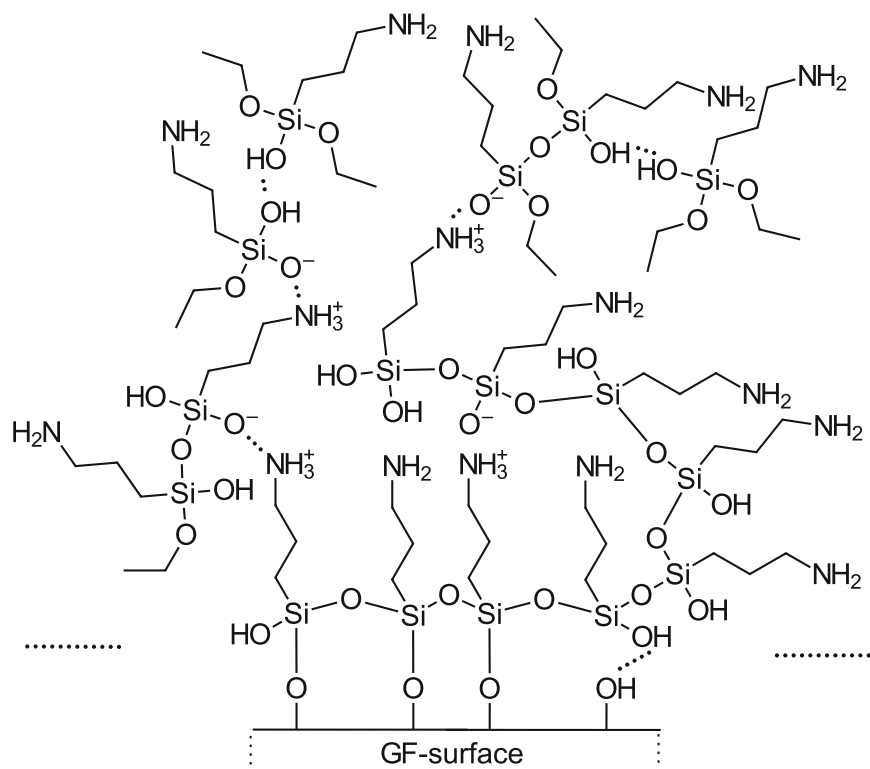


**Fig. 20** Aminosilane network formed on glass fibre surface by protonated aminogroups, hydrogen bonding and covalent interactions (adapted from [92,111,112]).

### 3.1.4 Polymeric film formers in glass fibre direct sizings

Polymeric film formers are not contained in glass fibre finishes but are essentially the main ingredient of direct sizings and constitute up to 60-90 wt% of the sizing's dry solids. A film former is chemically similar, identical or miscible with the intended matrix resin and composed of low- or high molecular weight polymers (or copolymers) based on polyurethanes, polyvinylpyrrolidones, polyesters, modified polyolefins, epoxy resins, polyetherimides, polyimides, polyetherketones and so on [33,116,117]. Since these polymers are often insoluble in water, many film formers require a significant amount of surfactant to be added in order to be dispersed or emulsified in water [33]. Examples of suitable surfactants for use in film former emulsification or dispersion include, but are not limited to, sodium dodecyl sulfate, benzalkonium chloride, octoxinol 9 (Triton<sup>®</sup> X-100) or ethylene oxide/propylene oxide copolymers (poloxameres also known as Pulronic<sup>®</sup>), which constitute up to 10-20 wt% of sizing dry solids [118,119]. The resultant particle size of many film formers is frequently within a region of 100-900 nm [118,120].

The film former plays a decisive role in protecting the fibres from abrasion and keeping them in a cohesive strand prior to composite processing [116,121]. Since the film former creates a “new interface” that differs from the original fibre surface, compatibility and wet-out are also largely determined by the chemistry of the film former [120]. Due to matrix miscibility, the film former also promotes the separation of fibres when in contact with the matrix polymer

[34]. If the chosen film former is incompatible with the later matrix material, there can be a severe performance knock-down, up to the point where the resulting material is essentially unusable for any application [22,25].

Even though the contained silane adhesion promoters in a direct sizing have affinities for certain polymers, so do the film formers. From this circumstance it can be deduced that a direct sizing must be formulated very meticulously, otherwise the formula could be incompatible with itself. To this end, the silanes, film formers and final matrix polymer need to complement each other for optimal performance. As mentioned, film formers are often well miscible or partly miscible with the matrix. The diffusion of film former and loosely bound silane layers into the matrix and vice versa is a commonly reported phenomenon, forming the interphase as shown in Fig. 21 [92,116,122]. These complex network structures are frequently termed semi-interpenetrating networks (IPN). IPN formation is thought to contribute greatly to the overall mechanical properties in thermoplastic composites [30].

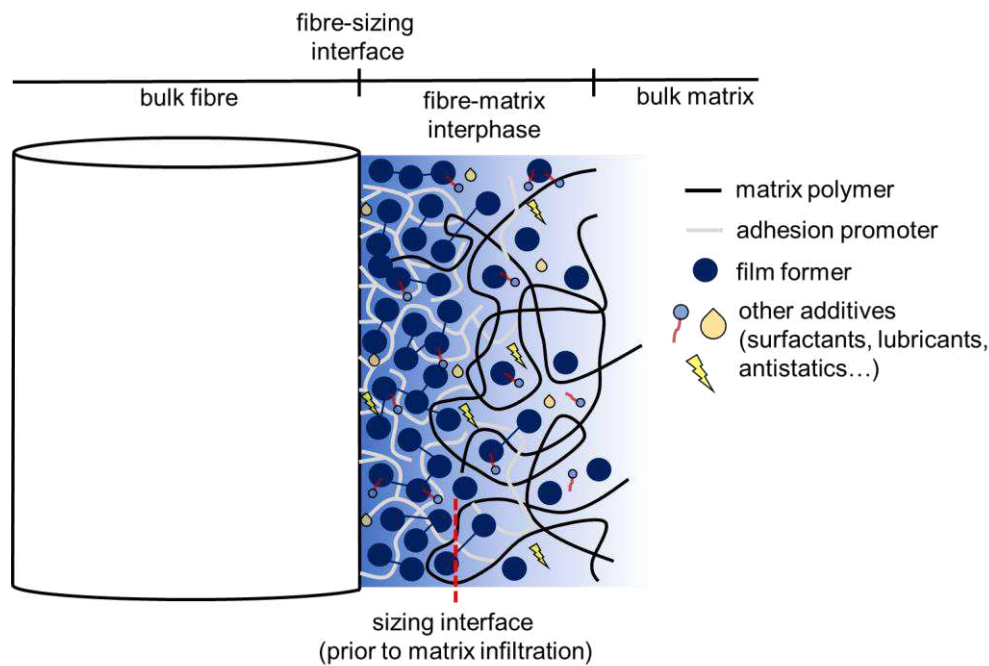


**Fig. 21** Scheme of an interpenetrating network (IPN) formed between a glass fibre direct sizing and a polymer matrix. The adhesion promoter (silane) is deposited closest to the glass surface. Note, the scheme is not to scale (adapted from [29]).

Epoxy-based film formers are the most used film formers in the industry for epoxy resin-compatible sizings or multi-compatible thermoset sizings [33]. Film formers based on polyurethanes (aliphatic, cross-linked, blocked [123]) are very versatile and give compatibility to both thermosets as well as to many thermoplastics (especially polyamides). According to a patent by glass fibre manufacturer Johns Manville, the film former does not enhance the mechanical performance of fibre-reinforced products [121]. Unlike silanes, there is no clear proof that film formers are chemically bound to the fibre surface. Nonetheless, there is a special class of film formers called reactive film formers. Blocked polyurethanes have blocked

isocyanate groups which will undergo deblocking when exposed to a specific temperature [60]. The formed isocyanates possibly interact with silanes and matrices covalently. In reactive film former formulations care must be taken that the film former does not “consume” all of the reactive sites of the adhesion promoter. For polypropylene applications, the use of polyurethane film formers and maleic anhydride grafted polypropylene (MAH-g-PP) film formers is common [33]. MAH-g-PP is also a reactive film former type that can potentially react with aminosilanes as outlined in Fig. 22. As found by Kiss et al. (**Publication I**) the amount of deposited MAH-g-PP within a PP-compatible direct sizing does not suffice to promote adequate adhesion in GF-PP laminates [22]. The use of additional MAH-g-PP blended into the PP-matrix is required.

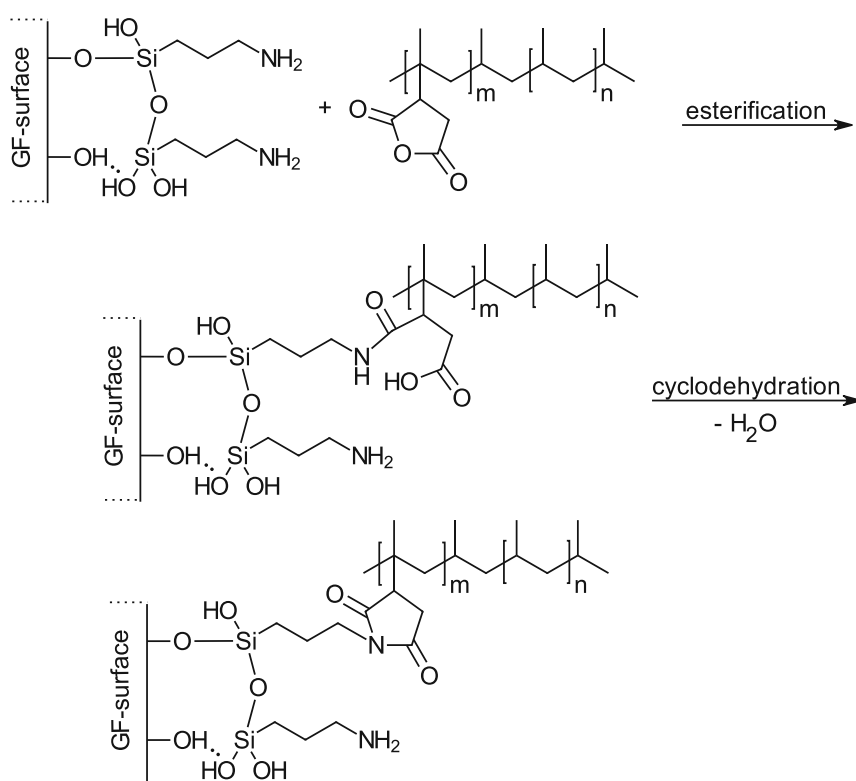


**Fig. 22** Possible interaction of silanized GF-surface with reactive film former type (MAH-g-PP) for PP compatibilization (adapted from [108]).

### 3.1.5 Auxiliary agents in glass fibre direct sizings

- Non-ionic lubricants: are “external” lubricants and convey lubricity to the entire fibre strand during handling and processing. In a preferred embodiment, non-ionic lubricants are stearyl ethanolamides (Lubesize K-12), waxes, polyethylene glycols (PEG 200, PEG 400, PEG 600) or fatty acid esters thereof [33,119]. PEG laurates, oleates or stearates may also simultaneously be used as surfactants.
- Cationic lubricants: adsorb to the glass fibre surface and are therefore “internal” lubricants [33]. They protect the fibres from interfilamentary abrasion (fibre-fibre abrasion). Due to their affinity to adsorb to the fibre surface, cationic lubricants compete with silane adhesion promoters. Hence, cationic lubricants are added in low amounts to



the sizing composition. Candidates for cationic lubricants are for instance polyethyleneimine polyamide salts (KATAX<sup>®</sup> 6760L) [119]. Cationic lubricants may also fulfil the simultaneous role of an antistatic since charge build up can be reduced by internal lubricity.

- Antistatic agents: are quaternary ammonium compounds, such as tetraethylammonium chloride that are soluble in a sizing (EMERSTAT or LAROSTAT) [119]. Antistatics reduce the fibres from generating electrostatic potential when handled.
- pH adjuster: the pH of the sizing is adjusted by means of acids or bases to hydrolyse the silane adhesion promoters efficiently. Typical acids are acetic-, formic-, phosphoric-, boric- or citric acid. Typical bases are ammonia or sodium hydroxide [33].
- Fungicides and bactericides: are agents which inhibit microbial growth in the organic sizing [121].
- Defoaming agents: to reduce or hinder the formation of foam, for example by the addition of polydimethylsiloxane derivatives.

A generic composition of a glass fibre direct sizing is listed in Table 3. The majority of glass fibre direct sizings are composed of these ingredients in varying amounts.

**Table 3** Generic composition of a water-based glass roving direct sizing [33,119].

Sizing component	Sizing dry solids [wt%]	Role of the component
Film formers	60-90	fibre protection, compatibility, control wet-out
Silane adhesion promoters	10-15	compatibility, fibre-matrix adhesion
Surfactants	10-20	dispersion of film former and other water insoluble ingredients
Non-ionic lubricants	5-20	fibre protection
Cationic lubricants	< 1	reduction of fibre-fibre friction, antistatic
Antistatic agents	< 0.5	reduction of static charge build up
pH adjusters	0.5-3	hydrolysis of silane
Defoaming agents	0.1	reduction of foam during sizing application
Fungicides and bactericides	ppm range	inhibit microbial growth
Distilled water	-	carrier medium, dilution to desired concentration

### 3.1.6 Glass fibre direct sizings vs finishes

Since the exact formulations of direct sizings are closely guarded secrets by the glass fibre manufacturers, the information shared in technical datasheets is very basic. The information provided, usually includes the matrix-compatibilities of the roving and that the coating is “silane” based. Neither the type of film former, nor the exact type of silane(s) and other additives used in the direct sizing are disclosed which is frequently a problem during material development. The use of finished fabrics with known adhesion promoter composition is therefore the only possibility to find glass fibre-polymer compatibilities in academic research.

Aside from many unknowns in the formulation of direct sizings, it should be mentioned that the long-term influences due to migration of many low-molecular weight additives (surfactants, lubricants, antistatics...) on composite mechanical properties are unknown to this day [33]. Migration could alter the interphase of the material and deteriorate its properties over time. In aerospace applications it is often desirable not to have this kind of unknown factor in safety critical parts. Therefore, finished yarn fabrics with pure adhesion promoter formulations are usually preferred over roving products. Many technical glass fibre yarn finishes, and finished glass yarn fabrics are qualified for aerospace applications according to BMS 9-3 (Boeing Commercial Airplanes specification) and several other certification standards [106,124].

The advantage of finishing yarn fabrics is that the weaver has a high flexibility to adapt the coating to specific customer requirements - this is usually not possible with mass produced rovings. In some cases, the exact type of adhesion promoter finish applied to the yarn fabric is disclosed e.g., “A-1100 aminosilane”. Of course, there are also proprietary finish blends. Overall, finishes are said to promote better adhesion than direct sizings since they do not contain any auxiliary agents [34]. However, the required heat cleaning step prior to finishing has a detrimental effect on fibre strength. After the usual heat treatment process at 400 °C, the residual tensile strength of E-glass yarns is in a region between 50-75% of their initial tensile strength [35,125]. Therefore, the better fibre-matrix adhesion obtained by finished fabrics is potentially compromised by their inherently lower fibre tensile strengths compared to direct sized fibres [22].

A legitimate question is “why are glass yarns not provided with direct sizings similar to roving sizings?”. Indeed, there are exceptions. Special yarns with matrix-compatible direct sizings have been developed by the industry which do not need to undergo heat cleaning. Early direct sizing formulations for yarns did not allow high-speed weaving operations without causing active sizing ingredients to degrade due to the high temperatures arising from friction. Such direct sized yarns were restricted mostly to braiding or stitching [12]. However, recent advances in sizing chemistry allowed the production of direct sized yarns for high-speed weaving. The cheaper price of these fabrics compared to finished fabrics most possibly comes at the expense of inferior fibre-matrix adhesion and slower wet-out, but with the advantage of higher fibre

strengths. An interesting range of direct sized yarn products with thermoplastic compatibilities are produced by AGY as found during literature review [126]. However, it is unknown precisely which weavers process these special yarns into fabrics.

Despite the long history of glass fibre production, the designation system for fibre coatings is not well standardised. Confusingly, both direct sized yarn fabrics and roving fabrics are frequently termed “silane” fabrics. Consequently, one may deduce that these fabrics contain silane-only coatings. As mentioned, this is not the case. A direct sizing is always a complex formulation of multiple ingredients among which silane adhesion promoters are contained, whereas silane-only coatings are applied exclusively to heat cleaned yarn fabrics during finishing [11].

Lastly, a factor which should always be considered when processing sized or finished glass fibres with thermoplastics is the thermal stability of the organic coatings. Many silanes and film formers are prone to oxidative degradation in a range of merely 200-300 °C [107,127–129]. This thermal stability suffices for processing most, but not all thermoplastics. Decomposition of the sizing or finish at these elevated temperatures may lead to defects in the fibre-matrix interphase and deteriorate mechanical properties of the composite significantly [123].

### 3.2 Carbon fibre sizings

Most intricacies discussed so far about glass fibre sizing formulations are not directly applicable to carbon fibres. Unfortunately, carbon fibre sizing formulations are affected by the same form of confidentiality that is found throughout the glass fibre sizing business. However, what has been deduced from research so far, it appears that sizings applied to carbon fibres are not of the same importance for interfacial adhesion compared to the sizings which are applied to glass fibres [12,25]. It is comprehensible that this fundamental difference in the role of sizings between carbon fibres and glass fibres is contributing to much confusion in the composites community. It is almost certain that formulation-wise carbon fibre sizings differ vastly from glass fibre direct sizings in that they do not contain silane adhesion promoters and are composed mostly or solely from polymeric film formers.

Most carbon fibre sizings are formulated for use with epoxy resins. As a consequence, they are coated with epoxy-based (EP) film formers (low-molecular weight bisphenol-A or novolac epoxy resins). These EP-sizings are potentially applied without hardeners, or even partly crosslinked (details are unknown) from solution or emulsion [130]. Film formers employed in carbon fibre sizings fulfil the same purpose as glass fibre film formers, namely, to protect the fibres from abrasion, to guarantee tow integrity and to control wet-out. The matrix compatibility of sized carbon fibres is dictated by the type of film former applied. For example, if a bisphenol-A-sized carbon fibre is combined with an unsaturated polyester resin or vinyl ester resin (VE),

good compatibility is not guaranteed, unless the sizing is modified to be multi-compatible (e.g., by epoxy modified unsaturated polyester resin film formers [131,132]).

Despite extensive investigation, the literature contains conflicting findings regarding the role of carbon fibre sizings on interfacial adhesion. Many scholars report improved fibre-matrix adhesion of sized carbon fibres [98,133–135], while others report improved adhesion when the carbon fibre sizing is removed or unsized fibres are used [64,136,137]. Yet, even carbon fibre manufacturers state that carbon fibre sizing materials are applied to aid in handling and not primarily to improve adhesion [12,106,138]. Therefore, film formers in carbon fibre sizings may be considered as handling agents or pre-wetting agents. Due to the better strand integrity, sized carbon fibre tows limit resin pickup, which results in parts with higher fibre volume fractions.

The carbon fibre to matrix adhesion is most likely determined by the functionality of the carbon surface [12]. Activation or functionalisation of the carbon surface is conducted by electrochemical surface treatment in industrial practice prior to sizing application [53] as illustrated in Fig. 23.

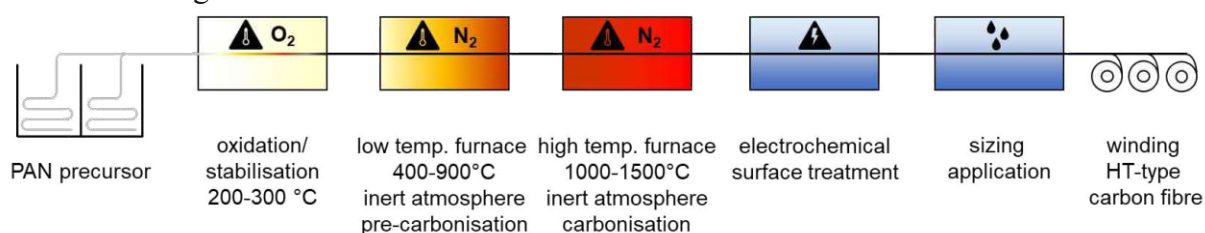


**Fig. 23** Carbon fibre (HT-type) production process from a PAN-copolymer based precursor: oxidation of the PAN-precursor, carbonisation in inert gas furnaces, electrochemical surface treatment (activation), sizing application and winding (adapted from [31]).

It appears that the electrochemically activated and unsized carbon fibre surface is already compatible with most thermosets and thermoplastics [139]. Commonly found surface functionalities of the carbon surface are depicted in Fig. 24 which promote adhesion through either covalent or non-covalent interactions. In contrast, an unsized glass surface would promote only very weak adhesion with polymers due to the different surface functionality of glass compared to carbon [24].

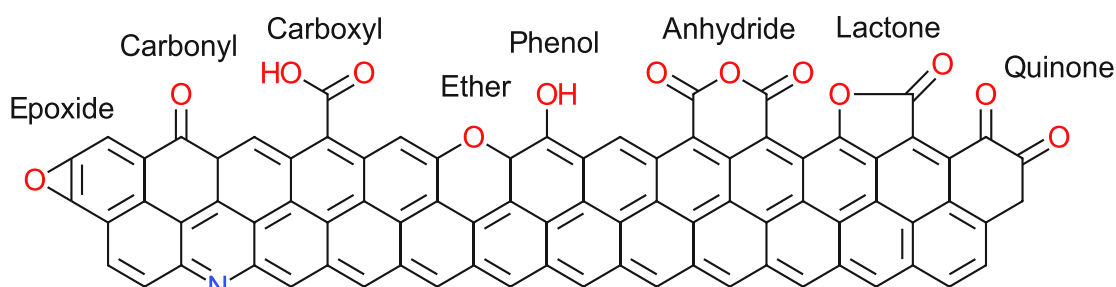


**Fig. 24** Functional groups on an electrochemically oxidised (activated) carbon fibre surface (adapted from [140–142])

### 3.2.1 Continuous carbon fibres in the thermoplastic process

Since structural applications of continuous carbon fibres with thermoplastics are relatively new, the development of tailored thermoplastic sizings has only recently gained attention by carbon fibre manufacturers [143,144]. While some evidence can be gathered from industrial material development reports, generally, scientific literature on the compatibilisation of thermoplastics with carbon fibres is rather limited.

Thermoplastic UD-tapes have been frequently made industrially from unsized carbon fibres [145–147]. However, a new trend has emerged in UD-tape production by utilisation of 12K-50K tows with tailored thermoplastic sizings. The product quality can be improved significantly with less broken filaments due to the protective nature of the thermoplastic compatible sizing.

In the case of technical fabrics, carbon fibres in the 3K tow range are most commonly used in TPCL production. Unlike 12K-50K tows, 3K tows are currently not available with thermoplastic sizings and only supplied with EP-sizings [143,144]. It is important to note that EP-sizings are incompatible with most thermoplastics, not only chemically but also from a processing point of view due to a decomposition onset of around 250 °C [25,148,149].

Unsize carbon fibres are impossible to weave due to excessive fibre breakage and fuzzing. Therefore, any generic EP-sized 3K carbon fibre tow may be selected to protect and lubricate the fibres during weaving. Consequently, the EP-sizing requires to be removed from the woven fabrics [148]. This type of desizing may be considered similar to the heat cleaning process of glass yarn fabrics. However, relatively little is known about industrial carbon fibre desizing processes due to proprietary reasons [106]. Batch oven desizing of large carbon fibre fabric rolls (thousands of metres in length) may not be as effective as batch oven desizing of glass yarn fabric rolls since the decomposition behaviour of EP-sizings is different than that of glass yarn textile sizings. It appears that infrared-irradiation, or gas-fired ovens are effective for desizing carbon fibre fabrics in continuously operated processes [25,149].

Desizing of carbon fibre fabrics should be conducted in a region of 350-400 °C in air atmosphere to decompose the EP-sizing effectively without causing degradation of the carbon fibres [25]. Unlike E-glass fibres, carbon fibres do not experience strength degradation at said desizing temperatures and only start to degrade around 500 °C in air. It appears that the oxidised carbon fibre surface suffices for bonding many thermoplastics with highly satisfactory results as reported by Kiss, Stadlbauer, Burgstaller and Archodoulaki (**Publication IV**) [25]. The application of tailored thermoplastic sizings is therefore not a necessity for high-performance carbon fibre TPCL production. As of yet, it is not entirely clear whether desizing carbon fibre fabrics in air atmosphere reconstitutes the fibre surface to a “factory state” prior to sizing. Another possible explanation is that the graphitic planes of carbon fibres, or edges of the graphitic planes [92] could be additionally functionalised at typical desizing temperatures, as reported with pristine graphite [150].

## 4 TPCL manufacturing processes

The aim of manufacturing woven TPCL is to obtain fully impregnated, void-free laminates without distorting the weave structure of the reinforcement (fibre wash-out or in-plane waviness). Put in other words, displacing all the interstitial air between the fibres by the thermoplastic matrix and simultaneously maintaining the orientation of the reinforcement.

The main advantage of TPCL is that generally less waste material is generated during their manufacture and subsequent part manufacturing processes compared to thermoset preregs. Neither backers (prepreg release films), nor storage in freezers is required as with thermoset preregs.

There are numerous methods for the manufacture of TPCL from woven fibre reinforcements. In general, three types of compression moulding processes are used. Depending on the hydraulic press configuration, a moderate material throughput of roughly 20 m/h can be achieved. All conventional TPCL pressing processes have in common that the dry fibre bundles are impregnated by a thermoplastic matrix melt at elevated temperatures (solvent or slurry impregnation is not considered here). After a sufficient dwell time above the melting temperature of the polymer matrix, the laminate is cooled (solidified) and consolidated (compacted) into its final thickness. Since thermoplastic polymers have high viscosities, fibre impregnation is carried out mainly in the thickness direction of the material stacks.

### 4.1 Matrix forms and pressing processes

Thermoplastics for TPCL production come in the form of pellets (direct melt processing), polymer powder, polymer film, or polymer fibre as depicted in Fig. 25 [149].

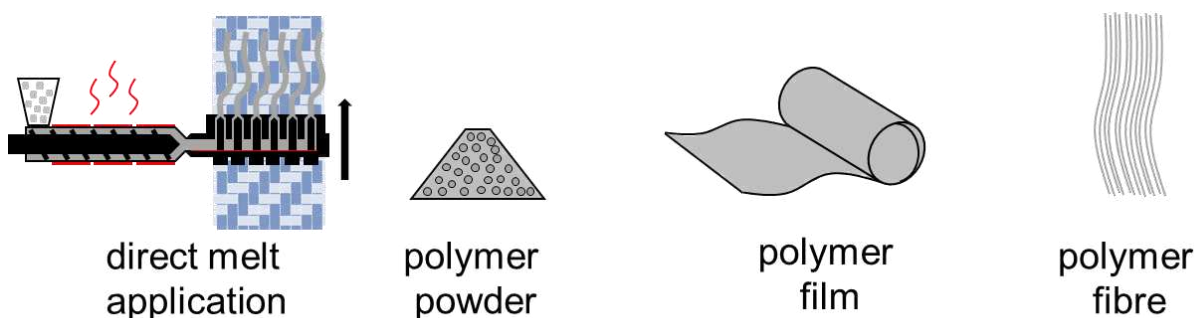


**Fig. 25** Polymer matrix forms for TPCL production provided as direct melt, polymer powder, polymer film or polymer fibre.

Every matrix form comes with its own processing advantages and disadvantages. Therefore, certain forms of thermoplastic matrices are best suited only for specific pressing technologies.

Pressing technologies include discontinuous (static) pressing, semi-continuous (intermittent) pressing or continuous (double belt) pressing as displayed in Fig. 26.

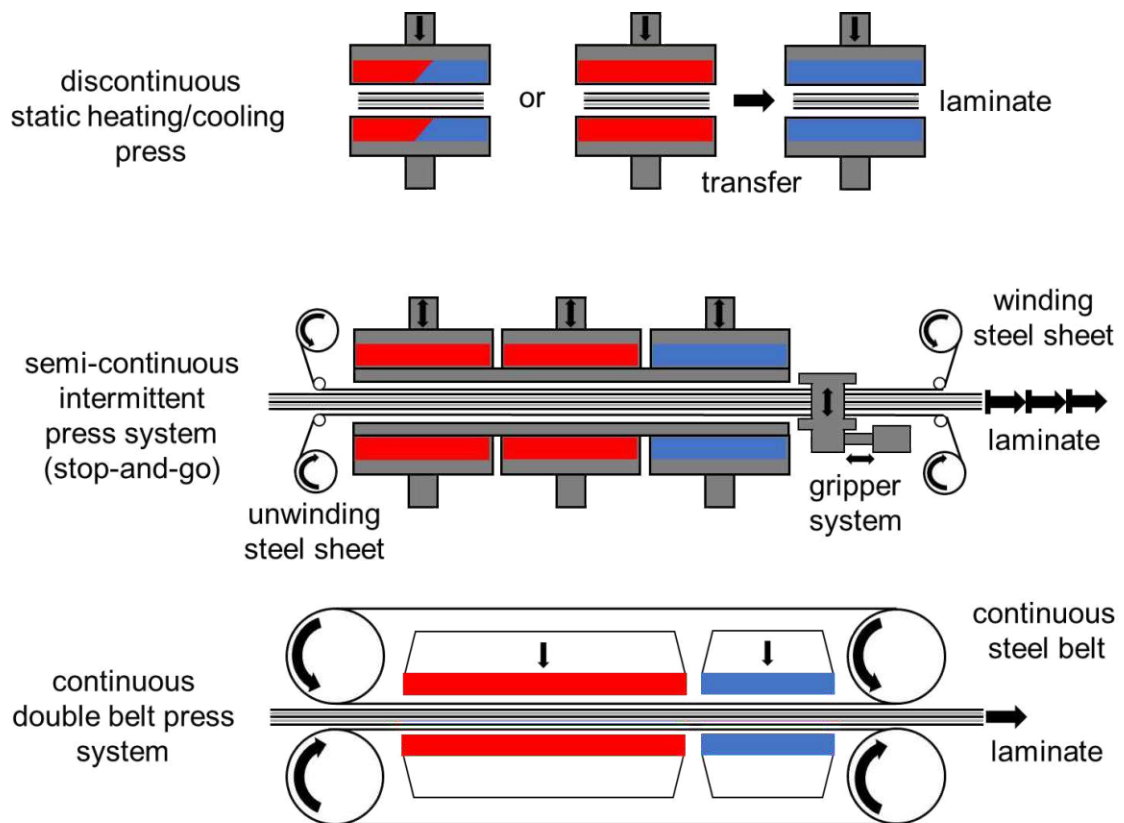


**Fig. 26** Press configurations for processing TPCL including static pressing, intermittent pressing, or continuous pressing.

#### 4.1.1 Discontinuous (static) pressing

Discontinuous pressing is certainly the most versatile pressing technology for research & development or frequent material change and corresponds to a batch process. The process is characterised by long heating and cooling times. Therefore, material output is restricted to low or medium production quantities. The process may be realised by a single heating/cooling press or optimised by retractable cooling platens. It is also possible to utilise a two-press system interconnected by a mould transportation shuttle. One press is used to heat and impregnate the material, while the other press is used to cool and consolidate the material. Another type of static press is a floor press which has multiple pressing floors and can therefore accommodate multiple material stacks at once. Woven fabric widths are often tailored to match the press platen dimension in order to minimise offcuts and material waste as far as possible.

Even though material output is relatively low, Toray Advanced Composites produces their Cetex<sup>®</sup> TPCL range of materials via compression moulding in four large static heating/cooling presses. Their presses have a capacity of producing laminates up to 3.6 m by 1.2 m in size and are operated around the clock to satisfy demand [151]. The achievable laminate and surface

qualities via discontinuous pressing are of the highest aerospace standards with void contents < 1%. A range of aerospace certified TPCL is displayed in Fig. 27.



**Fig. 27** Cetex<sup>®</sup> TPCL consolidated on static presses. CF-PPS fabric TC1100 (large panel background 500 · 500 mm<sup>2</sup>); TPCL from bottom left to top right: CF-LMPAEK UD, CF-PEI fabric, CF-PPS UD, CF-PPS fabric, CF-PEI UD, GF-PEI fabric, GF-PPS fabric. Samples kindly provided by Toray Advanced Composites.

Recent developments in inductively heated tools (e.g., Roctool LIT<sup>™</sup>) allow significant reduction of cycle times in static pressing with heating rates of up to 150 °C/min and a maximum operating temperature at 400 °C [152]. However, it is unknown whether this technology is used by industrial TPCL manufacturers to impregnate dry fibres.

#### 4.1.2 Semi-continuous (intermittent) pressing

An intermittent press is essentially a series of static heating and cooling press segments which open and close simultaneously. A material stack to be impregnated is incrementally pulled through the heating and cooling zones by means of a hydraulic gripper arm together with thin steel release sheets which prevent the molten matrix material from sticking to the pressing tool. Intermittent pressing is arguably the best method to meet current woven TPCL demand in terms of material output and machine investment cost. The investment cost of an intermittent press is higher by a factor of roughly 3-5 compared to a similar sized static press.

The intermittent pressing process, also referred to as CCM - continuous compression moulding was pioneered by Spelz and Schulze at Dornier Luftfahrt GmbH in the early 1990's [153,154]. The process was invented to manufacture shaped continuous TPCL profiles from



preimpregnated thermoplastic UD-tape material for the aerospace industry. Today, continuous TPCL profiles with variable cross sections and even hollow profiles are produced for example by XELIS GmbH via the CCM process. The use of intermittent pressing for the impregnation of dry fabrics to flat TPCL blanks is another field of application.

Modern intermittent press systems which have gained considerable attention in industrial TPCL manufacture are built by RUCKS Maschinenbau GmbH (larger machines) and Teubert Maschinenbau GmbH (smaller machines) [155,156]. Intermittent presses have platens with integrated heating and cooling zones (thermally separated). The top pressing tool may be chamfered or tilted slightly to take material compaction into account and displace air opposite to the processing direction [157–159]. Impregnation may be optimised by the adaption of the tool geometry, for instance by interchangeable shims with trapezoidal or “boomerang” shapes [159]. This adaption is crucial for the production of wide TPCL in order to assure sufficient air displacement in the transverse direction. The pressing tools are also designed to prevent the molten polymer from leaking sideways (similar to a stamp impregnation tool) but with a large enough gap to allow easy feeding and air displacement. A sideways closed mould reduces the risk of fibre wash-out and the width of edge trims significantly.

The stop-and-go-operation of the intermittent press imparts a characteristic step-like or striated pattern to the surface of the TPCL as can be seen in Fig. 28. The pattern arises due to polymer shrinkage and a pressure drop when the molten material passes the transition zone between the heating and cooling segments of the machine [159]. A thickness profile ( $\pm 10$  microns) forms across the surface which is visible to the naked eye. However, there is no measurable effect on the mechanical performance due to the pattern [157]. If the TPCL is subsequently stamp formed, the step pattern disappears once the matrix is remelted.



**Fig. 28** Step pattern arising from semi-continuous pressing of a 50” wide Tepex<sup>®</sup> 202 CF-PA6 TPCL produced by Bond Laminates GmbH.

The feed distance per intermittent stroke is typically around 50-100 mm. However, the exact production speed (dwell time under pressure) cannot be derived from the step pattern. Theoretical production speeds of the machines are up to 2 m/min. However, the actual production speeds are in the region of 0.1-0.4 m/min. The material output is largely determined by the impregnation time of the individual fibre bundles (micro-impregnation), which is

dependent on the fibre architecture, ply count, flow front optimisation, polymer type, impregnation temperature profile, impregnation zone length, and pressure applied by the machine.

One major disadvantage of this technology comes with the required top and bottom steel release sheets. In industrial production, the utilised stainless-steel coils are up to 100-200 metres in length (sufficient to cover one production shift). The sheets must be equipped with non-stick plasma coatings or optionally treated with liquid based release agents and can therefore be rather costly. Since the sheets are limited in length, strategies must be found to ensure seamless production. Either new release sheets are bolted to the end of the consumed sheets, or the consumed sheets are reinstalled again at the unwinder. Due to the machine design, it was not possible so far to implement continuous steel belts in intermittent presses. Certainly, such an implementation would make this technology more attractive and accessible for upcoming TPCL producers.

### 4.1.3 Continuous (double belt) pressing

Continuous double belt presses are complex machines and the technology for TPCL production is still maturing. There have been countless attempts and concepts to manufacture TPCL by double belt pressing since higher demands can be satisfied with this technology compared to intermittent pressing [160–163]. The investment cost of a high-temperature double belt press can exceed several millions of euros, which is the main reason why many TPCL manufacturers are hesitant to make use of this technology. Due to its overall larger size, the operating cost of a double belt press is also higher compared to an intermittent press.

A major challenge to be overcome in double belt pressing technology is the high friction between the typical steel belts and the heating/cooling segments of the machine. Since the composite material is impregnated under constant motion there are also several problems with TPCL quality, including poor wet-out, air entrapment, fibre wash-out, in-plane fibre waviness and large edge trims as reported in several studies [160,162,163]. It is also more difficult to influence the polymer flow front in a targeted manner since specific pressing tool geometries or shims cannot be implemented in double belt presses.

The belt materials are either made from stainless steel for the impregnation of high temperature thermoplastics up to 400 °C, or Teflon® (PTFE-polytetrafluoroethylene)-glass fabrics for the impregnation of thermoplastics up to 250 °C (cheaper machines). TPCL produced via Teflon-glass fabric belts are characterised by a print-through of the belt fabric on the TPCL surface.

Once suitable processing parameters and machine configurations are found, input material can be fed endlessly. This is possibly the main advantage of the double belt press technology over other pressing techniques. Release agent application to steel belts is also more convenient compared to the steel coils used in intermittent pressing. The surface appearance of laminates

produced via steel belts is excellent (no step pattern) and comparable to discontinuous static pressed TPCL [157]. However, start-up losses in belt presses are high and can exceed several metres of waste material. In the case of carbon fibre multi-ply material stacks, such start-up waste could cost thousands of euros.

Processing speeds are generally also limited by the fibre impregnation time and not the actual capabilities of the machines. Since double belt presses typically have longer heating zones, processing speeds are somewhat higher than the production capabilities of intermittent presses. A high-temperature double belt press pilot plant for TPCL production is currently available at Berndorf Band GmbH [164].

#### 4.1.4 Direct melt processing

The utilisation of an extruded polymer melt for TPCL production is both an energy saving and cost-effective approach since the energy invested to melt the polymer is harnessed directly for impregnation of the reinforcement. All other intermediate matrix forms (powder, film, fibre) require at least one additional production step before the reinforcing fibres can be impregnated.

While direct melt impregnation processes are state-of-the-art in thermoplastic UD-tape production, impregnation of fabrics with direct melts is technologically more complex due to possible risk of fibre wash-out or distortion of weft strands. As far as is known, only Neue Materialien Fürth GmbH have successfully implemented a plasticising unit by ENGEL GmbH in combination with a hot runner system on their intermittent press for direct melt impregnation of fabrics [159,165]. The melt extrusion is coupled to the stop-and-go motion of the press and the melt is applied between two fabric plies. The limitation of the process is that multi-ply stacks (more than two) are difficult to process due to the long impregnation distance of the melt from the core to the outer plies.

#### 4.1.5 Polymer powder processing

Some high-temperature thermoplastics such as PEEK or PEI are readily available in powder form. However, standard and engineering thermoplastics are almost exclusively available in granule form. The production of polymer powder involves cryogenic grinding of the polymer granules which is an expensive process. Polymer powder is used for the preparation of an intermediate product, called powder-semipregs. Powder-semipregs are produced by scattering polymer powder onto the surface of glass or carbon fabrics and quickly melting the applied powder by means of heat (e.g., infrared irradiation) in a continuous process [149]. The molten powder particles coalesce into droplets on the surface of the fabric and adhere to the outermost fibres. The product may be cooled subsequently by calendaring. The application of polymer powder can also be realised by electrostatic attraction [146]. Typical powder particles are larger in size than the fibre diameters. Therefore, sprinkled particles cannot penetrate the fibre bundles

effectively. As the name “semipreg” implies, the material is only negligibly impregnated. A CF-semipreg is depicted in Fig. 29, where polymer powder was applied to both sides of the fabric.



**Fig. 29** CF-polymer powder-semipreg (top left, top right and bottom left), and compression moulded laminate therefrom (bottom right).

The advantages of semipregs are, that they can be wound into rolls, stored indefinitely, and used in combination with all pressing technologies. Handling is improved dramatically and the risk of ply misalignment or crease formation due to inaccurate machine feeding is drastically reduced. Modern powder scattering machines are capable of applying polymer powder onto fabrics with high precision and are made for instance by Maschinenfabrik Herbert Meyer GmbH [166]. Despite the high cost of cryogenic grinding and semipreg production, powder-semipregs are the most widely used fibre-matrix intermediate form in modern TPCL production.

For components which are too large to be processed by hydraulic presses, high-temperature autoclave processing of thermoplastic powder-semipregs is common practice in aerospace engineering [46,167]. High-temperature vacuum bagging materials (polyimide films) are required for impregnation and consolidation of parts manufactured in this manner. However, the shape complexity is restricted to planar or slightly curved components due to the limited drapeability of powder-semipregs.

#### 4.1.6 Polymer film processing

The production of polymer films requires the upstream process of cast film extrusion. The thickness of the films can be controlled precisely, and the obtained laminates made from compression moulded stacks of alternating fabric plies and film layers are generally of very high quality. Special care has to be taken when stacks are assembled to prevent misalignment of the dry fabrics.

The film stacking method is commonly used in all types of pressing processes. However, continuously fed films tend to wrinkle when heated unevenly. Thus, manufacturing defects may arise during continuous laminate production. For fibre impregnation, injection moulding grade thermoplastics with low viscosity are favoured over extrusion grade thermoplastics. In some instances, the melt stiffness of injection moulding grade thermoplastics may not suffice to be extruded into thin films. Therefore, other types of matrix processing technologies have to be used (mainly powder).

The impregnation distance between films and the centre of a fibre bundle is comparable to powder-semipregs.

#### 4.1.7 Polymer fibre (commingling) processing

Polymers fibres may be melt spun and subsequently or immediately commingled (intermixed) with reinforcing fibres via an air jet nozzle into a continuous hybrid strand [168]. A typical hybrid strand and woven commingled fabric is shown in Fig. 30.



**Fig. 30** Commingled GF-PP roving (left) and commingled GF-PP roving fabric (right).

Commingling generally results in a lot of fibre breaks, which is the reason why woven commingled fabrics are rarely used in top-of-the-line TPCL. Historically, commingled fabrics were marketed under the name “Twintex”. The main advantage of commingled fabrics is the

ease of handling and the shorter impregnation distance compared to other matrix forms. Since many commingled fabrics are relatively well drapeable, complex shapes may be draped directly. Diaphragm- or vacuum bagging processes are suitable for impregnation and direct part manufacturing routes without the need to press a flat TPCL blanks first.

Table 4 summarises viable combinations of pressing processes and fibre-matrix intermediate forms for woven fabrics.

**Table 4** Compatibility chart of pressing processes and fibre-matrix intermediate forms for dry woven fabrics

	Discontinuous (static) pressing	Semi-continuous (intermittent) pressing	Continuous (double belt) pressing
Direct melt impregnation	-	o	-
Powder-semipreg	+	+	+
Film stacking	+	o	o
Commingled fabrics	+	+	+

+ well suited, o possible but not optimal, - unsuited

## 4.2 TPCL recycling

One of the major benefits of thermoplastic composites is their recyclability. Alongside virgin material development, material reclamation and reprocessing ideas should always be presented. A relatively simple and effective method is shredding of TPCL trims, offcuts, scrap parts or end-of-life parts via cutting mills or single shaft shredders (lower wear rates). Depending on the particle size, the obtained shredded material fraction can be injection moulded directly or reprocessed via compression moulding methods as displayed in Fig. 31. All these recycling processes have in common that the former continuous length fibres are cut and shortened into long- or short fibres. Essentially, these recycling processes are downcycling procedures which significantly deteriorate mechanical properties down to 10-30% of the initial TPCL properties [23].



**Fig. 31** Recycling route for TPCL via shredding and compression moulding

In an effort to retain the mechanical properties of recycled TPCL, Kiss et al. (**Publication II**) [23] successfully tested two approaches by:

- Co-moulding shredded TPCL material as a core with continuous fibre skins into “micro-sandwich” composite panels. The skin material is either a thin sheet of a fully consolidated laminate, a powder-semipreg or a dry reinforcement (film stack).
- Directly reshaping thermoformed parts into flat TPCL blanks for reuse via reverse thermoforming.

While the latter idea of reverse forming is rather experimental and definitely not applicable to highly complex part geometries, it could nonetheless be a viable method for recycling expensive carbon TPCL with limited geometrical complexity.

The former idea of remanufacturing shredded material into sandwich composites was found to be a highly viable method and a potential solution to introducing alternative recycled products to the market.

# 5 Materials and methods

## 5.1 Woven fabrics

Technical E-glass fibre fabrics used for TPCL manufacture are listed in Table 5. As mentioned previously, the type of adhesion promoter contained in a finish is usually disclosed, whereas the adhesion promoter of a direct sizing has the generic description of “silane”. Despite different areal weights of the fabrics, the attempt was to create comparable laminates in terms of fibre weight- and volume fraction by adjusting the utilised ply number.

**Table 5** Dry glass fibre fabrics used in the experiments. (**Publications I and III**)

2/2 twill E-glass fabric	Fibre diameter (microns)	Areal weight (g/m <sup>2</sup> )	Finish/sizing	Fabric plies used for 2 mm thick laminates
<sup>1</sup> GIVIDI Fabrics VR48	9	290	Heat cleaned/desized	8
<sup>1</sup> GIVIDI Fabrics VR48	9	290	A-1100 aminosilane <sup>a</sup>	8
<sup>1</sup> GIVIDI Fabrics VR48	9	290	G1 aromatic aminosilane <sup>a</sup>	8
<sup>1</sup> GIVIDI Fabrics VR48	9	290	GI496 aminosilane blend <sup>a</sup>	8
<sup>1</sup> GIVIDI Fabrics VR48	9	290	Z6040 epoxysilane <sup>a</sup>	8
<sup>2</sup> PI Interglas 92140 FK144	9	390	modified Volan <sup>®</sup> A chromium complex	6
<sup>3</sup> HexForce <sup>®</sup> 01038	9	600	TF970 aminosilane	4
<sup>4</sup> PD GW 123-580K2	14	580	Silane, thermoset multi-compatible (UP, EP, VE)	4
<sup>4</sup> PD GW 173-600K2 E35	17	600	Silane, PP-compatible	4
<sup>5</sup> JM StarRov <sup>®</sup> 490	16	600	Silane, PP-compatible	4
<sup>6</sup> NEG TufRov <sup>®</sup> 4599	17	600	Silane, PP-compatible	4
<sup>5</sup> JM StarRov <sup>®</sup> 895	16	600	Silane, PA6-compatible	4
<sup>6</sup> NEG TufRov <sup>®</sup> 4588	17	600	Silane, thermoplastic multi-compatible (e.g., PP, PA6, PPS)	4

<sup>1</sup> GIVIDI Fabrics S.r.l., Italy

<sup>2</sup> Porcher Industries Germany GmbH, Germany

<sup>3</sup> Hexcel Corporation, France

<sup>4</sup> P-D Glasseiden GmbH Oschatz, Germany

<sup>5</sup> Johns Manville Slovakia a.s., Slovakia

<sup>6</sup> Nippon Electric Glass Co. Ltd., Japan

<sup>a</sup> equimolar finish concentration



The technical carbon fibre fabric used for TPCL production is listed in Table 6.

**Table 6** Dry carbon fibre fabric used in the experiments. (**Publication IV**)

2/2 twill HT carbon fabric	Fibre diameter (microns)	Areal weight (g/m <sup>2</sup> )	Sizing	Fabric plies used for 2 mm thick laminates
<sup>1</sup> ECC style 452-5, Tenax <sup>®</sup> -E HTA40 3K, 2/2 twill	7	200	E13-epoxy	8

<sup>1</sup> ECC - Engineered Cramer Composites, Germany

### 5.1.1 Thermoplastic matrices

The matrices used, consist of low to medium viscosity PP, PA6, PC, PPS and PEEK grades. The matrices were extruded to films in-house or provided in film form as outlined in Table 7.

**Table 7** Thermoplastic matrices used in the experiments. (**Publications I, III and IV**)

Matrix material	Material designation	Extruded film thickness (microns)	Film layers used for 2 mm thick laminates	specialty
PP	<sup>1</sup> HK060AE	130 ± 5	8	high heat stabilisation
PP copolymer	<sup>1</sup> BJ100HP	130 ± 5	8	contains coupling additive
PA6	<sup>2</sup> Ultramid <sup>®</sup> B3W	130 ± 5	9	pigmented black, heat stabilisation
PA6	<sup>3</sup> Durethan <sup>®</sup> B30S	120 ± 5	9	
PC	<sup>4</sup> Makrolon <sup>®</sup> LQ2647	120 ± 5	9	
PPS <sup>5</sup> LITE P	<sup>6</sup> Fortron <sup>®</sup> 0214 film	100, 120	9	
PEEK <sup>5</sup> LITE K	<sup>7</sup> Victrex <sup>®</sup> PEEK 151G film	120	9	

<sup>1</sup> Borealis AG, Austria

<sup>2</sup> BASF SE, Germany

<sup>3</sup> LANXESS AG, Germany

<sup>4</sup> Covestro AG, Germany

<sup>5</sup> LITE GmbH, Austria

<sup>6</sup> Celanese Corp., USA

<sup>7</sup> Victrex plc, UK

PP HK060AE required modification and was compounded with different concentrations and types of MAH-g-PP coupling agent and black pigment masterbatch as shown in Table 8.

**Table 8** Additives used for PP homopolymer modification. (**Publication I**)

Additive	Additive designation	MAH grafting level [wt%]	Melt mass-flow rate MFR [g/10 min]*
MAH-g-PP	<sup>1</sup> Polybond <sup>®</sup> 3000	1.2	405
Carbon black masterbatch	<sup>2</sup> Maxithen <sup>®</sup> PP 98981 black	-	-
MAH-g-PP (unpublished results)	<sup>3</sup> Scona <sup>®</sup> TPPP 9112 GA	1.0	70 - 120
MAH-g-PP (unpublished results)	<sup>3</sup> Scona <sup>®</sup> TPPP 9212 GA	1.8	80 - 140
MAH-g-PP (unpublished results)	<sup>4</sup> Orevac <sup>®</sup> CA100	1.0	>100
MAH-g-PP (unpublished results)	<sup>3</sup> Priex <sup>®</sup> 20097	0.45	>>1000 hyperfluid

<sup>1</sup> SI Group USA LLC, USA. Material supplied by Brenntag GmbH, Germany

<sup>2</sup> Gabriel-Chemie GmbH, Austria

<sup>3</sup> BYK-Chemie GmbH, Germany

<sup>4</sup> Arkema, France

\* (at 190 °C, 2.16 kg)

PA6 Ultramid<sup>®</sup> B3W was also modified with different concentrations of EBA-g-MAH (ethylene butyl acrylate copolymer functionalised with maleic anhydride) coupling and impact modifier as described in Table 9.

**Table 9** Additives used for PA6 homopolymer modification. (used in unpublished results)

Additive	Additive designation	MAH grafting level [wt%]	Melt volume-flow rate MVR [cm <sup>3</sup> /10 min]*
EBA-g-MAH	<sup>1</sup> Scona <sup>®</sup> TSEB 2113 GB	0.6	3-8

<sup>1</sup> BYK-Chemie GmbH, Germany

\* (at 190 °C, 2.16 kg)

### 5.1.2 Thermoset matrix

The low viscosity thermoset epoxy matrix used for carbon fibre resin infusion is specified in Table 10.

**Table 10** Thermoset epoxy matrix used for carbon fibre resin infusion. (used in unpublished results)

Matrix material	Material designation	Pot life when mixed at room temperature [min]	Mixing ratio [wt%]	Curing condition
Epoxy resin	<sup>1</sup> Biresin <sup>®</sup> CR83	60	100	70 °C for 8h
Amine hardener	<sup>1</sup> Biresin <sup>®</sup> CH83-2		30	

<sup>1</sup> Sika Deutschland GmbH, Germany

### 5.1.3 Industrial reference materials

For comparative purposes, industrial reference materials were chosen to resemble the in-house moulded TPCL as closely as possible. Industrial materials are listed in Table 11.

**Table 11** Industrial GF and CF reference materials. (0,90) represents one fabric ply. (Publications I-IV)

Material combination	Material designation	Areal weight per fabric ply (g/m <sup>2</sup> )	Fabric plies used in the laminates	Stacking sequence
GF-PP consolidated laminate	<sup>1</sup> Tepex <sup>®</sup> dynalite 104-RG600(4)/47% 2/2 twill	600	4	[(0,90) <sub>2</sub> ] <sub>s</sub>
GF-PA6 consolidated laminate	<sup>1</sup> Tepex <sup>®</sup> dynalite 102-RG600(4)/47% 2/2 twill	600	4	[(0,90) <sub>2</sub> ] <sub>s</sub>
GF-epoxy prepreg	<sup>2</sup> GGBD2807 2/2 twill	280	8	[(0,90) <sub>4</sub> ] <sub>s</sub>
CF-PA6 consolidated laminate	<sup>1</sup> Tepex <sup>®</sup> dynalite 202-C200(8)/45% 2/2 twill	200	8	[(0,90) <sub>4</sub> ] <sub>s</sub>

CF-PPS consolidated laminate	<sup>3</sup> Toray Cetex <sup>®</sup> TC1100 5-harness satin	280	6	(0,90) <sub>3</sub> /(0,90) <sub>r3</sub>
CF-PEEK consolidated laminate	<sup>4</sup> Tenax <sup>®</sup> -E TPCL PEEK-HTA40 5-harness satin	285	6	(0,90) <sub>3</sub> /(0,90) <sub>r3</sub>

<sup>1</sup> Bond-Laminates GmbH, Germany      <sup>3</sup> Toray Advanced Composites, Netherlands  
<sup>2</sup> Krempel GmbH, Germany      <sup>4</sup> Teijin Carbon Europe GmbH, Germany

Further tests included a comparison of TPCL with aerospace grade aluminium alloys listed in Table 12. The aluminium specimens were provided by LKR Ranshofen GmbH and were tested under the same testing conditions as their composite counterparts described in 5.2.3.

**Table 12** Aerospace grade aluminium alloy reference materials. (used in unpublished results)

Material combination	Material designation	Heat treatment	Sheet thickness (mm)
EN AW-2024	<sup>1</sup> Al-2024 T6	T6	2
EN AW-7075	<sup>1</sup> Al-7075 T6	T6	2

<sup>1</sup> LKR Leichtmetallkompetenzzentrum Ranshofen GmbH, Austria

#### 5.1.4 Cast film extrusion

All thermoplastics (except PPS and PEEK) were processed in-house to cast films by means of a cast film extrusion line PM30 (Plastik-Maschinenbau Geng-Meyer GmbH, Germany). All materials except PP were pre-dried prior to cast film extrusion. Processing parameters are given in Table 13.

**Table 13** Drying and processing conditions for cast film extrusion (**Publications I and III**)

Material	Pre-drying temperature and drying time	Barrel and die temperature during extrusion [°C]	Extruder throughput [kg/h]
PP	-	220 °C	10
PA6*	80 °C 6h	260 °C	10
PC*	120 °C 6h	290 °C	10

\* The cast film rolls were stored in hermetically sealed bags until used for TPCL pressing.

As required in the case of PP homopolymer, the thermoplastic material was modified by MAH-g-PP coupling agent in different concentrations. The dry blends were compounded in a co-rotating twin screw extruder TSE 24 MC (Thermo Scientific Fisher GmbH, Germany) and pelletised prior to cast film extrusion.

## 5.2 Methods

The chosen processing route for TPCL manufacture was film stacking and discontinuous hot compression moulding, followed by mechanical testing and morphological characterisation of the prepared laminates.

### 5.2.1 TPCL manufacture

TPCL manufacture involved cutting of the film layers and fabric plies, followed by manual stacking and compression moulding in a non-isothermal process. The steel stamp impregnation tool was treated properly with a high temperature resistant mould release agent (Frekote<sup>®</sup> 700 NC or Zyvox<sup>®</sup> Composite Shield) prior to hot pressing. A processing scheme is depicted in Fig. 32.

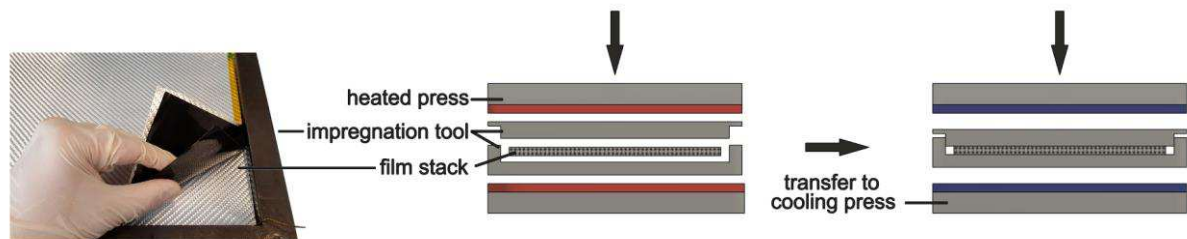


**Fig. 32** Processing scheme of TPCL manufacture via film stacking and hot compression moulding.

An overview of investigated fibre-matrix combinations is given in Table 14.

**Table 14** Overview of investigated TPCL fibre-matrix combinations.

Material	Glass fibres	Carbon fibres
PP	✓	
PA6	✓	✓
PC		✓
PPS	✓	✓
PEEK		✓

Depending on the thermoplastic matrix material, two different configurations of static presses were used. For matrices processable up to 300 °C, a combination of a heating and cooling press system (Wickert WLP 80/4/3 80-ton press and a Höfer H10 10-ton press) was used which were interconnected by a tool transport shuttle. For matrices which required higher processing temperatures, a high temperature heating/cooling press (Langzauner LZT-OK-220-L 220-ton press) capable of operating at up to 500 °C was utilised as shown in Fig. 33.



**Fig. 33** Static heating and cooling presses utilised in the experiments.

The temperature of every pressing cycle was monitored via thin-film thermocouples type-K 402-716 (TC Mess-und Regelungstechnik GmbH, Germany) positioned at the corner of the centre ply of the film stacks. A datalogger Testo 176 T4 (Testo SE, Germany) was used to record the temperature readings.

Some general TPCL processing guidelines for film stacking as practised throughout the work:

- Latex gloves are worn to prevent any contamination of the fabrics and films during handling.
- A clean cutting template e.g., steel sheet, which is marginally smaller than the cavity of the impregnation tool is used to cut fabric plies and film layers.
- Cutting of dry glass- and carbon fabrics is ideally conducted on a clean cutting mat with a roller cutter. Thermoplastic films are cut with a Stanley knife.
- The fabric rolls and cut fabric plies therefrom require very delicate handling in order to prevent weave distortion (sensitivity to trellis-shearing).
- The quality of impregnation can be influenced by the processing parameters temperature (polymer viscosity), dwell time and pressure.
- The hot press is pre-heated before insertion of the impregnation tool. By choosing an adequately high pre-heat temperature, faster tool heating is achieved. Additionally, possible thermal degradation of the polymer is greatly reduced. However, if the pre-heat temperature is set too high, uncontrolled temperature overshoot of the laminate is provoked. A heat up rate of 25-30 °C/min is targeted which is partly predetermined by

press system according to its heating performance, thermal masses involved and the material of the impregnation tool.

- The film stack is assembled carefully inside the cavity of the cold impregnation tool. The impregnation tool is closed with the top stamp and subsequently heated up in the press under low contact pressure e.g., 0.1-0.3 MPa. Low contact pressure is maintained until the thermoplastic polymer has reached its melting point. Macro impregnation around the fibre bundles commences and full impregnation pressure may be applied thereafter. As a rule of thumb, low contact pressure should be maintained roughly 10-20 °C above the polymer's melting point for at least one minute (semi-crystalline materials). If full impregnation pressure is applied from the get-go, severe fibre-washout will be provoked - the progressively melting polymer acts as an instable cushion which is displaced from higher pressure zones to lower pressure zones (edge of the mould).
- Optimal impregnation results for TPCL are observed with impregnation pressures of at least 0.5 MPa, ideally between 1.0-2.0 MPa and a dwell time of 5-10 minutes at least 20-40 °C above the polymer's melting point.
- If severe fibre-washout is still observed, the edges of the fabrics may be masked with high temperature polyimide adhesive tape to create creating a "resin dam" of sorts ("belts and braces approach"). The parallelism of the mould or press platens should also be checked and may need to be adjusted via shims. Apart from these potential factors, impregnation pressure may require to be lowered.
- Very high impregnation pressures >2-10 MPa can have an adverse effect on melt penetration due to compaction of the fibre bundles.
- In a two-press system TPCL are cooled with a cooling rate of roughly 10 °C/min and demoulded at 80-100 °C. The application of release agent to the mould prior to the pressing process is crucial for effortless demoulding.
- In general, the described TPCL manufacturing process is a non-isothermal process. The polymer viscosity which depends on the temperature, changes over the course of the process cycle. However, due to the low pressures and flow velocities involved during fabric impregnation an additional change in polymer viscosity (shear-thinning) is not occurring (compared to injection moulding). Therefore, during fabric impregnation by polymer melts quasi-Newtonian flow occurs [169,170]. The polymer viscosity can therefore only be lowered effectively by choosing higher processing temperatures [171].

Processing parameters of the utilised matrices are listed in Table 15.

**Table 15** Processing conditions of thermoplastic matrices during TPCL manufacture.

Material	Melting point [°C]	Impregnation pressure [MPa]	max. processing temperature [°C]	Dwell time above melting point [min.]
PP	165	1.5	220	10
PA6	220	1.5	260	10
PC	-	1.5	290	10
PPS	280	1.5	300,320	10
PEEK	343	1.5	380	10

### 5.2.2 GF-epoxy and CF-epoxy laminate manufacture

For comparative purposes, GF-epoxy and CF-epoxy laminates were prepared. The GF-epoxy material came as a deep-frozen prepreg and was processed via hot compression moulding, whereas the CF-epoxy laminates were manufactured by resin infusion as depicted in Fig. 34.



**Fig. 34** Vacuum assisted infusion of carbon fibre fabrics with epoxy resin. Resin inlet (left), resin outlet to vacuum pump (right) and infusion lines. Dry CF stack is covered by a peel ply, flow media and the vacuum bagging film (secured by sealant tape).

### 5.2.3 Analytical methods - specimen preparation, conditioning and mechanical testing

GF-TPCL, GF-epoxy and CF-epoxy laminates were cut on a water-cooled circular saw Diadisc 4200 (Mutronic Präzisionsgerätebau GmbH & Co. KG, Germany). CF-TPCL were cut on a circular saw Diadisc 5200 with a special saw blade for CF thermoplastic composites (Mutronic Diatool PKD-blade).



Specimens were cut according to specifications given in Fig. 35. The samples were subsequently conditioned in a climate chamber according to ISO 291 at 23 °C and 50% relative humidity [172].

The mechanical tests were carried out at 23°C and 50% relative humidity including:

- ILSS (apparent interlaminar shear strength) short beam flexural testing according to ISO 14130 [173] on a Zwick/Roell ZMART. Pro 10 kN universal testing machine. **(Publications III and IV)**
- Charpy impact testing according to ISO 179-1 [174] on a Zwick 5113.300 pendulum impact tester. **(Publications II and IV)**
- 3-point flexural testing according to ISO 14125 [175] on a Zwick/Roell ZMART. Pro 10 kN universal testing machine. **(Publications I-IV)**
- Tensile testing according to ISO 527-4 [176] on a 150 kN Zwick Z150 universal testing machine. **(Publication II)**
- Compression after impact (CAI) on an in-house constructed drop weight tower and compression test fixture according to ISO 18352 [177]. Compression tests were carried out on a 150 kN Zwick Z150 universal testing machine. **(Publication III)**
- Each sample set included 5 specimens (Charpy 10 specimens).

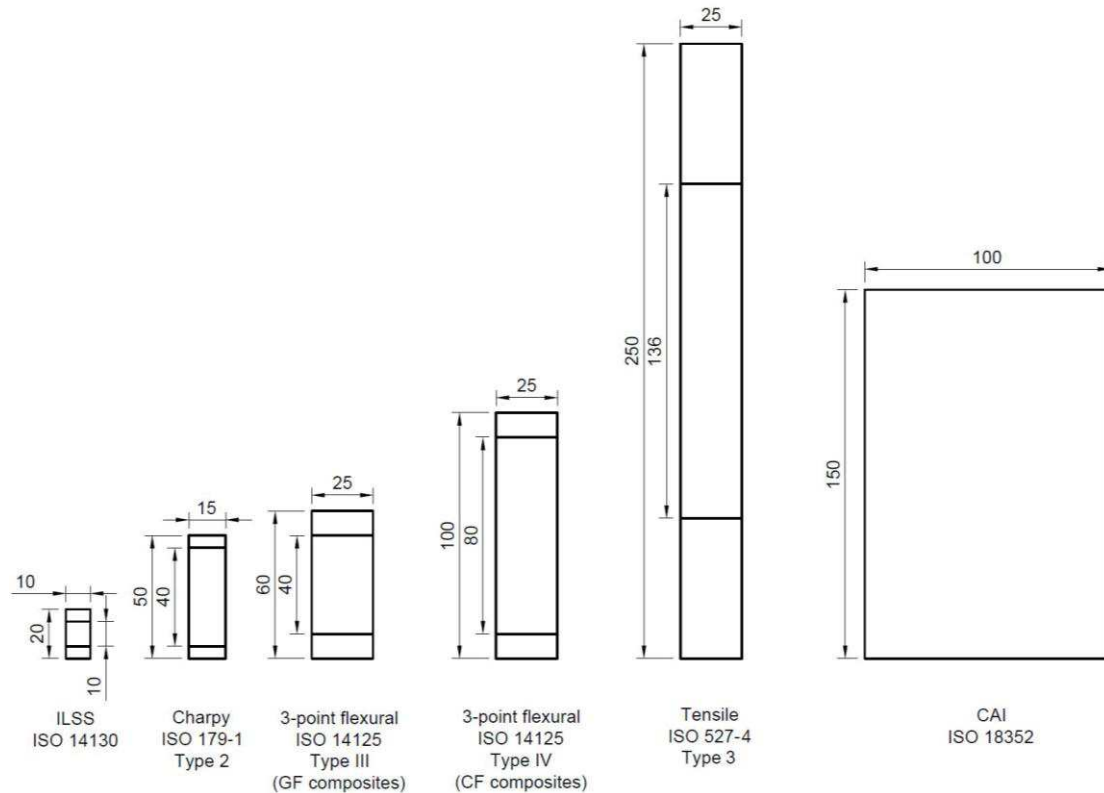


**Fig. 35** Standardised composite test specimens for  $2 \pm 0.2$  mm thick laminates. The inner dimension represents the support span or gage length, respectively. All dimensions are given in millimetres. Aluminium specimens were tested according to CF-composite specifications.

- Densities of composite samples  $\rho_{c\_experimental}$ , dry desized fibres  $\rho_f$  and matrices  $\rho_m$  were determined by buoyancy method in ethanol according to ISO 1183 [178]. (**Publications I-IV**)
- Thermogravimetric analysis of the same macroscopic samples (sample weight 1-2 grams) was carried out for the determination of fibre weight fraction  $\omega_f$  according to ISO 1172 resin burn-off method [179]. (**Publications I-IV**)
- The fibre volume fraction  $v_f$  (**Publications I-IV**) and sample porosity  $v_p$  (**Publication III**) were calculated according to equations (1), (2) and (3):

$$v_f = \frac{\omega_f \cdot \rho_{c\_experimental}}{\rho_f} \cdot 100 \quad (1)$$

$$v_p = \frac{\rho_{c\_theoretical} - \rho_{c\_experimental}}{\rho_{c\_theoretical}} \cdot 100 \quad (2)$$

$$\rho_{c\_theoretical} = \frac{1}{\frac{\omega_f}{\rho_f} + \frac{1-\omega_f}{\rho_m}} \quad (3)$$

- Alternatively, specimens were scanned via X-ray micro-computed tomography on a Phoenix/X-ray Nanotom 180NF (General Electric, USA) for a porosity/inclusion analysis. (**Publication IV**) Porosity/inclusions of the digital volume data was analysed by means of computer software Volume Graphics Studio (Volume Graphics, Germany).

### 5.2.4 Microscopical analyses

The quality of impregnation, consolidation and fracture behaviour was assessed via optical microscopy and SEM imaging of polished specimens. Specimens were embedded in epoxy resin and polished on a LaboPol-5 polishing machine (Struers GmbH, Germany) by means of silicon carbide discs and water. (**Publications I-IV**) The quality of fibre-matrix adhesion was assessed via SEM analysis. (**Publications I, III and IV**)

- Optical microscopy was carried out on a stereo microscope Stemi 2000-C (Carl Zeiss GmbH, Austria) (**Publication IV**)
- SEM imaging was carried out on a Vega II LMU (Tescan, Czech republic) (**Publications I-III**) and an FESEM MIRA3 (Tescan, Czech republic), preferably by back scattered electron imaging. (**Publications III and IV**)

## 6 Results and discussion

The following section reports on major findings that were made throughout the TPCL development efforts. The results will be discussed in the following order - publications focussing on TPCL development (**Publication I, III and IV**) and subsequently TPCL recycling (**Publication II**).

It should be pointed out that the most reliable mechanical test to differentiate interfacial adhesion between sets of TPCL samples was found by flexural strength testing. Other mechanical tests including interlaminar shear, tensile, compression or impact testing were found to be either unreliable (specimen slippage during compression testing or inelastic deformation during interlaminar shear testing) or providing no meaningful testing outcome to differentiate interfacial adhesion between specimens (tensile and impact testing). While the published scientific papers by Kiss et al. contain many additional mechanical property data of the developed TPCL, the following section focuses mainly on the flexural properties. While it can be argued that the flexural strength in the longitudinal direction is a fibre-dominated property, which it certainly is, it should be pointed out that the maximal strength properties of the fibres upon bending may be harnessed only by high interfacial adhesion.

### 6.1 GF-PP laminates (Publication I)

The first investigations revolved around the development of GF-PP TPCL. Due to their non-polar nature, PP matrices require modification with a slightly polar or reactive coupling agent, for instance MAH-g-PP. While short or long fibre GF-PP injection moulding compounds are common input materials in engineering, it is quite certain that a coupling agent is always used within the material mix. However, raw material suppliers usually do not disclose the amount of coupling agent added to the PP matrix, which strongly depends on the glass fibre loading. Therefore, it was necessary to assess the required MAH-g-PP concentration for adequate mechanical performance in TPCL with a fibre volume fraction in a region of 50% (=74 wt%). Since good adhesion cannot be expected solely by the addition of a coupling agent, compatible fibre coatings had also to be found. A comprehensive screening study was conducted, whereby several direct sized roving fabrics and finished glass yarn fabrics were tested.

Composite strength was highly sensitive to the concentration of MAH-g-PP coupling agent as displayed in Fig 36. It should be noted that the grafting level of the utilised MAH-g-PP coupling agent Polybond 3000 (1.2 wt% grafted MAH) was normalised to the active MAH content in the blend with PP homopolymer HK060AE. Without the presence of MAH-g-PP, the PP-

compatible roving fabric StarRov 490 offered higher strength compared to the FK144 Volan A chromium complex finished yarn fabric. This initial difference in strength was apparently due to an MAH-g-PP based film former in the direct sizing of StarRov 490, which facilitated interfacial adhesion. Upon addition of MAH-g-PP coupling agent to the PP matrix the initial advantage of StarRov 490 was compensated and both fabrics exhibited similar mechanical performance. The exceptional compatibility of Volan A chromium complex with modified PP was unexpected and reported as a novel finding [22]. Overall, a saturation effect in mechanical performance came into existence in a region between 0.04-0.06% MAH for an average fibre volume fraction of 50%. Higher MAH concentrations did not result in significant strength gains. Due to an efficiency driven study, 0.04% MAH additive was chosen for further investigations.

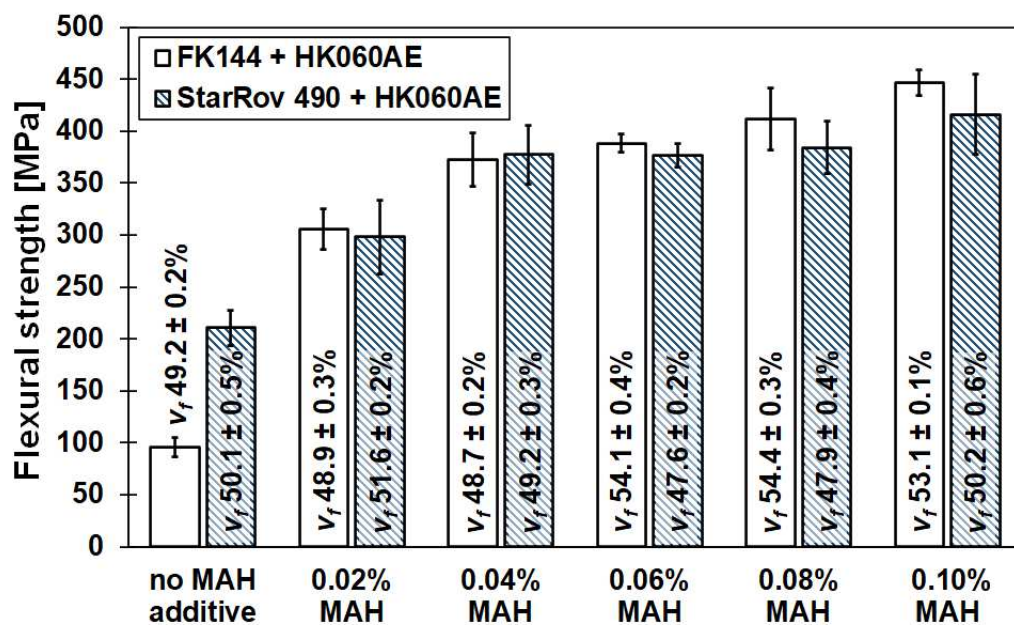


**Fig. 36** Flexural strength vs. active MAH content (Polybond 3000) in HK060AE (PP matrix). Fabrics used: FK144 (Volan A chromium complex GF finish) and StarRov 490 (PP-compatible GF direct sizing). (**Publication I** [22]).

The fact that MAH-based coupling agents are also utilised in the industrial GF-PP reference material Tepex dynalite 104 could be verified by ignition of the PP matrix and identification of a slightly pungent odour characteristic for MAH-g-PP additives. The strength level of 370 MPa of the Tepex 104 material could be reached with certain fabrics as depicted in Fig. 37. It was recognised that Tepex 104 might have had a slightly higher degree of modification than 0.04% MAH, due to a lower fibre volume fraction of 45% compared to the in-house moulded TPCL with an average fibre volume fraction of 50%. Therefore, the MAH modification of Tepex 104 could have been in the range of 0.05-0.06%.

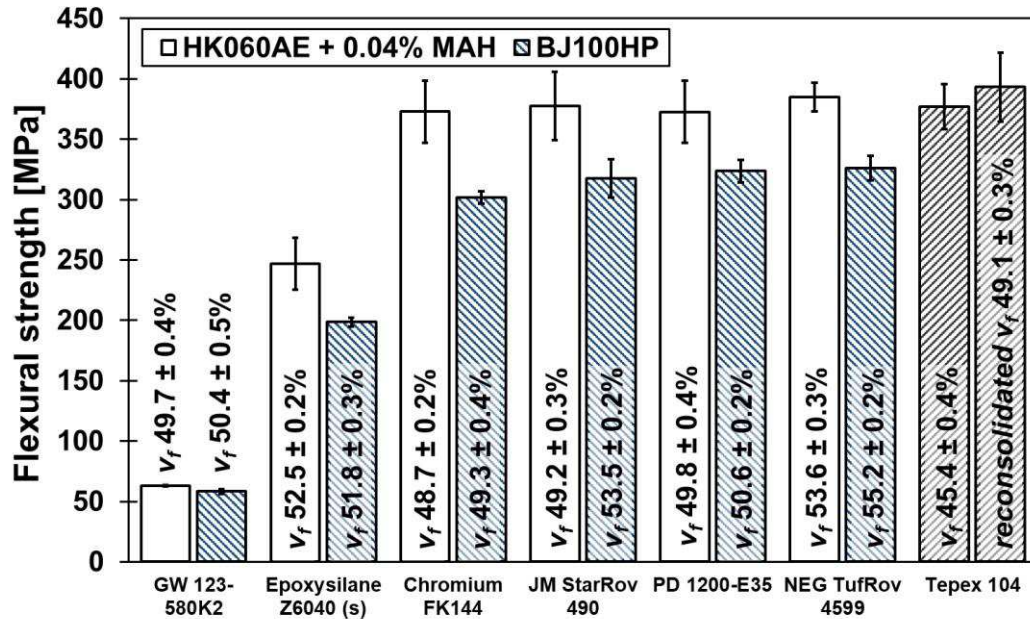
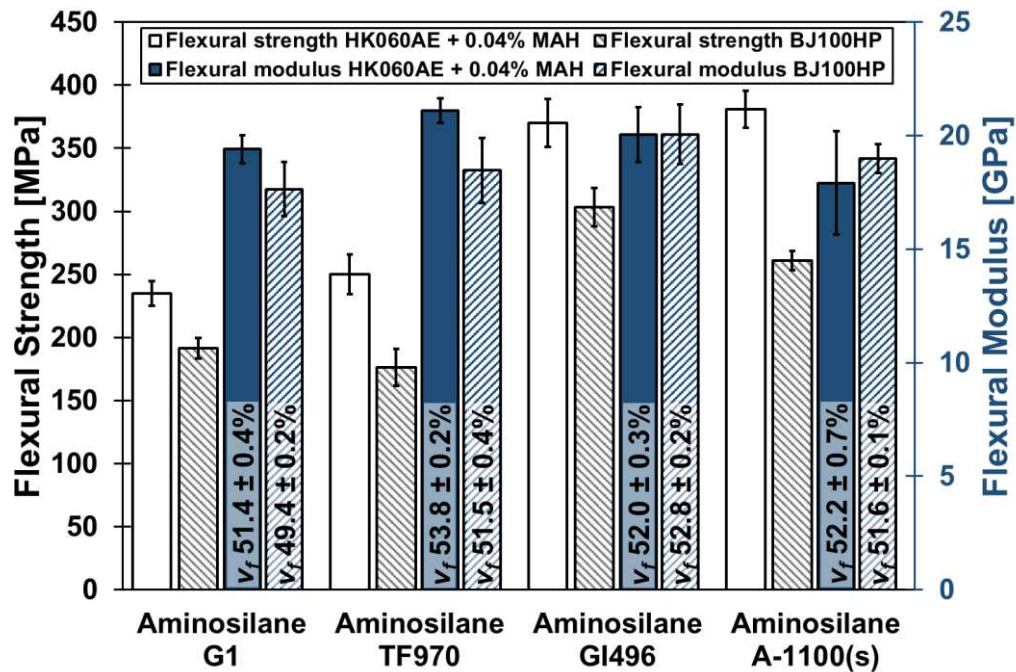


Fig. 37 Flexural strength of in-house moulded TPCL vs different fabrics and industrial reference TPCL. (**Publication I** [22]).

Different PP-compatible direct sized roving fabrics (StarRov 490, PD 1200-E35 and TufRov 4599) were found to perform equally. Even though the direct sizings of these rovings contained many unknown ingredients that supposedly impede adhesion, their performance was on a par with finished fabrics. The advantage of finished fabrics, was most likely influenced by a performance knock down due to the upstream heat cleaning process which is known to deteriorate fibre strength. The industrial grade copolymer PP BJ100HP (with factory coupling agent modification) did result in lower laminate strengths throughout. Due to this observation, a lower level than 0.04% MAH was expected within this compound. It is highly likely that PP BJ100HP is optimised for injection moulding of short fibre-reinforced composites, which typically have considerably lower fibre contents than TPCL. Since similarly modified PP grades are not available on the market, in-house preparation of modified PP is a necessity for high-performance TPCL production.

The flexural stiffness of the GF-PP TPCL was relatively constant. In general, the flexural modulus is measured at low strains and therefore mostly sensitive to the fibre orientation and fibre content rather than on interfacial adhesion. The flexural stiffness of most TPCL was measured in a region of 20 GPa with slight deviations for PP-incompatible fabrics (such as GW 123-580 K2 thermoset compatible). The different behaviour of the GW 123 fabric arose most possibly due to due to an incompatible film former, which caused poor wettability and interfacial void formation.

Further comparisons included different aminosilane finished fabrics. The most effective aminosilane for GF-PP compatibilization was the aminosilane type A-1100 as depicted in Fig. 38. The aromatic aminosilane G1 and the two proprietary aminosilane blends TF970 and GI496 did not outperform the aminosilane type A-1100.



**Fig. 38** Flexural properties of aminosilane finished fabrics in GF-PP TPCL. (Publication I [22]).

In GF-PP TPCL the interfacial adhesion was expected to be the result from wetting, chemical adhesion, interdiffusion and entanglement. An acid-base reaction between the aminosilanes and maleic anhydride (or its hydrolysed form maleic acid - a dicarboxylic acid) was thought to occur during composite processing, following the formation of amides or even further reaction to imides. As observed, the selected aminosilane type is of high significance for laminate performance. Here, the aminosilane with a primary amine group (A-1100) offered the best mechanical properties compared to aminosilanes with aromatic groups (G1) for example. The aromatic aminosilanes may have offered reduced reactivity or lower accessibility for interdiffusion of MAH-g-PP. In conclusion, it is evident that direct sizings most possibly contain an aminosilane component such as A-1100.

Different adhesion promoters including epoxysilanes and Volan A chromium complex also yielded high to very high laminate strengths. Epoxides could react with water, giving di-alcohols followed by the formation of bis-esters with maleic anhydride or maleic acid. In the case of Volan A chromium complex some form of radical crosslinking reaction with the methacrylic group or organometallic reactions between chromium and maleic anhydride were inferred. Unfortunately, ATR-IR (attenuated total reflection infrared spectroscopy) analysis did not provide any meaningful experimental confirmation of chemical bond formation since the

fractured fibre interfaces were always covered by too much of the bulk matrix material. The attained IR-spectra were strictly that of pure PP.

### 6.1.1 GF-PP laminates unpublished results

In preliminary experimental trials, PP films were extruded with natural colour (no carbon black masterbatch added) and moulded with FK144 Volan A chromium complex finished glass yarn fabrics. A relatively interesting effect was noticed, in that the FK144 Volan A chromium complex finished laminates changed in hue depending on the MAH coupling agent concentration. To demonstrate this effect clearly, strips of differently modified PP films were stacked side-by-side and compression moulded with the fabric. Clear boundaries appeared between the regions of different coupling agent concentration as shown in Fig. 37. The effect that Volan A chromium complex finished fabrics result in blueish-green tinted laminates has been only reported for strongly coupled thermoset resins so far [30]. Clearly, there had to be some sort of chemical reaction, or extremely good wetting between Volan A chromium complex and MAH-g-PP to achieve this sort of effect.

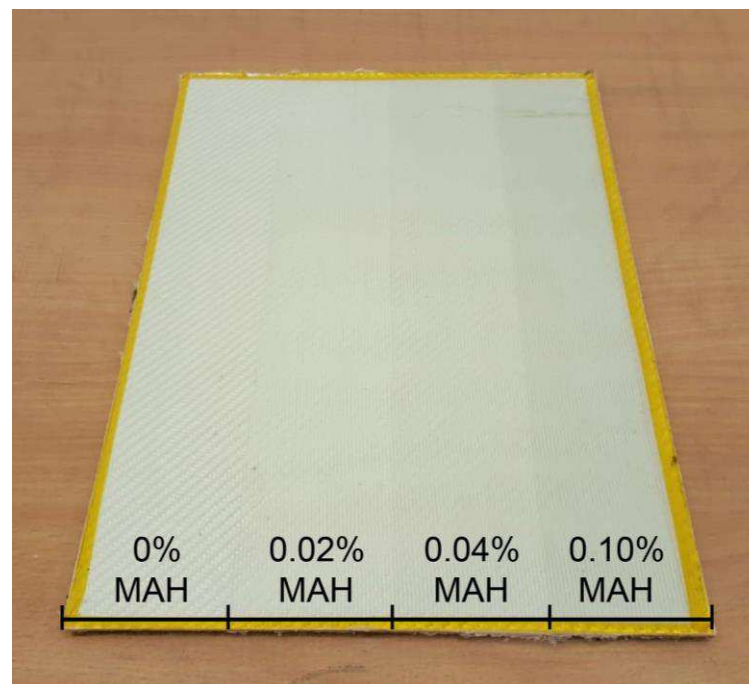


**Fig. 39** FK144 Volan A chromium complex finished glass yarn fabric laminate, impregnated with strips of natural coloured PP HK060AE films with different MAH coupling agent concentrations. The change in hue indicates improved wettability or coupling between MAH and the Volan A chromium complex finish.

When the compression moulding experiments were subsequently focussed on coarsely woven roving fabrics, undesirable visual effects were noticed that did not occur with formerly tested tightly woven yarn fabrics. The gaps between adjacent rovings (low weave density) resulted in

translucent matrix-rich areas with the clear PP matrix as demonstrated in Fig. 40. Quite interestingly, the 2/2 twill woven roving fabric also appeared as if it had been plain-woven. This second effect occurred most likely due to similar refractive indices of glass, its sizing and the PP matrix. Due to the partial translucency of intersecting strands an optical loss of the weave structure was provoked. The visual appearance of woven roving laminates could be subsequently improved dramatically by the addition of carbon black masterbatch. The 2/2 weave pattern was visible again in the laminate upon addition of 1.0 wt% carbon black masterbatch. Therefore, all subsequent laminates were modified with 2.0 wt% carbon black pigment masterbatch. A detrimental effect on mechanical performance due to possible adsorption of MAH-g-PP to the carbon black masterbatch was not observed.



**Fig. 40** Required amount of carbon black masterbatch to make GF-PP TPCL visually more appealing.

In Fig. 41, a visual comparison between the industrial reference Tepex dynalite 104 is given with an in-house moulded TPCL based on StarRov 490 600 gsm roving fabric + PP HK060AE + 0.04% MAH + 2.0 wt% carbon black master batch.



**Fig. 41** Comparison of industrial reference TPCL Tepex dynalite 104 (left) overlapped with in-house developed GF-PP TPCL with 2.0 wt% carbon black masterbatch (right background). Apart from the visual optimisation of GF-PP TPCL the effect of different MAH-g-PP coupling agents on mechanical performance was examined in a screening test. For the sake of clarity, the blend formulations of MAH-g-PP with PP homopolymer are outlined in Table 16. The different



grafting levels of the MAH-g-PP additives were normalised to active MAH content in the PP blends for a fair comparison.

**Table 16** Blend formulations of MAH-g-PP and PP HK060AE homopolymer. Additives sorted according to fluidity.

MAH-g-PP additive	MAH grafting level [wt%]	0.04% MAH blend formulation*	0.10% MAH blend formulation*	Melt mass-flow rate MFR [g/10 min]**
Scona <sup>®</sup> TPPP 9112 GA [wt%]	1.0	4.0	10.0	70 - 120
Scona <sup>®</sup> TPPP 9212 GA [wt%]	1.8	2.2	5.6	80 - 140
Orevac <sup>®</sup> CA100 [wt%]	1.0	4.0	10.0	>100
Polybond <sup>®</sup> 3000 [wt%]	1.2	3.3	8.3	405
Priex <sup>®</sup> 20097 [wt%]	0.45	8.9	22.2 - not tested due to unrealistic additive quantity	>>1000 hyperfluid

\* MAH-g-PP quantity utilised in the blend normalised to active MAH content depending on the grafting level of the additive for fair comparison.

\*\* (at 190 °C, 2.16 kg)

The experimental results are displayed in Fig. 42 and Fig. 43. The results were generally expected to be more pronounced due to the difference in molecular weight of the MAH-g-PP polymer chains. Notwithstanding, a very slight trend among different MAH-g-PP coupling agents could be observed. MAH-g-PP coupling agents with higher fluidity (higher melt mass-flow rate) resulted in slightly better mechanical performance possibly due to better wet-out and faster migration of the additive to the fibre surface during manufacturing. MAH-g-PP coupling agents with low MFR resulted in slightly lower mechanical properties despite their supposedly longer polymer chains and likelihood of facilitating entanglements. However, the higher molecular weight could have also hindered the migration of the additive to the fibre surface, considering the low-shear TPCL compression moulding process. Polybond 3000 was subsequently chosen as the main input additive due to the well-balanced properties of both tested fabrics. This is not to say that the other MAH-g-PP coupling agents are not equally effective for TPCL production.

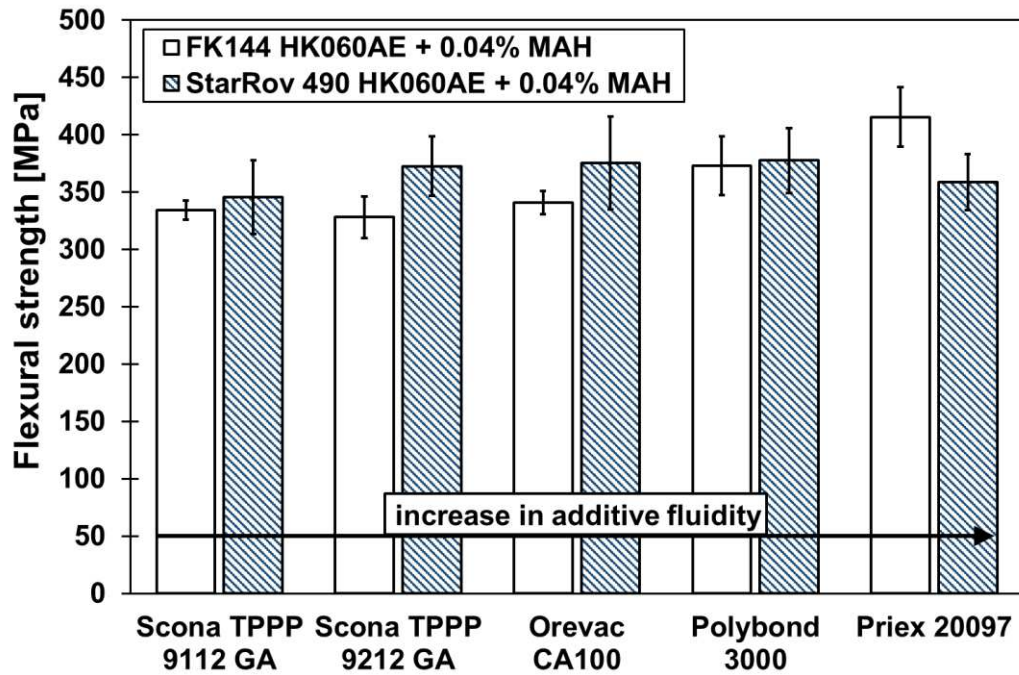


**Fig. 42.** Flexural strengths of different MAH-g-PP coupling agent additives in GF-PP TPCL at an active MAH concentration of 0.04%.

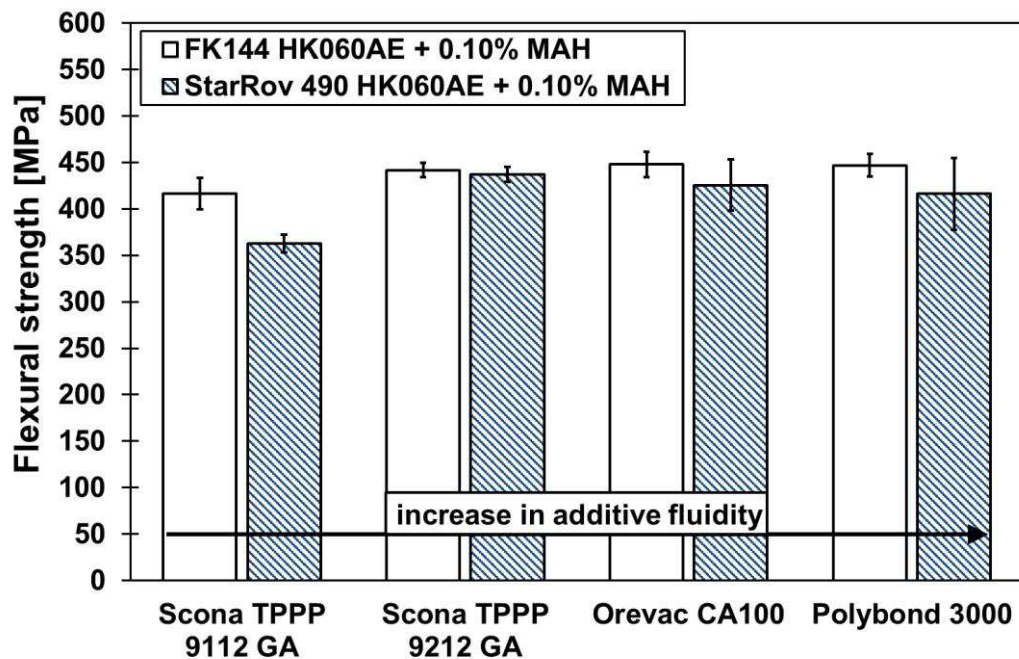


**Fig. 43** Flexural strengths of different MAH-g-PP coupling agent additives in GF-PP TPCL at an active MAH concentration of 0.10%

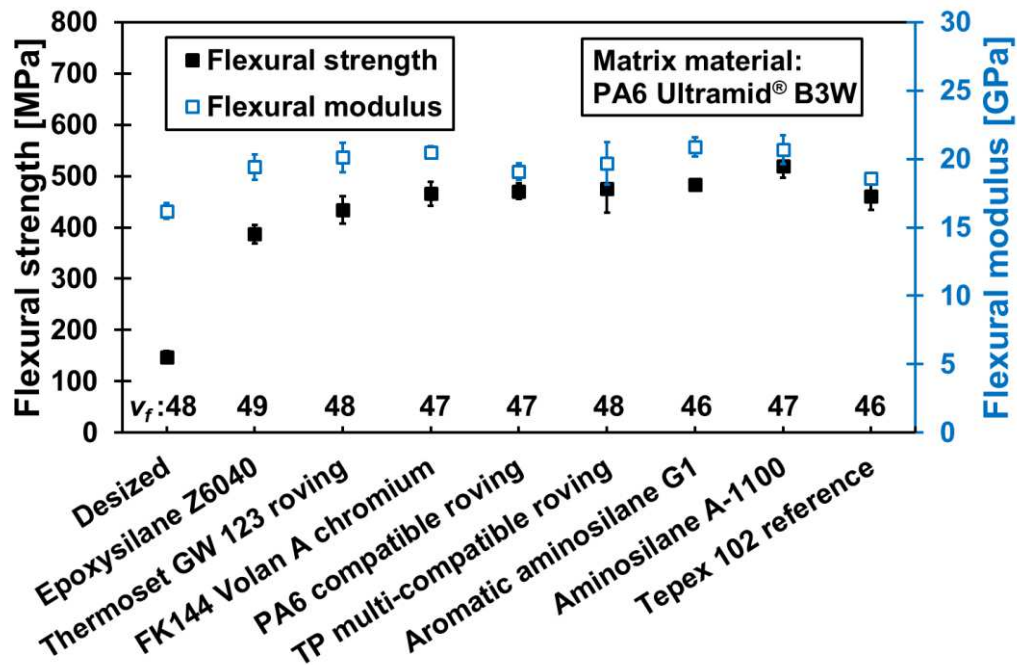
Summarising, GF-PP TPCL were developed successfully in terms of high mechanical performance and optimised visual appearance. The combination of an MAH-g-PP coupling agent together with a suitable fibre coating system (preferably an aminosilane based coating)

was found to be decisive for promoting sufficient interfacial adhesion for high-performance applications. An MAH concentration range of 0.04-0.06% was optimal for attaining high laminate strengths in the region of industrial products.

## 6.2 GF-PA6 laminates (Publication III)

After successful development of GF-PP TPCL, research was focussed on the development of GF-PA6 TPCL. Basic pressing parameters including 1.5 MPa impregnation pressure and 0.5 MPa consolidation pressure were carried over from the first study. In the GF-PA6 compatibility study several glass fibre fabrics with different finish or sizing compositions were compared to identify potential high-performance candidates.

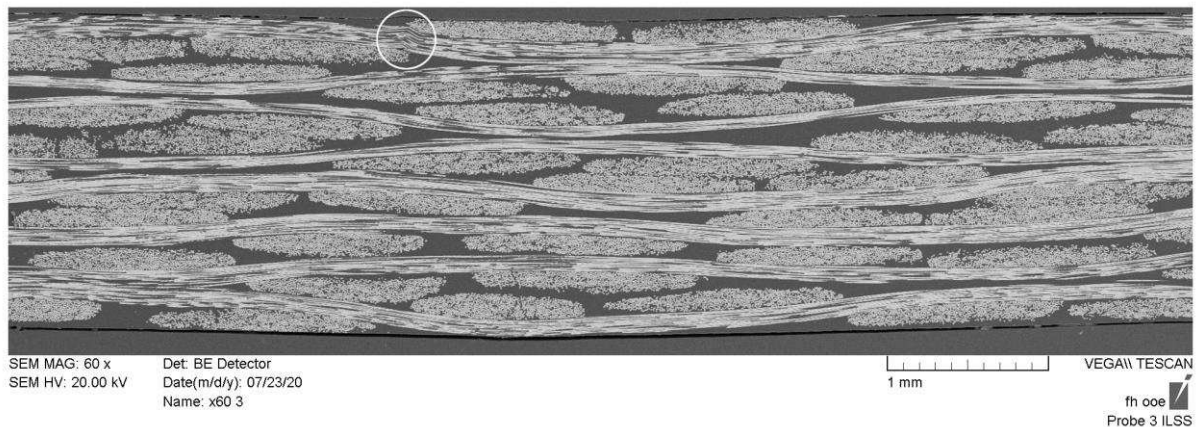
As can be seen in Fig. 44, it became apparent that the flexural modulus of the laminates was in a relatively constant region of 20 GPa and not affected largely by interfacial adhesion, whereas flexural strength varied greatly depending on the fibre coating. The sample sets had a fibre volume fraction of 46-49%, which ensured good comparability. The GF-PA6 laminate prepared with desized (heat cleaned) glass fibres boasted a mean flexural strength of merely 150 MPa. Upon usage of specific finishes or sizings, the mean flexural strength increased up to 520 MPa. The flexural properties of the industrial GF-PA6 reference material Tepex dynalite 102 could be surpassed, e.g. by the aminosilane A-1100 finished GF-PA6 TPCL.



**Fig. 44** Flexural properties of GF-PA6 TPCL prepared from differently modified glass fibre fabrics and neat PA6 matrix. GF-PA6 specimens were tested in conditioned state (23 °C, 50% relative humidity, 14 days duration of conditioning). (**Publication III** [24])

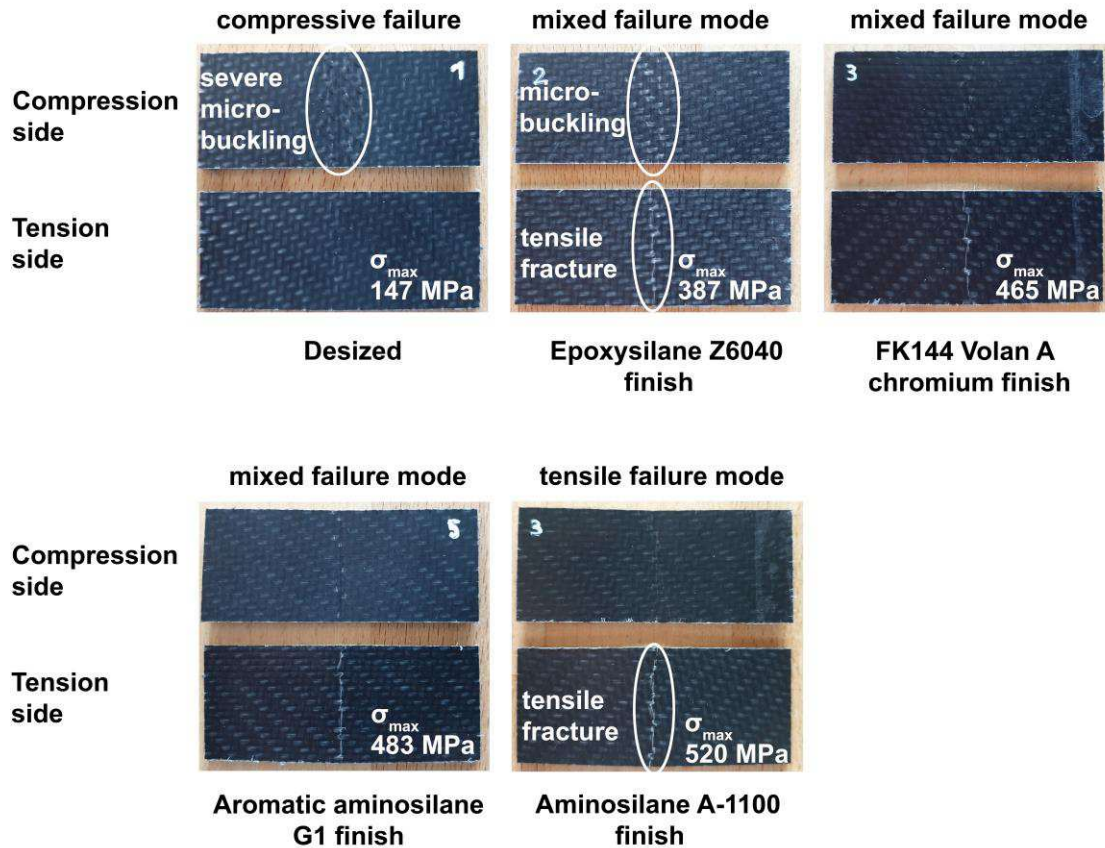
Interestingly, the film former of the thermoset compatible roving fabric GW 123 that was formerly reported to be completely incompatible with PP, offered great compatibility with PA6. The GW 123 GF-PA6 laminate boasted a mean flexural strength of 434 MPa. This unexpected result verified that compatibility studies with specific fabrics are crucial during composite material development. In this case, the GW 123 fabric can be considered a low-cost alternative to the generally more expensive fabrics with PA6-tailored sizings such as StarRov 895.

Fig. 45 shows a cross-section of a GF-PA6 ILSS test specimen with A-1100 aminosilane finish. The image shall demonstrate the impregnation quality and void-free structure of the in-house prepared laminates.



**Fig. 45** Cross-section of compression moulded 8-ply GF-PA6 TPCL with A-1100 finish. The microstructure of the laminate appeared fully impregnated and void-free. (**Publication III [24]**)

Among the GF-PA6 TPCL flexural sample sets a distinctive behaviour in the failure mechanism could be identified depending on the adhesion promoter used. As displayed in Fig. 46, the desized (no adhesion promoter) GF-PA6 TPCL failed due to compressive micro-buckling only, indicating poor interfacial adhesion. In the case of finished glass fibres with adhesion promoters such as epoxysilane, Volan A or aromatic aminosilane G1 the failure pattern changed to a mixed compressive-tensile failure mode. Eventually, the laminate with the highest mean flexural strength of 520 MPa (aminosilane A-1100 finished glass fibres) failed primarily in tensile mode with minimal signs of micro-buckling. This circumstance was indicative of good interfacial adhesion between the aminosilane A-1100 and PA6. Failure mechanisms changing from the compression side to the tension side of TPCL specimens depending on the adhesion promoter used has not been demonstrated in literature so far.



**Fig. 46** Different specimen failure mechanisms of flexural tested GF-PA6 TPCL. Failure mechanisms changing from compressive micro-buckling to mixed compressive-tensile failure depending on the adhesion promoter and quality of interfacial adhesion (adapted from [24]).

### 6.2.1 GF-PA6 laminates unpublished results

In an attempt to improve the strength properties of GF-PA6 TPCL, PA6 was modified with EBA-g-MAH coupling agent and impact modifier (ethylene butyl acrylate copolymer functionalised with maleic anhydride - Scona<sup>®</sup> TSEB 2113 GB) as outlined in Table 17.

**Table 17** Blend formulations of EBA-g-MAH and PA6 Ultramid<sup>®</sup> B3W homopolymer.

EBA-g-MAH additive	MAH grafting level [wt%]	0.04% MAH blend formulation*	0.06% MAH blend formulation*	Melt volume-flow rate MVR [g/10 min]**
Scona <sup>®</sup> TSEB 2113 GB [wt%]	0.6	6.7	10.0	3 - 8

\* EBA-g-MAH quantity utilised in the blend normalised to active MAH content depending on the grafting level of the additive.

\*\* (at 190 °C, 2.16 kg)

At sufficiently high concentrations, the additive did neither improve the flexural nor the Charpy impact properties as displayed in Fig. 47 and Fig. 48. The mean flexural strength remained unaffected within a region of 480 MPa. Likewise, the mean Charpy impact strength remained unaffected within 110 kJ/m<sup>2</sup>. It is thinkable that the EBA-g-MAH additive is potentially more effective in improving the properties of short fibre compounds.

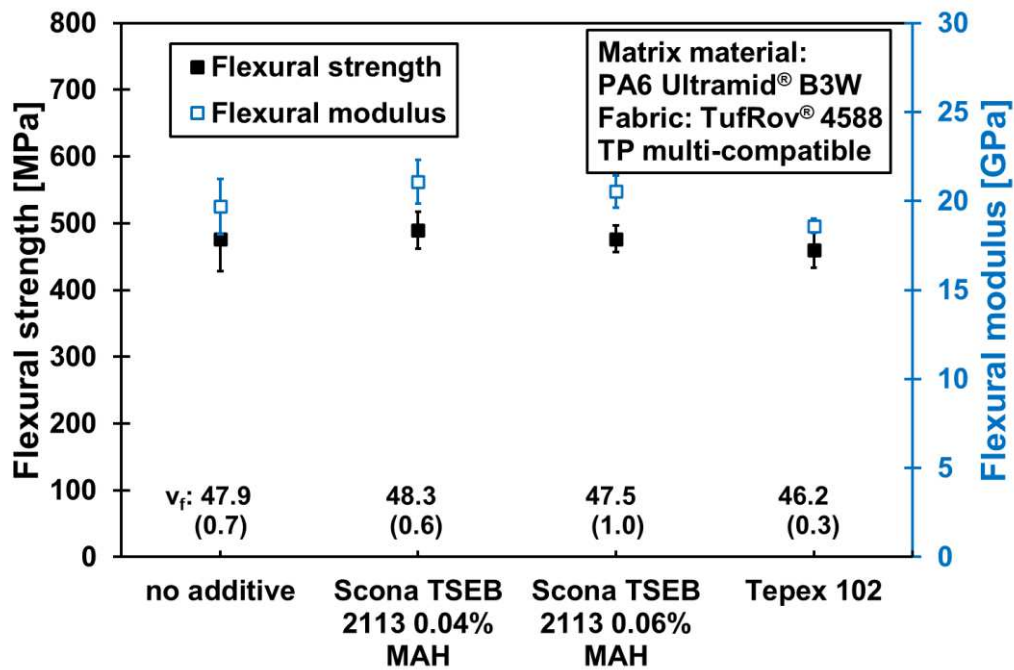


Fig. 47 Flexural properties of GF-PA6 TPCL modified with coupling agent EBA-g-MAH.

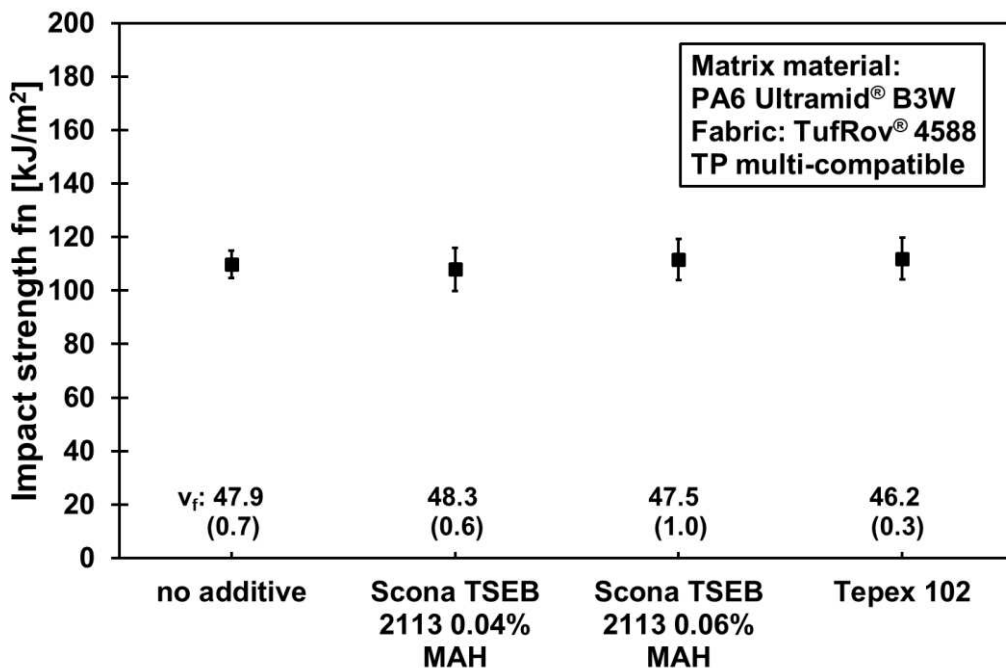


Fig. 48 Charpy impact properties of GF-PA6 TPCL modified with coupling agent EBA-g-MAH.

Ultimately, the mechanical properties of GF-PA6 TPCL could not be improved further by means of matrix modification. Neat PA6 offered sufficient interfacial adhesion for the production of high-strength TPCL with fibre coatings based on aminosilanes.

### 6.3 GF-PPS laminates (Publication III)

Parallel to the GF-PA6 TPCL development, GF-PPS TPCL were developed in an effort to utilise the capabilities of a high-performance thermoplastic matrix. Promising findings were obtained for compatibilisation of PPS with continuous glass fibres through flexural testing. As shown in Fig. 49, the highest performing glass fibre fabrics were based on the TP-multicompatible roving (TufRov<sup>®</sup> 4588 direct sizing) and yarn fabrics with aminosilane A-1100 and FK144 Volan A chromium complex finish.

The exceptional compatibilities of aminosilane A-1100 and FK144 Volan A chromium complex with PPS have not been reported in literature to date. The mean flexural strength of GF-PPS TPCL with FK144 Volan A chromium complex finish topped out at 772 MPa ( $v_f$ : 56%), which is quite an impressive value for a woven glass fibre-reinforced laminate. In comparison, an industrial GF-epoxy prepreg performed moderately to the best performing GF-PPS TPCL. Unfortunately, an industrial GF-PPS reference TPCL could not be acquired at the time of testing.

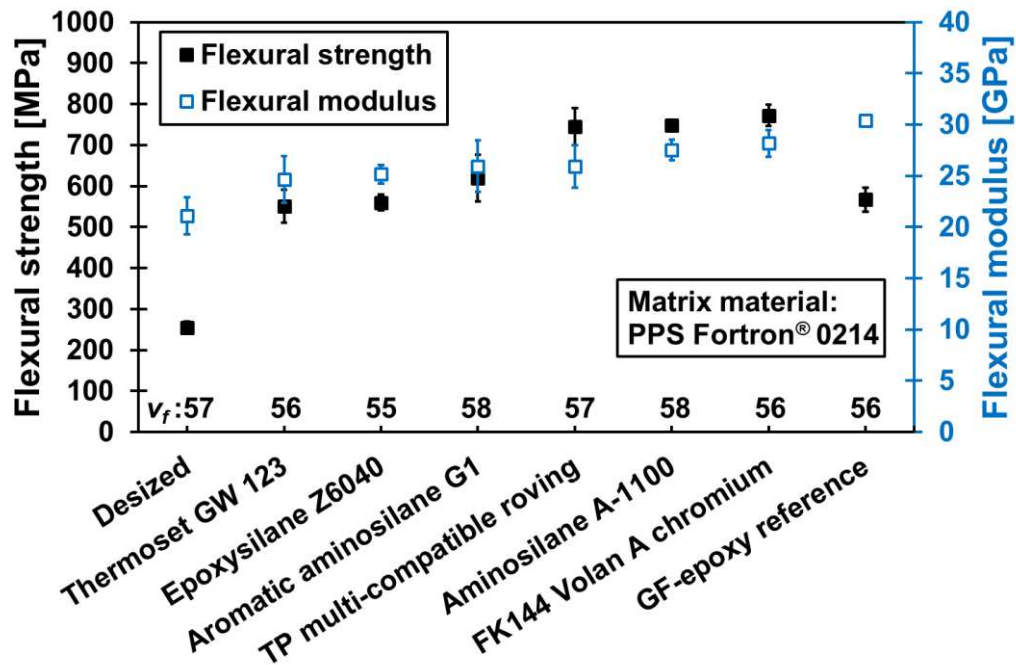
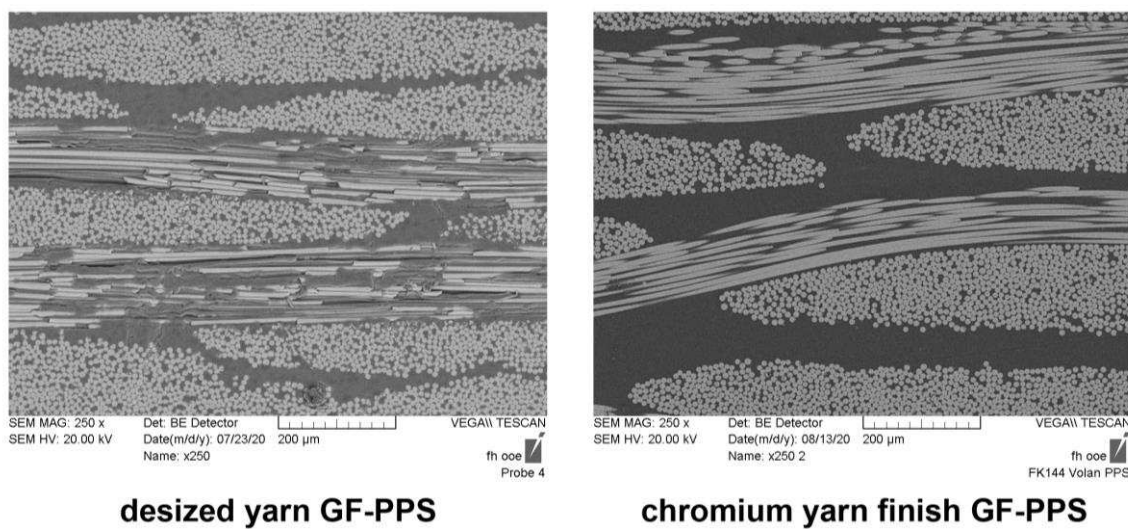


Fig. 49 Flexural properties of GF-PPS TPCL prepared from differently modified glass fibre fabrics and neat PPS matrix. (Publication III [24])

Importantly, the only GF-PPS TPCL that evinced no sign of oxidative discolouration (browning) after moulding were the desized TPCL, thermoset GW 123 TPCL, and FK144

Volan A chromium finish based TPCL. The epoxysilane and aminosilane based TPCL (including the TP-multicompatible roving Tufrov 4588<sup>®</sup>) were prone to slight oxidation at moulding temperatures close to 300 °C and a dwell time of 10-15 minutes at that temperature. Considering the high performance characteristics and oxidative resistance given by FK144 Volan A chromium complex, it appeared as a viable candidate for future PPS based TPCL developments.

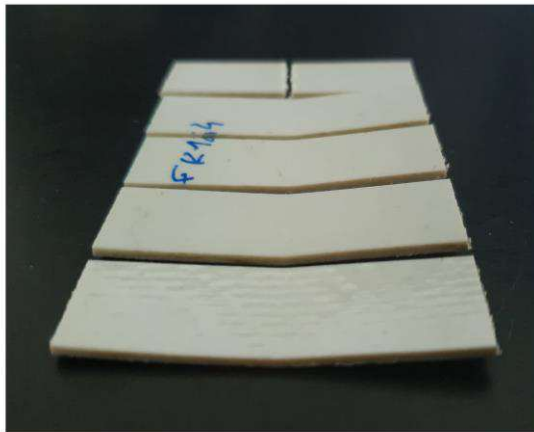
Fig. 50 shows cross-sections of the lowest performing GF-PPS laminate (desized) and the highest performing laminate (FK144 Volan A chromium complex). It can be seen that both laminates were fully impregnated by the matrix and thereby comparable. The materials differed only in their interfacial adhesion, visible by the fibre pull-outs within the desized laminate.



**Fig. 50** GF-PPS TPCL cross-sections indicating good impregnation of both desized (left) and FK144 Volan A chromium finished (right) materials. (**Publication III** [24])

Quite astonishingly, the FK144 Volan A chromium complex based GF-PPS TPCL was the only laminate to show pure tensile fracture, which is indicative of very high adhesion strength. The flexural tested series is displayed in Fig. 51.





**chromium yarn finish GF-PPS  
compression side**



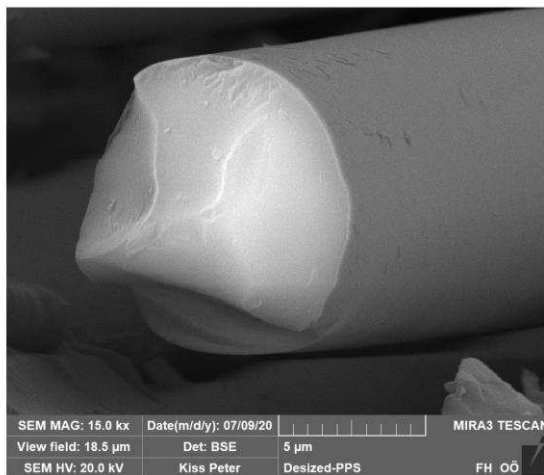
**chromium yarn finish GF-PPS  
tension side**

**Fig. 51** Flexural tested GF-PPS TPCL based on FK144 Volan A chromium complex finish.

The test specimens evinced tensile fracture only without compressive micro-buckling.

**(Publication III [24])**

In fact, a clear difference in microscale adhesion was observed during SEM imaging as shown in Fig. 52. While the flexural tests were indirect methods to assess the quality of interfacial adhesion, the experimental results correlated very well with the fracture morphology. The effect of interfacial adhesion on macroscopic composite properties could be demonstrated quite clearly.



**desized yarn GF-PPS**



**chromium yarn finish GF-PPS**

**Fig. 52** SEM images of fractured GF-PPS TPCL. Left: Desized GF-PPS laminate with interfacial debonding and no adherent PPS matrix on the glass fibre. Right: GF-PPS laminate with FK144 Volan A chromium complex finish exhibiting cohesive failure and a fully adhered layer of PPS matrix on the glass fibre. **(Publication III [24])**

For glass fibre TPCL, both Volan A chromium complex and aminosilane A-1100 seemed to be highly potent multi-compatible finishes. They promoted exceptionally high interfacial adhesion with PP, PA6 and PPS matrices. Potentially, even a multitude of other thermoplastics might be compatibilised with these adhesion promoters.

#### 6.4 CF-PA6, CF-PPS and CF-PEEK laminates (Publication IV)

The final part of TPCL development work focussed on carbon fibre-reinforced thermoplastics. The eventual approach taken for the compatibilisation of carbon fibres with thermoplastics was quite different to the aforementioned successful technique of glass fibres silanization.

Preliminary compression moulding trials with PA6 and epoxy-sized (EP-sized) carbon fibre fabrics resulted in highly unsatisfactory material properties. Despite a high impregnation pressure and a moulding temperature of 260 °C the EP-sized carbon fibre fabrics did not wet-out properly. The laminates displayed excessive fraying during cutting and the overall material performance during flexural testing was very poor (mean flexural moduli of 9 GPa and strength of 82 MPa).

It became clear that the EP-sizing had caused this major incompatibility and that the sizing had to be removed, ideally, by a quick and efficient measure before the TPCL compression moulding process. MTGA analyses helped to investigate the decomposition behaviour of the EP-sizing as illustrated in Fig. 53. The loss on ignition (LOI, % weight loss) in air atmosphere and 400 °C was identified at 1.1%, which roughly corresponded to the sizing amount specified by the fibre manufacturer (1.3%). Moreover, the MTGA curve progression indicated that the sizing was decomposable within a short timeframe. This observation assisted the selection of a fabric desizing method, eventually turning to desizing via infrared-irradiation.

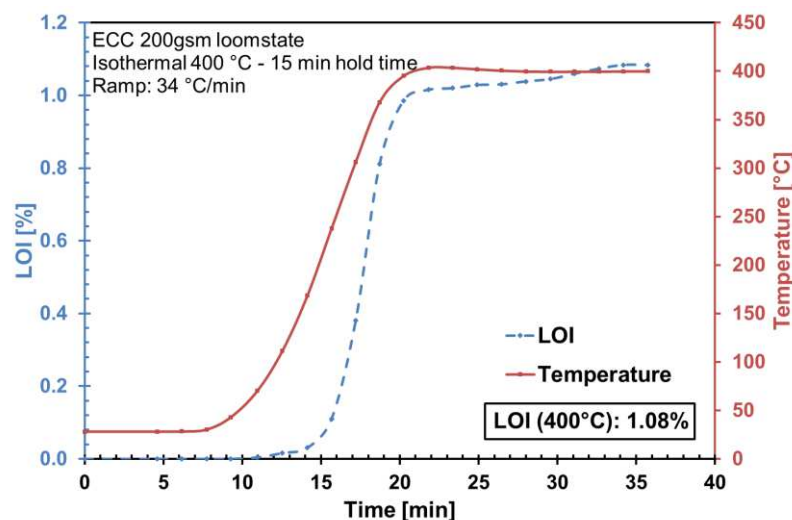


**Fig. 53** Decomposition behaviour of EP-sizing measured by thermogravimetric analysis. A decomposition onset of the EP-sizing at roughly 250 °C was observed. (Publication IV [25])

Subsequently, infrared desizing (IR-desizing) experiments were conducted in-house on single fabric plies (1·1 m<sup>2</sup>) as demonstrated in Fig. 54. The fabric temperature was brought to 400 °C within 1 minute and subsequently held for 20 seconds. No more decomposition gasses were generated thereafter.

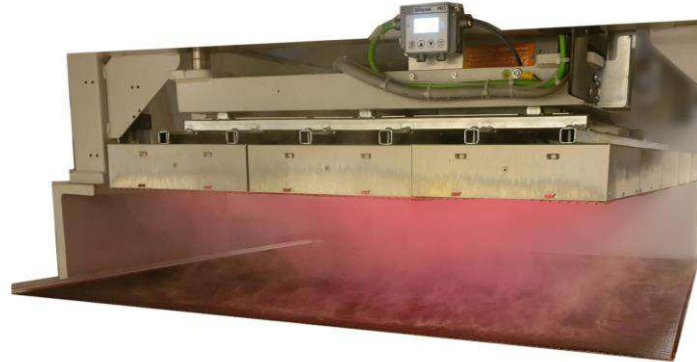


**Fig. 54** CF-fabric desizing by means of infrared irradiation (IR-desizing) at 380-400 °C.  
(Publication IV [25])

The desizing results were reviewed by SEM analyses. As can be seen in Fig. 55, the IR-desized carbon fibre reinforcement appeared free from sizing residues on the microscale following IR-exposure at 400 °C.

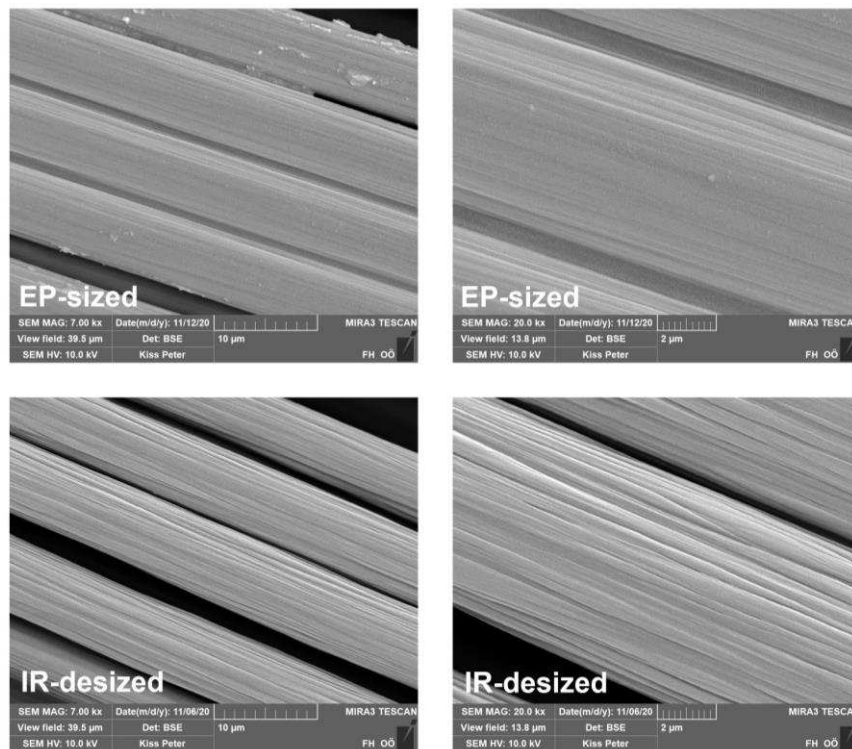


**Fig. 55** SEM images of EP-sized (top) and IR-desized (bottom) carbon fibre reinforcement. Note, the IR-desized fibres appeared completely free from sizing residues after heating to 400 °C in air atmosphere. (Publication IV [25])

Iterative MTGA analyses of the IR-desized carbon fibre fabrics verified that the fabrics were desized fully. The LOI of desized carbon fibre fabrics typically did not exceed 0.05% as shown in Fig. 56.

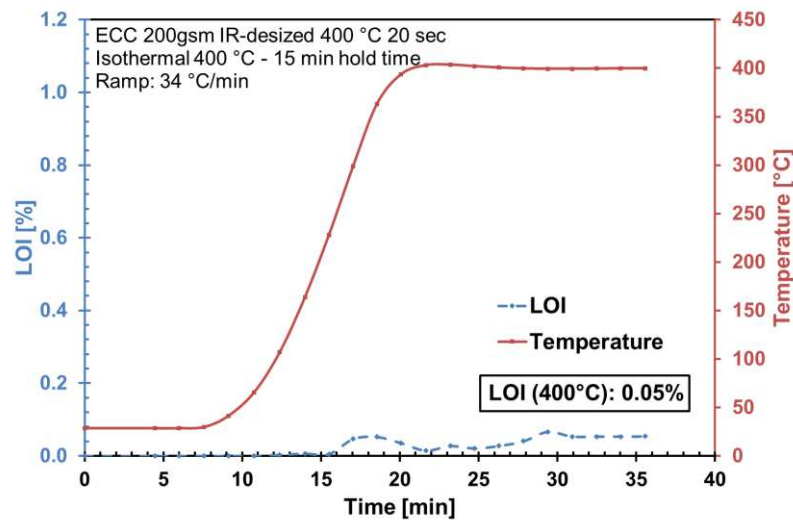


**Fig. 56** MTGA analysis of an IR-desized carbon fibre fabric indicating full removal of the sizing due to the low LOI measured. (Publication IV [25])

Subsequent TPCL compression moulding experiments with the IR-desized carbon fibre fabrics resulted in promising mechanical results with PA6, PPS and PEEK matrices as presented in Fig. 57.

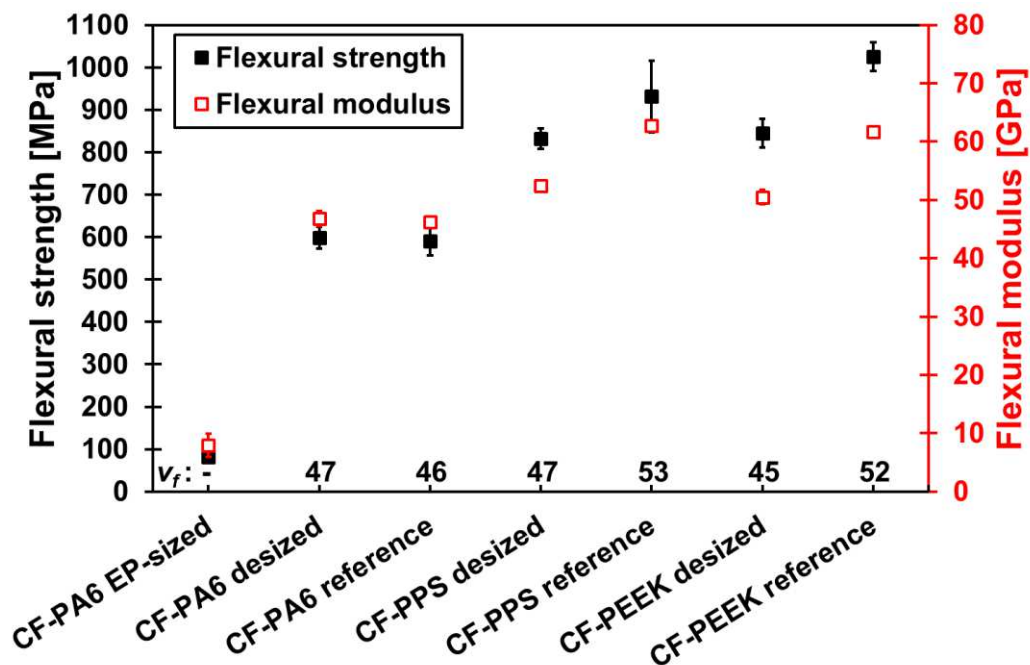


**Fig. 57** Flexural properties of in-house moulded CF TPCL vs. industrial reference CF TPCL. (Publication IV [25])

While the performance range of the industrial CF-PA6 reference could be matched by the IR-desizing approach, the industrial CF-PPS and CF-PEEK laminates exhibited higher mechanical performance compared to their in-house moulded TPCL counterparts. This higher performance of the industrial TPCL was rather attributed to higher fibre volume fractions and a different weave style (5 harness satin) than to any special sizing used.

Thermal desizing of carbon fibre fabrics turned out to be a key approach for TPCL production, imparting thermoplastic multi-compatibility to the fibres. The effect of incompatible sizing removal from carbon fibres resulted in a strength performance gain of roughly 700% in the case of CF-PA6 laminates (conditioned samples) and roughly 1000% in the case of CF-PPS and CF-PEEK laminates.

#### 6.4.1 CF laminates unpublished results

In complementary experiments to the CF TPCL development, CF-EP (EP-sized), CF-EP (desized) and CF-PC (desized) laminates were investigated. It was recognised throughout numerous vacuum assisted resin infusions, that the CF-EP (desized) laminates were thicker by roughly 20% and therefore exhibited lower fibre volume fractions. Within the CF-EP (EP-sized) laminates the sticky EP-sizing limited resin pickup, whereas fibre separation was facilitated by the desized fibre bundles (soaking up more resin). Nonetheless, the flexural performance of the laminates is outlined in Fig. 58. At a fibre volume fraction of 38% the CF-EP (desized) laminate exhibited a mean flexural strength of 734 MPa compared to the CF-EP (EP-sized) laminate with a fibre volume fraction of 45% and mean flexural strength of 839 MPa. This 100 MPa difference between the samples can be attributed to the difference in fibre volume fraction rather than any meaningful difference in interfacial adhesion. According to these observations, it is identifiable that EP-sized carbon fibres perform identically to the desized carbon fibres in combination with epoxy resin matrices. The CF-PC laminate exhibited a somewhat lower flexural strength compared to the epoxy matrices, which can be explained by the overall lower matrix properties of the PC matrix.

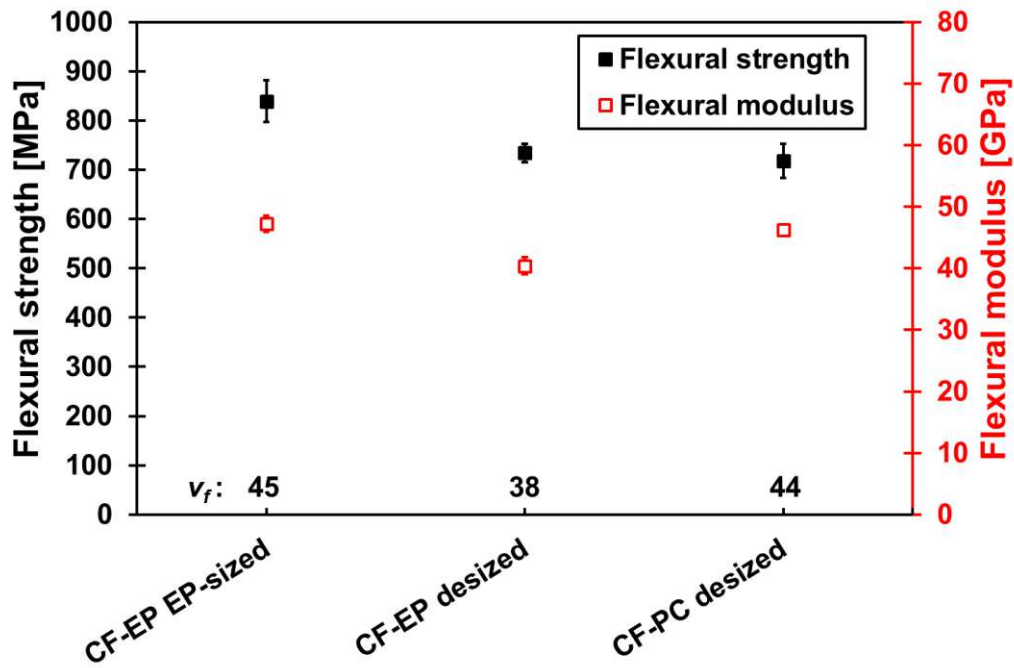


Fig. 58 Flexural properties of CF-EP and CF-PC laminates.

All examined CF laminates exhibited catastrophic brittle fracture and moderate impact strengths. The low impact resistance of carbon fibre composites is certainly one of the downsides of this material class. Even the polycarbonate matrix could only convey a marginal improvement in fracture toughness to the CF composites in the Charpy impact tests as shown in Fig. 59. Overall, the CF composites exhibited impact strengths in a range of 40-50 kJ/m<sup>2</sup>.

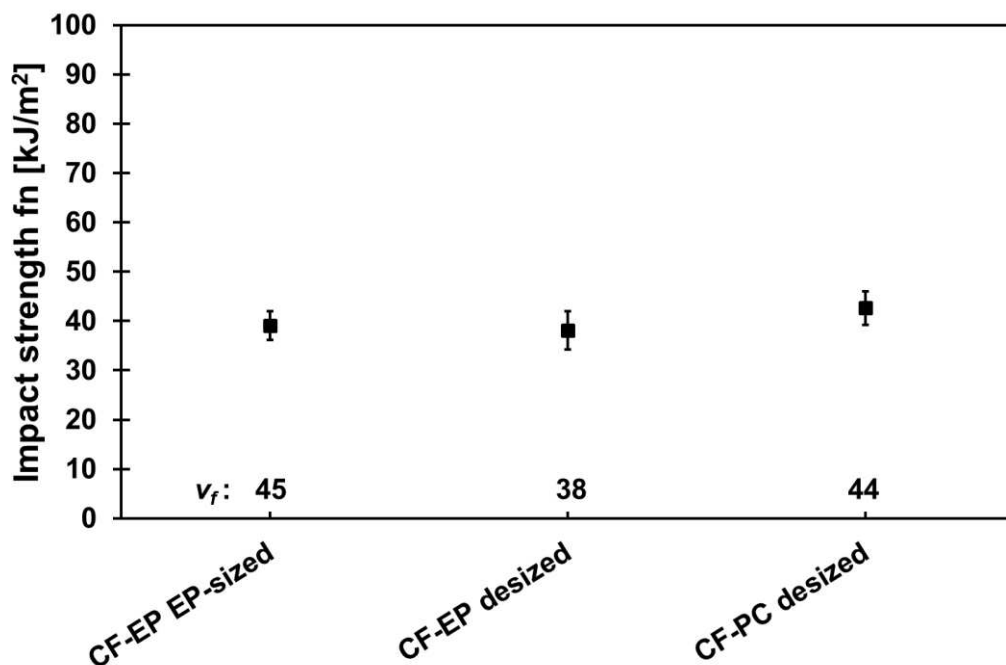
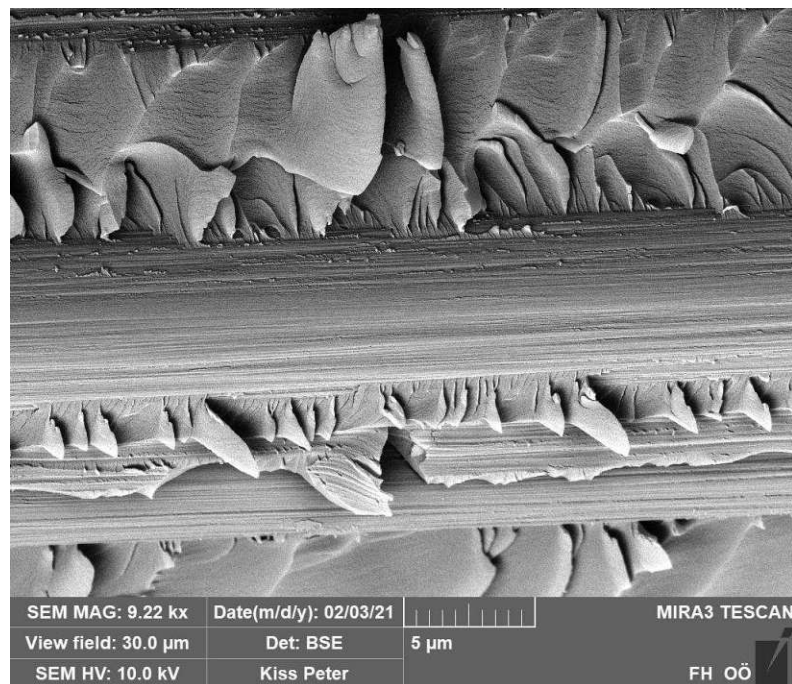


Fig. 59 Charpy impact strengths of CF-EP and CF-PC laminates.

Since the elongation at break of carbon fibres is very low (< 2%), it is challenging to find an effective method to boost impact resistance without sacrificing other properties. A possible

method for an improvement in impact resistance of TPCL could be realised by incorporation of  $\pm 45^\circ$  plies, or possibly by the use of partly desized (partly incompatible) fibres. Due to the  $\pm 45^\circ$  plies or partial incompatibility impact strength could potentially be improved by delamination, fibre-matrix debonding or crack deviation effects. As mentioned, composite strengths and moduli will both be affected adversely by any of these measures. Notwithstanding, the impact behaviour of carbon fibre composites can also be used to an advantage in certain cases. Impact damage from spherical objects often tend to be localised. As such, many times, only a small area is affected by the impact event while the rest of the structure may still provide sufficient integrity.

The microstructure of fractured CF laminates is illustrated in Figs. 60, 61, and 62. While the fractured samples evinced differences in matrix ductility (thermoset vs thermoplastic) on the microscale, these fracture properties did not translate to the Charpy impact toughness on macroscopic test samples. A plausible explanation for this behaviour is the low elongation at break of the carbon fibre reinforcement. Once the fibres break, especially in an impact event (high strain rate) the surrounding matrix is overstressed causing easy crack propagation. Throughout the figures, it is observable that wetting and mechanical interlocking played an important role in interfacial adhesion of CF composites.



**Fig. 60** SEM image of fractured CF-EP (EP-sized) laminate. The sample shows good wetting of the carbon fibre with the epoxy resin and brittle fracture behaviour of the matrix.

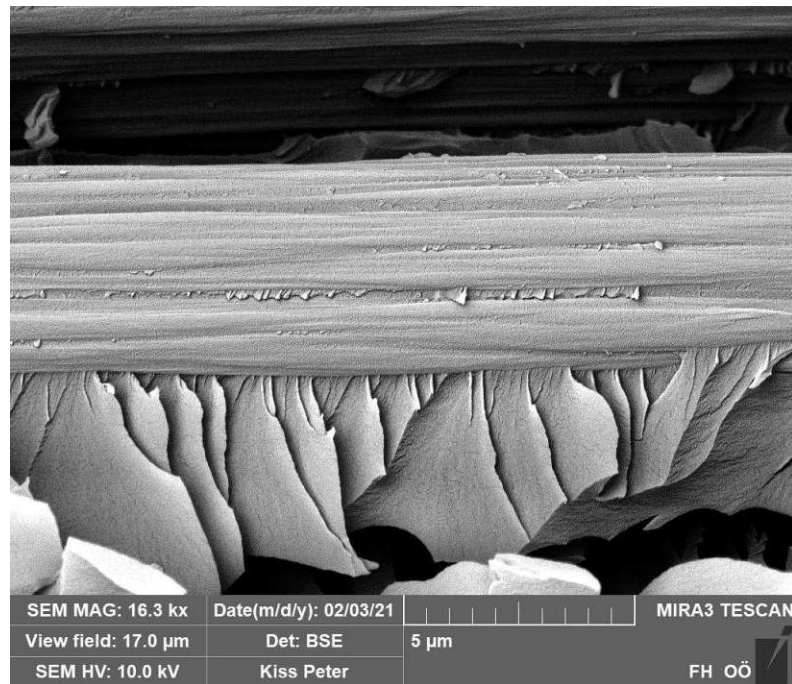


**Fig. 61** SEM image of fractured CF-EP (desized) laminate. The sample shows good wetting of the carbon fibre with the epoxy resin and brittle fracture behaviour of the matrix.

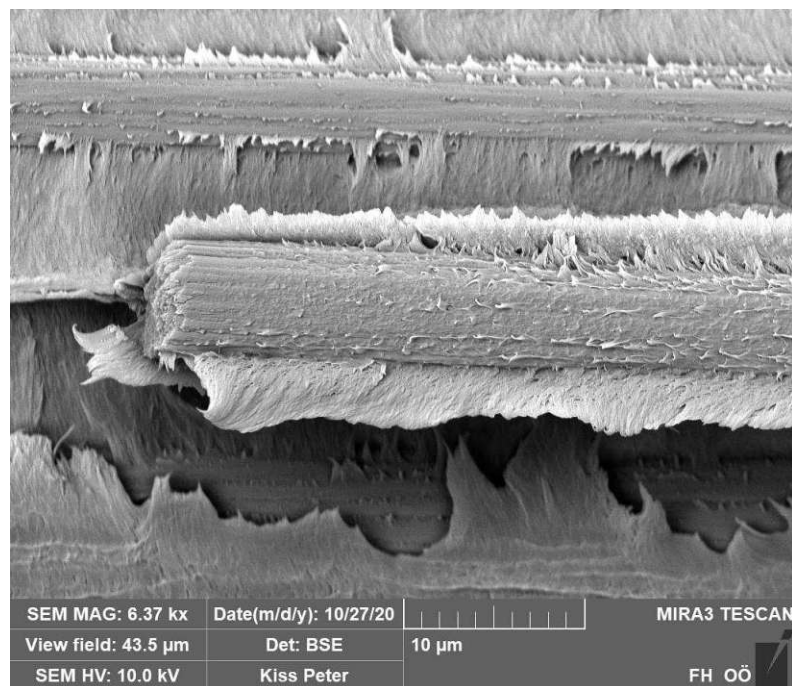


**Fig. 62** SEM image of fractured CF-PC (desized) laminate. The sample shows good wetting of the carbon fibre with polycarbonate and ductile fracture behaviour of the matrix.

### 6.5 TPCL recycling (Publication II)

In a TPCL recycling study, several in-house recycling methods were tested by shredding, compression moulding and thermoforming experiments. Panels made of purely shredded TPCL feedstock (referred to as thermoplastic sheet moulding compounds TP-SMC) were compared



to sandwich panels (shredded core materials co-moulded with continuous TPCL skins) and virgin monolithic (as-received) TPCL. As depicted in Fig. 63, the TP-SMCs with their random fibre orientations resulted in poor flexural strengths in a range of 100-200 MPa. This was expected, as randomly oriented short- or long fibre composites do not offer the same reinforcing effect as oriented continuous reinforcements. Unexpectedly, the flexural performance of co-moulded sandwich panels with a 50% recycled material core was on a par with their virgin material counterparts.

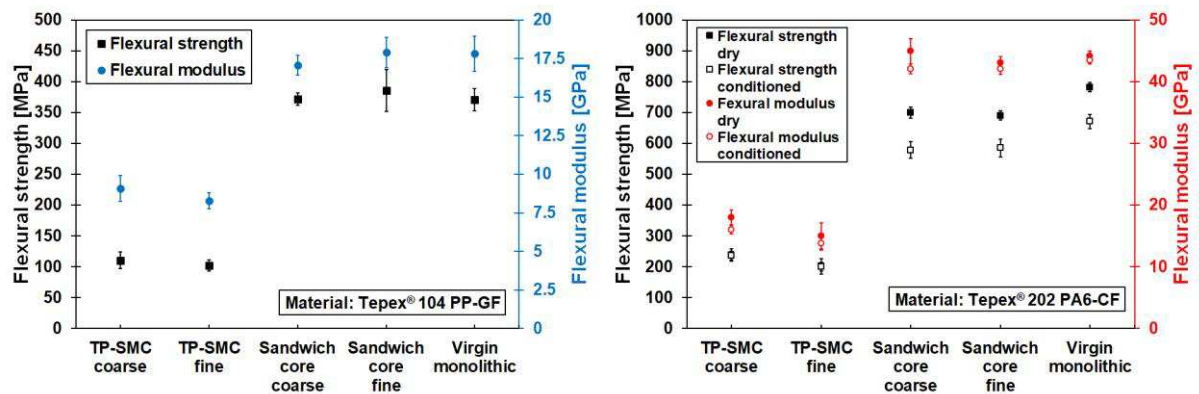


**Fig. 63** Flexural properties of recycled TPCL. Left: recycled GF-PP TPCL, right: recycled CF-PA6 TPCL.

The co-moulding process was found to be a highly viable recycling method for industrial TPCL waste treatment and a virgin material input of 50%. For comparison, the cross-sections of a TP-SMC and a sandwich panel with a 50% recycled core are depicted in Fig. 64.

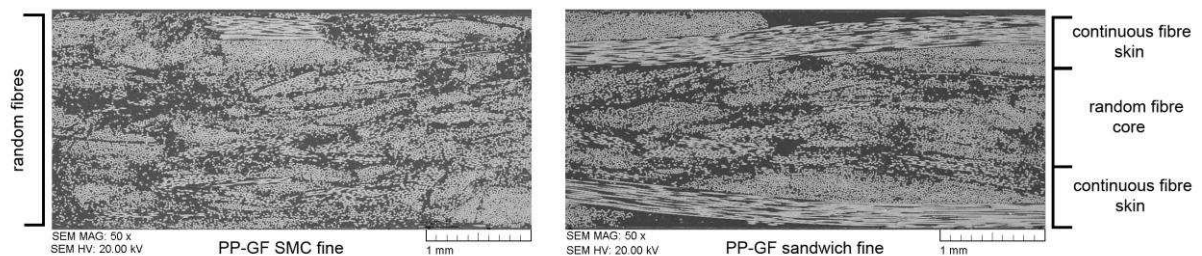


**Fig. 64** SEM micrographs of polished specimen cross-sections. Left: recycled TP-SMC panels, right: recycled sandwich panels with shredded material core and continuous fibre skins.

A second innovative idea for in-house recycling techniques was presented by reverse thermoforming, shown in Fig. 65. Thermoformed parts were subjected to IR-irradiation and spring-loaded clamp holders, whereby they were reshaped/pulled back into flat blanks for re-use. Ultimately, the reverse formed blanks evinced no deterioration in their mechanical properties.

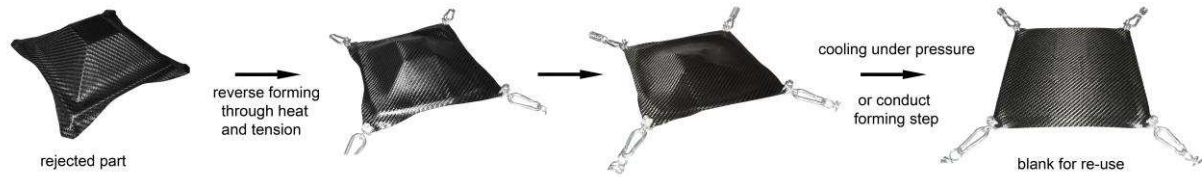


**Fig. 65** Direct recycling of TPCL by reverse thermoforming. A complexly shaped part is reshaped into its initial flat geometry by means of heat and tension.

As frequently discussed by the industry, chemical and thermal recycling by depolymerisation of the matrices are considered viable recycling methods for large TPCL waste volumes. However, the mechanical recycling route, as presented here, could likely have benefits over chemical and thermal recycling methods. In the case of glass fibres, the sizing or finish is possibly retained in mechanical recycling, whereas it could possibly be decomposed in chemical/thermal recycling. Such glass fibres stringently require re-sizing or re-finishing, making the chemical/thermal recycling process somewhat ineffective. As shown previously, a sizing or finish is essential for the performance of glass fibre composites.

In the case of carbon fibre recycling, high depolymerisation temperatures usually have an adverse effect the surface oxides of the carbon fibres. Essentially, when pyrolyzing carbon fibres, most of their activated sites are lost. As discussed, these surface oxides are potentially contributing to the good wettability of carbon fibres with thermoplastics.

Therefore, mechanical recycling is arguably the most convenient way of treating TPCL waste in low to medium volumes.

## 6.6 Summary of TPCL investigations

Summarising all experiments, the performance range of in-house developed TPCL was gathered into a single comparative chart, presented Fig. 66. While woven GF TPCL offer high strengths and good cost-effectiveness, their downsides are clearly the low moduli of 20-30 GPa and high density of 1.7-2.0 g/cm<sup>3</sup>. With respect to this, woven CF TPCL excel in very high strengths of up to 1000 MPa, high moduli of up to 60 GPa and low densities of 1.4-1.6 g/cm<sup>3</sup>. In a direct comparison, aluminium AW-7075 T6 offered similar flexural strength to CF TPCL at a flexural modulus of 70 GPa and density of 2.7 g/cm<sup>3</sup>. The aluminium specimens were tested under the same testing conditions (described in 5.2.3) as their CF-composite counterparts.

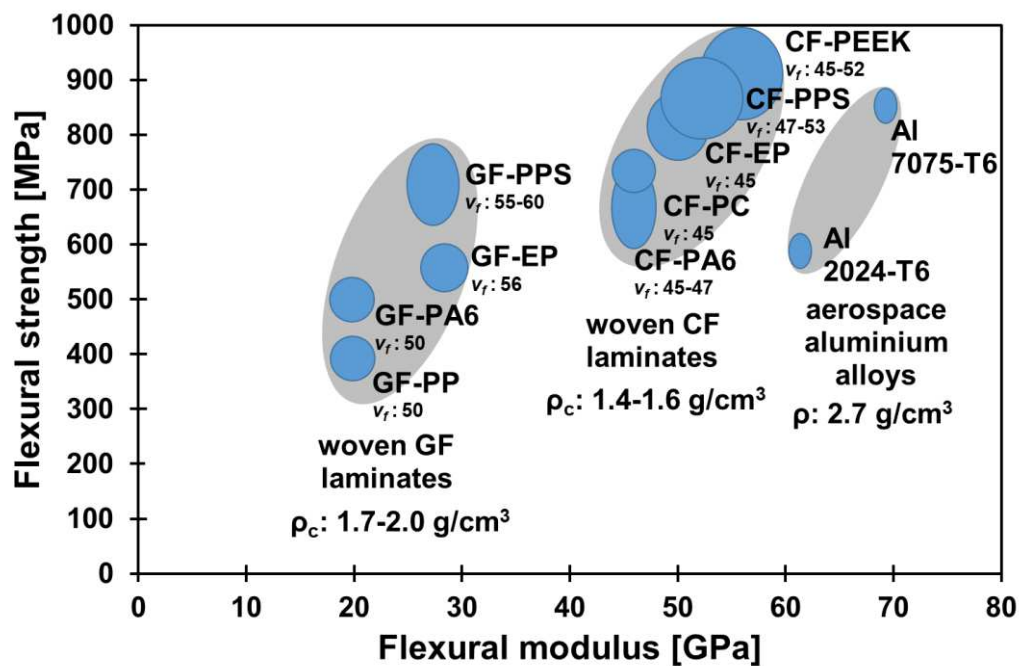


**Fig. 66** Performance range of in-house developed woven TPCL with bidirectional ply layout vs. aerospace grade aluminium alloys.

The performance characteristics of these materials should not be evaluated solely by their static strengths but also by their impact toughness. Despite different thermoplastic matrices, the Charpy impact strength ( $f_n$  - tested in flatwise normal configuration) was rather unaffected for each respective fibre type as shown in Fig 67. The energy required to fracture TPCL samples remained within a very tight range for both GF TPCL and CF TPCL, regardless of the matrix type used. GF TPCL offered an impact strength of 110-130 kJ/m<sup>2</sup>, whereas CF TPCL offered poor impact strengths in a 40-50 kJ/m<sup>2</sup> range. The elongation at break of the materials appeared to be related strongly to the measured impact characteristics. Since GF TPCL could deflect more, both due to their lower moduli and higher elongation at break, these samples evinced 2-3 times higher impact strengths compared to CF TPCL. The impacted GF TPCL specimens stayed mostly intact, evincing broken fibres on the compression and tension surface. Conversely, CF TPCL exhibited catastrophic failure resulting in completely fractured specimens or hinge breaks. A much better impact performance was observed by the aluminium

alloys. They offered impact strengths at over 300 kJ/m<sup>2</sup> due to their overall higher ductility compared to any of the composites produced.

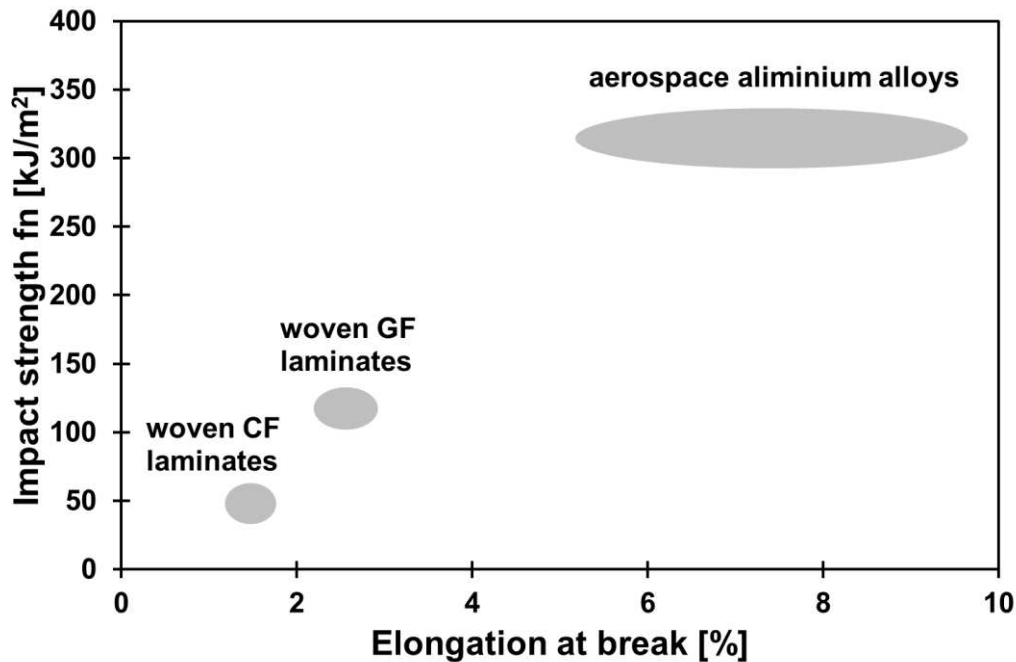


**Fig. 67** Impact performance of in-house developed woven TPCL with bidirectional ply layout vs. aerospace grade aluminium alloys.

Ultimately, the applicability of woven TPCL depends strongly on cost, fuel/energy saving measures, operating environments (temperature, chemicals, fluids), damage and fatigue tolerance, and processability. With this in mind, GF TPCL based on PP and PA6 matrices are undoubtedly a potential solution for automotive applications. GF-PPS on the other hand, offers exceptional performance for lightweight aircraft wing componentry or interior parts.

CF TPCL were found to be highly susceptible to impact damage. Therefore, they should be optimally used in areas which are not exposed to frequent impact events. Due to the high cost of carbon fibres, only CF-PA6 and CF-PC (lowest matrix prices) come into question for selected lightweight automotive parts. In applications where temperature, humidity and chemical resistance are required, CF-PPS and CF-PEEK offer unprecedented strength and stiffness performance.

## 7 Conclusion

Within this thesis, several high-performance thermoplastic composite laminates (TPCL) were engineered by a practice-oriented approach. A major focus was put on finding appropriate fibre surface treatments, or preparation techniques in order to facilitate interfacial adhesion between different thermoplastics and reinforcing fibres (glass and carbon).

In the case of glass fibre reinforcements, silane adhesion promoters were found to be highly effective in facilitating interfacial adhesion with thermoplastics, giving laminate mechanical properties on a par with industrial materials or even beyond. Especially  $\gamma$ -aminopropyltriethoxysilane (A-1100) treated glass fibre fabrics were found to be multi-compatible with several thermoplastic matrices tested, among which excellent adhesion was promoted to modified PP, neat PA6 and neat PPS. In the case of PPS an even more potent adhesion promoter could be found, a non-silane adhesion promoter based on a chromium (III) methacrylate complex (Volan<sup>®</sup> A).

Since industrial glass fibre rovings generally contain adhesion promoters in the form of silanes, it can be inferred from the mechanical testing results that most proprietary glass fibre direct sizings with thermoplastic compatibilities are formulated with aminosilane A-1100. The main adhesion mechanisms between thermoplastics and glass fibres were inferred to be wetting, interdiffusion and entanglement, and possibly covalent bonding.

### Highlights GF-TPCL

- GF-PP requires modification with adhesion promoters and a coupling agent. The coupling agent is preferably MAH-g-PP (maleic anhydride grafted PP) within a concentration range of 0.04-0.06% MAH.
- GF-PA6 only requires modification with adhesion promoters, preferably aminosilane A-1100. The neat PA6 matrix has high affinity to the aminosilane.
- GF-PPS only requires modification with adhesion promoters, preferably aminosilane A-1100 or chromium (III) methacrylate complex (Volan<sup>®</sup> A). The use of a neat PPS matrix suffices to generate exceptionally high laminate properties.

In the case of carbon fibre reinforcements, silanes play no commanding role in interfacial adhesion. The adhesion mechanisms of carbon fibres are generally different to glass fibres. Carbon fibres are often rough, whereby mechanical interlocking of polymers can be observed. Since specific carbon fibre sizings with thermoplastic compatibilities are not available in the

woven fabric 3K tow range, other possibilities had to be explored in the experimental investigations. Eventually, by the removal of the incompatible “standard” epoxy-based sizing a breakthrough was achieved for thermoplastic compatibilization. Sizing removal was conducted by means of a fabric heat treatment. All subsequently compression moulded laminates between thermally desized carbon fibre fabrics and thermoplastic matrices PA6, PC, PPS and PEEK offered unprecedented flexural performance near the industrial material range. It can be concluded that thermal desizing is the main approach taken by the industry for high-performance woven CF TPCL.

### Highlights CF-TPCL

- CF-PA6, CF-PC, CF-PPS and CF-PEEK require desized carbon fibres for ultimate laminate performance. The desized carbon fibres facilitate wetting and mechanical interlocking with the neat matrices.
- An industrially viable desizing process was found by infrared irradiation of the CF fabrics at 400 °C.

In times where material recyclability becomes ever more important, strategies for TPCL waste treatment must be investigated. In this recycling effort, some very promising results were obtained. incorporating shredded TPCL waste material as a core between continuous fibre skins. These micro-sandwich laminates with 50% recycle content offered flexural performance near their virgin material counterparts. A second promising recycling route was found, which truly harnessed the properties of the thermoplastic matrix. Thermoformed parts could be effectively reshaped into their flat geometry via a reverse thermoforming step.

### Highlights GF-TPCL and CF-TPCL recycling

- Shredded TPCL material feedstock can be reused easily by means of compounding, injection moulding or compression moulding methods.
- Co-moulding of shredded material cores with continuous fibre skins to flat laminates offer similar flexural and impact properties as monolithic laminates.
- The properties of the thermoplastic matrix can be harnessed directly by reshaping thermoformed parts into new geometries in a reverse forming process.
- Reverse forming is conducted by infrared-heating and application of restoring forces on the part. Once the matrix softens and melts, the part transitions back into its initial flat geometry.
- Reverse formed blanks offer similar mechanical performance as their virgin material counterparts.

## Outlook

The material combinations and manufacturing techniques investigated offer a great basis for laboratory and industrial scale-up trials. According to the findings, several material combinations can be readily applied in highly demanding engineering applications. By providing insight into the techniques how to optimise interfacial adhesion between glass and carbon fibres with several key thermoplastics, some guidelines were established for upcoming material developers and manufacturers in this field. A pressing issue that may not be overlooked, is the waste treatment problem of composites. Here, some innovative ideas were presented and successfully put into practice, hopefully sparking some interest by the industry.

---

## List of References

- [1] Mallick PK. Composites Engineering Handbook. CRC Press; 1997. doi:10.1201/9781482277739.
- [2] Tadano S, Giri B. X-ray diffraction as a promising tool to characterize bone nanocomposites. *Sci Technol Adv Mater* 2011;12:064708. doi:10.1088/1468-6996/12/6/064708.
- [3] Teischinger A. Opportunities and limits of timber in construction. WCTE 2016 - World Conf. Timber Eng., ISSN 1066-5757, 2016.
- [4] Jabbari E. Challenges for Natural Hydrogels in Tissue Engineering. *Gels* 2019;5:30. doi:10.3390/gels5020030.
- [5] Chew E, Liu JL, Tay TE, Tran LQN, Tan VBC. Improving the mechanical properties of natural fibre reinforced laminates composites through Biomimicry. *Compos Struct* 2021;258:113208. doi:10.1016/j.compstruct.2020.113208.
- [6] Mencattelli L, Pinho ST. Ultra-thin-ply CFRP Bouligand bio-inspired structures with enhanced load-bearing capacity, delayed catastrophic failure and high energy dissipation capability. *Compos Part A Appl Sci Manuf* 2020;129:105655. doi:10.1016/j.compositesa.2019.105655.
- [7] Vincent JFV, Bogatyreva OA, Bogatyrev NR, Bowyer A, Pahl A-K. Biomimetics: its practice and theory. *J R Soc Interface* 2006;3:471–82. doi:10.1098/rsif.2006.0127.
- [8] Gibson LJ, Ashby MF. The design of sandwich panels with foam cores. *Cell. Solids*, Cambridge University Press; 1997, p. 345–86. doi:10.1017/CBO9781139878326.011.
- [9] European Green Deal - European Commission website 2023. [https://ec.europa.eu/info/strategy/priorities-2019-2024/european-green-deal\\_en](https://ec.europa.eu/info/strategy/priorities-2019-2024/european-green-deal_en) (accessed February 27, 2023).
- [10] Pickering SJ. Recycling technologies for thermoset composite materials-current status. *Compos Part A Appl Sci Manuf* 2006;37:1206–15. doi:10.1016/j.compositesa.2005.05.030.
- [11] Oliveux G, Dandy LO, Leeke GA. Current status of recycling of fibre reinforced polymers: Review of technologies, reuse and resulting properties. *Prog Mater Sci* 2015;72:61–99. doi:10.1016/j.pmatsci.2015.01.004.
- [12] Juska TD, Puckett PM. “Matrix Resins and Fiber/Matrix Adhesion” in *Composites Engineering Handbook*, P.K. Mallick. New York, USA: Marcel-Dekker, Inc.; 1997.
- [13] Krause W, Henning F, Tröster S, Geiger O, Eyerer P. LFT-D - A process technology for large scale production of fiber reinforced thermoplastic components. *J Thermoplast Compos Mater* 2003;16:289–302. doi:10.1177/0892705703016004001.
- [14] Ning H, Lu N, Hassen AA, Chawla K, Selim M, Pillay S. A review of Long fibre thermoplastic (LFT) composites. *Int Mater Rev* 2020;65:164–88. doi:10.1080/09506608.2019.1585004.
- [15] Rohan K, Mcdonough TJ, Ugresic V, Potyra E, Henning F. Mechanical Study of Direct Long Fiber Thermoplastic Carbon/Polyamide 6 and its Relations to Processing Parameters. *Soc Plast Eng Automot Compos Conf Exhib* 2015;c:1–24.
- [16] Dittmar H, Plaggenborg H. Lightweight vehicle underbody design. *Reinf Plast* 2019;63:29–32. doi:10.1016/j.repl.2017.11.014.
- [17] BASF and Toray partnership to develop composite tapes. *Reinf Plast* 2019;63:286. doi:10.1016/j.repl.2019.10.029.
- [18] Fisher M, Hampe H. Interview with Hinrich Hampe, Toho Tenax. *Reinf Plast*



- 2017;61:330–1. doi:10.1016/j.repl.2017.04.055.
- [19] BİLGE Ç, AYDINER T, AKDENİZ Ç, SOYER AM, AKSEL L. Weight Reduction of Automobile Using Glass-Mat Thermoplastic Composites in Spare-Wheel Well. *Eur Mech Sci* 2020;4:7–11. doi:10.26701/ems.573687.
- [20] Han P, Butterfield J, Price M, Buchanan S, Murphy A. Experimental investigation of thermoforming carbon fibre-reinforced polyphenylene sulphide composites. *J Thermoplast Compos Mater* 2015;28:529–47. doi:10.1177/0892705713486133.
- [21] Akkerman R, Bouwman M, Wijskamp S. Analysis of the Thermoplastic Composite Overmolding Process: Interface Strength. *Front Mater* 2020;7:1–16. doi:10.3389/fmats.2020.00027.
- [22] Kiss P, Stadlbauer W, Burgstaller C, Archodoulaki V-M. Development of high-performance glass fibre-polypropylene composite laminates: Effect of fibre sizing type and coupling agent concentration on mechanical properties. *Compos Part A Appl Sci Manuf* 2020;138:106056. doi:10.1016/j.compositesa.2020.106056.
- [23] Kiss P, Stadlbauer W, Burgstaller C, Stadler H, Fehringer S, Haeuserer F, et al. In-house recycling of carbon- and glass fibre-reinforced thermoplastic composite laminate waste into high-performance sheet materials. *Compos Part A Appl Sci Manuf* 2020;139:106110. doi:10.1016/j.compositesa.2020.106110.
- [24] Kiss P, Schoefer J, Stadlbauer W, Burgstaller C, Archodoulaki V-M. An experimental study of glass fibre roving sizings and yarn finishes in high-performance GF-PA6 and GF-PPS composite laminates. *Compos Part B Eng* 2021;204:108487. doi:10.1016/j.compositesb.2020.108487.
- [25] Kiss P, Glinz J, Stadlbauer W, Burgstaller C, Archodoulaki V-M. The effect of thermally desized carbon fibre reinforcement on the flexural and impact properties of PA6, PPS and PEEK composite laminates: A comparative study. *Compos Part B Eng* 2021;108844. doi:10.1016/j.compositesb.2021.108844.
- [26] Gao S-L, Mäder E. Characterisation of interphase nanoscale property variations in glass fibre reinforced polypropylene and epoxy resin composites. *Compos Part A Appl Sci Manuf* 2002;33:559–76. doi:10.1016/S1359-835X(01)00134-8.
- [27] Müssig J, Graupner N. Test Methods for Fibre/Matrix Adhesion in Cellulose Fibre-Reinforced Thermoplastic Composite Materials: A Critical Review. *Rev Adhes Adhes* 2020;8:68–129. doi:10.7569/RAA.2020.097306.
- [28] Wang R-M, Zheng S-R, Zheng Y-P. Interface of polymer matrix composites. *Polym. Matrix Compos. Technol.*, Elsevier; 2011, p. 169–548. doi:10.1533/9780857092229.1.169.
- [29] Liu Z, Zhang L, Yu E, Ying Z, Zhang Y, Liu X, et al. Modification of Glass Fiber Surface and Glass Fiber Reinforced Polymer Composites Challenges and Opportunities: From Organic Chemistry Perspective. *Curr Org Chem* 2015;19:991–1010. doi:10.2174/138527281911150610100914.
- [30] Plueddemann EP. *Silane Coupling Agents*. Boston, MA: Springer US; 1991. doi:10.1007/978-1-4899-2070-6.
- [31] Lengsfeld H, Mainka H, Altstädt V. *Carbonfasern - Herstellung, Anwendung, Verarbeitung*. Carl Hanser Verlag München; 2019.
- [32] Bledzki AK, Mamun AA, Faruk O. Abaca fibre reinforced PP composites and comparison with jute and flax fibre PP composites. *Express Polym Lett* 2007;1:755–62. doi:10.3144/expresspolymlett.2007.104.
- [33] Thomason JL. *Glass Fibre Sizing: A Review of Size Formulation Patents*. Blurb, Glasgow, Scotland; 2015.
- [34] Thomason JL. Glass fibre sizing: A review. *Compos Part A Appl Sci Manuf* 2019;127:105619. doi:10.1016/j.compositesa.2019.105619.

- [35] Biron M. Thermoplastics and Thermoplastic composites - Technical Information for Plastics Users. *Cult Trends* 2007;944.
- [36] Starr TF. Continuous Filament Yarns. *Glas. Datab.*, Dordrecht: Springer Netherlands; 1993, p. 51–63. doi:10.1007/978-94-011-1492-9\_4.
- [37] Fu Z, Liu B, Deng Y, Ma J, Cao C, Wang J, et al. The suitable itaconic acid content in polyacrylonitrile copolymers used for PAN-based carbon fibers. *J Appl Polym Sci* 2016;133. doi:10.1002/app.43919.
- [38] Hao J, Wei H, Lu C, Liu Y. New aspects on the cyclization mechanisms of Poly(acrylonitrile-co-itaconic acid). *Eur Polym J* 2019;121:109313. doi:10.1016/j.eurpolymj.2019.109313.
- [39] Kim K-y, Park W-r, Shin D-g, Han J-w, Jung Y-s. Acrylonitrile copolymer for pan based carbon fiber precursor, Patent KR20120115029A, 2011.
- [40] Brodmann IGL, Lawton EL, Park A, Wiley J. Warp sizing composition. US Patent 4,530,876, 1985.
- [41] Wang S, Zhou Z, Zhang J, Fang G, Wang Y. Effect of temperature on bending behavior of woven fabric-reinforced PPS-based composites. *J Mater Sci* 2017;52:13966–76. doi:10.1007/s10853-017-1480-0.
- [42] Groves S, Highsmith A. Compression Response of Composite Structures. 100 Barr Harbor Drive, PO Box C700, West Conshohocken, PA 19428-2959: ASTM International; 1994. doi:10.1520/STP1185-EB.
- [43] Ksouri I, De Almeida O, Haddar N. Long term ageing of polyamide 6 and polyamide 6 reinforced with 30% of glass fibers: physicochemical, mechanical and morphological characterization. *J Polym Res* 2017;24:133. doi:10.1007/s10965-017-1292-6.
- [44] Sang L, Wang Y, Wang C, Peng X, Hou W, Tong L. Moisture diffusion and damage characteristics of carbon fabric reinforced polyamide 6 laminates under hydrothermal aging. *Compos Part A Appl Sci Manuf* 2019;123:242–52. doi:10.1016/j.compositesa.2019.05.023.
- [45] LANXESS Deutschland GmbH. Datasheet DURETHAN® B30S 2020. [https://techcenter.lanxess.com/scp/americas/en/products/datasheet/LANXESS\\_Durethan\\_B30S\\_000000\\_ISO\\_EN.pdf?docId=31442939](https://techcenter.lanxess.com/scp/americas/en/products/datasheet/LANXESS_Durethan_B30S_000000_ISO_EN.pdf?docId=31442939) (accessed February 27, 2023).
- [46] Mathijssen D. Leading the way in thermoplastic composites. *Reinf Plast* 2016;60:405–7. doi:10.1016/j.repl.2015.08.067.
- [47] Audoit J, Rivière L, Dandurand J, Lonjon A, Dantras E, Lacabanne C. Thermal, mechanical and dielectric behaviour of poly(aryl ether ketone) with low melting temperature. *J Therm Anal Calorim* 2019;135:2147–57. doi:10.1007/s10973-018-7292-x.
- [48] Holmes M. Aerospace looks to composites for solutions. *Reinf Plast* 2017;61:237–41. doi:10.1016/j.repl.2017.06.079.
- [49] Carbon fiber tapes suitable for aerospace. *Reinf Plast* 2021;65:3. doi:10.1016/j.repl.2020.12.017.
- [50] Drzal LT, Herrera-Franco PJ, Ho H. Fiber–Matrix Interface Tests. *Compr. Compos. Mater.*, Elsevier; 2000, p. 71–111. doi:10.1016/B0-08-042993-9/00036-X.
- [51] Pickering KL, Efendy MGA, Le TM. A review of recent developments in natural fibre composites and their mechanical performance. *Compos Part A Appl Sci Manuf* 2016;83:98–112. doi:10.1016/j.compositesa.2015.08.038.
- [52] Carnevale P. Fibre-matrix interfaces in thermoplastic composites A meso-level approach. 2014. <https://repository.tudelft.nl/islandora/object/uuid%3A880605ea-fb4c-4b9b-a25e-ad610d94a5cd> (accessed February 27, 2023)
- [53] Gulyás J, Földes E, Lázár A, Pukánszky B. Electrochemical oxidation of carbon fibres: surface chemistry and adhesion. *Compos Part A Appl Sci Manuf* 2001;32:353–60.

- doi:10.1016/S1359-835X(00)00123-8.
- [54] Drzal LT, Rich MJ, Koenig MF, Lloyd PF. Adhesion of Graphite Fibers to Epoxy Matrices: II. The Effect of Fiber Finish. *J Adhes* 1983;16:133–52. doi:10.1080/00218468308074911.
- [55] Tran LQN, Yuan XW, Bhattacharyya D, Fuentes C, Van Vuure AW, Verpoest I. Fiber-matrix interfacial adhesion in natural fiber composites. *Int J Mod Phys B* 2015;29:1540018. doi:10.1142/S0217979215400184.
- [56] Tran LQN, Fuentes CA, Dupont-Gillain C, Van Vuure AW, Verpoest I. Understanding the interfacial compatibility and adhesion of natural coir fibre thermoplastic composites. *Compos Sci Technol* 2013;80:23–30. doi:10.1016/j.compscitech.2013.03.004.
- [57] Fuentes CA, Zhang Y, Guo H, Woigk W, Masania K, Dransfeld C, et al. Wettability and interphase adhesion of molten thermoplastics on glass fibres. *ICCM 21 Int Conf Compos Mater* 2017;2017-Augus:20–5.
- [58] Chen P, Lu C, Yu Q, Gao Y, Li J, Li X. Influence of fiber wettability on the interfacial adhesion of continuous fiber-reinforced PPESK composite. *J Appl Polym Sci* 2006;102:2544–51. doi:10.1002/app.24681.
- [59] Zisman WA. INFLUENCE OF CONSTITUTION ON ADHESION. *Ind Eng Chem* 1963;55:18–38. doi:10.1021/ie50646a003.
- [60] Cevahir A. Glass fibers. *Fiber Technol. Fiber-Reinforced Compos.*, Elsevier; 2017, p. 99–121. doi:10.1016/B978-0-08-101871-2.00005-9.
- [61] Liu X, Jones FR, Thomason JL, Roekens BJ. An XPS study of organosilane and sizing adsorption on E-glass fibre surface. *ICCM Int Conf Compos Mater* 2007:1–6.
- [62] Ulkem I, Schreiber HP. The role of interactions at interfaces of glass-fiber reinforced composites. *Compos Interfaces* 1994;2:253–63. doi:10.1163/156855494X00111.
- [63] Pisanova E, Mäder E. Acid–base interactions and covalent bonding at a fiber–matrix interface: contribution to the work of adhesion and measured adhesion strength. *J Adhes Sci Technol* 2000;14:415–36. doi:10.1163/156856100742681.
- [64] Dilsiz N, Wightman J. Effect of acid–base properties of unsized and sized carbon fibers on fiber/epoxy matrix adhesion. *Colloids Surfaces A Physicochem Eng Asp* 2000;164:325–36. doi:10.1016/S0927-7757(99)00400-8.
- [65] Fowkes FM. Role of acid-base interfacial bonding in adhesion. *J Adhes Sci Technol* 1987;1:7–27. doi:10.1163/156856187X00049.
- [66] Johannson OK, Stark FO, Vogel GE, Fleischmann RM. Evidence for Chemical Bond Formation at Silane Coupling Agent Interfaces. *J Compos Mater* 1967;1:278–92. doi:10.1177/002199836700100304.
- [67] Wang Q, Xiao Z, Wang W, Xie Y. Coupling pattern and efficacy of organofunctional silanes in wood flour-filled polypropylene or polyethylene composites. *J Compos Mater* 2015;49:677–84. doi:10.1177/0021998314525065.
- [68] Park J-M, Kim D-S, Kim S-R. Improvement of interfacial adhesion and nondestructive damage evaluation for plasma-treated PBO and Kevlar fibers/epoxy composites using micromechanical techniques and surface wettability. *J Colloid Interface Sci* 2003;264:431–45. doi:10.1016/S0021-9797(03)00419-3.
- [69] Zisman WA. Surface Chemistry of Plastics Reinforced by Strong Fibers. *Ind Eng Chem Prod Res Dev* 1969;8:98–111. doi:10.1021/i360030a002.
- [70] Fuentes CA, Brughmans G, Tran LQN, Dupont-Gillain C, Verpoest I, Van Vuure AW. Effect of roughness on the interface in natural fibre composites: Physical adhesion and mechanical interlocking. *16th Eur Conf Compos Mater ECCM 2014* 2014.
- [71] Ishida H, Kumar G. *Molecular Characterization of Composite Interfaces*. Berlin, Heidelberg: Springer Berlin Heidelberg; 1985. doi:10.1007/978-3-662-29084-2.

- 
- [72] Cogswell FN. Thermoplastic Aromatic Polymer Composites. Butterworth Heinemann Ltd; 1992.
- [73] Hassan EAM, Yang L, Elagib THH, Ge D, Lv X, Zhou J, et al. Synergistic effect of hydrogen bonding and  $\pi$ - $\pi$  stacking in interface of CF/PEEK composites. *Compos Part B Eng* 2019;171:70–7. doi:10.1016/j.compositesb.2019.04.015.
- [74] Koenig JL, Ishida H. Controlled Interphases in Composite Materials: Proceedings of the Third International Conference on Composite Interfaces. Springer Netherlands; 1990.
- [75] Shin P-S, Baek Y-M, Kim J-H, Park H-S, Kwon D-J, Lee J-H, et al. Interfacial and wetting properties between glass fiber and epoxy resins with different pot lifes. *Colloids Surfaces A Physicochem Eng Asp* 2018;544:68–77. doi:10.1016/j.colsurfa.2018.02.017.
- [76] Aranguren M. Polymer Composites. *Encycl. Surf. Colloid Sci.* Third Ed., CRC Press; 2015, p. 5682.
- [77] Mäder E. Study of fibre surface treatments for control of interphase properties in composites. *Compos Sci Technol* 1997;57:1077–88. doi:10.1016/S0266-3538(97)00002-X.
- [78] Wang J, Fuentes CA, Zhang D, Wang X, Van Vuure AW, Seveno D. Wettability of carbon fibres at micro- and mesoscales. *Carbon N Y* 2017;120:438–46. doi:10.1016/j.carbon.2017.05.055.
- [79] Duchoslav J, Unterweger C, Steinberger R, Fürst C, Stifter D. Investigation on the thermo-oxidative stability of carbon fiber sizings for application in thermoplastic composites. *Polym Degrad Stab* 2016;125:33–42. doi:10.1016/j.polymdegradstab.2015.12.016.
- [80] Roe R-J. Surface tension of polymer liquids. *J Phys Chem* 1968;72:2013–7. doi:10.1021/j100852a025.
- [81] Zitzenbacher G, Huang Z, Längauer M, Forsich C, Holzer C. Wetting behavior of polymer melts on coated and uncoated tool steel surfaces. *J Appl Polym Sci* 2016;133:n/a-n/a. doi:10.1002/app.43469.
- [82] Cattanaich JB, Guff G, Cogswell FN. The Processing of Thermoplastics Containing High Loadings of Long and Continuous Reinforcing Fibers. *J Polym Eng* 1986;6. doi:10.1515/POLYENG.1986.6.1-4.345.
- [83] Pangelinan AB, Mccullough RL, Kelley MJ. Fiber-Matrix Interactions in Thermoplastic Composites. *J Thermoplast Compos Mater* 1994;7:192–207. doi:10.1177/089270579400700302.
- [84] Zisman WA. *Surface Chemistry of the Reinforcement of Plastics by Glass Fibers and Flakes.* Soc. Plast. Ind. Inc., 1963.
- [85] Pillay S, Vaidya UK, Janowski GM. Liquid Molding of Carbon Fabric-reinforced Nylon Matrix Composite Laminates. *J Thermoplast Compos Mater* 2005;18:509–27. doi:10.1177/0892705705054412.
- [86] Cousins DS, Suzuki Y, Murray RE, Samaniuk JR, Stebner AP. Recycling glass fiber thermoplastic composites from wind turbine blades. *J Clean Prod* 2019;209:1252–63. doi:10.1016/j.jclepro.2018.10.286.
- [87] Juska T. Effect of Water Immersion on Fiber/Matrix Adhesion in Thermoplastic Composites. *J Thermoplast Compos Mater* 1993;6:256–74. doi:10.1177/089270579300600401.
- [88] Raghavendran VK, Drzal LT, Askeland P. Effect of surface oxygen content and roughness on interfacial adhesion in carbon fiber–polycarbonate composites. *J Adhes Sci Technol* 2002;16:1283–306. doi:10.1163/156856102320252813.
- [89] Suzuki Y, Saitoh J. The interaction between poly-ether-imide and gamma-

---

aminopropyl-triethoxysilane on high strength glass fiber. *Control. Interphases Compos. Mater.*, Dordrecht: Springer Netherlands; 1990, p. 417–22. doi:10.1007/978-94-011-7816-7\_40.

- [90] Ishida H, Nakata K. Role of aminosilanes on the adhesion promotion at the E / glass / poly ( butylene terephthalate ) interface. 42nd Annu. Conf. Soc. Plast. Ind. Inc., Sampe Q; 1987.
- [91] Fuentes CA, Tran LQN, Dupont-Gillain C, Van Vuure AW, Verpoest I. Interfacial adhesion and mechanical behaviour of natural fibre composites: Effect of surface energy and physical adhesion. *ICCM Int Conf Compos Mater 2013;2013-July:6670–6.*
- [92] Jones FR. A Review of Interphase Formation and Design in Fibre-Reinforced Composites. *J Adhes Sci Technol 2010;24:171–202.* doi:10.1163/016942409X12579497420609.
- [93] Beland S. *High Performance Thermoplastic Resins and Their Composites.* Noyes Publications, Park Ridge, USA; 1990.
- [94] Israelachvili J. *Intermolecular and Surface Forces.* Elsevier; 2011. doi:10.1016/C2011-0-05119-0.
- [95] Mezenov YA, Krasilin AA, Dzyuba VP, Nominé A, Milichko VA. Metal–Organic Frameworks in Modern Physics: Highlights and Perspectives. *Adv Sci 2019;6:1900506.* doi:10.1002/advs.201900506.
- [96] Yang Q-S, Liu X. Mechanical behavior of extra-strong CNT fibers and their composites. *Toughening Mech. Compos. Mater.*, Elsevier; 2015, p. 339–72. doi:10.1016/B978-1-78242-279-2.00013-5.
- [97] Mathijssen D. The black magic of carbon fiber reinforced thermoplastics. *Reinf Plast 2015;59:185–9.* doi:10.1016/j.repl.2015.02.012.
- [98] Eyckens DJ, Arnold CL, Simon Ž, Gengenbach TR, Pinson J, Wickramasingha YA, et al. Covalent sizing surface modification as a route to improved interfacial adhesion in carbon fibre-epoxy composites. *Compos Part A Appl Sci Manuf 2021;140:106147.* doi:10.1016/j.compositesa.2020.106147.
- [99] Bowland C. A FORMULATION STUDY OF LONG FIBER THERMOPLASTIC POLYPROPYLENE ( PART 1 ) : THE EFFECTS OF COUPLING AGENT , GLASS CONTENT & RESIN PROPERTIES ON THE MECHANICAL PROPERTIES. 8th Annu. Automot. Compos. Conf. Exhib. ACCE 2008, 2008.
- [100] Bowland C. A formulation study of long fiber thermoplastic polypropylene (Part 2): The effects of coupling agent type and properties. 9th Annu. Automot. Compos. Conf. Exhib. ACCE 2009, 2009, p. 168–78.
- [101] Bowland C, Busche B, Woude J v. A formulation study of long fiber thermoplastic polypropylene (part 3): Mechanical properties of PP DLFT composites. *Soc. Plast. Eng. - 11th-Annual Automot. Compos. Conf. Exhib. ACCE 2011, 2011.*
- [102] Mäder E, Pisanova E. Characterization and design of interphases in glass fiber reinforced polypropylene. *Polym Compos 2000;21:361–8.* doi:10.1002/pc.10194.
- [103] McMican R. Sizing stability is a key element for glass fibre manufacturing. *Reinf Plast 2012;56:29–32.* doi:10.1016/S0034-3617(12)70110-8.
- [104] Moody V, Needles HL. Primary and Secondary Backing Construction. *Tufted Carpet*, Elsevier; 2004, p. 67–81. doi:10.1016/B978-188420799-0.50006-3.
- [105] Gandhi KL. Yarn preparation for weaving: Warping. *Woven Text.* 2nd ed., Elsevier; 2020, p. 81–118. doi:10.1016/B978-0-08-102497-3.00003-9.
- [106] Hexcel Corporation. *HexForce® Technical Fabrics Handbook 2017.* [https://www.hexcel.com/user\\_area/content\\_media/raw/HexForce\\_FabricsHandbook.pdf](https://www.hexcel.com/user_area/content_media/raw/HexForce_FabricsHandbook.pdf) (accessed February 27, 2023).
- [107] Pape PG. Adhesion Promoters. *Appl. Plast. Eng. Handb.*, vol. 3, Elsevier; 2011, p.

- 503–17. doi:10.1016/B978-1-4377-3514-7.10029-7.
- [108] Liu K, Stadlbauer W, Zitzenbacher G, Paulik C, Burgstaller C. Effects of surface modification of talc on mechanical properties of polypropylene/talc composites. *AIP Conf. Proc.*, vol. 1713, 2016, p. 120008. doi:10.1063/1.4942323.
- [109] Yates PC, Trebilcock JW. The chemistry of chromium complexes used as coupling agents in fiberglass resin laminates. *Polym Eng Sci* 1961;1:199–213. doi:10.1002/pen.760010411.
- [110] Rössler M. *Repairs of Aircraft Composite Structures*. Norderstedt: BoD Books on Demand; 2015.
- [111] Jones FR. Interphase Formation and Control in Fibre Composite Materials. *Key Eng Mater* 1995;116–117:41–60. doi:10.4028/www.scientific.net/KEM.116-117.41.
- [112] Liu X, Thomason JL, Jones FR. XPS and AFM Study of Interaction of Organosilane and Sizing with E-Glass Fibre Surface. *J Adhes* 2008;84:322–38. doi:10.1080/00218460802004386.
- [113] Arkles B, Steinmetz JR, Zazyczny J, Mehta P. Factors contributing to the stability of alkoxysilanes in aqueous solution. *J Adhes Sci Technol* 1992;6:193–206. doi:10.1163/156856192X00133.
- [114] Shi H, Villegas IF, Bersee HEN. Strength and failure modes in resistance welded thermoplastic composite joints: Effect of fibre–matrix adhesion and fibre orientation. *Compos Part A Appl Sci Manuf* 2013;55:1–10. doi:10.1016/j.compositesa.2013.08.008.
- [115] Matisons JG. Silanes and Siloxanes as Coupling Agents to Glass: A Perspective 2012;281–98. doi:10.1007/978-94-007-3876-8\_10.
- [116] Mäder E, Moos E, Karger-Kocsis J. Role of film formers in glass fibre reinforced polypropylene — new insights and relation to mechanical properties. *Compos Part A Appl Sci Manuf* 2001;32:631–9. doi:10.1016/S1359-835X(00)00156-1.
- [117] Giraud I, Franceschi S, Perez E, Lacabanne C, Dantras E. Influence of new thermoplastic sizing agents on the mechanical behavior of poly(ether ketone)/carbon fiber composites. *J Appl Polym Sci* 2015;132:38. doi:10.1002/app.42550.
- [118] Giraud I, Franceschi-Messant S, Perez E, Lacabanne C, Dantras E. Preparation of aqueous dispersion of thermoplastic sizing agent for carbon fiber by emulsion/solvent evaporation. *Appl Surf Sci* 2013;266:94–9. doi:10.1016/j.apsusc.2012.11.098.
- [119] Hartman D, Peters L, Antle J. Sizing for high performance glass fibers and composite materials incorporating same. Patent WO2007100816A2, 2006.
- [120] Zinck P, Mäder E, Gerard JF. Role of silane coupling agent and polymeric film former for tailoring glass fiber sizings from tensile strength measurements. *J Mater Sci* 2001;36:5245–52. doi:10.1023/A:1012410315601.
- [121] Kriskova A, Wiesenganger T. Sizing composition for fibers, sized fibers and method of sizing fibers. Patent EP2559673A1, 2013.
- [122] Petersen H, Kusano Y, Brøndsted P, Almdal K. Preliminary Characterization of Glass Fiber Sizing. *Proc 34th Risø Int Symp Mater Sci* 2013;34:333–40.
- [123] Vercoulen P, Amato L, Villa S. Film-forming dispersion and sizing dispersion, Patent WO2019038249A1, 2018.
- [124] *Aerospace specifications for fibre-reinforced materials 2023*. <http://www.bgf.com/technical/specifications/> (accessed February 27, 2023).
- [125] Jenkins PG, Yang L, Liggat JJ, Thomason JL. Investigation of the strength loss of glass fibre after thermal conditioning. *J Mater Sci* 2015;50:1050–7. doi:10.1007/s10853-014-8661-x.
- [126] *AGY Thermoplastics 2023*. <https://www.agy.com/markets/> (accessed February 27,

- 2023).
- [127] Tiefenthaler AM, Urban MW. Thermal stability of silane coupling agents on Nextel fibres. *Composites* 1989;20:145–50. doi:10.1016/0010-4361(89)90642-3.
- [128] Rudzinski S, Häußler L, Harnisch C, Mäder E, Heinrich G. Glass fibre reinforced polyamide composites: Thermal behaviour of sizings. *Compos Part A Appl Sci Manuf* 2011;42:157–64. doi:10.1016/j.compositesa.2010.10.018.
- [129] Thomason JL, Nagel U, Yang L, Bryce D. A study of the thermal degradation of glass fibre sizings at composite processing temperatures. *Compos Part A Appl Sci Manuf* 2019;121:56–63. doi:10.1016/j.compositesa.2019.03.013.
- [130] Drzal LT, Madhukar M. Fibre-matrix adhesion and its relationship to composite mechanical properties. *J Mater Sci* 1993;28:569–610. doi:10.1007/BF01151234.
- [131] Wang Z, Yang W, Feng X, Tian J, Jia F, Li J, et al. SYNTHESIS AND CHARACTERIZATION OF EPOXY-MODIFIED WATERBORNE UNSATURATED POLYESTER AND THEIR USE IN FIBER SIZING AGENTS. *Top. Chem. Mater. Eng.*, vol. 1, Volkson Press; 2018, p. 105–9. doi:10.26480/icnmim.01.2018.107.109.
- [132] Bang Y-h, Jo C-h, Wang Y-s, Kim S-r. Sizing agent for carbon-fiber, and carbon-fiber manufactured by using the same. Patent KR101683345B1, 2014.
- [133] Zhang Q, Liu L, Jiang D, Yan X, Huang Y, Guo Z. Home-made epoxy emulsion sizing agent for treating carbon fibers: Thermal stability and mechanical properties. *J Compos Mater* 2015;49:2877–86. doi:10.1177/0021998314557298.
- [134] Liu F, Shi Z, Dong Y. Improved wettability and interfacial adhesion in carbon fibre/epoxy composites via an aqueous epoxy sizing agent. *Compos Part A Appl Sci Manuf* 2018;112:337–45. doi:10.1016/j.compositesa.2018.06.026.
- [135] Hu J, Li F, Wang B, Zhang H, Ji C, Wang S, et al. A two-step combination strategy for significantly enhancing the interfacial adhesion of CF/PPS composites: The liquid-phase oxidation followed by grafting of silane coupling agent. *Compos Part B Eng* 2020;191:107966. doi:10.1016/j.compositesb.2020.107966.
- [136] Dai Z, Shi F, Zhang B, Li M, Zhang Z. Effect of sizing on carbon fiber surface properties and fibers/epoxy interfacial adhesion. *Appl Surf Sci* 2011;257:6980–5. doi:10.1016/j.apsusc.2011.03.047.
- [137] Luo Y, Zhao Y, Duan Y, Du S. Surface and wettability property analysis of CCF300 carbon fibers with different sizing or without sizing. *Mater Des* 2011;32:941–6. doi:10.1016/j.matdes.2010.08.004.
- [138] Toho Tenax America. Tenax® datasheet EP-sizing 2010. <https://www.swiss-composite.ch/pdf/t-Tenax-Datenblatt.pdf> (accessed February 27, 2023).
- [139] HexTow® Continuous Carbon Fiber, Sizings Available with HexTow® Continuous Carbon Fiber Products 2023. <https://www.hexcel.com/Products/Carbon-Fiber/HexTow-Continuous-Carbon-Fiber> (accessed February 27, 2023).
- [140] Figueiredo J., Pereira MF., Freitas MM., Órfão JJ. Modification of the surface chemistry of activated carbons. *Carbon N Y* 1999;37:1379–89. doi:10.1016/S0008-6223(98)00333-9.
- [141] Matos I, Bernardo M, Fonseca I. Porous carbon: A versatile material for catalysis. *Catal Today* 2017;285:194–203. doi:10.1016/j.cattod.2017.01.039.
- [142] Casimero C, Hegarty C, McGlynn RJ, Davis J. Ultrasonic exfoliation of carbon fiber: electroanalytical perspectives. *J Appl Electrochem* 2020;50:383–94. doi:10.1007/s10800-019-01379-y.
- [143] Teijin Carbon Europe GmbH. Tenax® Carbon Fiber HTS45/IMS65 P12/P22 Product Information on Safe Handling 2018. [https://www.tejincarbon.com/fileadmin/user\\_upload/PISH\\_Tenax\\_Carbon\\_Fiber\\_P-](https://www.tejincarbon.com/fileadmin/user_upload/PISH_Tenax_Carbon_Fiber_P-)

- 
- Size\_v02\_en\_2018-07-15\_EN.pdf (accessed February 27, 2023).
- [144] SGL Carbon. SIGRAFIL® continuous carbon fiber tows 2020. <https://www.sglcarbon.com/pdf/SGL-Broschure-The-Enablers-EN.pdf> (accessed February 27, 2023).
- [145] Kibayashi M, Seike S, Rau A. Thermoplastic resin impregnated tape. Patent WO2013086118A1, 2011.
- [146] Muzzy J, Varughese B, Thammongkol V, Tincher W. Electrostatic prepregging of thermoplastic matrices. *Int SAMPE Symp Exhib* 1989;34:1940–51.
- [147] Sloan J. I want to say two words to you: “Thermoplastic tapes” 2018. <https://www.compositesworld.com/articles/i-want-to-say-two-words-to-you-thermoplastic-tapes> (accessed February 27, 2023).
- [148] Lenferink RG, Van Dreumel WHM. Method for preparing a fabric substantially consisting of carbon fibers. United States Patent US7252726B2, 2007.
- [149] Mitschang P, Blinzler M, Wöginger A. Processing technologies for continuous fibre reinforced thermoplastics with novel polymer blends. *Compos Sci Technol* 2003;63:2099–110. doi:10.1016/S0266-3538(03)00107-6.
- [150] Nair SS, Saha T, Dey P, Bhadra S. Thermal oxidation of graphite as the first step for graphene preparation: effect of heating temperature and time. *J Mater Sci* 2021;56:3675–91. doi:10.1007/s10853-020-05481-x.
- [151] Black S. Thermoplastic composites technology: A view from Europe 2015. [https://www.toraytac.com/media/bb9f2d08-2f05-4a80-bcbc-cf91d6301cb5/5MZmdQ/TAC/Documents/Articles/Toray\\_Thermoplastic-Composites\\_A-View-from-Europe\\_CW.pdf](https://www.toraytac.com/media/bb9f2d08-2f05-4a80-bcbc-cf91d6301cb5/5MZmdQ/TAC/Documents/Articles/Toray_Thermoplastic-Composites_A-View-from-Europe_CW.pdf) (accessed February 27, 2023).
- [152] Schaal L. Roctool LIT: A high performance and cost-effective solution for automotive and aeronautical applications. *Reinf Plast* 2018;62:307–13. doi:10.1016/j.repl.2017.10.002.
- [153] Pantelakis S, Baxevani E, Spelz U. An automated technique for manufacturing thermoplastic stringers in continuous length. *Compos Struct* 1993;26:115–21. doi:10.1016/0263-8223(93)90060-4.
- [154] Spelz U, Schulze V. Herstellung profilierter Stringer. Patent DE4017978C2, 1993.
- [155] RUCKS Maschinenbau GmbH intermittent press system 2021. [https://www.rucks.de/de\\_sonderanlagen.html?oncekeys=id%7Ccode%7Ctemplate](https://www.rucks.de/de_sonderanlagen.html?oncekeys=id%7Ccode%7Ctemplate) (accessed February 27, 2023).
- [156] Teubert Maschinenbau GmbH intermittent press system 2021. <https://teubert.de/composites/> (accessed February 27, 2023).
- [157] Wöginger A. Prozesstechnologien zur Herstellung kontinuierlich faserverstärkter thermoplastischer Halbzeuge. ISBN 9783934930377, TU Kaiserslautern, Germany, 2004.
- [158] Christmann M, Medina L, Mitschang P. Effect of inhomogeneous temperature distribution on the impregnation process of the continuous compression molding technology. *J Thermoplast Compos Mater* 2017;30:1285–302. doi:10.1177/0892705716632855.
- [159] Piott F, Krämer A, Lück A, Hoffmann L, Mitschang P, Drummer D. Increasing the performance of continuous compression moulding by local pressure adaption. *Adv Manuf Polym Compos Sci* 2021;0:1–14. doi:10.1080/20550340.2021.1888209.
- [160] Hofbauer D. Herstellung endlosfaserverstärkter, thermoplastischer Halbzeuge für Karosseriestrukturbauteile in Großserie. *Technol Light Struct* 2017;1. doi:10.21935/tls.v1i1.75.
- [161] Mayer C, Wang X, Neitzel M. Macro- and micro-impregnation phenomena in continuous manufacturing of fabric reinforced thermoplastic composites. *Compos Part*



- A Appl Sci Manuf 1998;29:783–93. doi:10.1016/S1359-835X(98)00056-6.
- [162] Wang X, Mayer C, Neitzel M. Some issues on impregnation in manufacturing of thermoplastic composites by using a double belt press. *Polym Compos* 1997;18:701–10. doi:10.1002/pc.10323.
- [163] Liu D, Zhu Y, Ding J, Lin X, Fan X. Experimental investigation of carbon fiber reinforced poly(phenylene sulfide) composites prepared using a double-belt press. *Compos Part B Eng* 2015;77:363–70. doi:10.1016/j.compositesb.2015.03.062.
- [164] Double Belt Presses Berndorf Band GmbH 2023. <https://www.berndorfband-group.com/products/modular-double-belt-press/> (accessed February 27, 2023).
- [165] Functionalized Fiber Reinforced Thermoplastic Composite Materials - Neue Materialien Fürth GmbH 2023. <https://www.nmfgmbh.de/wp-content/uploads/2022/06/Faserverbundhalbzeuge-deutsch-1.pdf> (accessed February 27, 2023).
- [166] Scattering Machines Meyer 2023. <https://www.meyer-machines.com/en/scattering/scattering-machines/> (accessed February 27, 2023).
- [167] CompositesWorld. Thermoplastic composites gain leading edge on the A380 2006. <https://www.compositesworld.com/articles/thermoplastic-composites-gain-leading-edge-on-the-a380>.
- [168] Köhler T, Gries T, Seide G. Development of PLA hybrid yarns for biobased self-reinforced polymer composites. *IOP Conf Ser Mater Sci Eng* 2017;254:042016. doi:10.1088/1757-899X/254/4/042016.
- [169] Gennaro R, Greco A, Maffezzoli A. Numerical simulation of the microscale impregnation in commingled thermoplastic composite yarns. *Adv Polym Technol* 2010;29:122–30. doi:10.1002/adv.20179.
- [170] Gennaro R, Christmann M, Greco A, Rieber G, Mitschang P, Maffezzoli A. Experimental measurement of transversal micro- and macro permeability during compression molding of PP/Glass composites. *Polym Compos* 2014;35:105–12. doi:10.1002/pc.22639.
- [171] Hopmann C, Wilms E, Beste C, Schneider D, Fischer K, Stender S. Investigation of the influence of melt-impregnation parameters on the morphology of thermoplastic UD-tapes and a method for quantifying the same. *J Thermoplast Compos Mater* 2019;089270571986462. doi:10.1177/0892705719864624.
- [172] DIN EN ISO 291:2008-08, Plastics - Standard atmospheres for conditioning and testing (ISO 291:2008); German version EN ISO 291:2008, 2008. doi:10.31030/1441132.
- [173] DIN EN ISO 14130:1998-02, Fibre reinforced plastic composites - Determination of apparent interlaminar shear strength by short beam-method (ISO 14130:1997); German version EN ISO 14130:1997, 1998. doi:10.31030/7433990.
- [174] Plastics - Determination of Charpy impact properties - Part 1: Non-instrumented impact test (ISO 179-1:2010); German version EN ISO 179-1:2010, 2010. doi:10.31030/1625765.
- [175] DIN EN ISO 14125:2011-05, Fibre-reinforced plastic composites - Determination of flexural properties (ISO 14125:1998 + Cor.1:2001 + Amd.1:2011); German version EN ISO 14125:1998 + AC:2002 + A1:2011, 2011. doi:10.31030/1753441.
- [176] Plastics - Determination of tensile properties - Part 4: Test conditions for isotropic and anisotropic fibre-reinforced plastic composites (ISO 527-4:1997); German version EN ISO 527-4:1997, 1997. doi:10.31030/7360910.
- [177] DIN EN ISO 18352:2009 Carbon-fibre-reinforced plastics - Determination of compression-after-impact properties at a specified impact-energy level, 2009. doi:https://dx.doi.org/10.31030/2755048.
- [178] DIN EN ISO 1183-1:2019-09, Plastics - Methods for determining the density of non-

---

cellular plastics - Part 1: Immersion method, liquid pycnometer method and titration method (ISO 1183-1:2019, Corrected version 2019-05); German version EN ISO 1183-1:2019, 2019. doi:10.31030/3023324.

- [179] DIN EN ISO 1172:1998-12, Textile-glass-reinforced plastics - Prepregs, moulding compounds and laminates - Determination of the textile-glass and mineral-filler content; calcination methods (ISO 1172:1996); German version EN ISO 1172:1998, 1998. doi:10.31030/8003549.



# Development of high-performance glass fibre-polypropylene composite laminates: Effect of fibre sizing type and coupling agent concentration on mechanical properties

Peter Kiss<sup>a,c,\*</sup>, Wolfgang Stadlbauer<sup>a</sup>, Christoph Burgstaller<sup>b</sup>, Vasiliki-Maria Archodoulaki<sup>c</sup>

<sup>a</sup> University of Applied Sciences Upper Austria, School of Engineering, Stelzhamerstrasse 23, 4600 Wels, Austria

<sup>b</sup> Transcenter fuer Kunststofftechnik GmbH, Franz-Fritsch-Strasse 11, 4600 Wels, Austria

<sup>c</sup> TU Wien, Institute of Materials Science and Technology, Getreidemarkt 9, 1060 Vienna, Austria

## ARTICLE INFO

### Keywords:

- A. Glass fibres
- B. Fibre/matrix bond
- C. Laminate mechanics
- E. Forming

## ABSTRACT

A selection of woven roving and woven filament yarn E-glass fabrics, equipped with different sizing and finish formulae, were tested for compatibility with maleic anhydride functionalised polypropylene (MAH-g-PP) matrices. Glass fibre-polypropylene laminates (GF-PP) were prepared at 50% fibre volume fraction via film stacking and flat panel compression moulding. The effectivity of the utilised coupling agent concentration on interfacial adhesion was characterised through indirect method in 3-point flexural tests. Besides aminosilane A-1100 and PP-compatible fabrics, FK144 Volan "A" chromium complex finished fabrics showed exceptional compatibility and performance in combination with MAH-g-PP modified PP matrices, which has not been reported in the literature before. Mean flexural properties of FK144 laminates peaked at 450 MPa for strength and 21 GPa for modulus at 0.10% MAH loading and a fibre volume fraction of 53%. Possible coupling mechanisms were discussed, which may explain the basic compatibility between the chromium complex and PP.

## 1. Introduction

In recent years, industrial interest has been focusing on finding weight reduction measures for transportation means, thereby improving upon energy efficiency and fuel economy. Through re-design and material substitution of specific components with lighter materials, substantial efforts are being undertaken towards reduced environmental impacts across vehicles life cycles. Continuous fibre-reinforced thermoplastics represent a lightweight structural material group, which are gaining popularity in various technical applications, especially in the automotive sector. The possibility of sub-one-minute thermoforming cycles makes these materials very attractive for high-volume production. At the same time, fibre-reinforced thermoplastics meet the requirements of circular economy concepts due to general recyclability and therefore higher sustainability compared to thermoset composites.

Pre-impregnated glass fibre-polypropylene (GF-PP) laminates, also known as "GF-PP organo sheets", come in a favourable cost to performance ratio as an engineering material. They are suited for use in mild temperature conditions with typical areas of application below 100 °C. Chemical resistance, moisture resistance and basically unlimited shelf life, in addition to excellent thermoforming characteristics are just a

few advantages of polypropylene (PP) composite laminates. However, material development of high-quality pre-impregnated laminates poses many challenges in terms of base material selection, given by the large quantity of available fibrous products, polypropylene types, additives and combinations thereof.

Owing to the nonpolar nature of polypropylene, glass fibre-reinforced polypropylene composites made of unfunctionalised matrices, suffer from poor fibre adhesion and therefore low mechanical properties [1]. To promote fibre adhesion, a coupling agent such as maleic anhydride grafted polypropylene (MAH-g-PP) may be introduced into the matrix, which provides some degree of polarity, reactivity and compatibilisation of the two phases [2]. The addition of up to 10 wt% MAH-g-PP concentrate in the matrix phase for short-, long- or continuous fibre glass reinforced PP is common practice documented in literature [3–7]. The amount of coupling agent to be blended with the PP base polymer depends, besides the graft level, viscosity and fibre content, in practice mainly on the cost factor and the mechanical requirements of the composite. For this reason, PP composites can in a certain performance range be mechanically fine-tuned fairly easily compared to other polymer systems. However, high mechanical performance of GF-PP composites cannot be expected solely by the

\* Corresponding author at: University of Applied Sciences Upper Austria, School of Engineering, Stelzhamerstrasse 23, 4600 Wels, Austria.  
E-mail address: [peter.kiss@fh-wels.at](mailto:peter.kiss@fh-wels.at) (P. Kiss).

addition of MAH-g-PP. A fundamental prerequisite for an MAH-g-PP modified PP matrix to yield high-performance composites is the ability to properly wet the reinforcement fibre surface, chemically react with it and entangle (interdiffusion) with the bulk of the polymer [8,9]. In general, adhesion at the fibre interface occurs mainly due to: physical adhesion related to wettability and compatibility which are controlled by the surface energies of the materials, and chemical bonding which depends on the chemical functionality of the matrix and the fibre coatings [10]. Mechanical interlocking (mechanical adhesion) due to surface roughness is less important in the case of glass fibre reinforcement.

Continuous glass fibre strands which are used for fabric weaving can be differentiated by their fibre diameter and linear densities into roving and filament yarn. Roving refers to strands with filaments typically over 13  $\mu\text{m}$  in diameter and linear densities of 300–4800 Tex. Filament yarn refers to strands with filaments typically under 14  $\mu\text{m}$  in diameter and linear densities under 300 Tex. Roving fabrics and filament yarn fabrics can be further differentiated by the method of coating application, either by sizing or finishing. It is important to note that the terms sizing and finish shall not be used interchangeably. Direct roving fabrics, which are used in this work, are equipped with a permanent coating immediately applied after melt spinning to the rovings, called a direct sizing. Apart from film formers and the important silane adhesion promoters, direct sizings may contain several other additives, including antistatics and lubricants which facilitate weaving and prevent fibre breakage [11]. Sizing formulations are proprietary and no information on the exact adhesion promoter is given.

Filament yarns are used to produce tightly woven fabrics, usually with lower grammage compared to roving fabrics. In certain cases, filament yarns may be equipped with a direct sizing for immediate use after weaving, however, more common is the use of filament yarns for the finishing process [12]. Filament yarns used for finishing contain a specially formulated protective coating which needs removal after weaving. This woven (loomstate) product is cleaned by either heat or chemical treatment, followed by re-coating of the fabric with a chemically pure adhesion promoter, thereafter, called a finished fabric. Silane-finished fabrics used in this work are silane-only coatings and do not contain any other additives. The active adhesion promoter applied in a finish is generally disclosed, e.g. “Z6040 epoxypropylsilane” [12–14]. A finish can be tailored to yield compatibility towards certain resins. Fibre wettability is an important topic and adhesion to fibres may be impeded if an incompatible coating is selected in terms of surface energy. For bonding to occur, which is important for effective stress transfer, the fibres and matrix must be brought into intimate contact; wettability can therefore be regarded as an essential prerequisite for chemical bonding [10,15]. An optimised fibre coating can make the difference between a low- or high-performance composite as for example Sambale, Schönreich and Stommel concluded [16]. A wide range of fibre adhesion promoters are available, most of which were specifically developed for thermoset resin systems in the form of reactive silanes. The majority of silane-based fibre coatings are highly heat resistant (200–300 °C) in oxidising atmospheres, which makes them also suitable for thermoplastic composite processing [17,18]. A lot of research has gone into aminosilane coated fibres, which are most commonly referred to as very good adhesion promoters for a variety of thermoplastics, especially for maleated polypropylene [11]. Silanised

fabrics with organofunctionalities other than amino, such as epoxy, vinyl, or methacrylic and non-silane-based fabrics containing chromium complexes are easily available, but not sufficiently analysed for polypropylene compatibility [14,19].

Nevertheless, especially for compression moulded continuous GF-PP composites, the influence of fibre coatings and coupling agent was not investigated in detail until now. Therefore, the aim of this work was to investigate the influence of MAH coupling agent content in combination with different fibre coating types on the mechanical properties and to reach laminate strengths at least in the range of an industrial GF-PP laminate product. Initially two fabrics were compared, a roving fabric with a PP-compatible sizing and a filament yarn fabric containing a chromium methacrylate complex finish called Volan. Laminates made of these fabrics were tested in 3-point flexural tests in an MAH-concentration range between 0.02 and 0.10% in 0.02% steps. Through these measurements, a reasonable amount of coupling agent could be assessed which was then used for a fibre coating study comparing eight further coating types. Apart from mechanical optimisation and characterisation, a processing method is presented in the final chapter of the paper for drastically improved laminate surface quality comparable to industrial standards.

## 2. Materials and methods

### 2.1. Materials

A PP-homopolymer, specifically developed for fibre impregnation applications, PP HK060AE (supplied by Borealis AG, Austria) with an MFR of 125 g/10 min (melt flow rate at 230 °C, 2.16 kg) and a density of 905 kg/m<sup>3</sup> was selected for the experiments. HK060AE was functionalised with an easy flowing MAH-g-PP grade, Polybond® 3000, hereinafter abbreviated as PB3000 (supplied by Brenntag GmbH, Germany) at different concentrations. The utilised coupling agent PB3000 had high MFR, 400 g/10 min (at 190 °C, 2.16 kg) at an MAH grafting level of 1.2%. Blends of PP and MAH-g-PP were prepared based on active MAH substance. Therefore, it was necessary to calculate weight adjustment to obtain the required MAH concentration depending on the grafting level. Additionally, carbon black PP-homopolymer masterbatch Maxithen® PP black 98981 (supplied by Gabriel-Chemie GmbH, Austria) containing 40% carbon black pigment, was added at 2.0 wt% to all HK060AE blend formulations for improved contrast between fibres and the matrix. The exact blend formulations used, are outlined in Table 1.

From these formulations, films were produced in-house by dry blending the constituents, melt compounding and flat film extrusion. Melt compounding was carried out in a co-rotating twin-screw extruder TSE 24 MC (Thermo Fisher Scientific GmbH, Germany) with 24 mm screw diameters, L/D ratios of 40, at screw speeds of 280 rpm and throughput of 12.0 kg/h. The barrel temperature was adjusted to 200 °C during compounding. The extruded strands were pelletised and further processed by flat film extrusion on a flat film extrusion line PM30 (Plastik Maschinenbau Geng-Meyer GmbH, Germany) with a 35 mm screw diameter, an L/D ratio of 18, at a screw speed of 50 rpm and throughput of 9.5 kg/h. The barrel temperature was set to 220 °C and the flat film extrusion die was adjusted to 130  $\pm$  5  $\mu\text{m}$  film thickness.

For comparative reasons, a special PP-copolymer grade, “containing

**Table 1**  
Blend formulations with PP HK060AE base resin.

Additive	MAH grafting level (%)	no MAH blend	0.02% MAH blend*	0.04% MAH blend*	0.06% MAH blend*	0.08% MAH blend*	0.10% MAH blend*
Polybond 3000 (wt%)	1.2	–	1.67	3.33	5.0	6.67	8.33
Maxithen black 98981 (wt%)	–	2.0	2.0	2.0	2.0	2.0	2.0

\* MAH-g-PP quantity normalised to active MAH content.

**Table 2**  
Overview of selected E-glass fibre 2x2 twill fabrics and composite build up used in this work.

Glass fabric	Fibre type	Areal weight(g/ m <sup>2</sup> )	Fibre coating	Number of fabric plies and films (130 µm) used
<sup>1</sup> GIVIDI VR48	EC9 filament	290	A-1100 aminosilane soft finish	8/8
<sup>1</sup> GIVIDI VR48	EC9 filament	290	G1 aromatic aminosilane finish	8/8
<sup>1</sup> GIVIDI VR48	EC9 filament	290	G1496 enhanced aminosilane finish	8/8
<sup>1</sup> GIVIDI VR48	EC9 filament	290	Z6040 epoxysilane soft finish	8/8
<sup>2</sup> PI Interglas 92140	EC9 filament	390	FK144 chromium complex finish	6/8
<sup>3</sup> HexForce® 01038	EC9 filament	600	TF970 aminosilane finish	4/8
<sup>4</sup> PD GW 123-580K2 1200	EC14 roving	580	Silane sizing, thermoset application UP, VE, EP	4/8
<sup>4</sup> PD 1200-E35 (new designation: GW 173-600K2)	EC17 roving	600	Silane sizing, PP-compatible	4/8
<sup>5</sup> JM StarRov® 490 1200	EC16 roving	600	Silane sizing, PP-compatible	4/8
<sup>6</sup> NEG TufRov® 4599	EC17 roving	600	Silane sizing, PP-compatible	4/8

<sup>1</sup> GIVIDI Fabrics S.r.l., Italy

<sup>2</sup> Porcher Industries Germany GmbH, Germany

<sup>3</sup> Hexcel Composites Dagneux, France

<sup>4</sup> P-D Glasseiden GmbH Oschatz, Germany

<sup>5</sup> Johns Manville Slovakia a.s., Slovakia

<sup>6</sup> Nippon Electric Glass Co. Ltd., Japan

an additive package for optimum glass fibre coupling”, PP BJ100HP (supplied by Borealis AG, Austria), with an MFR of 90 g/10 min (at 230 °C, 2.16 kg) and a density of 904 kg/m<sup>3</sup> was also included in the experiments. Due to proprietary reasons, no further information on the additive package of BJ100HP was provided. BJ100HP was directly processed to 130 ± 5 µm films in-house without addition of carbon black pigment.

An overview of the utilised glass fibre fabrics with different sizing and finish compositions for composite lamination is given in Table 2. All listed fabrics made of EC9 fibres contained adhesion promoters applied via finishing process. Yarn coating-removal of VR48 loomstate fabric rolls was conducted by GIVIDI Fabrics S.r.l. through stationary oven heat-treatment at a peak temperature of 350 °C and short dwell-times at that temperature. Such heat-treatment processes are optimised to yield a glass fibre surface with an optimal distribution and quantity of hydroxyl groups for the subsequent silanisation process. The cooled fabric rolls were unwound and drawn through finishing-baths which contained aqueous solutions of silanes/silane-mixtures. The silanes were deposited on the fabrics followed by a drying, washing and winding step. The terminology “soft finish” refers to an adapted composition or low concentration of the silane adhesion promoter. The rest of the fabrics made of direct roving reinforcement had proprietary direct sizings applied to the fibres. As a reference for mechanical properties, an industrially manufactured GF-PP consolidated laminate, Tepex® dynalite 104-RG600(4)/47% – 2.0 mm (supplied by Bond-Laminates GmbH, Brilon) based on 1200 Tex roving reinforcement was benchmarked.

## 2.2. Methods

### 2.2.1. Weaving of PP-compatible fabrics

Since woven fabrics made of PP-optimised direct rovings Johns Manville StarRov® 490 and Nippon Electric Glass TufRov® 4599 both with a linear density of 1200 Tex were not commercially available, fabrics were produced in-house from roving bobbins by manual weaving. A simple handloom was built for this application as shown in Fig. 1, on which 2x2 twill fabrics were woven for comparative tests with a thread count of approximately 2.5 threads per cm and grammage of approximately 600 g/m<sup>2</sup>. During unwinding of the rovings from the bobbins, the initially hard and stiff direct rovings, held together by the film former, had to be mechanically crimped for softening. This was realised by redirection of the rovings as described by Henninger and Friedrich, which spread the rovings into soft fibre bundles [20]. Only through these measures micro-impregnation of the self-woven fabrics



Fig. 1. Loom constructed for manual weaving of PP-compatible rovings.

could be guaranteed.

### 2.2.2. Laminate production by compression moulding

Reinforcement fabrics and plastic films were cut to dimensions of 350 × 250 mm and alternately stacked layer by layer inside a transportable hardened steel impregnation tool as shown in the processing scheme in Fig. 2. The impregnation tool was properly treated with a high temperature heat resistant release agent Loctite Frekote 700-NC (Loctite Deutschland GmbH, Germany) prior to laminate pressing. All fabric layers were stacked with the warp yarn arranged in the same, i.e. longitudinal direction. To reach a final laminate thickness of 2 ± 0.2 mm conforming to EN ISO 14125, eight filament glass fabric layers of 300 g/m<sup>2</sup> were stacked with eight layers of 130 µm thick polymer film [21]. Laminates made of high grammage fabrics were processed by stacking four layers of 600 g/m<sup>2</sup> reinforcement fabric and eight layers of 130 µm polymer film. Hot pressing was carried out on a laboratory press Wickert WLP 80/4/3 (Wickert Maschinenbau GmbH, Germany). For fast tool heat up, the temperature of the heating press was adjusted to the maximum of 300 °C. To avoid over-heating of the laminates, the temperature of the film stacks was monitored inside the impregnation tool by insertion of thin-film thermocouples type-K, 402–716 (TC Mess- und Regeltechnik GmbH, Germany) in combination with a temperature data logger Testo 176 T4 (Testo SE & Co. KGaA, Germany). Cooling of the impregnation tool was carried out on a water-cooled press Höfer H10 (Höfer Presstechnik GmbH, Austria). During the heat up phase of the impregnation tool, the hot press was closed at approximately 0.1–0.2 MPa to allow for contact heating without excessive compaction. Once processing temperature

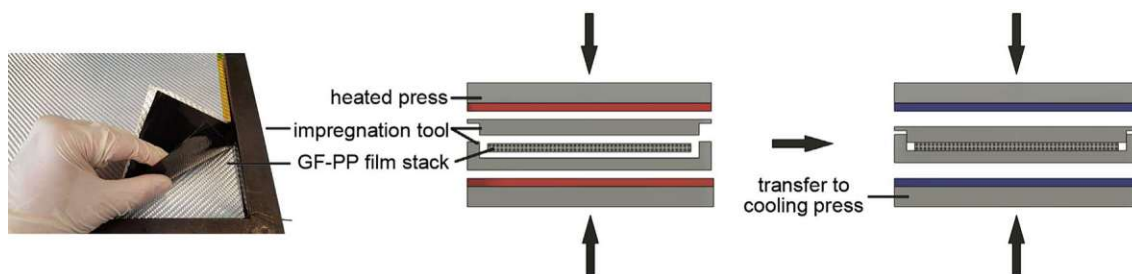


Fig. 2. Film stacking and flat compression moulding processing scheme.

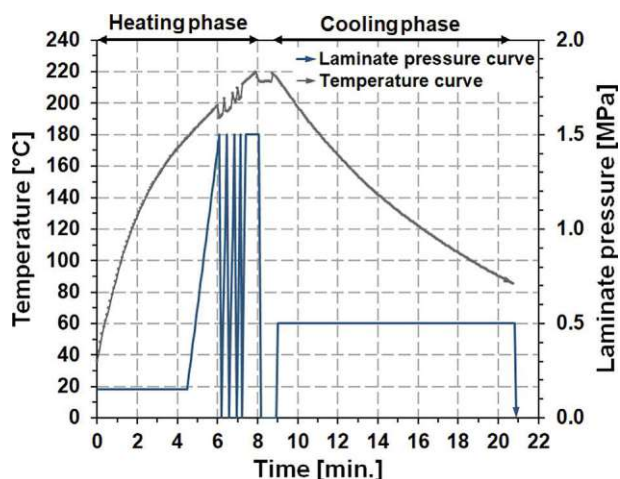


Fig. 3. Representation of a laminate processing cycle, temperature taken inside impregnation tool and pressure exerted upon laminate.

reached 180 °C inside the tool, impregnation pressure was slowly increased by manual operation of the press to 1.5 MPa (gauge pressure: 5.0 MPa). The pressure-cycling method, also referred to as pressure-unloading was exerted at 200 °C laminate temperature for at least five times. Several authors found this method to aid impregnation by partially restoring permeability of fibre bundles during the unloading action, resulting in better wet-out and practically void-free laminates [22–24]. Moreover, the pressure-cycling technique is somewhat related to intermittent pressing, frequently used in thermoplastic composite laminate manufacturing. After pressure cycling, the tool was kept inside the heating press at constant pressure for one minute until the laminate temperature reached 220 °C. The tool was subsequently transferred into the cooling press via a shuttle system. The laminates were cooled and consolidated under 0.5 MPa static pressure (gauge pressure: 10.0 MPa, smaller piston) followed by demoulding at 90 °C. Representative processing temperature- and pressure curves can be seen in Fig. 3.

### 2.2.3. Laminate analysis

In order to evaluate the influence of MAH concentration and fibre coating variation on the mechanical properties of woven GF-PP laminates, 3-point flexural tests were carried out on a Zwick/Roell ZMART.PRO 10 kN universal testing machine. According to EN ISO 14125 a crosshead speed of 1 mm/min and a span length of 40 mm was selected [21]. Specimens were cut out of filament glass fabric reinforced laminates with dimensions of 60 × 15 mm. For laminates made of coarse roving glass reinforcement, the selection of a wider specimen size (60 × 25 mm) was applied to reduce deviation within the test series according to EN ISO 14125 [21]. Samples were cut in the fabric warp direction utilising a saw blade for thermoplastic composites on a water-cooled circular saw Diadisc 4200 (Mutronic Präzisionsgerätekombi GmbH & Co.KG, Germany) and conditioned according to EN ISO 291 [25]. The densities of the composite plates were determined according to EN ISO 1183 [26]. With the knowledge of the composite

specimen density  $\rho_c$  it was possible to calculate for the respective fibre volume fraction via thermogravimetric analysis. The glass fibre mass fraction  $\omega_f$  of the composite samples was determined via calcination at 625 °C on a macro thermogravimetric analyser LECO TGA801 (Leco Instrumente GmbH, Germany) according to EN ISO 1172 [27]. The fibre volume fraction  $\nu_f$  was obtained by Eq. (1):

$$\nu_f = \frac{\omega_f \cdot \rho_c}{\rho_f} \cdot 100 \quad (1)$$

where  $\rho_f$  is the fibre density provided by the fibre manufacturers, here 2.58 g/cm<sup>3</sup>.

Fully impregnated laminates established the foundation upon which a comparison was eligible to be made. SEM micrographs were taken from polished specimens at different magnifications at 20 kV accelerating voltage and back scattered electron imaging. Low magnification images were taken via SEM Vega II LMU (Tescan, Czech Republic). High magnification images were taken via FESEM MIRA3 LMH (Tescan, Czech Republic).

### 2.2.4. Validation of a radical grafting mechanism between PP and the FK144 Volan “A” chromium methacrylate complex finish

Upon inspection of the chemical structure of Volan A, a possibility for radical coupling was suspected between polypropylene and the methacrylate ligand contained within the chromium complex. A series of film stacks were prepared, which were moulded with different amounts of radical initiator dicumylperoxide 98%, abbreviated as DCP (Alfa Aesar GmbH & Co KG, Germany) deposited on PP films. To ensure a possible radical grafting reaction to take place in-situ during impregnation, DCP-acetone solutions were prepared with which unmodified PP HK060AE films of 130 µm thickness were wetted. The respective amounts of DCP, 0.01, 0.10 and 0.30 wt% were weighed according to the mass of unmodified PP films utilised in the film stacks and dissolved in acetone at room temperature. The DCP-acetone solutions were poured over the PP films and spread evenly by shuffling of the films. The acetone was let to evaporate off the films prior to film stacking and laminate pressing. The consolidated laminates were tested in 3-point flexural tests with the same parameters as described previously.

## 3. Results and discussion

### 3.1. Determination of optimal coupling agent concentration by mechanical testing

Several testing methods are available to determine fibre–matrix interfacial shear strength by micromechanical testing. Since the focus of this work was on macromechanical properties, an interface sensitive macromechanical testing method had to be chosen. Macromechanical tests such as compression, flexural or ILSS tests may be used to gather interface sensitive information for comparison of laminates with the same processing history. Compressive strength is a strong function of fibre–matrix adhesion, since poor interfacial adhesion lowers the critical stress for micro-buckling through a reduction of fibre support

[28,29]. Bending of specimens leads to a combination of compressive and tensile loads. Because failure occurs on the compression side of flexural specimen for most composites, it can be used as an effective substitute for compression testing [12]. Tran et al. have done extensive work on single-fibre wetting analysis as well as micro- and macro-mechanical testing, and concluded that the flexural strength in longitudinal fibre direction of composites is largely correlated with their interfacial adhesion [30]. Flexural strength, either in longitudinal or transverse fibre direction, is frequently used as a measure for the quality of interfacial adhesion [15,28–36]. Support against fibre micro-buckling in bending is afforded by the rigidity (shear modulus) and (shear) strength of the matrix [29]. Further important factors to consider are proper fibre wetout, fibre orientation, fibre stiffness, fibre strength, fibre volume fraction, void content and fibre–matrix adhesion to effectively transmit loads. Support against buckling is particularly important in woven fabric laminates where the fibres exhibit significant waviness [29]. The ILSS (interlaminar shear strength) is also a measure for determining the quality of fibre–matrix adhesion [37]. However, based on our testing experience with woven glass fibre reinforced polypropylene composites, specimens of such do not fail caused by interlaminar shear due to their high inherent toughness and insufficient stiffness in the short beam ILSS test. This corresponds with the findings of several authors who made similar observations with woven glass fibre reinforced thermoplastic composites in which specimens showed inelastic deformation, rather than failure through delamination [38,39]. Therefore, we opted not to perform ILSS tests and focus on 3-point flexural tests instead.

Experimental data obtained from the 3-point laminate flexural tests are compared in the following figures, which depict the mechanical properties of woven GF-PP laminates as a function of increasing coupling agent concentration.

As can be seen in Fig. 4 the progressions of GF-PP laminates based on PP-compatible glass fibres StarRov 490 and filament glass fibres with FK144 Volan “A” chromium methacrylate complex finish show more or less identical results in terms of bending strength with increasing MAH content. The only major difference between the two reinforcement fabrics was measured with PP HK060AE matrix (no MAH additive), which is an indicator of StarRov 490 having better initial compatibility to polypropylene possibly due to an MAH-g-PP film former [18]. At MAH concentrations greater than 0.04%, a plateau was reached for StarRov 490, showing only marginal increase in flexural strength thereafter. This is probably due to the arising fibre surface saturation with MAH-g-PP as described by Sammartino et al., after which no noteworthy, or only a minor improvement in mechanical properties is occurring [40]. As we could observe from our testing results, fibre surface saturation may start as early as in the 0.04% MAH concentration range. The outcome therefore indicated that the addition

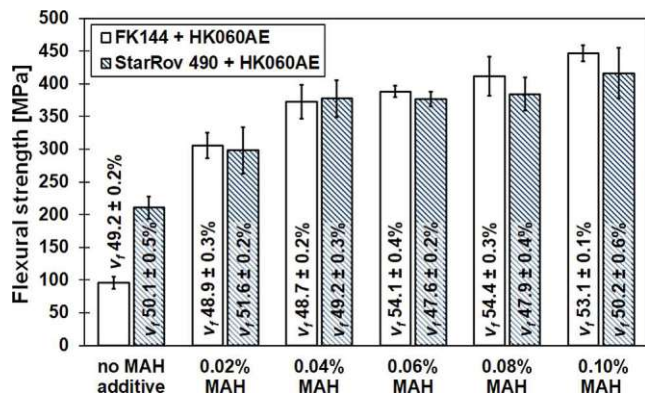


Fig. 4. Flexural strength versus increasing MAH concentration in HK060AE matrix of FK144 and StarRov 490 GF-PP laminates; MAH (PB3000) concentrations ranging from no additive to 0.10% in 0.02% steps.

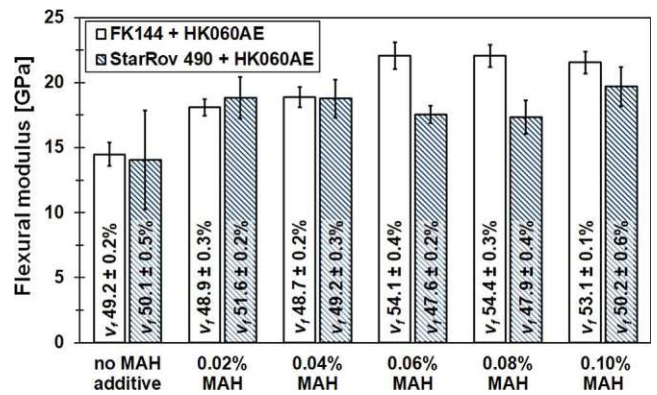


Fig. 5. Flexural moduli and fibre volume fractions of laminates with increasing MAH (PB3000) concentrations from no additive to 0.10% MAH in 0.02% steps. Comparison of two fabrics FK144 and StarRov 490 with HK060AE matrix.

of 0.04% MAH additive is adequate to reach high material performance at modest coupling additive usage. For this reason, all further laminate comparisons were carried out at an MAH concentration of 0.04%. Bending strengths of FK144 fabrics were slightly higher at high MAH loading compared to StarRov 490 and peaked at 450 MPa with 0.10% MAH additive. It is important to note that fibre volume fractions differed among the test series, especially in the case of FK144 laminates at high coupling agent contents. We are aware, that the increase in flexural strength of FK144 laminates past 0.04% MAH is not necessarily attributable solely to better coupling, but rather also in the higher fibre volume fractions ranging between 53 and 54% compared to the other laminates having 48–50% fibre volume content.

Composite stiffness is governed mainly by fibre content and fibre orientation, rather than interfacial adhesion. However, there have also been reports of MAH-g-PP affecting the flexural modulus significantly, depending on the coupling agent concentration [41]. In our case, we could also observe a difference in flexural stiffness between specimens containing no coupling additive and specimens containing coupling additive at identical fibre volume fractions, shown in Fig. 5. It seems that a certain amount of coupling agent is necessary in polypropylene composites to give reliable stiffness readings. This may have to do with interfacial wetting and improved load transfer at low strains. At 0.02% MAH additive and above, flexural modulus readings were relatively well correlated to the respective fibre volume fractions.

Taking into account the difference in the fibre diameters of 9 μm (FK144) and 16 μm (StarRov 490) for specimens at identical fibre volume fractions, it may be hypothesised that the PP-compatible StarRov 490 fibres performed better overall. This is due to the fact that 16 μm fibres have a smaller surface area and therefore fewer binding sites compared to 9 μm fibres. Sizing and finish adhesion promoter concentrations were unknown, which could also affect coupling performance. Furthermore, it is known that the heat-treatment step of filament glass fabrics causes detrimental effects on fibre strength. Dry fabric tensile strength data provided by the fabric manufacturers indicated that there was a slight difference between roving and filament fabric strength, with roving fabrics showing higher strength. However, both fabric types were still in a very comparable range. Nevertheless, the exceptional compatibility of FK144 Volan “A” chromium methacrylate complex to MAH-g-PP is highly interesting and has not been mentioned in the open literature before. Thus, FK144 finish underwent further detailed investigations, which are discussed shortly.

### 3.2. Effect of fibre sizing on mechanical properties

As we demonstrated before, MAH-g-PP is clearly affecting flexural strength, yielding higher values at higher MAH loading most possibly by improving fibre wetting and interfacial bond formation. In the

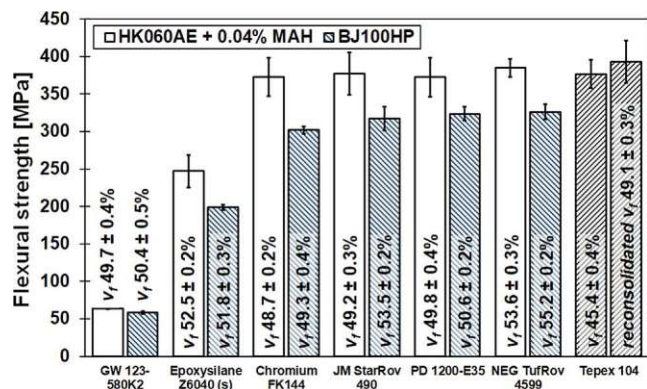


Fig. 6. Flexural strength of GF-PP laminates with different fibre coating types obtained by use of different PP matrices; HK060AE + 0.04% MAH (PB3000) and PP BJ100HP. Tepex 104 tested as reference material.

following comprehensive fibre coating study, which involved the comparison of eight additional fabrics, a strong dependence of the fibre coating on the resulting mechanical performance could be verified. Our own blend of HK060AE containing 0.04% MAH (PB3000) and carbon black masterbatch (CB) was compared with a commercially available glass fibre compatible polypropylene grade BJ100HP. For the sake of comparison, the values obtained at 0.04% MAH of StarRov 490 and FK144 are provided again in Fig. 6.

The importance of fibre coatings on the mechanical performance could be shown very clearly by comparing samples made of thermoset compatible direct roving fabric GW 123-580K2 and the three PP-compatible roving fabrics JM StarRov 490, PD 1200-E35 and NEG TufRov 4599. All laminates made of PP-compatible rovings performed equally in a region of 370 MPa, while a 300 MPa difference in mean flexural strength was observed between the thermoset compatible and PP-compatible rovings. The presence of an incompatible film former within the GW 123 thermoset compatible sizing could have prohibited complete fibre wetting. This would have resulted in poor fibre-matrix load transfer, hence the low flexural strengths and low moduli. The results therefore proved that tailored thermoplastic sizings for direct rovings, in the case of polypropylene matrices, are of utmost importance for wettability and coupling. The use of thermoset compatible roving fabrics with direct sizings equipped for compatibility with epoxy-, unsaturated polyester- and vinyl ester resins lead to highly unsatisfactory laminate properties in combination with functionalised PP matrices. Thus, they should be avoided in GF-PP organo sheet applications due to fibre matrix incompatibility. The reference material Tepex dynalite 104-RG600(4)/47% – 2.0 mm was tested in delivery condition as well as in reconsolidated state (subjected to the same processing cycle as shown previously in Fig. 3). Tepex 104 mean flexural strength was measured at 377 MPa, which is in accordance with the datasheet of the material supplier. Higher bending strengths of Tepex 104 were obtained in reconsolidated state due to compaction of the laminate from 2.0 mm to 1.84 ± 0.04 mm thickness and smaller specimen cross sections as a consequence. The mean flexural strength of epoxysilane Z6040 (soft) laminate at 247 MPa indicated that coupling between modified PP and the epoxysilane may have occurred. If maleic anhydride is present in hydrolysed form as maleic acid, there is a possibility of reaction with glycidyl groups through addition, similar to high temperature anhydride curing epoxy resins. Hydrolysis of maleic anhydride may take place during lamination with traces of water usually adsorbed to the fibre surface [42,43]. Furthermore, water present may react with the epoxide group, giving di-alcohols which could react with MAH giving bis-esters. Still, the epoxysilane finish could not quite match mechanical performance of PP-optimised sizings and FK144 finish. However, the epoxysilane-only (finished) fabric is capable of providing much improved properties over the thermoset compatible fabric GW 123-580K2

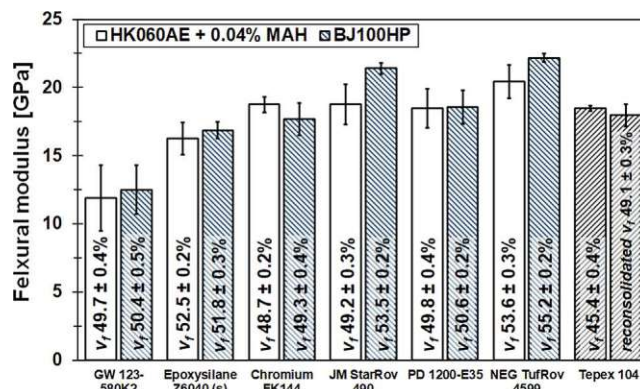


Fig. 7. Flexural moduli of GF-PP laminates with different fibre coating types obtained by use of different PP matrices; HK060AE + 0.04% MAH (PB3000) and PP BJ100HP. Tepex 104 as reference material.

(containing a vinyl-, epoxy- or aminosilane sizing). The absence of an incompatible film former within the finished fabric has most possibly improved wettability and bonding compared to GW 123-580K2. Overall, the comparison illustrated, that the compatibility of FK144 Volan “A” chromium methacrylate complex to MAH modified PP matrices is truly exceptional. Equal performance of the FK144 finish to PP-adapted silane sizings was not expected beforehand and is a novel finding.

Laminates made of PP type BJ100HP reached lower flexural strength performance throughout, yet equal to higher flexural moduli were attained for most laminates compared to modified HK060AE composites as can be seen in Fig. 7. The strength difference between BJ100HP laminates and our modified HK060AE laminates may be due to a difference in coupling agent concentration or also due to a difference in matrix strength and modulus between the two PP types. Fibre wetting characteristics were comparable (see Fig. 10, chapter 3.3), even though HK060AE had higher MFI in the delivery state. Mean flexural moduli of the tested laminates lied in a region of 16–22 GPa except for the thermoset optimised roving laminates GW 123-580K2 that were lower at around 12 GPa, supporting the theory of matrix incompatibility.

A comparison between FK144 at 0.04% MAH, StarRov 490 at 0.04% MAH and Tepex 104 was eligible, because of mean flexural moduli lying in a region of 18 GPa for all of these specimens. However, Tepex 104 showed fibre volume fractions around 45% in delivery state, whereas our laminates had fibre volume fractions in the region of 50%. Even though Tepex 104 has around 5% lower fibre volume content, it exhibits similar flexural strengths to our laminates. This could indicate that in Tepex 104 a slightly higher MAH concentration than 0.04% is used.

In the fibre coating study, a further comparison between four aminosilane finish types with both polymers (HK060AE + 0.04% MAH PB3000 and BJ100HP) was conducted. Aminosilane treated surfaces are suspected to form amide bonds with maleic anhydride or very stable imide ring systems through further reaction via cyclodehydration [44]. Regardless, the performance of aminosilane-finished fabrics with MAH-g-PP functionalised PP matrices is still dependent on their exact chemical composition as Fig. 8 confirms. Functionalised PP HK060AE showed medium compatibility to aromatic aminosilane G1 finish and TF970 aminosilane finish. On the other hand, enhanced aminosilane GI496 and A-1100 aminosilane soft finished fabrics exhibited very good compatibility to MAH-g-PP and therefore high flexural strengths of close to 400 MPa at 0.04% MAH loading. Mean flexural moduli were measured at 20 GPa in the case of GI496 laminate and 18 GPa for the A-1100 laminate. In a recent publication by Thomason et al., the authors clarified that modern PP compatible glass fibre sizings are made up of APS (aminopropylsilanes) and MAH-g-PP film formers [18]. It is clear



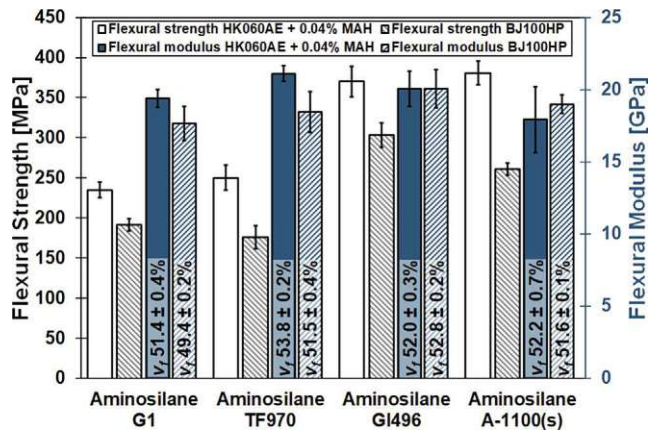


Fig. 8. Flexural strength values of GF-PP laminates built up from different aminosilane treated fabrics and two different PP matrices; HK060AE + 0.04% MAH (PB3000) and PP BJ100HP.

from the results that the aminosilane type A-1100 is a possible candidate for these applications in direct sizings because of its mechanical performance in combination with MAH-g-PP. Likewise, as previously observed, PP type BJ100HP showed inferior flexural strength performance compared to modified HK060AE across all tested aminosilane laminates. However, BJ100HP still showed reasonably good results in combination with all PP-optimised rovings, FK144 finish and enhanced aminosilane finish GI496 at mean bending strengths of 300–325 MPa. Even though all aminosilanes should in theory chemically couple in the same way, the differences among the aminosilanes were surprising. It is suspected that the silane-backbone could pose differences in polarity, wetting or accessibility for coupling.

3.3. SEM micrographs

SEM micrographs given in Fig. 9 unveil the morphology of broken

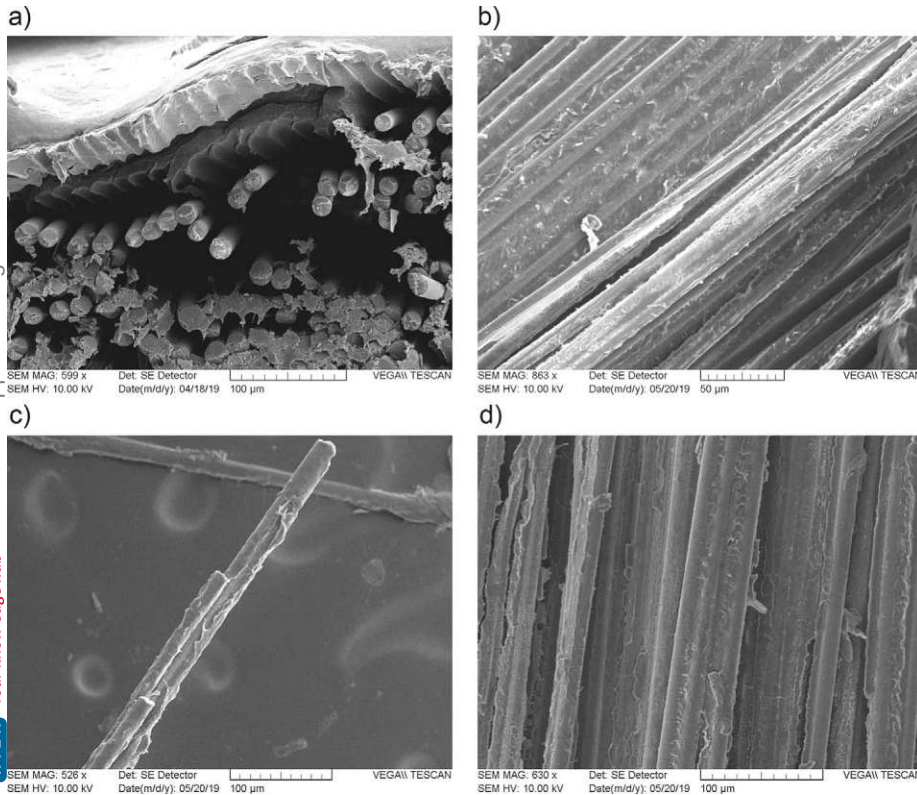


Fig. 9. SEM microsections; (a) EC14 GW 123-580 K2 HK060AE + 0.04% MAH (PB3000) matrix peeling off fibres (b) EC9 FK144 HK060AE + 0.04% MAH (PB3000) showing thoroughly embedded fibres within the PP matrix (c) EC16 StarRov 490 with complete fibre wetting with HK060AE + 0.04% MAH (PB3000) (d) Tepex 104 exhibiting proper fibre wetting.

specimens. Images of the thermoset compatible GW 123-580K2 laminate had to be taken from a cryo cut sample as it showed no brittle failure from testing. GW 123-580 K2 laminated with PP + 0.04% MAH showed the matrix peeling smoothly off the fibres, leaving no matrix residue, which is an indication for incompatibility of the fibres and the matrix. Furthermore, GW 123-580K2 showed wetting issues at the microscale possibly due to the presence of an incompatible film former. A broken EC9 FK144 specimen gives an example of good fibre wet out with PP and matrix cracking rather than interfacial debonding. The same was observed in Tepex 104 laminates, which showed thoroughly wetted fibres and no interfacial debonding. StarRov 490 PP-compatible fibres also exhibited proper coating of fibres with the PP matrix, again verifying the importance of adapted sizings in the case of direct rovings.

All fabrics (except GW 123-580K2) used in the study, regardless of fibre coating and fibre diameter, PP grade, matrix modification or ply count were fully impregnated and practically void-free on both the macro- and microscale. A selection of SEM images taken from polished specimens of high-strength laminates are presented in Fig. 10.

3.4. Investigations of the FK144 Volan “A” chromium methacrylate complex finish

Interestingly, the initial flexural strength value of the FK144 laminate series without the addition of MAH coupling agent seemed to be relatively high at 100 MPa in comparison to the thermoset compatible roving laminate GW 123-580K2 at 60 MPa (which additionally contained 0.04% MAH). This difference in flexural strength led us to believe that there had been some kind of reaction between PP (no MAH involved) and the FK144 chromium complex. Extensive research on interactions between such chromium complexes and laminating thermoset resins has been conducted by Yates and Trebilcock. The authors suggested a variety of mechanisms such as hydrogen bonding, coordinate complex bonding to chromium, acid-base interactions and the involvement of the methacrylic double bond in matrix bonding [45]. The complexed methacrylic group within the Volan chromium adhesion

Die approbierte gedruckte Originalversion dieser Dissertation ist an der TU Wien Bibliothek verfügbar. The approved original version of this doctoral thesis is available in print at TU Wien Bibliothek.

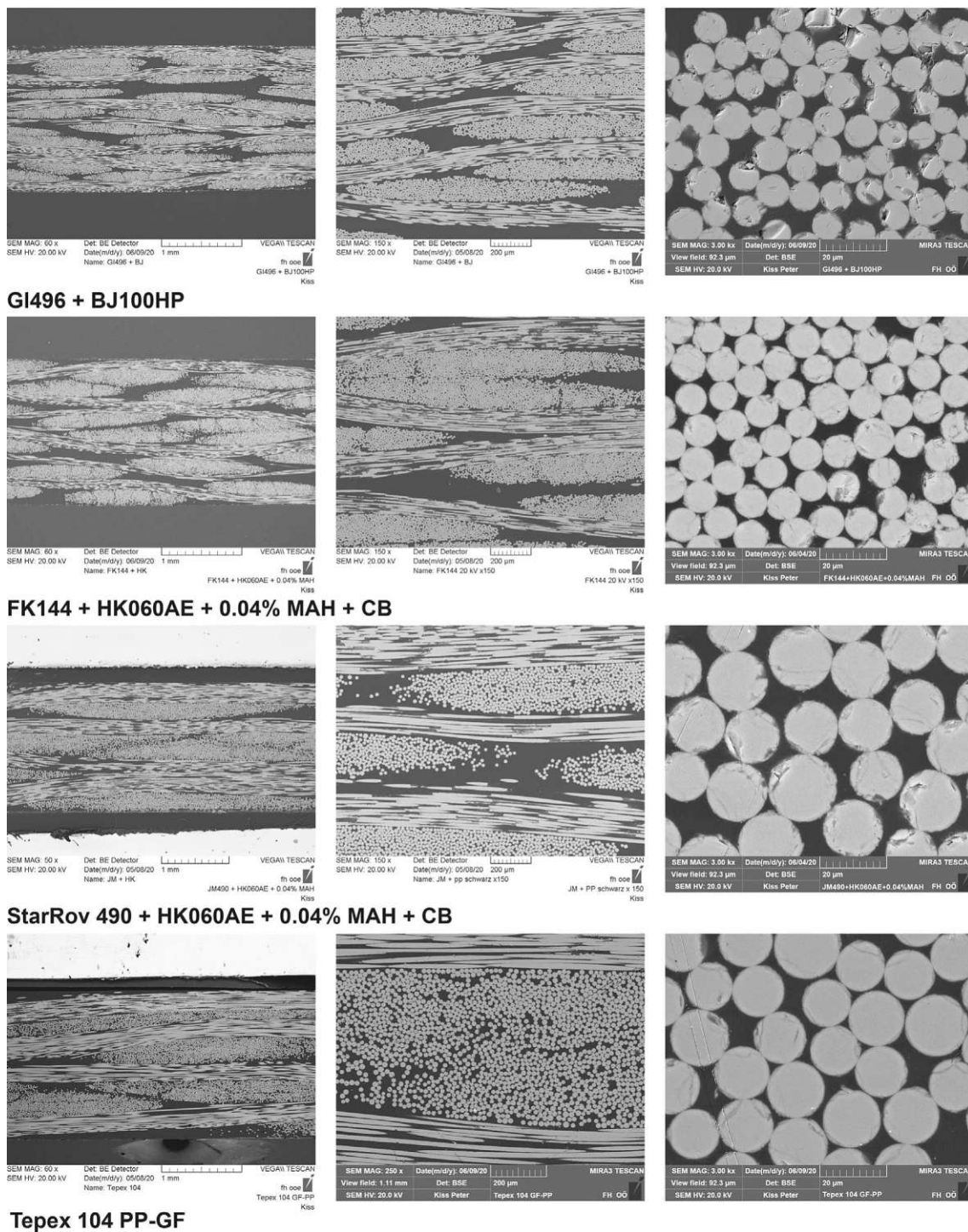


Fig. 10. SEM microsections of polished high-strength laminates GI496, FK144, JM StarRov 490 and Texpex 104.

Die approbierte gedruckte Originalversion dieser Dissertation ist an der TU Wien Bibliothek verfügbar. The approved original version of this doctoral thesis is available in print at TU Wien Bibliothek.

**TU** **Bibliothek**  
WIEN  
Your knowledge hub

promoter provides a possible binding site in the form of a double bond for radical addition. As radical addition is a known method for grafting polyolefins to silanes containing double bonds, we suspected a similar radical binding mechanism of PP and the chromium methacrylic group [9,46,47]. Wang has proven, if coupling sites are created within PP by the addition of peroxides such as DCP, a significant increase in flexural strength is to be observed in combination with methacrylic silanes [48]. A control of sorts would be to have the radical initiator decompose in-situ during the laminate impregnation process and conducting flexural tests on the obtained laminates. Therefore, laminates of FK144 and A-1100 fabric were prepared with PP-films (no MAH) coated in 0.01, 0.1

and 0.3 wt% DCP-acetone solution as radical initiator. In the case of A-1100 aminosilane, a strength increase with the addition of DCP is unlikely since there is no possibility for aminosilanes to undergo radical reactions. In fact, the test series with FK144 revealed a substantial strength increase when additional radical initiator was present, indicating that radical grafting could be involved in PP-FK144 composites. A-1100 showed no significant increase in strength across the DCP concentration range. Test results are presented in Fig. 11. A possible reaction mechanism between the chromium complex and polypropylene was proposed and is depicted in Fig. 12.

The extraordinarily high mechanical strengths reached by FK144

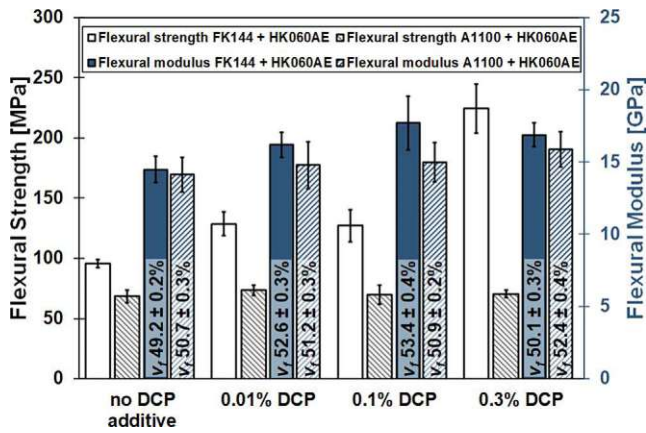


Fig. 11. Flexural properties of FK144-PP HK060AE and A-1100 (s)-PP HK060AE laminates containing no DCP additive as well as 0.01, 0.10 and 0.30 wt% DCP based on PP film mass. No MAH involved.

laminates in combination with MAH-g-PP modified PP matrices could be explained by a further mechanism which is also based on PP-radicals. Alongside the possibility of PP-radicals to react with the methacrylic ligand within the chromium complex, thermally induced PP-radicals could also oxidise Cr(III) to a Cr(VI) species. In this case, additional coordination possibilities would be created. Subsequently, maleic anhydride could interact with Cr(VI) by being priorly ring-opened to a di-carboxylic acid in the presence of water or alcohol. This may be giving a coordination of the di-carboxylic acid to the Cr(VI) generated from a peroxide.

### 3.5. Process optimisation: Effect of film stacking sequence on the laminate surface quality

Besides an optimisation in mechanical properties we also wanted to provide a processing technique for generating an improved material surface quality, which was found during the compression moulding experiments. The visual surface quality of materials is of paramount importance in today's aesthetics and design. Industrial woven glass fibre thermoplastic laminates are known for their special appearance, showing the weave structure of the fabric on the laminate surface and are therefore frequently used as visible parts. Lamination by film stacking with uncoloured films is generally susceptible to visual defects originating from processing flaws such as inclusions of dust and other particulate matter. Glass fibres provide especially high contrast to dark inclusions, which is why thermoplastic matrices of natural colour are frequently coloured with pigments. Carbon black pigments not only provide great visual contrast at low concentrations, but also the added benefit of faster heat-up during thermoforming due to high absorption

in the IR-range [49].

When utilising the film stacking method for multi-layer laminates, the stacking sequence may be started by either the polymer film or the reinforcement layer. In the literature, the stacking sequence is almost exclusively started and ended by the polymer films, which we call standard stacking sequence [50–56]. In contrast, starting and ending the stacking sequence with reinforcement fibre layers, i.e. fibres touching the mould surfaces, is called alternative stacking sequence in this context. The required impregnation time is generally slightly increased by the alternative stacking sequence, as impregnation commences only from the inside of the stack to the outer layers. This must be accounted for in longer dwell times. However, the attained laminate surface finish, achievable by this method resulted in the often-desired “carbon-fibre-like” looks of GF-PP composite laminates which is usually achieved by powder prepregging or commingling. The results of laminates produced by the alternative film stacking sequence versus laminates produced by the standard stacking sequence are compared in Fig. 13. By alternative stacking, the structure of the weave is clearly emerging on the laminate surface and gives the same visual quality as industrially manufactured organo sheets. The prerequisite for generating this surface appearance on both laminate sides by film stacking is the use of at least two reinforcement layers. In the case of single-ply laminates, one laminate side stays mostly matte depending on the coloured film thickness.

## 4. Conclusions

Basic research was conducted in the form of a fibre coating study in order to assess the requirements for high-performance GF-PP composite laminates. The modification of the PP matrix with MAH-g-PP coupling agent showed to be the decisive factor in reaching high strength composites in combination with suitable fibre coatings. Even though direct rovings may be coated with a PP-compatible sizing (possibly containing an MAH-g-PP film former), it was found that the incorporation of further MAH-g-PP into the PP matrix is mandatory for reaching high laminate strengths. It could be shown that in a region of 50% fibre volume fraction, a matrix MAH content in the extent of 0.04% (which accounted for 3.33 wt% of the used MAH-g-PP additive) is required, to reach a strength plateau near 400 MPa. Flexural strength properties may be further improved by incorporation of higher MAH concentrations, however, the additional additive cost may not justify the improvement in material performance.

Finished fabrics, containing adhesion promoter-only coatings, showed proper wetout despite their smaller fibre diameters. Nonetheless, substantial differences in flexural strengths have been identified among different finishes. Since equal wet-out, an equal processing history and comparable fibre volume fractions were obtained, the strength variations within the laminates were attributed to differences in interfacial adhesion. Among the highest performing fabric

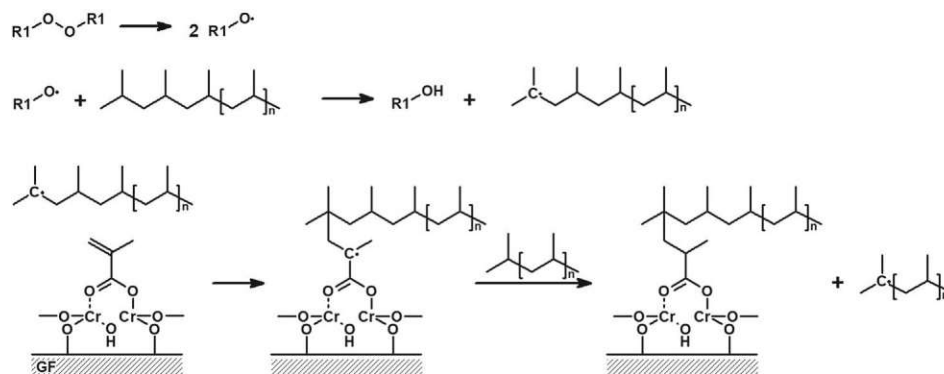
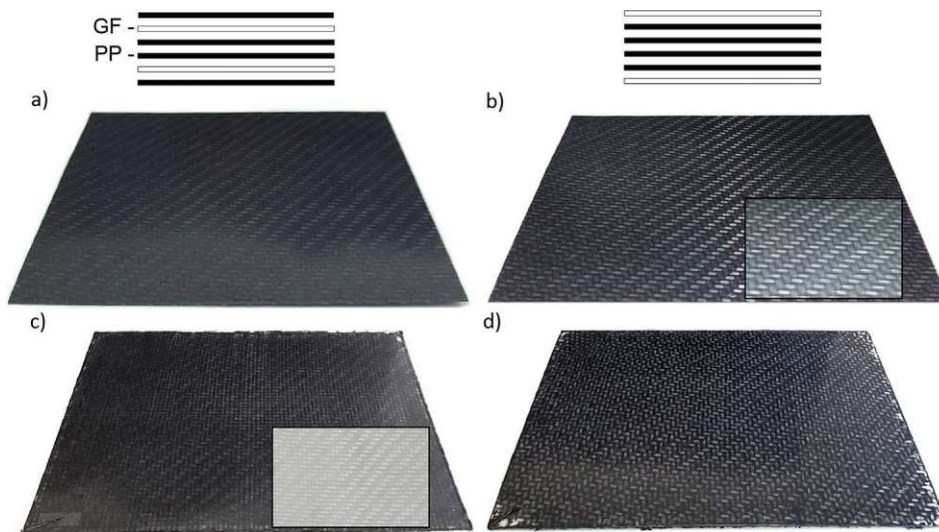


Fig. 12. Proposed radical reaction mechanism of PP and GF chromium complex finish; (top: breakdown of peroxide radical initiator, middle: abstraction of hydrogen from PP chain, bottom: proposed coupling reaction between PP and chromium methacrylate complex based finish on the glass fibre).



**Fig. 13.** Results of laminate surface finish depending on stacking sequence of polymer films; (a) standard stacking sequence filament fabric, matte surface (b) alternative stacking sequence filament fabric, weave clearly emerging on surface; picture in picture: camera flash (c) standard stacking sequence PP-compatible roving fabric; picture in picture: natural PP film HK060AE (d) alternative stacking sequence PP-compatible roving fabric.

finishes were A-1100 aminosilane and the finish FK144 chromium complex. Laminates prepared from these finished fabrics resulted in flexural strengths of close to 400 MPa at 0.04% MAH loading. FK144 finish being on par with the performance of PP-adapted direct roving sizings was highly surprising and a novel finding.

However, due to intricate postprocessing steps involved during the production of finished fabrics, such fabrics tend to be more expensive than direct roving fabrics. Finished fabrics did not show a substantial performance gain over directly sized PP-compatible roving fabrics, even though finishes are of higher chemical purity. The best price to performance ratio is therefore provided by direct roving fabrics.

Finally, an optimised processing method for film stacking was presented with which the visual appearance of laminates could be enhanced significantly. By changing the film stacking sequence from starting with a polymer film, to starting with the reinforcement fabric, impregnation commenced inside-out. Using this method, the outer fabrics in contact with the mould surfaces were wetted with the optimal amount of polymer, leaving the visual appearance of the weave structure intact. This way, equal appearance to industrial GF-PP laminates was achieved.

In summary, continuous glass fibre-reinforced polypropylene consolidated laminates were successfully developed in terms of high mechanical strength and superior laminate surface finish.

#### CRediT authorship contribution statement

**Peter Kiss:** Conceptualization, Investigation, Resources, Writing - original draft, Visualization. **Wolfgang Stadlbauer:** Conceptualization, Validation, Project administration, Writing - review & editing. **Christoph Burgstaller:** Conceptualization, Investigation, Resources, Writing - review & editing. **Vasiliki-Maria Archodoulaki:** Methodology, Writing - review & editing, Supervision.

#### Declaration of Competing Interest

The authors declare that they have no known competing financial interests or personal relationships that could have appeared to influence the work reported in this paper.

#### Acknowledgements

We would like to thank Borealis AG, Brenntag GmbH, Gabriel-Chemie GmbH, GIVIDI Fabrics S.r.l, Johns Manville Slovakia a.s., Neue Materialien Fürth GmbH and Tissa Glasweberei AG for providing their materials for research purposes.

The authors are grateful to the State Government of Upper Austria and the European Regional Development Fund for providing financial support for this research in the programme EFRE-IWB 2020 for the project:



#### References

- [1] Nerenz BA, Fuqua MA, Chevali VS, Ulven CA. Processing and characterization of a polypropylene biocomposite compounded with maleated and acrylated compatibilizers. *Int J Polym Sci* 2012;2012. <https://doi.org/10.1155/2012/472078>.
- [2] Kufel A, Kuciel S. Basalt/wood hybrid composites based on polypropylene: morphology, processing properties, and mechanical and thermal expansion performance. *Materials (Basel)* 2019;12:2557. <https://doi.org/10.3390/ma12162557>.
- [3] Kano-Ibarretxe J, Anakabe J, Iturrondobeitia M, Hernandez R, Arrillaga A. Effect of the processing conditions and maleation on the properties of basalt fibre reinforced polypropylene. *ECCM 2012 - Compos Venice, Proc 15th Eur Conf Compos Mater* 2012:24–8.
- [4] Van Den Oever M, Peijs T. Continuous-glass-fibre-reinforced polypropylene composites II. Influence of maleic-anhydride modified polypropylene on fatigue behaviour. *Compos Part A Appl Sci Manuf* 1998;29:227–39. [https://doi.org/10.1016/S1359-835X\(97\)00089-4](https://doi.org/10.1016/S1359-835X(97)00089-4).
- [5] Kulkarni MB, Mahanwar PA. Studies on the effect of maleic anhydride-grafted polypropylene with different MFI on mechanical, thermal and morphological properties of fly ash-filled PP composites. *J Thermoplast Compos Mater* 2014;27:1679–700. <https://doi.org/10.1177/0892705712475009>.
- [6] Arbelaz A, Fernández B, Ramos JA, Retegi A, Llano-Ponte R, Mondragon I. Mechanical properties of short flax fibre bundle/polypropylene composites: Influence of matrix/fibre modification, fibre content, water uptake and recycling. *Compos Sci Technol* 2005;65:1582–92. <https://doi.org/10.1016/j.compscitech.2005.01.008>.
- [7] Troltzsch J, Stiller J, Hase K, Roth I, Helbig F, Kroll L. Effect of maleic anhydride modification on the mechanical properties of a highly filled glass fibre reinforced, low-viscosity polypropylene for injection moulding. *J Mater Sci Res* 2016;5:111. <https://doi.org/10.5539/jmsr.v5n2p111>.
- [8] Knob A, Lukes J, Drzal LT, Cech V. Further progress in functional interlayers with controlled mechanical properties designed for glass fiber/polyester composites. *Fibers* 2018;6. <https://doi.org/10.3390/fib6030058>.
- [9] Liu Z, Zhang L, Yu E, Ying Z, Zhang Y, Liu X, et al. Modification of glass fiber surface and glass fiber reinforced polymer composites challenges and opportunities: from organic chemistry perspective. *Curr Org Chem* 2015;19:991–1010. <https://doi.org/10.2174/138527281911150610100914>.
- [10] Tran LQN, Yuan XW, Bhattacharyya D, Fuentes C, Van Vuure AW, Verpoest I. Fiber-matrix interfacial adhesion in natural fiber composites. *Int J Mod Phys B* 2015;29:1540018. <https://doi.org/10.1142/S0217979215400184>.
- [11] Thomason JL. Glass fibre sizing: A review. 105619 *Compos Part A Appl Sci Manuf* 2019;127. <https://doi.org/10.1016/j.compositesa.2019.105619>.
- [12] Mallick PK. *Composites engineering handbook*. CRC Press 1997. <https://doi.org/10.1201/9781482277739>.
- [13] GiViDi-Fabrics S.r.l. Fabric finishes 2020. <https://www.gividi-fabrics.com/finishes/> (accessed January 9, 2020).
- [14] BGF-Industries. Glass Fabric Finishes 2020. <http://www.bgf.com/technical/glass-fabric-finishes/> (accessed January 9, 2020).

- [15] Pickering KL, Efendy MGA, Le TM. A review of recent developments in natural fibre composites and their mechanical performance. *Compos Part A Appl Sci Manuf* 2016;83:98–112. <https://doi.org/10.1016/j.compositesa.2015.08.038>.
- [16] Sambale AK, Schöneich M, Stommel M. Influence of the processing parameters on the fiber-matrix-interphase in short glass fiber-reinforced thermoplastics. *Polymers (Basel)* 2017;9:221. <https://doi.org/10.3390/polym9060221>.
- [17] Tiefenthaler AM, Urban MW. Thermal stability of silane coupling agents on Nextel fibres. *Composites* 1989;20:145–50. [https://doi.org/10.1016/0010-4361\(89\)90642-3](https://doi.org/10.1016/0010-4361(89)90642-3).
- [18] Thomason JL, Nagel U, Yang L, Bryce D. A study of the thermal degradation of glass fibre sizings at composite processing temperatures. *Compos Part A Appl Sci Manuf* 2019;121:56–63. <https://doi.org/10.1016/j.compositesa.2019.03.013>.
- [19] GiViDi-Fabrics S.r.l. Fabric finishes 2020. <https://www.gividi-fabrics.com/finishes/> (accessed January 8, 2020).
- [20] Henninger F, Friedrich K. Thermoplastic filament winding with online-impregnation. Part A: Process technology and operating efficiency. *Compos Part A Appl Sci Manuf* 2002;33:1479–86. [https://doi.org/10.1016/S1359-835X\(02\)00135-5](https://doi.org/10.1016/S1359-835X(02)00135-5).
- [21] DIN EN ISO 14125:2011-05, Fibre-reinforced plastic composites - Determination of flexural properties (ISO 14125:1998 + Cor.1:2001 + Amd.1:2011); German version EN ISO 14125:1998 + AC:2002 + A1:2011, doi:10.31030/1753441.
- [22] Zaixia F, Zhangyu Yanmo C, Hairu L. Effects of pre-stretching on the tensile properties of knitted glass fiber fabric reinforced polypropylene composite. *J Thermoplast Compos Mater* 2006;19:399–411. <https://doi.org/10.1177/0892705706059744>.
- [23] Barrera Betanzos F, Gimeno-Fabra M, Segal J, Grant D, Ahmed I. Cyclic pressure on compression-moulded bioresorbable phosphate glass fibre reinforced composites. *Mater Des* 2016;100:141–50. <https://doi.org/10.1016/j.matdes.2016.03.108>.
- [24] Zhao L, Yu Y, Huang H, Yin X, Peng J, Sun J, et al. High-performance polyphenylene sulfide composites with ultra-high content of glass fiber fabrics. *106790 Compos Part B Eng* 2019;174. <https://doi.org/10.1016/j.compositesb.2019.05.001>.
- [25] DIN EN ISO 291:2008-08, Plastics - Standard atmospheres for conditioning and testing (ISO 291:2008); German version EN ISO 291:2008, doi:10.31030/1441132.
- [26] DIN EN ISO 1183-1:2019-09, Plastics - Methods for determining the density of non-cellular plastics - Part 1: Immersion method, liquid pycnometer method and titration method (ISO 1183-1:2019, Corrected version 2019-05); German version EN ISO 1183-1:2019, doi:10.31030/3023324.
- [27] DIN EN ISO 1172:1998-12, Textile-glass-reinforced plastics - Prepregs, moulding compounds and laminates - Determination of the textile-glass and mineral-filler content; calcination methods (ISO 1172:1996); German version EN ISO 1172:1998, doi:10.31030/8003549.
- [28] Rijdsdijk HA, Contant M, Peijs AAJM. Continuous-glass-fibre-reinforced polypropylene composites: I. Influence of maleic-anhydride-modified polypropylene on mechanical properties. *Compos Sci Technol* 1993;48:161–72. [https://doi.org/10.1016/0266-3538\(93\)90132-Z](https://doi.org/10.1016/0266-3538(93)90132-Z).
- [29] Groves S, Highsmith A. Compression response of composite structures. 100 barr harbor drive, PO Box C700, West Conshohocken, PA 19428–2959: ASTM. International 1994. <https://doi.org/10.1520/STP1185-EB>.
- [30] Tran LQN, Fuentes CA, Dupont-Gillain C, Van Vuure AW, Verpoest I. Understanding the interfacial compatibility and adhesion of natural coir fibre thermoplastic composites. *Compos Sci Technol* 2013;80:23–30. <https://doi.org/10.1016/j.compscitech.2013.03.004>.
- [31] Mehndiratta A, Bandyopadhyaya S, Kumar V, Kumar D. Experimental investigation of span length for flexural test of fiber reinforced polymer composite laminates. *J Mater Res Technol* 2018;7:89–95. <https://doi.org/10.1016/j.jmrt.2017.06.010>.
- [32] Chen F, Bazhenov S, Hiltner A, Baer E. Flexural failure mechanisms in unidirectional glass fibre-reinforced thermoplastics. *Composites* 1994;25:11–20. [https://doi.org/10.1016/0010-4361\(94\)90062-0](https://doi.org/10.1016/0010-4361(94)90062-0).
- [33] Chen P, Lu C, Yu Q, Gao Y, Li J, Li X. Influence of fiber wettability on the interfacial adhesion of continuous fiber-reinforced PPESK composite. *J Appl Polym Sci* 2006;102:2544–51. <https://doi.org/10.1002/app.24681>.
- [34] Brocks T, Cioffi MOH, Voorwald HJC. Effect of fiber surface on flexural strength in carbon fabric reinforced epoxy composites. *Appl Surf Sci* 2013;274:210–6. <https://doi.org/10.1016/j.apsusc.2013.03.018>.
- [35] Goriparthi BK, Suman KNS, Mohan Rao N. Effect of fiber surface treatments on mechanical and abrasive wear performance of polylactide/jute composites. *Compos Part A Appl Sci Manuf* 2012;43:1800–8. <https://doi.org/10.1016/j.compositesa.2012.05.007>.
- [36] Kim H-S, Lee B-H, Choi S-W, Kim S, Kim H-J. The effect of types of maleic anhydride-grafted polypropylene (MAPP) on the interfacial adhesion properties of bio-fiber-filled polypropylene composites. *Compos Part A Appl Sci Manuf* 2007;38:1473–82. <https://doi.org/10.1016/j.compositesa.2007.01.004>.
- [37] DIN EN ISO 14130:1998-02, Fibre reinforced plastic composites - Determination of apparent interlaminar shear strength by short beam-method (ISO 14130:1997); German version EN ISO 14130:1997, doi:10.31030/7433990.
- [38] d'Hooghe EL, Edwards CM. Thermoplastic composite technology; tougher than you think. *Adv Mater* 2000;12:1865–8. [https://doi.org/10.1002/1521-4095\(200012\)12:23<1865::AID-ADMA1865>3.0.CO;2-N](https://doi.org/10.1002/1521-4095(200012)12:23<1865::AID-ADMA1865>3.0.CO;2-N).
- [39] Zahid S, Nasir MA, Nauman S, Karahan M, Nawab Y, Ali HM, et al. Experimental analysis of ILSS of glass fibre reinforced thermoplastic and thermost textile composites enhanced with multiwalled carbon nanotubes. *J Mech Sci Technol* 2019;33:197–204. <https://doi.org/10.1007/s12206-018-1219-0>.
- [40] Sammartino EK, Reboredo MM, Aranguren MI. Natural fiber-polypropylene composites made from caranday palm. *J Renew Mater* 2016;4:101–12. <https://doi.org/10.7569/JRM.2014.634144>.
- [41] Harper LT, Burn DT, Johnson MS, Warrior NA. Long discontinuous carbon fibre/polypropylene composites for high volume structural applications. *J Compos Mater* 2018;52:1155–70. <https://doi.org/10.1177/0021998317722204>.
- [42] Ortega-Toro R, Santagata G, Gomez D'Ayala G, Cerruti P, Talens Oliag P, Chiralat Boix MA, et al. Enhancement of interfacial adhesion between starch and grafted poly( $\epsilon$ -caprolactone). *Carbohydr Polym* 2016;147:16–27. <https://doi.org/10.1016/j.carbpol.2016.03.070>.
- [43] Jiang X, Huang H, Zhang Y, Zhang Y. Dynamically cured PP/epoxy blends compatibilised with MAH-g-PP. *Polym Polym Compos* 2004;12:29–42. <https://doi.org/10.1177/096739110401200103>.
- [44] Chandra A, Turg L-S, Gopalan P, Rowell RM, Gong S. Semitransparent poly(styrene-*r*-maleic anhydride)/alumina nanocomposites for optical applications. *J Appl Polym Sci* 2007;105:2728–36. <https://doi.org/10.1002/app.26349>.
- [45] Yates PC, Trebilcock JW. The chemistry of chromium complexes used as coupling agents in fiberglass resin laminates. *Polym Eng Sci* 1961;1:199–213. <https://doi.org/10.1002/pen.760010411>.
- [46] Clemons CM, Sabo RC, Kaland ML, Hirth KC. Effects of silane on the properties of wood-plastic composites with polyethylene-polypropylene blends as matrices. *J Appl Polym Sci* 2011;119:1398–409. <https://doi.org/10.1002/app.32566>.
- [47] Stori A, Dahl IM. Grafting of Polyolefins to Silane Treated Surfaces by Free-Radical Reactions. *Control. Interphases Compos. Mater.*, Dordrecht: Springer Netherlands; 1990, p. 321–33. doi:10.1007/978-94-011-7816-7\_31.
- [48] Wang Q, Xiao Z, Wang W, Xie Y. Coupling pattern and efficacy of organofunctional silanes in wood flour-filled polypropylene or polyethylene composites. *J Compos Mater* 2015;49:677–84. <https://doi.org/10.1177/0021998314525065>.
- [49] Forrest M. Recycling of polyethylene terephthalate. Berlin: De Gruyter; 2019.
- [50] Jespersen ST, Wakeman MD, Michaud V, Cramer D, Månson J-AE. Film stacking impregnation model for a novel net shape thermoplastic composite preforming process. *Compos Sci Technol* 2008;68:1822–30. <https://doi.org/10.1016/j.compscitech.2008.01.019>.
- [51] Bar M, Alagirusamy R, Das A. Properties of flax-polypropylene composites made through hybrid yarn and film stacking methods. *Compos Struct* 2018;197:63–71. <https://doi.org/10.1016/j.comstruct.2018.04.078>.
- [52] Grouve WJB, Akkerman R. Consolidation process model for film stacking glass/PPS laminates. *Plast Rubber Compos* 2010;39:208–15. <https://doi.org/10.1179/174328910X12647080902457>.
- [53] Kim JW, Lee JS. Influence of interleaved films on the mechanical properties of carbon fiber fabric/polypropylene thermoplastic composites. *Materials (Basel)* 2016;9. <https://doi.org/10.3390/ma9050344>.
- [54] Loendersloot R, Grouve W, Lamers E, Wijskamp S. Textile impregnation with thermoplastic resin – models and application. *Flow Process Compos Mater* 2012;11:344–51.
- [55] Kim JW, Lee JS. The effect of the melt viscosity and impregnation of a film on the mechanical properties of thermoplastic composites. *Materials (Basel)* 2016;9. <https://doi.org/10.3390/ma9060448>.
- [56] Sadighi M, Rabizadeh E, Kermansaravi F. Effects of laminate sequencing on thermoforming of thermoplastic matrix composites. *J Mater Process Technol* 2008;201:725–30. <https://doi.org/10.1016/j.jmatprotec.2007.11.239>.



# In-house recycling of carbon- and glass fibre-reinforced thermoplastic composite laminate waste into high-performance sheet materials



Peter Kiss<sup>a,c,\*</sup>, Wolfgang Stadlbauer<sup>a</sup>, Christoph Burgstaller<sup>b</sup>, Hannes Stadler<sup>b</sup>, Stefan Fehringer<sup>a</sup>, Florian Haeuserer<sup>a</sup>, Vasiliki-Maria Archodoulaki<sup>c</sup>

<sup>a</sup> University of Applied Sciences Upper Austria, School of Engineering, Stelzhamerstrasse 23, 4600 Wels, Austria

<sup>b</sup> Transfercenter fuer Kunststofftechnik GmbH, Franz-Fritsch-Strasse 11, 4600 Wels, Austria

<sup>c</sup> TU Wien, Institute of Materials Science and Technology, Getreidemarkt 9, 1060 Vienna, Austria

## ARTICLE INFO

### Keywords:

- A. Laminates
- D. Mechanical testing
- E. Compression moulding
- E. Recycling

## ABSTRACT

As the paradigm of production, use and consumption is currently shifting towards a circular economy, measures must be taken in the field of composite laminate recycling in order to prevent environmental pollution. In an effort to capitalise on the recyclability of thermoplastic composite laminates, a selection of in-house recycling and reuse routes are highlighted and compared in this research paper. Reprocessed compression moulded panels from shredded laminates demonstrated only 10–30% strength of monolithic virgin materials. Therefore, a largely unexplored recycling method was applied by co-moulding shredded material as a core layer between continuous fibre skins. These sandwich-like panels had true upcycling potential to achieve monolithic laminate properties in flexural and impact loading; in tensile loading around 50% performance was reached. Lastly, a promising reuse method was examined by reverse-thermoforming rejected parts. Wrinkle-free flat blanks with virgin-like properties could be produced for reuse purposes out of complexly shaped parts.

## 1. Introduction

Since the scope of applications and demand for continuous fibre-reinforced thermoplastics is ever-growing, research regarding closed-loop recycling techniques for composite waste treatment is currently a central environmental issue. When considering post-consumer and post-industrial waste accumulations of these materials in the near future [1–3], it becomes of great significance to find effective, viable and financially attractive recycling routes now. As such, every effort must be made to reduce the amount of waste material that is sent either to landfill or incineration, by reusing and recycling waste as far as possible. The objective is to develop alternative lower-cost products out of waste material, whilst retaining the mechanical integrity of recycled parts.

Compared to cured thermoset matrix resins, which are problematic to dispose of and difficult to recycle, thermoplastic matrices are in essence easier to handle during recycling operations since they are repeatedly meltable [1–8]. An overview of existing recycling concepts for continuous fibre-reinforced thermoplastic composite laminates (TPCL) was recently compiled by Vincent [9]. Despite the fact that TPCLs boast

an inherent potential for material recycling, up until now real world recycling applications for these materials have been lacking [7,9–11]. Straightforward procedures in feedstock preparation during material recycling involve size reduction by shredding, grinding, or cutting up rejected parts, trimmings, offcuts or end-of-life components. Shredding TPCL waste generated in-house, presorted according to fibre type and matrix material is a simple task for material recovery and is quick to perform [9–13].

For the downstream processing of shredded or ground laminate feedstock, laminate manufacturers recommend compounding and injection moulding [13]. However, the shear-intensive compounding and injection moulding operations cause substantial fibre attrition, often yielding sub-millimetre short fibre composites [14–16]. While such injection moulded composite parts can still provide excellent stiffness and good strength properties due to flow-induced fibre orientation, the impact strength of short fibre composites is usually very low [17]. The performance of recycled composite parts is therefore highly sensitive to parameters such as fibre length, fibre length distribution, fibre orientation, fibre content, fibre–matrix adhesion, void content, matrix degradation and possible contaminants [15,17–21]. By selecting more

\* Corresponding author at: University of Applied Sciences Upper Austria, School of Engineering, Stelzhamerstrasse 23, 4600 Wels, Austria.  
E-mail address: [peter.kiss@fh-wels.at](mailto:peter.kiss@fh-wels.at) (P. Kiss).

<https://doi.org/10.1016/j.compositesa.2020.106110>

Received 16 May 2020; Received in revised form 25 August 2020; Accepted 2 September 2020

Available online 09 September 2020

1359-835X/ © 2020 Elsevier Ltd. All rights reserved.

gentle reprocessing methods, high aspect ratio fibres can be kept mostly intact without breakage, providing improved impact strength [9,22]. De Bruijn and Vincent showed that shredded centimetre-sized TPCL flakes can be reprocessed by heated low-shear mixers into a homogenised dough-like mass for net-shape stamp forming, similar to direct long fibre thermoplastics (LFT-D) or thermoset bulk moulding compounds (BMC) [9,23,24]. Schinner, Brandt and Richter [25], Eguemann et al. [26], Howell and Fukumoto [27,28] together with Rasheed [11] pursued a more direct approach without the use of upstream homogenisation. Loose, long chopped unidirectional carbon fibre thermoplastic tapes (UD-tapes) [25-28], or chopped centimetre-sized TPCL flakes [11] were fused by variothermal compression moulding to simple or complex parts. Visually, flat compression moulded sheets produced in this manner are reminiscent of thermoset sheet moulding compounds (SMC). Subsequently, flat sheet materials pressed from shredded TPCL feedstock are referred to as thermoplastic SMC (TP-SMC) in the further course of this work.

Without an upstream fibre alignment process, the fibres in such compression moulded TP-SMCs are randomly oriented. Research has found that randomly oriented short or long fibre composites do not exhibit such high performance levels as provided by continuous fibre composites with fibres predominantly oriented in the load direction [10,15,17,18,24,29-31]. To overcome these limitations, researchers at the University of Bristol have developed a recycling technique by dissolving the thermoplastic matrix of long fibre composites, followed by an alignment process of the recovered fibres termed HiPerDiF [32-36]. It was established that working with up to 6 mm long fibres was optimal for process stability, and that panels made from aligned fibre preforms exhibited tensile properties close to those of continuous fibre composites [32-36]. While the HiPerDiF method is a promising recycling technique, fibre lengths of shredded TPCL materials are often far in excess of 6 mm [9,11,22]. As of yet, shredded TPCLs (with > 6 mm long fibres) must be reprocessed using more conventional methods and the resulting components frequently undergo a considerable performance loss compared to their former continuous fibre architecture [37]. Hence, they are classified as downcycled products.

In order to create upcycled products out of shredded TPCL materials, a reprocessing method may be applied by incorporating the shredded material as a core/filler layer between two continuous fibre skins/faces [38]. Skins and core are co-moulded to generate a “sandwich-like structure”. Such thermoplastic composite sandwich structures with fibrous cores have been discussed by Schaefer [39], Wakeman et al. [40,41], as well as Lahr and Paessler [42]. Since then, this method has remained largely unmentioned and unexplored in the field of thermoplastic composite recycling. Therefore, its potential is highlighted through further analysis in this paper.

A reuse method involving blank reconstruction through reshaping rejected thermoformed parts, has likewise gained limited attention. “Reverse-forming” is an intricate yet effective method, as thermoformed TPCLs may be reshaped multiple times depending on matrix thermal stability [10,43,44]. Cousins et al. have straightened sections of a slightly curved wind turbine spar cap made of TPCL for reuse purposes by means of contact hot pressing [10]. However, a more complex geometrical part cannot be simply compressed in a heated press, as severe fibre misalignments will appear in the resulting sheet. The challenge of reverse-forming therefore lies in finding parameters to avoid the formation of creases (out-of-plane) and in-plane fibre misalignments for generating high-quality reusable blanks.

The goal of the present work is to compare recycled sheet materials with regard to mechanical performance in the framework of tensile, flexural and impact tests. The focus was placed on TP-SMC production, sandwich panel lamination (with recycled material cores) and reverse-forming of monolithic laminates. The recycling methods under discussion had to be performable in-house, with as few reprocessing steps as possible. The target material for recycling was waste generated in-house, such as laminate trimmings, offcuts and scrap parts. End-of-life

waste, its collection, separation and treatment, was not considered in this work.

## 2. Materials and methods

Two recycling topics were covered in this paper. Firstly, the recycling of industrial glass fibre (GF) and carbon fibre (CF) laminates based on Tepex® products was addressed by shredding and hot compression moulding methods, followed by mechanical testing. Secondly, reverse-formability of Tepex® laminates was examined and blank quality was assessed via mechanical tests.

### 2.1. Materials

Tepex® dynalite consolidated composite laminates, based on Polypropylene (PP) and Polyamide 6 (PA6) matrices were utilised for shredding, TP-SMC pressing, sandwich panel lamination and reverse-forming. Both base materials under discussion, Tepex® dynalite 104-RG600(x)/47% PP-GF and Tepex® dynalite 202-C200(x)/45% PA6-CF were produced and supplied by Bond-Laminates GmbH (Brilon, Germany).

### 2.2. Methods

#### 2.2.1. Material preparation for recycling by shredding

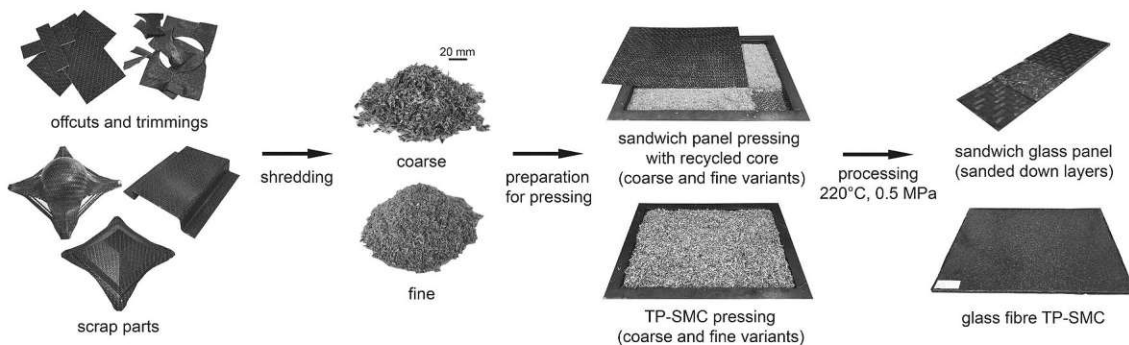
A mixture of Tepex® laminate offcuts, trimmings and scrap parts from thermoforming was fed into a staggered rotor cutting mill MAS 1 (Wittmann Kunststoffgeraete GmbH, Germany) with a throughput of roughly 10 kg/h and motor output of 2.2 kW. The materials were shredded to coarse and fine fractions by means of interchangeable bottom sieves within the cutting mill. Sieves with hole openings of 4 mm and 8 mm in diameter were utilised for shredding. Material shredded with 4 mm hole openings resulted in 0.5–7 mm long fibres (fine fraction). Material shredded with 8 mm hole openings resulted in fibres with 5–25 mm length (coarse fraction). Fibre lengths were determined by electron microscopy on a Vega II LMU SEM (Tescan, Czech Republic) at an accelerating voltage of 10.0 kV and VegaTC software (Tescan, Czech Republic) length measurement.

#### 2.2.2. Recycling and reprocessing methods by compression moulding

Material recycling by hot compression moulding was conducted in a stamp impregnation tool on a static laboratory hot press Wickert WLP 80/4/3 (Wickert Maschinenbau GmbH, Germany) preheated to 300 °C and a water-cooled static press Höfer H10 (Höfer Presstechnik GmbH, Austria). Laminate consolidation pressure amounted to 0.5 MPa on both presses. Low consolidation pressure was chosen as the materials only needed to be fused and to reduce squeeze flow. PP materials were heated to 220 °C, while PA6 materials were heated to 260 °C. To prevent the laminates from overheating, the temperature was monitored inside the impregnation tool by inserting thin-film thermocouples type-K, 402-716 (TC Mess- und Regeltechnik GmbH, Germany) and by a temperature data logger Testo 176 T4 (Testo SE & Co. KGaA, Germany). Once the required temperature had been reached, the tool was immediately transferred to the cooling press (no holding time). Full processing cycles (heating and cooling to 100 °C) required 20 minutes for PP based materials and 25 minutes for PA6 based materials.

As described by Howell and Fukumoto [27], the required amount of shredded material for compression moulding can be simply determined by calculating the volume of the mould cavity or the volume of the intended panel and multiplying that by the composite density. Fig. 1 shows the processing schemes of TP-SMC and sandwich panels based on PP-GF and PA6-CF materials. Shredded material was strewn inside the mould and spread evenly with a flat spatula. Both panel types (TP-SMC and sandwich) were prepared with both coarse and fine shredded material to yield a thickness of 2.0 mm. 0.5 mm thick skins were used for sandwich panel lamination.

### PP-GF recycling route



### PA6-CF recycling route

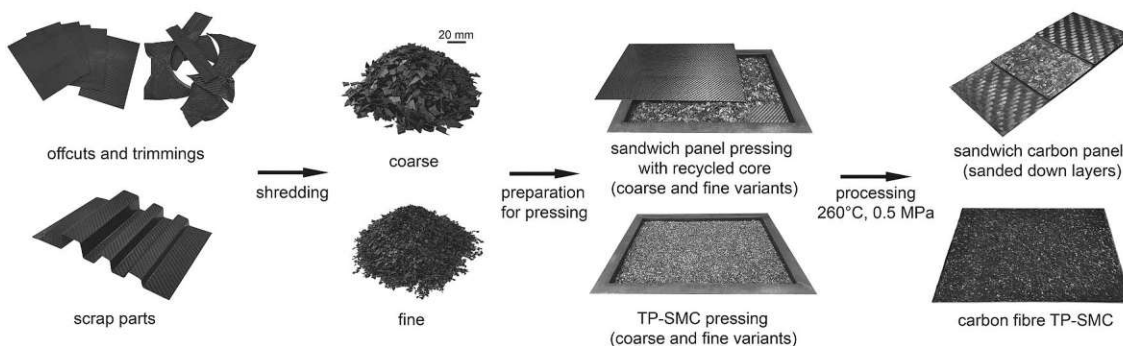


Fig. 1. Recycling routes for PP-GF and PA6-CF based TPCLs.

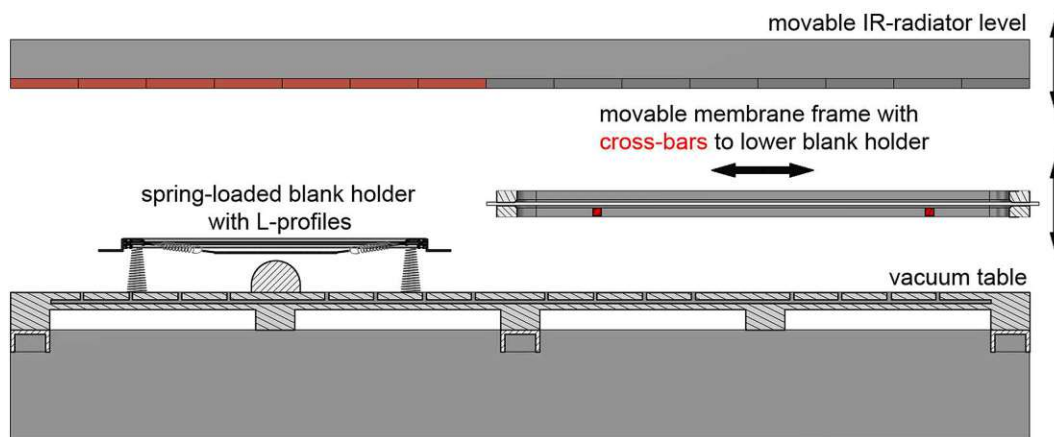


Fig. 2. Single diaphragm forming (SDF) machine setup with lowerable spring-loaded blank holder.

#### 2.2.3. Reverse-forming

The reverse-forming of laminates for testing the direct reuse potential of TPCLs was carried out on a fully automated single-diaphragm vacuum forming (SDF) machine LZ-SO 0110-00013 (Langzauner GmbH, Austria). A novel diaphragm machine setup, depicted schematically in Fig. 2, was utilised for these trials with a movable membrane to remain in a separate area from the blank heating region upon blank heating. This setup ensured that the membrane material was not exposed to the severe heating conditions and did not shield the blank during heating. The TPCL blanks were supported by a spring-loaded blank holder.

Thermoformed parts made of 250 · 250 · 1 mm blanks were clamped, heated and reverse-formed into their initial flat form again by means of tension springs (peak spring force 55 N) as shown in Fig. 3.

PP-GF laminates were heated to 220 °C; PA6-CF laminates were heated to 260 °C by 1 kW metal foil IR-radiators Krelus G14-25-2.5 MM3 (Krelus AG, Switzerland) at 100% heater power, controlled by IR-pyrometers MI3 (Raytek GmbH, Switzerland) and a heater distance of 100 mm. The machine was equipped with a silicone rubber membrane, type MS1 (Rapha-Systems Handels GmbH, Austria) and a vacuum table to carry out the forming and shape fixation operations. Reverse-forming cycles as short as 60–90 s could be realised using this setup.

#### 2.2.4. Laminate testing

For the evaluation of laminate performance, both virgin laminates and recycled laminates were inspected in flexural, impact and tensile tests. Specimens of fabric-reinforced panels were cut in the fabric warp direction.

Die approbierte gedruckte Originalversion dieser Dissertation ist an der TU Wien Bibliothek verfügbar. The approved original version of this doctoral thesis is available in print at TU Wien Bibliothek.



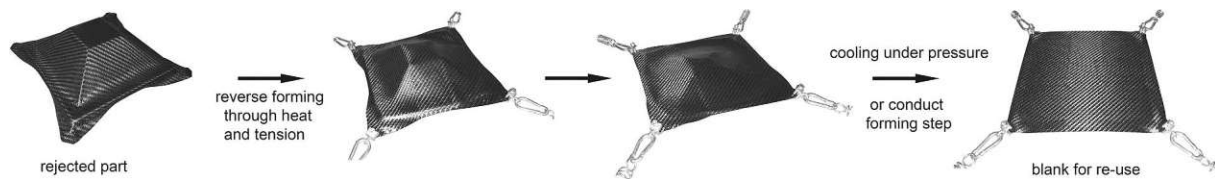


Fig. 3. Reuse route for thermoformed parts by reverse-forming.

3-point flexural tests were carried out on a Zwick/Roell ZMART.PRO 10 kN universal testing machine. According to EN ISO 14125:2011, 60 · 25 · 2 mm (length-width-height) flexural test specimens were prepared and tested at a crosshead speed of 1 mm/min and a span of 40 mm [45].

Tensile tests were carried out on a 150 kN Zwick Z150 universal testing machine. According to EN ISO 527-4:1997, 250 · 25 · 2 mm specimens were prepared and tested at a crosshead speed of 2 mm/min and gauge length of 136 mm [46].

Charpy impact tests were carried out on a Zwick 5113.300 pendulum impact tester. In accordance with EN ISO 179-1:2010, 50 · 15 · 2 mm specimens were prepared and tested in flatwise normal (fn) manner with a 7.5 Joule impactor and impact speed of 3.85 m/s [47]. A span of 40 mm was chosen for impact testing according to EN ISO 179-1:2010 [47].

PP-GF composites were conditioned according to EN ISO 291 at 23 °C and 50% relative humidity for 14 days [48]. PA6-CF composites were tested both in conditioned state at 23 °C and 50% relative humidity (conditioning time: 14 days) and in dry state (dried at 80 °C for 24 h and left to cool).

#### 2.2.5. Determination of laminate fibre volume fractions

The densities of composite samples were measured via buoyancy method with a density determination kit YDK01 (Sartorius AG, Germany) according to EN ISO 1183 [49]. The fibre mass fraction of the composite samples was determined by burning off the matrix via a macro thermogravimetric analyser LECO TGA801 (Leco Instrumente GmbH, Germany) according to EN ISO 1172 [50]. With knowledge of the composite specimen density, the fibre density and respective fibre mass fraction, it was possible to calculate the fibre volume fraction.

#### 2.2.6. Microscopic analysis of laminates

Composite panels and tested specimens were embedded in epoxy resin and polished on a LaboPol-5 polishing machine (Struers GmbH, Germany) by means of silicon carbide grinding disks and water. Imaging of gold sputtered specimens was carried out on a SEM Vega II LMU (Tescan, Czech Republic). PP-GF specimens were analysed by back scattered electron imaging at an accelerating voltage of 20.0 kV. PA6-CF specimens were analysed by secondary electron imaging at an accelerating voltage of 10.0 kV.

### 3. Results and discussion

Testing results obtained from flexural, impact and tensile specimens of compression moulded laminates are compared in the following figures, commencing with PP based TPCL and PA6 based TPCL recycling, followed by reverse-forming.

#### 3.1. Fibre volume fractions of recycled PP-GF and PA6-CF based laminates

The fibre volume fractions measured, differed in the region of 1% across virgin and recycled laminates. The results, displayed in Table 1, indicated that the fibre volume fraction of recycled panels remained unaffected by selected reprocessing parameters. The uniformity within the fibre volume fractions created a good basis for a mechanical comparison between virgin panels and recycled panels. PP-GF samples exhibited a fibre volume fraction in the range of 45% - two percentage points lower than stated by the manufacturer (47%) [51]. For PA6-CF,

the measured fibre volume fraction correlated very well with the specifications given by the manufacturer (45%) [51].

Comparing the mechanical properties of 2.0 mm thick recycled materials and virgin materials in Fig. 4, it is clearly evident that TP-SMCs demonstrate significantly lower mechanical performance compared to sandwich or virgin monolithic laminates. The testing results therefore underline the importance of continuous fibre-reinforcement and fibre orientation for high performance applications. The difference in mechanical performance between coarse and fine SMCs was only marginal, despite the coarse shredded fraction displaying fibres up to 25 mm in length. It was assumed that the random fibre orientation of SMCs was the cause for the poor mechanical performance. To isolate this factor, coarse shredded PP-GF material was injection moulded for fibre alignment and mechanical property comparison. The following Section 3.1.3 is dedicated to this topic, which proves that random SMCs would clearly benefit from an alignment process.

In flexural tests, considerably lower moduli were obtained from TP-SMCs, approximately 50% of their respective virgin monolithic laminate variants for PP-GF SMCs, and roughly 40% for PA6-CF SMCs. As mentioned previously, this was most likely due to the random fibre orientation of the TP-SMCs. Flexural strength was likewise strongly affected by the random fibre orientation; around 30% of the monolithic counterpart properties of both PP-GF and PA6-CF SMCs was measured. Dry and conditioned PA6-CF SMC samples exhibited the same flexural strength, while slightly higher moduli were attained by dry specimens.

An interesting result was obtained from the sandwich panels. PP-GF sandwich panels had the potential to show flexural properties on par with virgin monolithic laminates in the range of 370 MPa strength and 18 GPa modulus. PA6-CF sandwich panels fully maintained flexural moduli in the range of 44 GPa, however, they did show a decrease in flexural strength of roughly 10–14% from monolithic PA6-CF laminates. This can be explained by the high stress conditions in PA6-CF sandwich specimens. According to Schaefer [39] the failure of sandwich beams with thin cores is defined by reaching the failure stress of the skin material, which is also dependent on the skin thickness. Such tensile or compressive yield of the skins could be confirmed by microscopic analysis of test specimens (Section 3.1.4). As flexural loads are placed on the sandwich specimens, the stiffer skins are stressed more than the core material [39,52]. Apparently, the carbon skins were too thin to exhibit monolithic laminate performance. In PP-GF sandwich specimens the overall lower stresses occurring, were effectively carried by the skins and the core, thereby enabling monolithic material properties to be attained.

In tensile tests, PP-GF SMCs reached approximately 50% of the modulus (9–9.5 GPa) of monolithic PP-GF laminates (18.5 GPa). Theoretically, sandwich specimens in tension demonstrate a combined tensile modulus of both the monolithic laminate and the TP-SMC multiplied by the fraction of each material. The calculated tensile modulus for a PP-GF sandwich specimen (constructed of 50% monolithic laminate and 50% TP-SMC in this work) was approximately 14 GPa. In fact, the measured tensile moduli of PP-GF sandwich specimens correlated relatively well with this basic modulus consideration at  $14.35 \pm 0.35$  GPa for coarse core sandwich specimens, and  $13.71 \pm 1.04$  GPa for fine core sandwich specimens. With a slight deviation, this consideration also applied to the PA6-CF sandwich specimens, by combining half the modulus of the monolithic PA6-CF laminate (48GPa) with half the modulus of the PA6-CF SMCs (17–18 GPa) resulting in roughly 33 GPa. The data measured, indicated moduli of 36–37 GPa for coarse PA6-CF sandwich specimens and 33–34 GPa for fine

**Table 1**  
Fibre volume fractions of the laminates examined in this work.

Material	Measured composite density $\rho_c$ [g/cm <sup>3</sup> ]	Fibre weight fraction $\omega_f$ (%)	Fibre volume fraction $\nu_f$ (%)
PP-GF SMC coarse	1.64 ± 0.01	70.5 ± 0.7	44.9 ± 0.8
PP-GF SMC fine	1.63 ± 0.01	70.2 ± 0.5	44.2 ± 0.5
PP-GF Sandwich core coarse	1.64 ± 0.00	70.0 ± 0.1	45.2 ± 0.1
PP-GF Sandwich core fine	1.63 ± 0.00	70.4 ± 0.3	44.6 ± 0.3
PP-GF Virgin monolithic	1.65 ± 0.01	70.6 ± 0.3	45.4 ± 0.4
PA6-CF SMC coarse	1.41 ± 0.00	56.2 ± 0.1	44.7 ± 0.1
PA6-CF SMC fine	1.41 ± 0.00	55.6 ± 0.1	44.1 ± 0.1
PA6-CF Sandwich core coarse	1.42 ± 0.01	57.4 ± 0.9	45.7 ± 0.9
PA6-CF Sandwich core fine	1.42 ± 0.00	56.7 ± 0.6	45.1 ± 0.5
PA6-CF Virgin monolithic	1.42 ± 0.01	57.3 ± 0.8	45.7 ± 0.9

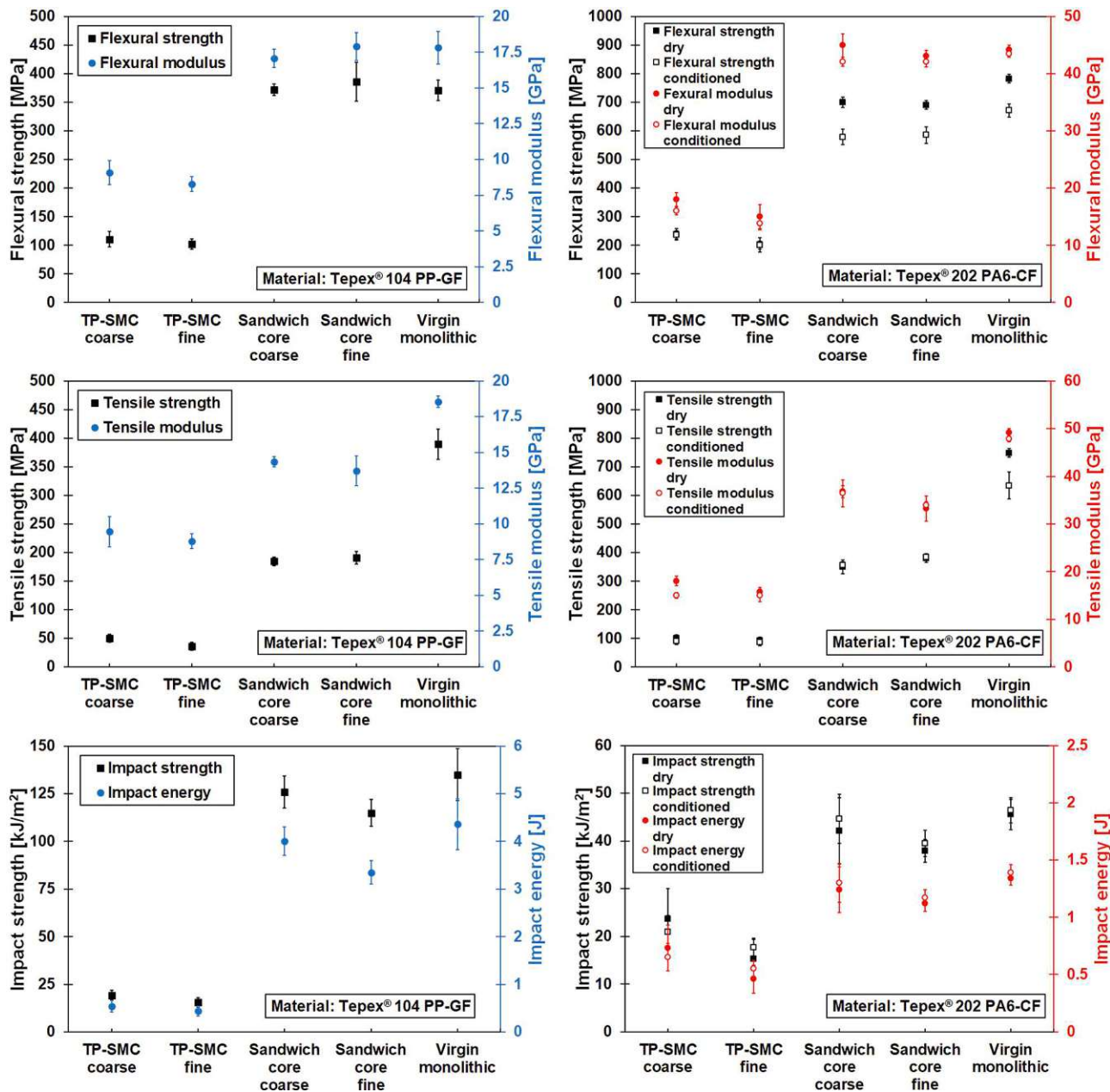
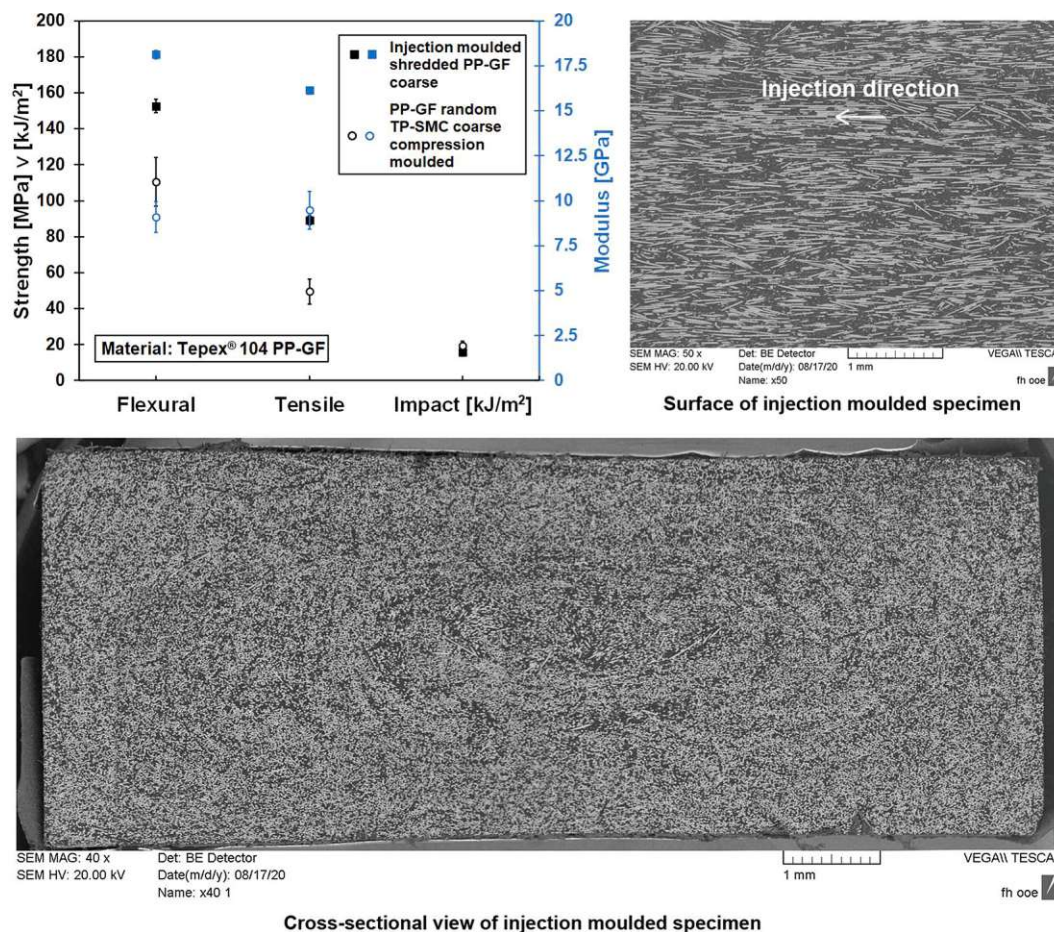


Fig. 4. Mechanical test results of recycled and virgin panels with 2 mm thickness; (left: PP-GF based materials, right: PA6-CF based materials).

PA6-CF sandwich specimens.

Tensile strength obtained from PP-GF SMCs was very low, yielding below 50 MPa (12.5% of virgin laminate). The PP-GF sandwich

specimens yielded around the 200 MPa mark (50% of virgin laminate), while virgin monolithic PP-GF laminates yielded close to 400 MPa. A similar pattern was observed with PA6-CF specimens, with SMCs



**Fig. 5.** Injection moulded TPCL exhibiting improved mechanical performance over compression moulded TP-SMC due to strong flow-induced fibre alignment (top left: mechanical properties of injection moulded material vs. compression moulded material; top right: SEM micrograph of injection moulded specimen as seen from the surface; bottom: SEM micrograph showing the cross-section of an injection moulded specimen with strong fibre alignment in the flow direction).

yielding at 100 MPa, sandwich specimens at approximately 400 MPa and monolithic laminates at 750 MPa in dry condition. Only in monolithic PA6-CF laminates was a significant difference between dried and conditioned tensile samples discernible.

In impact tests conducted in flatwise normal specimen configuration, TP-SMCs performed rather poorly. While PP-GF SMCs performed equally to PA6-CF SMCs, their impact strength was nonetheless merely within a range of 20 kJ/m<sup>2</sup>. A discontinuous and random fibre architecture is therefore not favourable in terms of high impact resistance. Fortunately, sandwich specimens performed closely to monolithic laminates. The outermost laminate layers are mainly responsible for energy absorption in charpy impact loading, enabling close-to-virgin material performance to be attained. PA6-CF sandwich and monolithic laminates exhibited an impact strength of 40–46 kJ/m<sup>2</sup>. By comparison, a virtual threefold increase in impact strength was observed in PP-GF sandwich and monolithic laminates (125–130 kJ/m<sup>2</sup>). Similarly, the literature reports an impact strength difference by a factor of 3–5 between continuous glass and carbon fibre laminates [53,54], which correlates well with the findings of this work. Dry and conditioned PA6-CF specimens did not differ greatly in impact strength, which hinted at the carbon fibres being responsible for the low impact strength due to their brittle nature and lower strain-to-failure ratio compared to glass fibres [54].

It is well known that the mechanical properties of neat PA6 differs between conditioned and dry state [55,56]. In conditioned state, neat PA6 accumulates moisture up to 10 wt% (fibre-reinforced up to 5wt%) after a prolonged period of moisture exposure [57]. Water acts as a plasticiser between the polymer chains, hence the PA6 matrix becomes more ductile and an increase in impact strength is generally observed

[58]. However, in PA6-based composites, water absorption is also accompanied by a loss of adhesion between the fibres and the matrix, negatively influencing mechanical performance [57]. In dry state, the PA6 matrix exhibits higher stiffness and tensile strength, but a lower elongation at break. Clearly, in flexural and tensile tests of monolithic PA6-CF laminates this kind of behaviour was observed, where dry specimens boasted higher strength and stiffness compared to conditioned specimens. However, in charpy impact tests the fibre type and continuous fibre architecture seemed to be more important than the moisture state of the PA6 matrix. Here, the apparently higher ductility of a conditioned PA6 matrix did not contribute to an improvement in impact properties; the differences were only marginal between dry and conditioned samples. Furthermore, in tensile and impact tests of sandwich and TP-SMC PA6-CF samples, there was also no difference in mechanical performance between dry and conditioned state. The premature failure of these samples could generally be dependent on stress-concentration buildup at the fibre ends of the random shredded material, rather than being affected by the moisture content.

Summarising the observations from the mechanical tests, the difference in fibre length between the coarse and fine shredded material fractions had only a negligible effect on the testing outcomes. TP-SMCs showed only acceptable stiffness properties but lacked high strength and impact resistance. In order to obtain the best performance from shredded TPCLs, it is advisable to process them into a sandwich structure as a core material. Such sandwich laminates are optimal for bending loads and are capable of competing with monolithic laminates. Recycling in-house TPCL production waste by means of compression moulding was found to be realisable with relatively low effort, and

therefore being readily up-scalable. In contrast, recycling of end-of-life TPCL waste most definitely requires more complex pretreatment. End-of-life TPCL waste may come highly contaminated, with degraded polymer matrices and significant fibre damage, which would most likely lead to worse mechanical performance of reprocessed panels as observed in this work. Therefore, such waste would need careful collection, sorting, cleaning and removal of possible metallic inserts or fasteners before being eligible for reprocessing. Depending on the severity of matrix degradation, intermixing of virgin polymer or polymer stabilisers and/or antioxidants may also be required [59].

### 3.2. Injection moulding of shredded material for fibre alignment

In order to investigate the influence of fibre orientation on the mechanical properties of the shredded material, it was processed by injection moulding according to EN ISO 294-1 [60]. Coarse shredded PP-GF material was directly fed into an Engel Victory 330/80 (Engel Austria GmbH, Austria) injection moulding machine at a barrel temperature of 220 °C and 85 MPa injection pressure. By comparison, the injection moulded samples displayed higher tensile and flexural properties at the same density and fibre volume fraction ( $\rho_c: 1.64 \text{ g/cm}^3$ ,  $v_f: 45.0\%$ ) to the compression moulded TP-SMC. The mechanical properties and SEM images of the injection moulded samples vs. compression moulded TP-SMC are outlined in Fig. 5. Injection moulded samples exhibited excellent fibre alignment, at the expense of fibre length. Nevertheless, the results indicated that fibre orientation clearly affects performance. Flexural and tensile moduli of the injection moulded specimens were almost double that of TP-SMCs, while strength was 25–50% higher. However, the impact strength of injection moulded samples was lower, which is attributable to the excessive fibre attrition (< 1 mm long fibres) and agrees well with Thomason's model [17] (influence of fibre length on the relative properties).

### 3.3. Microscopic laminate analysis

Micrographs of recycled PP-GF panel cross sections, depicted in Fig. 6, show a clear difference between the shred sizes of coarse and fine PP-GF SMCs. In the case of coarse PP-GF SMCs, the elliptically shaped roving bundles were still mostly intact, while the fine PP-GF SMCs consisted of roving fragments. Fibre distribution and packing were observed to be slightly better in fine PP-GF SMCs. However, as previously mentioned, this did not lead to improved mechanical properties of fine PP-GF SMCs compared to PP-GF SMCs. The reprocessed panels were practically void-free as the micrographs unveiled. In sandwich laminates a seamless transition was observed between the fusion

bonded cores and skins.

Lateral cross sections of tested PP-GF flexural and impact specimens revealed that the failure mechanism of monolithic laminates and sandwich laminates was very similar. The main failure mechanism for PP-GF laminates in bending was buckling of the fibres on the compression side, illustrated in Fig. 7. No shear induced separation (mode II failure/in-plane shear) of cores and skins was detected in sandwich specimens, indicating a good fusion bond.

One of the mechanisms for energy dissipation of PP-GF sandwich and monolithic laminates in impact tests was permanent plastic deformation with partial fibre breakage on the compression- and tension side (no continuous crack through the thickness of the specimen). Owing to their lower rigidity and their higher strain at failure, glass fibres are ideal for energy attenuation during an impact.

Recycled PA6-CF panel cross sections, depicted in Fig. 8, exhibited a less distinctive difference between coarse and fine PA6-CF SMCs at first glance. However, in some areas very long carbon fibre tows were visible in coarse PA6-CF SMC micrographs compared to fine PA6-CF SMCs. Very low void content and small void size (< 25  $\mu\text{m}$ ) were detected in these materials.

Fig. 9 shows a comparison between PA6-CF monolithic and sandwich specimens from flexural and impact tests. PA6-CF specimens demonstrated a different failure mechanism in contrast to PP-GF specimens. In flexural tests, PA6-CF laminates mostly yielded in tension, or a combination of compression and tension failure. The monolithic PA6-CF laminate was accompanied by delamination (white arrows), while crack propagation was halted more effectively in sandwich specimens. Sandwich skin debonding was not observed.

The low impact tolerance due to the brittle nature of carbon fibres led to catastrophic failure in impact tests, mostly resulting in hinge breaks or complete breaks without plastic deformation. Crack propagation could not be halted in the PA6-CF specimens as opposed to PP-GF specimens. The crack path of PA6-CF sandwich specimens appeared more complex compared to the virtually straight crack path of monolithic specimens. However, crack path deviation in sandwich specimens did not affect impact energy absorption to yield higher impact strength values.

### 3.4. Reuse potential by reverse-forming laminates

In the reverse-forming experiments, the focus was placed on multiply Teplex® laminates constructed of woven fabrics with consistent ply orientation. It is widely known that trellis shearing is one of the main deformation modes in thermoforming of woven fibre laminates [61,62]. Depending on the mould geometry, blank size and blank holder force, additional yarn slippage can occur during thermoforming, as described

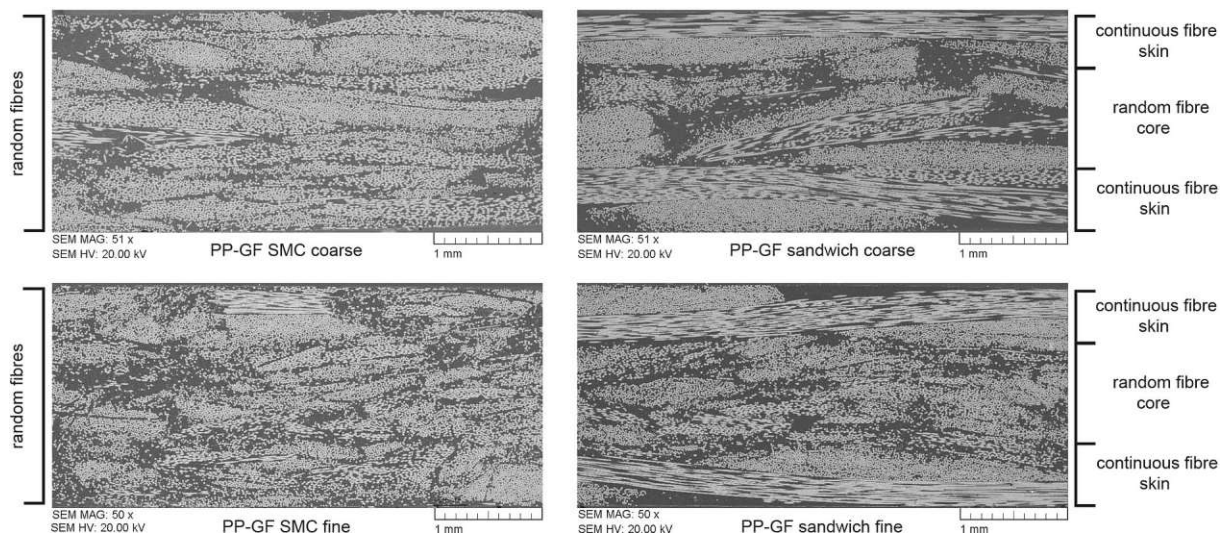


Fig. 6. SEM micrographs of recycled PP-GF laminates.

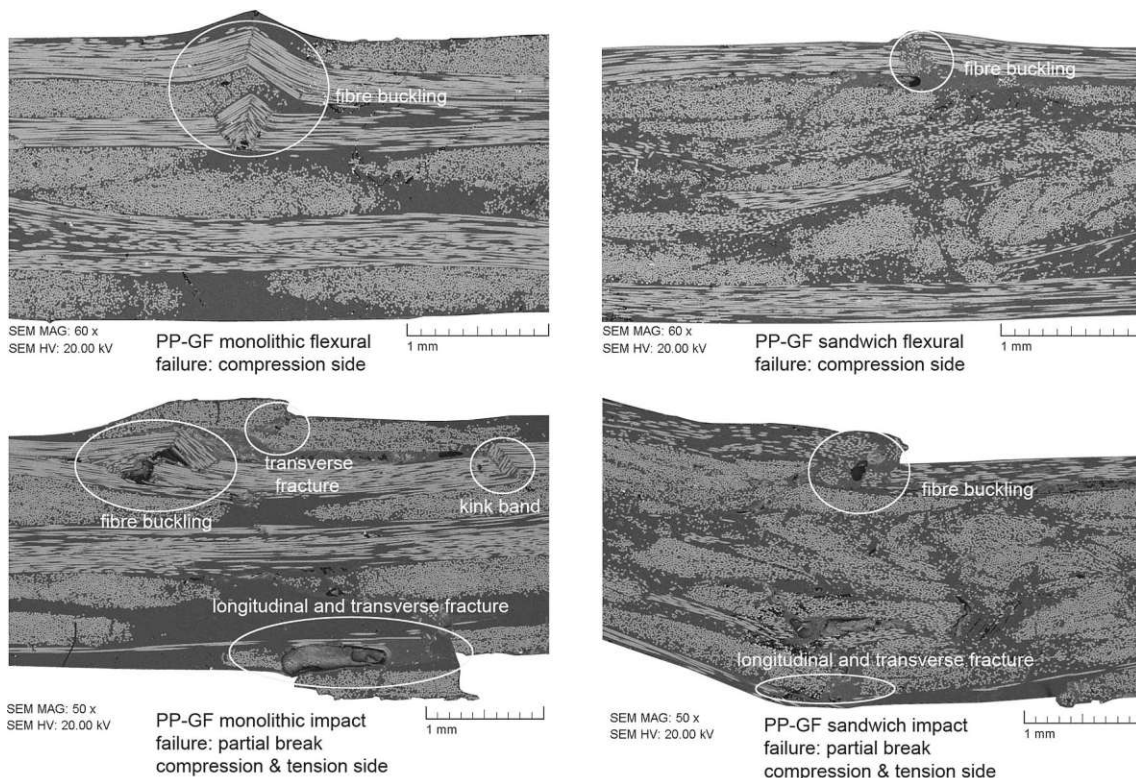


Fig. 7. SEM micrographs of tested PP-GF specimens; force was applied vertically (top side) to the specimens depicted.

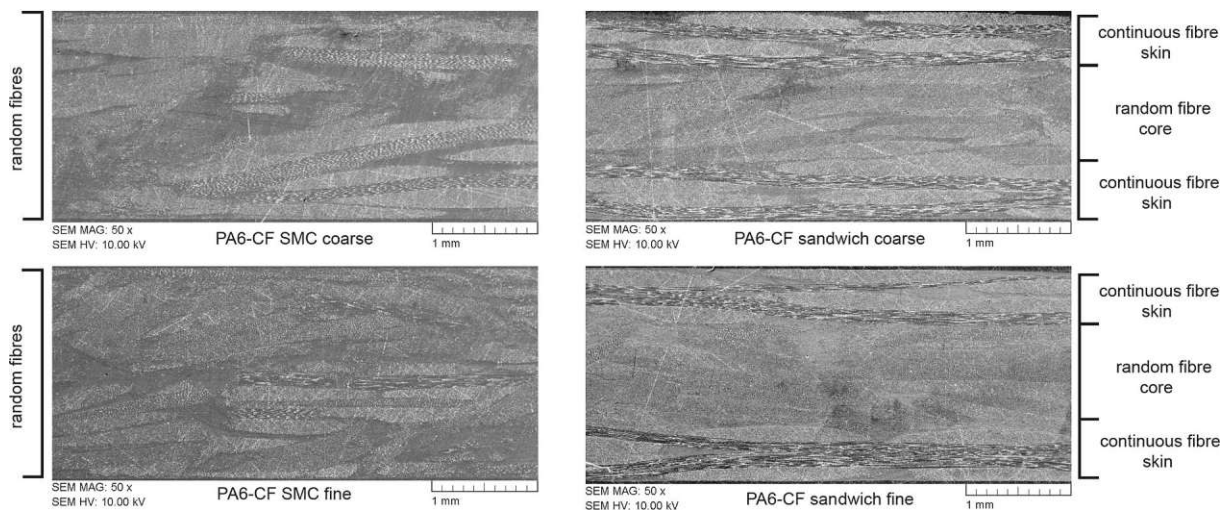


Fig. 8. SEM micrographs of recycled PA6-CF laminates.

Die approbierte gedruckte Originalversion dieser Dissertation ist an der TU Wien Bibliothek verfügbar. The approved original version of this doctoral thesis is available in print at TU Wien Bibliothek.

**TU** **Bibliothek**  
WIEN  
Your knowledge hub

by Boisse, Hamila and Madeo [63].

The reverse-forming method is best suited for rejected parts with clamping spots still intact, for reintroduction of the blank holder forces. The method was found to work effectively in terms of a “reverse trellis shearing” operation. Moreover, the core premise of this method is that the parts to be reverse-formed do not exhibit any yarn slippage, i.e. a flawless weave structure. Friction between intersecting yarns (inter-yarn friction) was found to be responsible for defect-free reverse-formability. Slipped yarns, on the other hand, cause excess material that cannot be moved due to missing yarn friction, ultimately resulting in out-of-plane wrinkle formation. A comparison between PP-GF and PA6-CF reverse-formed blanks, showing the difference with and without slipped yarns is provided in Fig. 10. Yarn slippage was particularly prominent in hemispherical parts of glass roving-reinforced

laminates Fig. 10 (a), whereas carbon fibre laminates (made of 3 K-tows) showed less yarn slippage Fig. 10 (b). This resulted in overall better reverse-formability of PA6-CF parts. Nonetheless, parts that exhibited slipped yarns were always accommodated by wrinkle formation. Laminates which were thermoformed into pyramid stumps, Fig. 10(c) and (d) featured no yarn-slippage. Hence, reverse-forming resulted in wrinkle-free reusable blanks of both PP-GF and PA6-CF laminates.

Compared to their virgin material counterparts, rejected vacuum-formed parts and reverse-formed blanks showed pinholes between the yarn crossover points. This was an early indication that the applied vacuum pressure may not have sufficed for adequate laminate consolidation. It is known that heating well consolidated thermoplastic composite laminates causes deconsolidation and void formation within

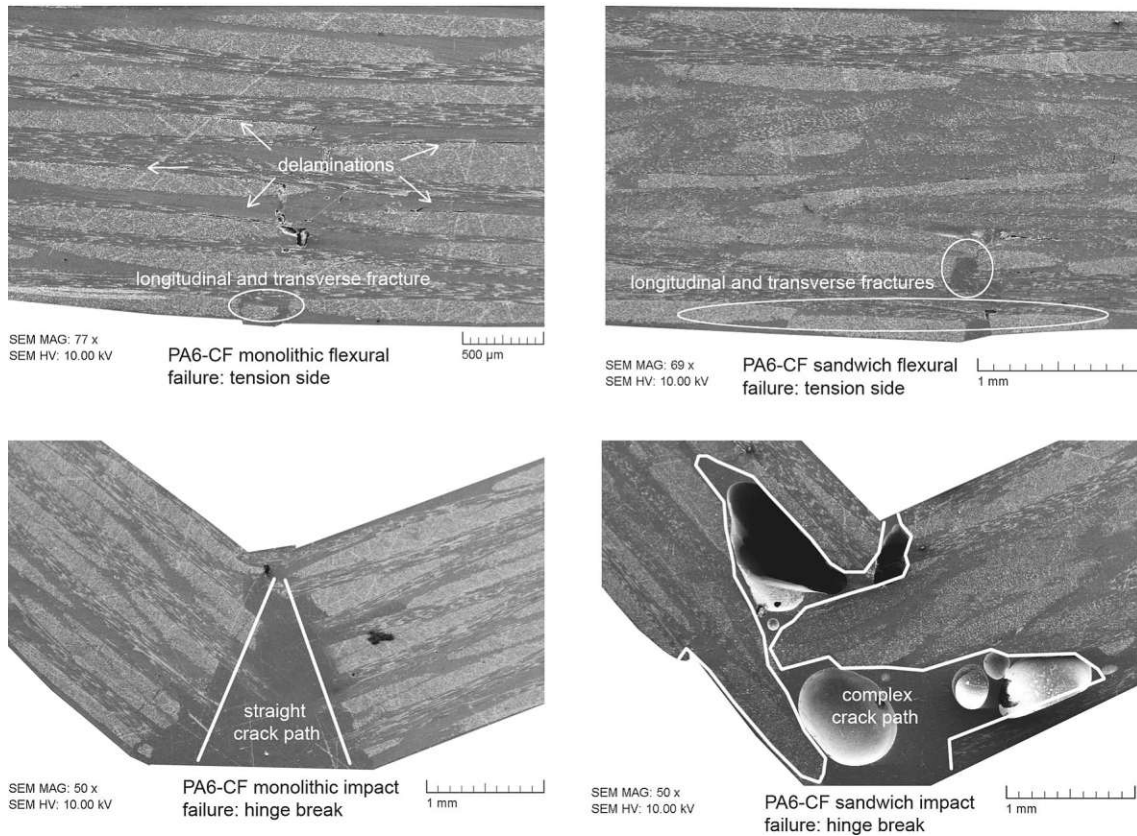


Fig. 9. SEM micrographs of tested PA6-CF specimens (PA6-CF sandwich impact specimen showing air pockets from embedding in epoxy resin); force was applied vertically (top side) to the specimens depicted.

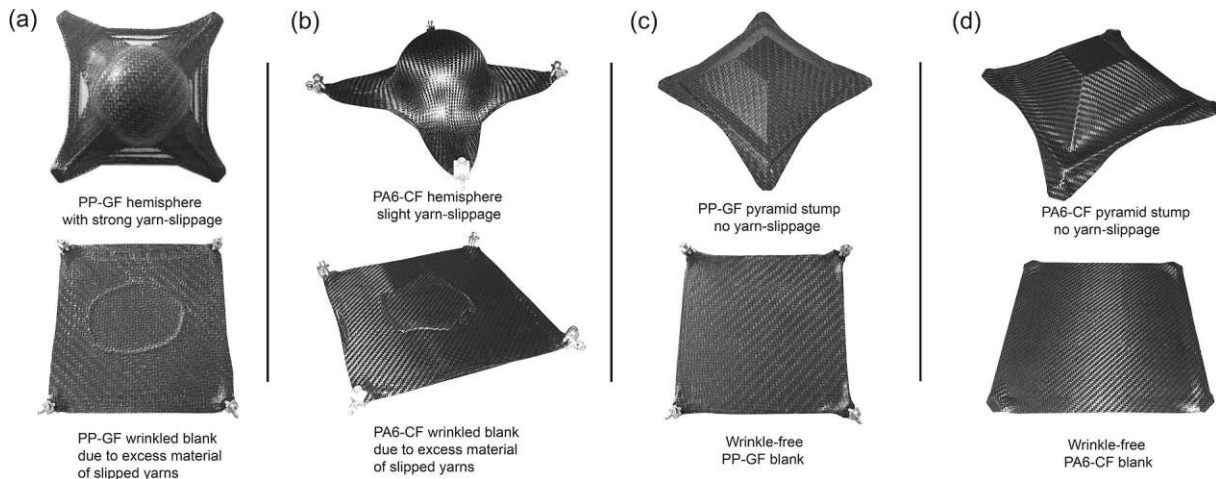


Fig. 10. Comparison of reverse-formed parts with attention to yarn slippage and wrinkle formation; (top: initial geometry, bottom: reverse-forming result); (a) PP-GF hemisphere, (b) PA6-CF hemisphere, (c) PP-GF pyramid stump, (d) PA6-CF pyramid stump; hemisphere mould height (70 mm), pyramid stump mould height (60 mm), blank size (250 · 250 · 1 mm).

Die approbierte gedruckte Originalversion dieser Dissertation ist an der TU Wien Bibliothek verfügbar. The approved original version of this doctoral thesis is available in print at TU Wien Bibliothek.



the matrix-rich laminate regions if reconsolidation pressure is low [40,64,65]. However, vacuum forming experiments of TPCLs are rarely conducted and little is known about void formation after vacuum forming. Cross-sectional micrographs taken from reverse-formed blanks in Fig. 11 confirmed that void formation had occurred during vacuum forming due to insufficient reconsolidation pressure. On average, the laminate thickness increased by 0.13 mm after heating and vacuum consolidation from an initial thickness of 1.0 mm. Mechanical tests were conducted for quality assessment of the reverse-formed blanks (Section 3.2.2). For comparative reasons, a series of wrinkle-free

reverse-formed blanks was subjected to reconsolidation in the heating and cooling press at 0.5 MPa. Most of the large voids collapsed during reconsolidation resulting in a virgin-like microstructure.

### 3.5. Mechanical properties of reverse-formed laminates

In subsequent mechanical tests, the high void content of the vacuum consolidated reverse-formed blanks resulted in reduced mechanical properties as can be seen in Fig. 12. The negative effects of voids were especially apparent in flexural tests, yielding both lower moduli and

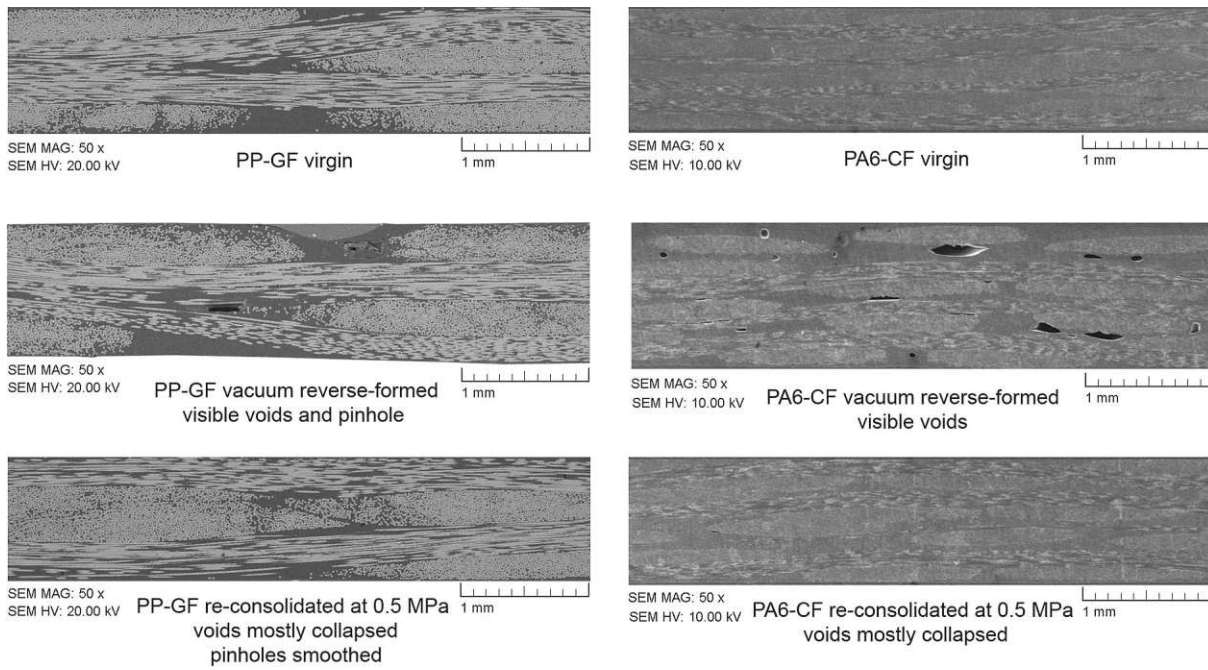


Fig. 11. Comparison of blank microstructure before and after reverse-forming; (top: virgin, middle: reverse-formed vacuum consolidated, bottom: re-consolidated reverse-formed blank at 0.5 MPa consolidation pressure).

strength of reverse-formed blanks. In tensile and impact tests, the negative effects of voids on the mechanical properties were less pronounced, yet, still detectable. Provided that wrinkle-free reverse-formed blanks are properly re-consolidated, it could be shown that they exhibit virgin-like properties. It can therefore be concluded that the reverse-forming operation is able to provide high-quality reusable blanks.

Overall, a discrepancy in the mechanical properties was detected between 1.0 mm and 2.0 mm thick virgin laminates (from Section 3.1.2), even though deliberate adjustments of the test setups were conducted. In flexural and impact tests, the span was adjusted according to a span-to-thickness ratio of 20. Nevertheless, reduced flexural strengths, flexural moduli and impact strengths (same 7.5 J pendulum) of 1 mm thick specimens were measured. Deviations in flexural and impact properties as a function of thickness are well documented. Nagai and Miyari experimentally verified that the impact strength varies widely with specimen thickness even with a constant span-to-thickness ratio for laminated composites [66]. The same is true for flexural testing, where different spans and thicknesses lead to different flexural property readings [67]. Tensile properties of 1 mm thick specimens (unchanged gauge length of 136 mm) showed a similar reduction compared to 2 mm thick specimens, which was unexpected. The elongation at break of both PP-GF and PA6-CF 1 mm thick specimens decreased by 0.2% compared to 2 mm thick specimens in tensile tests, even though lateral failure inside the gauge section was mostly observed. Decreased tensile properties of thinner specimens is reported in some cases for metals [68] and is documented only in one case

for composites [69], but is otherwise uncommon in composite materials [70]. The mechanical values obtained from 1 mm thick specimens should therefore be considered as a separate comparison. A performance downgrade due to matrix degradation could not be observed from the present study.

In summary, reverse-forming is a viable recycling method in that it avoids the need for shredding (and other labour-intensive reprocessing steps). It can be utilised as a means of correcting any forming mistakes. However, several boundary conditions must be met by the rejected parts in order to achieve reuse potential. Respectively, a continuous, woven-fibre architecture and an intact weave structure facilitate this methodology. In addition to these factors, parameters such as consolidation pressure, part size, geometrical complexity, clamping possibilities and the ply stacking sequence must be considered.

#### 4. Conclusion

Recycling thermoplastic composite laminates was successfully carried out under laboratory conditions by means of shredding, compression moulding methods and laminate reverse-forming. Panels made of purely shredded material, abbreviated as TP-SMC in this work, demonstrated insufficient properties for high performance applications due to their random fibre orientation. The random fibre orientation being responsible for poor mechanical performance of TP-SMCs was verified by injection moulded samples. Injection moulding resulted in

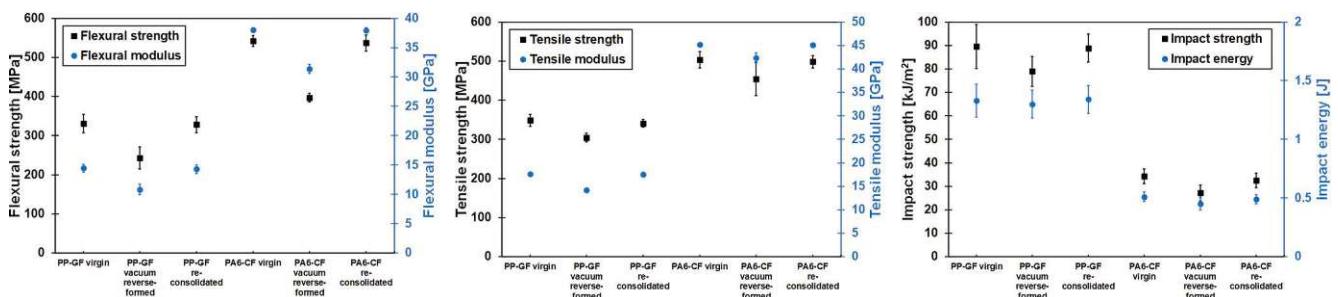


Fig. 12. Mechanical properties of PP-GF and PA6-CF 1 mm thick blanks in virgin state, vacuum reverse-formed state and re-consolidated state (0.5 MPa); PA6 materials tested only in conditioned state.

strong flow-induced fibre orientation and accordingly, significantly higher tensile and flexural properties were observed despite shear-induced fibre attrition. A dedicated long-fibre alignment process which would prevent attrition, could significantly improve TP-SMC performance. Squeeze flow in double belt presses or intermittent presses could help to orient fibres in the machine direction while keeping a high fibre aspect ratio. Overall, random TP-SMCs exhibited a special marbled appearance and could thus be used for decorative applications with less stringent performance requirements.

By incorporating shredded TPCL material as sandwich cores between two continuous fibre skins, it was possible to achieve virgin monolithic material properties in flexural and impact loading. Sandwich panel lamination by co-fusion provides an incentive to reduce virgin material usage for thick laminates and to save raw material costs. It is conceivable that edge trimmings from high-volume monolithic laminate production with consistent material quality may be considered as important feedstock for recycling. As demonstrated in this work, 50% of the virgin materials volume was replaced by recycled cores. Sandwich skins consisted of preimpregnated sheets. To improve energy efficiency, a one-shot sandwich lamination process should be investigated to combine dry fabric skin impregnation alongside co-fusion with a shredded TPCL material core. Overall, sandwich panel lamination can be considered a feasible and readily up-scalable recycling method.

A rather experimental but novel method was examined for reuse, by reverse-forming complex thermoformed parts. It was shown that blank reconstruction is possible by applying heat (preferably by infrared radiation) and tension to thermoformed parts. In order to produce flat and defect-free blanks, the weave structure had to be fully intact. Parts that exhibited yarn slippage could not be reverse-formed into their initial flat shape without wrinkling. Reverse-forming is realisable on state-of-the-art composite thermoforming machines with spring-loaded clamping frames or robotic grippers.

#### CRediT authorship contribution statement

**Peter Kiss:** Conceptualization, Methodology, Investigation, Resources, Writing - original draft, Writing - review & editing, Visualization. **Wolfgang Stadlbauer:** Conceptualization, Validation, Resources, Project administration, Resources, Writing - review & editing. **Christoph Burgstaller:** Conceptualization, Resources, Writing - review & editing. **Hannes Stadler:** Conceptualization, Methodology. **Stefan Fehringer:** Investigation. **Florian Hauserer:** Investigation. **Vasiliki-Maria Archodoulaki:** Methodology, Writing - review & editing, Supervision.

#### Declaration of Competing Interest

The authors declare that they have no known competing financial interests or personal relationships that could have appeared to influence the work reported in this paper.

#### Acknowledgements

The authors are grateful to the State Government of Upper Austria and the European Regional Development Fund for providing financial support for this research, in the EFRE-IWB 2020 programme for the project: "ProFVK".

#### References

- [1] Khurshid MF, Hengstermann M, Hasan MMB, Abdkader A, Cherif C. Recent developments in the processing of waste carbon fibre for thermoplastic composites – A review. *J Compos Mater* 2019. <https://doi.org/10.1177/0021998319886043>.
- [2] Thomason JL, Yang L, Meier R. The properties of glass fibres after conditioning at composite recycling temperatures. *Compos Part A Appl Sci Manuf* 2014;61:201–8. <https://doi.org/10.1016/j.compositesa.2014.03.001>.
- [3] Thomason J, Jenkins P, Yang L. Glass Fibre Strength—A Review with Relation to Composite Recycling. *Fibers* 2016;4:18. <https://doi.org/10.3390/fib4020018>.
- [4] Chu J, Sullivan JL. Recyclability of a continuous e-glass fiber reinforced poly-carbonate composite. *Polym Compos* 1996;17:556–67. <https://doi.org/10.1002/pc.10646>.
- [5] Pickering SJ. Recycling technologies for thermoset composite materials-current status. *Compos Part A Appl Sci Manuf* 2006;37:1206–15. <https://doi.org/10.1016/j.compositesa.2005.05.030>.
- [6] Corvaglia P, Passaro A, Manni O, Barone L, Maffezzoli A. Recycling of PP-based Sandwich Panels with Continuous Fiber Composite Skins. *J Thermoplast Compos Mater* 2006;19:731–45. <https://doi.org/10.1177/0892705706067918>.
- [7] Otheguy ME, Gibson AG, Findon E, Cripps RM, Mendoza AO, Castro MTA. Recycling of end-of-life thermoplastic composite boats. *Plast Rubber Compos* 2009;38:406–11. <https://doi.org/10.1179/146580109X12540995045642>.
- [8] Asmatulu E, Twomey J, Overcash M. Recycling of fiber-reinforced composites and direct structural composite recycling concept. *J Compos Mater* 2014;48:593–608. <https://doi.org/10.1177/0021998313476325>.
- [9] Vincent G. Recycling of thermoplastic composite laminates: the role of processing. University of Twente 2019. <https://doi.org/10.3990/1.9789036548526>.
- [10] Cousins DS, Suzuki Y, Murray RE, Samaniuk JR, Stebner AP. Recycling glass fiber thermoplastic composites from wind turbine blades. *J Clean Prod* 2019;209:1252–63. <https://doi.org/10.1016/j.jclepro.2018.10.286>.
- [11] Abdul Rasheed MI. Compression molding of chopped woven thermoplastic composite flakes: a study on processing and performance. University of Twente 2016. <https://doi.org/10.3990/1.9789036541510>.
- [12] Oliveux G, Dandy LO, Leeke GA. Current status of recycling of fibre reinforced polymers: Review of technologies, reuse and resulting properties. *Prog Mater Sci* 2015;72:61–99. <https://doi.org/10.1016/j.pmatsci.2015.01.004>.
- [13] LANXESS Deutschland GmbH. Quality performs. Information for processors Texpex®; 2017.
- [14] Lunt JM, Shortall JB. The effect of extrusion compounding on fibre degradation and strength properties in short glass-fibre-reinforced nylon 6.6. *Plast Rubber Process* 1979;4:108–11.
- [15] Ning H, Lu N, Hassen AA, Chawla K, Selim M, Pillay S. A review of Long fibre thermoplastic (LFT) composites. *Int Mater Rev* 2020;65:164–88. <https://doi.org/10.1080/09506608.2019.1585004>.
- [16] Subasinghe ADL, Das R, Bhattacharyya D. Fiber dispersion during compounding/injection molding of PP/kenaf composites: Flammability and mechanical properties. *Mater Des* 2015;86:500–7. <https://doi.org/10.1016/j.matdes.2015.07.126>.
- [17] Thomason JL. The influence of fibre length and concentration on the properties of glass fibre reinforced polypropylene: 5. Injection moulded long and short fibre pp. *Compos Part A Appl Sci Manuf* 2002;33:1641–52. [https://doi.org/10.1016/S1359-835X\(02\)00179-3](https://doi.org/10.1016/S1359-835X(02)00179-3).
- [18] Thomason JL, Vlugg MA. Influence of fibre length and concentration on the properties of glass fibre-reinforced polypropylene: 4. Impact properties. *Compos Part A Appl Sci Manuf* 1997;28:277–88. [https://doi.org/10.1016/S1359-835X\(96\)00127-3](https://doi.org/10.1016/S1359-835X(96)00127-3).
- [19] Park J-M, Kim D-S, Kim S-R. Improvement of interfacial adhesion and non-destructive damage evaluation for plasma-treated PBO and Kevlar fibers/epoxy composites using micromechanical techniques and surface wettability. *J Colloid Interface Sci* 2003;264:431–45. [https://doi.org/10.1016/S0021-9797\(03\)00419-3](https://doi.org/10.1016/S0021-9797(03)00419-3).
- [20] Koziol M. The effect of reinforcing fabric type on mechanical performance of laminar FR epoxy composite. *Compos Theory Pract* 2012;1:60–5.
- [21] Kiss P, Stadlbauer W, Burgstaller C, Archodoulaki V-M. Development of high-performance glass fibre-polypropylene composite laminates: Effect of fibre sizing type and coupling agent concentration on mechanical properties. *Compos Part A Appl Sci Manuf* 2020;138:106056. <https://doi.org/10.1016/j.compositesa.2020.106056>.
- [22] Vincent GA, de Bruijn TA, Wijskamp S, Abdul Rasheed MI, van Drongelen M, Akkerman R. Shredding and sieving thermoplastic composite scrap: Method development and analyses of the fibre length distributions. *Compos Part B Eng* 2019;176:107197. <https://doi.org/10.1016/j.compositesb.2019.107197>.
- [23] De Bruijn TA, Vincent G, Van Hattum FWJ. Recycling C/PPS laminates into long fibre thermoplastic composites by low shear mixing. *ICCM Int Conf Compos Mater* 2017. 2017-Augus:20–5.
- [24] Krause W, Henning F, Tröster S, Geiger O, Eyerer P. LFT-D - A process technology for large scale production of fiber reinforced thermoplastic components. *J Thermoplast Compos Mater* 2003;16:289–302. <https://doi.org/10.1177/>



- 089270573016004001.
- [25] Schinner G, Brandt J, Richter H. Recycling Carbon-Fiber-Reinforced Thermoplastic Composites. *J Thermoplast Compos Mater* 1996;9:239–45. <https://doi.org/10.1177/089270579600900302>.
- [26] Eguémann N, Giger L, Roux M, Dransfeld C, Thiébaud F, Perreux D. Compression moulding of complex parts for the aerospace with discontinuous novel and recycled thermoplastic composite materials. In: *ICCM Int Conf Compos Mater* 2013;2013-July:6616–26.
- [27] Howell DDW, Fukumoto S. Compression molding of long chopped fiber thermoplastic composites. In: *CAMX 2014 - Compos Adv Mater Expo Comb Strength Unsurpassed Innov*; 2014.
- [28] Howell DDW. Compression molded billet: Advantages and usages. *CAMX 2016 - Compos Adv Mater Expo* 2016:0–8.
- [29] Fu S-Y, Lauke B, Mäder E, Yue CY, Hu X. Tensile properties of short-glass-fiber- and short-carbon-fiber-reinforced polypropylene composites. *Compos Part A Appl Sci Manuf* 2000;31:1117–25. [https://doi.org/10.1016/S1359-835X\(00\)00068-3](https://doi.org/10.1016/S1359-835X(00)00068-3).
- [30] Fu S-Y, Lauke B. Effects of fiber length and fiber orientation distributions on the tensile strength of short-fiber-reinforced polymers. *Compos Sci Technol* 1996;56:1179–90. [https://doi.org/10.1016/S0266-3538\(96\)00072-3](https://doi.org/10.1016/S0266-3538(96)00072-3).
- [31] Amuthakkannan P, Manikandan V, Winowlin Jappes JT, Uthayakumar M. Effect of fibre length and fibre content on mechanical properties of short basalt fibre reinforced polymer matrix composites. *Mater Phys Mech* 2013;16:107–17.
- [32] Tapper RJ, Longana ML, Hamerton I, Potter KD. A closed-loop recycling process for discontinuous carbon fibre polyamide 6 composites. *Compos Part B Eng* 2019;179:107418. <https://doi.org/10.1016/j.compositesb.2019.107418>.
- [33] Longana ML, Ong N, Yu H, Potter KD. Multiple closed loop recycling of carbon fibre composites with the HiPerDiF (High Performance Discontinuous Fibre) method. *Compos Struct* 2016;153:271–7. <https://doi.org/10.1016/j.compstruct.2016.06.018>.
- [34] Yu H, Potter KD, Wisnom MR. A novel manufacturing method for aligned discontinuous fibre composites (High Performance-Discontinuous Fibre method). *Compos Part A Appl Sci Manuf* 2014;65:175–85. <https://doi.org/10.1016/j.compositesa.2014.06.005>.
- [35] Longana ML, Yu H, Hamerton I, Potter KD. Development and application of a quality control and property assurance methodology for reclaimed carbon fibres based on the HiPerDiF (High Performance Discontinuous Fibre) method and interlaminated hybrid specimens. *Adv Manuf Polym Compos Sci* 2018;4:48–55. <https://doi.org/10.1080/20550340.2018.1456504>.
- [36] Tapper RJ, Longana ML, Yu H, Hamerton I, Potter KD. Development of a closed-loop recycling process for discontinuous carbon fibre polypropylene composites. *Compos Part B Eng* 2018;146:222–31. <https://doi.org/10.1016/j.compositesb.2018.03.048>.
- [37] Kemmochi K, Takayanagi H, Nagasawa C, Takahashi J, Hayashi R. Possibility of closed loop material recycling for fiber reinforced thermoplastic composites. *Adv Perform Mater* 1995;2:385–94. <https://doi.org/10.1007/BF00705318>.
- [38] Toray Advanced Composites. White Paper: Recycling thermoplastic composites: Beyond grinding the materials; 2018.
- [39] Schaefer J. Thermoplastic Sandwich Sheets with Glass Fabric Reinforced Facings and Random-in-Plane Orientated Glass Fibre Reinforced Cores. *Proc. ICCM-10 Vol. 6 Microstruct. Degrad. Des., Whistler, B.C.: Woodhead Publishing Limited*; 1995, p. 53–60.
- [40] Wakeman MD, Blanchard P, Månson JAE. Void evolution during stamp-forming of thermoplastic composites. *ICCM-15* 2005;1001:15.
- [41] Wakeman MD, Cain TA, Rudd CD, Brooks R, Long AC. Compression moulding of glass and polypropylene composites for optimised macro- and micro- mechanical properties 3. Sandwich structures of GMTS and commingled fabrics. *Compos Sci Technol* 1999;59:1153–67. [https://doi.org/10.1016/S0266-3538\(98\)00155-9](https://doi.org/10.1016/S0266-3538(98)00155-9).
- [42] Institut fuer Verbundwerkstoffe GmbH. Recycling of CFRP with thermoplastic matrix 2016. [http://www.transferinitiative-rlp.de/fileadmin/core/img/Veranstaltungen/2016-11-29\\_Recycling\\_CFK\\_Luftfahrtbauteile\\_incl\\_IVW.pdf](http://www.transferinitiative-rlp.de/fileadmin/core/img/Veranstaltungen/2016-11-29_Recycling_CFK_Luftfahrtbauteile_incl_IVW.pdf) (accessed February 20, 2020).
- [43] Kasper A. Recycling composites: FAQs. *Reinf Plast* 2008;52:39. [https://doi.org/10.1016/S0034-3617\(08\)70278-9](https://doi.org/10.1016/S0034-3617(08)70278-9).
- [44] Kim JW, Lee JS. Influence of interleaved films on the mechanical properties of carbon fiber fabric/polypropylene thermoplastic composites. *Materials (Basel)* 2016;9. <https://doi.org/10.3390/ma9050344>.
- [45] DIN EN ISO 14125:2011-05, Fibre-reinforced plastic composites - Determination of flexural properties (ISO 14125:1998 + Cor.1:2001 + Amd.1:2011); German version EN ISO 14125:1998 + AC:2002 + A1:2011, 2011. doi:10.31030/1753441.
- [46] Plastics - Determination of tensile properties - Part 4: Test conditions for isotropic and anisotropic fibre-reinforced plastic composites (ISO 527-4:1997); German version EN ISO 527-4:1997, 1997. doi:10.31030/7360910.
- [47] Plastics - Determination of Charpy impact properties - Part 1: Non-instrumented impact test (ISO 179-1:2010); German version EN ISO 179-1:2010, 2010. doi:10.31030/1625765.
- [48] DIN EN ISO 291:2008-08, Plastics - Standard atmospheres for conditioning and testing (ISO 291:2008); German version EN ISO 291:2008, 2008. doi:10.31030/1441132.
- [49] DIN EN ISO 1183-1:2019-09, Plastics - Methods for determining the density of non-cellular plastics - Part 1: Immersion method, liquid pycnometer method and titration method (ISO 1183-1:2019, Corrected version 2019-05); German version EN ISO 1183-1:2019, 2019. doi:10.31030/3023324.
- [50] DIN EN ISO 1172:1998-12, Textile-glass-reinforced plastics - Prepregs, moulding compounds and laminates - Determination of the textile-glass and mineral-filler content; calcination methods (ISO 1172:1996); German version EN ISO 1172:1998, 1998. doi:10.31030/8003549.
- [51] Bond-Laminates GmbH. *Teplex® Datasheets* 2020. <http://bond-laminates.com/downloads/data-sheets/>.
- [52] Gibson LJ, Ashby MF. The design of sandwich panels with foam cores. *Cell. Solids*, Cambridge University Press 1997:345–86. <https://doi.org/10.1017/CBO9781139878326.011>.
- [53] Uzay C, Boztepe MH, Geren N. Impact Energy Absorption Capacity of Fiber Reinforced Polymer Matrix (FRP) Composites. *Conf Int J Arts Sci* 2016;09:211–20.
- [54] Jogur G, Nawaz Khan A, Das A, Mahajan P, Alagirusamy R. Impact properties of thermoplastic composites. *Text Prog* 2018;50:109–83. <https://doi.org/10.1080/00405167.2018.1563369>.
- [55] Prabhakaran RTD, Andersen TL, Lystrup A. Influence of moisture absorption on properties of Fiber Reinforced Polyamide 6 composites. *2nd Jt US-Canada Conf Compos - Am Soc Compos 26th Annu Tech Conf Can Assoc Compos Struct Mater* 2011.
- [56] Ourahmoune R, Salvia M, Laborde J. Effect of temperature and moisture on mechanical properties of a woven and short fibre thermoplastic composites for load-bearing automotive parts. *ICCM Int Conf Compos Mater* 2017;2017-Augus:20–5.
- [57] Ksouri I, De Almeida O, Haddar N. Long term ageing of polyamide 6 and polyamide 6 reinforced with 30% of glass fibers: physicochemical, mechanical and morphological characterization. *J Polym Res* 2017;24:133. <https://doi.org/10.1007/s10965-017-1292-6>.
- [58] Kim YS, Kim JK, Jeon ES. Effect of the compounding conditions of polyamide 6, carbon fiber, and Al<sub>2</sub>O<sub>3</sub> on the mechanical and thermal properties of the composite polymer. *Materials (Basel)* 2019;12:1–14. <https://doi.org/10.3390/ma12183047>.
- [59] Maris J, Bourdon S, Brossard J-M, Cauret L, Fontaine L, Montembault V. Mechanical recycling: Compatibilization of mixed thermoplastic wastes. *Polym Degrad Stab* 2018;147:245–66. <https://doi.org/10.1016/j.polydegradstab.2017.11.001>.
- [60] Plastics - Injection moulding of test specimens of thermoplastic materials - Part 1: General principles, and moulding of multipurpose and bar test specimens (ISO 294-1:2017); German version EN ISO 294-1:2017, 2017. doi:https://dx.doi.org/10.31030/16209064.
- [61] Liu L. Analytical Model of Shear of 4-harness Satin Weave Fabrics. *AIP Conf. Proc.*, vol. 712, AIP; 2004, p. 338–43. doi:10.1063/1.1766547.
- [62] Akkerman R, Haanappel SP. Thermoplastic composites manufacturing by thermoforming. *Adv Compos Manuf Process Des*, Elsevier 2015:111–29. <https://doi.org/10.1016/B978-1-78242-307-2.00006-3>.
- [63] Boisse P, Hamila N, Madoe A. Modelling the development of defects during composite reinforcements and prepreg forming. *Philos Trans R Soc A Math Phys Eng Sci* 2016;374:20150269. <https://doi.org/10.1098/rsta.2015.0269>.
- [64] Ye L, Lu M, Mai YW. Thermal de-consolidation of thermoplastic matrix composites-I. Growth of voids. *Compos Sci Technol* 2002;62:2121–30. [https://doi.org/10.1016/S0266-3538\(02\)00144-6](https://doi.org/10.1016/S0266-3538(02)00144-6).
- [65] Ye L, Chen ZR, Lu M, Hou M. De-consolidation and re-consolidation in CF/PPS thermoplastic matrix composites. *Compos Part A Appl Sci Manuf* 2005;36:915–22. <https://doi.org/10.1016/j.compositesa.2004.12.006>.
- [66] Nagai M, Miyairi H. The study on Charpy impact testing method of CFRP. *Adv Compos Mater* 1994;3:177–90. <https://doi.org/10.1163/156855194X00033>.
- [67] Mehndiratta A, Bandyopadhyaya S, Kumar V, Kumar D. Experimental investigation of span length for flexural test of fiber reinforced polymer composite laminates. *J Mater Res Technol* 2018;7:89–95. <https://doi.org/10.1016/j.jmrt.2017.06.010>.
- [68] Yuan WJ, Zhang ZL, Su YJ, Qiao LJ, Chu WY. Influence of specimen thickness with rectangular cross-section on the tensile properties of structural steels. *Mater Sci Eng A* 2012;532:601–5. <https://doi.org/10.1016/j.msea.2011.11.021>.
- [69] Nozawa T, Hinoki T, Katoh Y, Kohyama A, Lara-Curzio E. Specimen Size Effects on Tensile Properties of 2D/3D SiC Composites. *Small Specimen. Test Tech. Fourth Vol., 100 Barr Harbor Drive, PO Box C700, West Conshohocken, PA 19428-2959: ASTM International*; 2002, p. 294–305. doi:10.1520/STP10828S.
- [70] Wisnom MR. Size effects in the testing of fibre-composite materials. *Compos Sci Technol* 1999;59:1937–57. [https://doi.org/10.1016/S0266-3538\(99\)00053-6](https://doi.org/10.1016/S0266-3538(99)00053-6).



## An experimental study of glass fibre roving sizings and yarn finishes in high-performance GF-PA6 and GF-PPS composite laminates

Peter Kiss<sup>a,c,\*</sup>, Joachim Schoefer<sup>a</sup>, Wolfgang Stadlbauer<sup>a</sup>, Christoph Burgstaller<sup>b</sup>, Vasiliki-Maria Archodoulaki<sup>c</sup>

<sup>a</sup> University of Applied Sciences Upper Austria, School of Engineering, Stelzhamerstrasse 23, 4600, Wels, Austria

<sup>b</sup> Transfercenter Fuer Kunststofftechnik GmbH, Franz-Fritsch-Strasse 11, 4600, Wels, Austria

<sup>c</sup> TU Wien, Institute of Materials Science and Technology, Getreidemarkt 9, 1060, Vienna, Austria

### ARTICLE INFO

#### Keywords:

- A. Glass fibres
- B. Adhesion
- E. Thermoplastic resin
- D. Mechanical testing

### ABSTRACT

In the present study a range of glass fibre (GF) coatings (roving sizings and yarn finishes) were investigated for the manufacture of high-performance composite laminates based on Polyamide 6 (PA6) and Polyphenylene Sulfide (PPS) matrices. Matrix compatibility and resulting composite performance of press-consolidated laminates was evaluated by macro-mechanical testing on the basis of 3-point flexural and short-beam-shear tests. Among the tested yarn finishes,  $\gamma$ -aminopropyltriethoxysilane (A-1100 aminosilane yarn finish) and chromium (III)methacrylate (Volan®A chromium yarn finish) stood out as highly efficient adhesion promoters for both PA6 and PPS. Flexural strength properties of laminates prepared from finished yarn fabrics (up to 770 MPa) surpassed industrial grade laminates. A GF-epoxy laminate yielded lower flexural strength (570 MPa) compared to the GF-PPS laminates at an identical fibre volume fraction of 56%. These findings exemplified that neat PA6 and PPS matrices require no further chemical modification, i.e. adhesion and resulting composite strength can be tailored most efficiently by fibre coating adaptation. SEM imaging further verified that PA6 and PPS polymers adhere strongly to specific glass fibre coatings. In contrast, laminates made from desized (uncoated) fabrics exhibited interfacial debonding, and hence the lowest laminate performance throughout. Additional compression, and compression after impact tests (50 J impact) revealed that laminates made from sized or finished fabrics boast superior impact attenuation when compared to their desized fabric counterparts.

### 1. Introduction

In times of environmental upheaval, considerations of sustainability require raw materials to be used responsibly when it comes to mass-scale production. With regard to fibre-reinforced composite materials, thermoplastic polymer matrix composites are envisioned for applications where structural lightweight design and high-volume manufacturing is desired. Thermoplastic composite laminates, also termed organo sheets, are a promising type of semi-finished product offering high stiffness- and strength-to-weight ratios while most importantly, being inherently recyclable [1].

Lately, thermoplastic composite laminates based on glass fibre-reinforced (GF) Polypropylene (PP) have gained popularity in automotive engineering (e.g. front-end supports, engine shields and underbody covers [2,3]) owing to their excellent thermoforming characteristics, good mechanical performance and cost effectiveness. However, the

main drawback of PP matrices is that they are of limited use at service temperatures in the region of 100 °C due to excessive softening. Instead, applications at such operating temperatures demand different thermoplastic matrices to be used, for example composites of glass fibres and Polyamide 6 (PA6) or Polyphenylene Sulfide (PPS). PA6 is lower cost compared to PPS, therefore, it is of interest for composite usage [3]. However, the mechanical properties of PA6 depend strongly on moisture uptake [4]. Moreover, the exposure of PA6-based composites in hot and humid environment can result in considerable performance loss due to hygrothermal aging induced fibre-matrix debonding [5,6]. PPS may therefore be applied in composites, if an improved gas and moisture barrier [7], inherent flame retardancy, or chemical inertness is required over PA6 [8]. In combination with glass fibre fabrics, PPS is for example extensively used in aircraft interiors and wing parts [9]. However, attaining good interfacial adhesion between glass fibres and PPS is challenging. Moreover, processing of PPS is more difficult due to its

\* Corresponding author. University of Applied Sciences Upper Austria, School of Engineering, Stelzhamerstrasse 23, 4600, Wels, Austria.

E-mail address: [peter.kiss@fh-wels.at](mailto:peter.kiss@fh-wels.at) (P. Kiss).

<https://doi.org/10.1016/j.compositesb.2020.108487>

Received 31 August 2020; Received in revised form 9 October 2020; Accepted 18 October 2020

Available online 22 October 2020

1359-8368/© 2020 Elsevier Ltd. All rights reserved.

higher melting point (280 °C) compared to PP (165 °C) and PA6 (220 °C).

Since the mechanical requirements in fibre-reinforced composites are stringently determined by the efficacy of stress transfer, interfacial adhesion is one of the most important parameters with regard to structural integrity [10]. Due to the high surface area provided by fibrous reinforcement, the role of the interface cannot be ignored. A commonly reported problem in thermoplastic composite processing is that of poor interfacial adhesion. Neat thermoplastics generally present a challenge in attaining proper adhesion, since wet-out is influenced by the high melt viscosities, and avenues for bonding are limited by the primarily inert chemical structures of the polymers.

Theories of interfacial adhesion associate mechanisms of a physical, mechanical and chemical nature, but neither of these theories on its own is sufficient to fully explain fibre-matrix adhesion, as research has demonstrated [10–14]. It is almost certain that a multitude of adhesion mechanisms occur simultaneously during composite manufacture. Glass fibres are practically always treated with an interfacial coating, designed for specific end-use and polymer compatibility. The utilisation of fibre coatings based on silanes, which act as bonding agents between fibres and the matrix, has found widespread application in the industry. Fibre manufacturers and weavers have started to adapt to the increased demand and interest in thermoplastic composites by developing proprietary fibre sizings or fabric finishes, compatible with specific thermoplastic polymers. Depending on the composition, such a coating alters the physico-chemical properties of a fibre surface considerably [15,16]. It can affect wetting, solubility, miscibility, interdiffusion and covalent reactivity with the matrix [15–18].

The impregnation process commences with fibre wetting, which is controlled by physical interface-related interactions (polar and dispersive forces) [11,14,15,19]. Wetting may be considered as a prerequisite for generating intimate contact between the fibre (coating) and the matrix [12]. A compatible polymer most possibly entangles with the fibre coating network and remains entangled upon cooling, forming an interphase region with roughly 100–300 nm thickness [20]. Plueddemann [18] suspected the formation of such interpenetrating networks (IPN) by entanglement of thermoplastic polymers with silane coating networks. It is thought that IPN or semi-IPN formation affects interfacial shear strength significantly [16,21–25]. Moreover, practical experience indicates that for optimal matrix adhesion, more than a monolayer of silane is required, which supports the IPN theory [18].

As far as chemical bonding of thermoplastics is concerned, it is a subject on which opinions diverge widely in literature. While covalent bonding appears to be vital to the formation of strong interfaces in thermoset composites [26], interfacial adhesion of thermoplastics is thought to be dominated by physical or mechanical effects [14,16,26–28]. In thermoplastic polymers other than modified polyolefins (often modified with reactive maleic anhydride additives [29]), covalent bond formation is not considered to be of primary relevance. Moreover, mechanical adhesion by interlocking due to surface roughness may be disregarded in the case of glass fibres, since the latter exhibit very smooth surfaces [30] compared to natural fibres or carbon fibres [31].

In static tests, well-engineered thermoplastic composites (especially high temperature thermoplastics) are generally capable of performing on a par with composites from highly reactive thermosets such as epoxies [32]. This raises the legitimate question whether physical and mechanical interactions of neat thermoplastics are sufficiently strong to account for such high performance. Zisman [33] contended that wetting forces alone would provide adhesive strengths far in excess of the cohesive strength of a polymer matrix, while according to Plueddemann [18] the high performance of thermoplastic composites is better explained by the IPN theory when there is no obvious chemical reaction of a silane and the thermoplastic matrix. However, Suzuki and Saitoh experimentally validated that A-1100 aminosilane apparently catalyses certain reactions with inert thermoplastics at high temperatures. They demonstrated that Polyether Imide (PEI), which has basically no

chemical functionality, underwent some kind of chemical crosslinking reaction with the aminosilane coating [34]. The same was observed by Ishida and Nakata in the case of Polybutylene Terephthalate (PBT) and A-1100 aminosilane [35]. The discussion on interfacial adhesion mechanisms has ever been a controversial topic since the early days of composite development. Ultimately, however, for processors it is of primary relevance whether a material combination is capable of meeting a certain performance requirement. In this context, fibre coating studies prove to be useful, even though some results may be unexpected and the underlying adhesion mechanisms are not entirely comprehensible.

A further topic of importance is the thermal stability of the fibre coatings [36]. Throughout the industry, film- or powder impregnation have become well-established methods for thermoplastic composite laminate manufacture, despite the drawbacks of long impregnation times [2,37]. In particular, if thick roving reinforcement needs to be impregnated, long dwell times at high temperatures exert significant thermal stress on the fibre coatings. Several studies have shown that commonly used silane-based adhesion promoters start to degrade somewhere between 200 and 300 °C in oxidising atmospheres, most of them being relatively stable up to 300 °C [21,22,36,38]. In the case of PA6 processing temperatures (250–270 °C), the thermal stability of these fibre coatings should be of lesser concern. However, the processing window required for PPS (290–320 °C) possibly leads to degradation of certain silane types.

Thermoplastic composite laminates have enormous lightweighting potential for future applications. However, material formulations remain largely undisclosed, especially with regard to which fibre coatings yield the highest performance. Therefore, the aim of the present work concerns the identification of candidate fibre coatings for manufacturing high-strength GF-PA6 and GF-PPS laminates. 3-Point flexural tests and short-beam-shear tests are used to assess material quality in this comparative study. To rule out improper impregnation as an influencing factor, the moulding process (impregnation time and pressure) is selected such that fully impregnated and comparable laminates are obtained. In the case of GF-PA6 composites, a fibre volume fraction of 47% is targeted and compared with a commercial GF-PA6 reference material. For further comparison, a commercial GF-epoxy reference, coming in a typical fibre volume fraction of 55% is compared with GF-PPS laminates. Finally, compression, and compression after impact tests (50 J impactor) are carried out on best-of-best and worst-of-worst panels (based on flexural testing results).

## 2. Materials and methods

### 2.1. Materials

A highly heat-stabilised PA6 grade, Ultramid® B3W black (supplied by BASF SE, Germany) with an MVR (melt volume-flow rate) of 130 cm<sup>3</sup>/10min (at 275 °C, 5 kg) was utilised for GF-PA6 laminate manufacture. PA6 films were extruded in-house by means of a flat-film extrusion line PM30 (Plastik-Maschinenbau Geng-Meyer GmbH, Germany). The pre-dried PA6 pellets (80 °C/6 h) were extruded to 130 µm films at a barrel temperature of 260 °C. The MVR values of the virgin pellets and extruded films were measured and did not deviate from the manufacturer's datasheet value. GF-PA6 laminates were prepared at a fibre volume fraction of roughly 47% for comparison with an industrial-grade GF-PA6 laminate, Texpex® dynalite 102-RG600(4)/47% - 2.0 mm (supplied by Bond-Laminates GmbH, Germany).

An industrial GF-epoxy prepreg type GGBD2807 (a blend of BADGE-type and novolac-type epoxies, supplied by Krempel GmbH, Germany) was utilised for comparison with GF-PPS laminates at a set fibre volume fraction of 55%. The 2 × 2 twill woven glass fabric carrier of the GF-epoxy prepreg had an aerial weight of 280 g/m<sup>2</sup>.

GF-PPS laminate manufacture involved the use of PPS films LITE P (supplied in 100 µm thickness by LITE GmbH, Austria) based on the linear PPS grade Celanese Fortron® 0214 with an MVR of 60 cm<sup>3</sup>/10min

(at 315 °C, 5 kg). GF-PPS laminates were prepared at a fibre volume fraction of 55%.

Commercially available 2 × 2 twill woven E-glass fabrics utilised for thermoplastic matrix impregnation are listed in Table 1, alongside the material abbreviations used in the further course of the work. The glass fabrics used in the present study were either made of woven continuous filament yarn (hereinafter referred to as “yarn”) or woven continuous direct roving (hereinafter referred to as “roving”). The difference between yarn and roving lies within their linear density, fibre diameter and area of application [29].

Glass yarns are generally tightly woven into low-grammage fabrics and require the removal of a protective coating (applied solely for reduction of friction during weaving) by heat-cleaning prior to finishing [39]. Finishing of fabrics is the term used for the application of a chemically pure adhesion promoter (e.g. diluted aminosilane) to the woven and heat-cleaned glass yarns by a complex wetting system [39]. The finishing process leaves great freedom with regard to adhesion promoter selection and concentration to be applied by a weaver. Finished fabrics used in this work contain adhesion promoters only. The different silane finishes of VR48 fabrics were applied equimolarly by Gividi Fabrics S.r.l. for comparability and the type of adhesion promoter was disclosed (e.g. A-1100 aminosilane).

Glass rovings are coarsely woven into fabrics, which are considered as heavy reinforcement. Roving fabrics are lower-cost compared to finished yarn fabrics, since they do not require intricate post-treatment.

**Table 1**  
Overview of selected E-glass fibre 2 × 2 twill fabrics, commercial laminate and prepreg used in the present work.

Woven glass fabrics, linear densities (Tex)	Fibre type	Areal weight (g/m <sup>2</sup> )	Fibre coating	Abbreviation
<sup>a</sup> GIVIDI VR48 desized, 68 Tex · 3	EC9 yarn	290	heat-cleaned, desized (no coating)	desized yarn
<sup>a</sup> GIVIDI VR48 A-1100	EC9 yarn	290	A-1100 aliphatic aminosilane finish*	aminosilane yarn finish
<sup>a</sup> GIVIDI VR48 G1	EC9 yarn	290	G1 aromatic aminosilane finish*	aromatic aminosilane yarn finish
<sup>a</sup> GIVIDI VR48 Z6040	EC9 yarn	290	Z6040 epoxysilane finish*	epoxysilane yarn finish
<sup>b</sup> PI Interglas 92140 FK144, 68 Tex · 5	EC9 yarn	390	modified Volan®A chromium complex finish	chromium yarn finish
<sup>c</sup> PD GW 123–580K2, 1200 Tex	EC14 roving	580	Silane sizing, thermoset application UP, VE, EP	thermoset-compatible roving
<sup>d</sup> JM StarRov® 895, 1200 Tex	EC16 roving	600	Silane sizing, PA6 compatible	PA6-compatible roving
<sup>a</sup> GIVIDI ST600 based on <sup>e</sup> NEG TufRov® 4588, 1200 Tex	EC17 roving	600	Silane sizing, PA6 and PPS compatible	thermoplastic multi-compatible roving
<sup>f</sup> Tepex® dynalite 102-RG600(4)/47%, 1200 Tex	EC roving	600	unknown	commercial GF-PA6 reference
<sup>g</sup> GGBD2807 GF-epoxy prepreg	EC9 yarn	280	unknown	commercial GF-epoxy reference

\*Equimolar silane-finish concentration.

<sup>a</sup> GIVIDI Fabrics S.r.l., Italy.

<sup>b</sup> Porcher Industries Germany GmbH, Germany.

<sup>c</sup> P-D Glasseiden GmbH Oschatz, Germany.

<sup>d</sup> Johns Manville Slovakia a.s., Slovakia.

<sup>e</sup> Nippon Electric Glass Co. Ltd., Japan.

<sup>f</sup> Bond-Laminates GmbH, Germany.

<sup>g</sup> Krempel GmbH, Germany.

The complex formulation of roving coatings (sizing) serves multiple purposes and is applied to the fibres immediately after fibre spinning. The knowledge of the exact sizing composition is exclusive to the glass fibre manufacturer and kept highly proprietary [39]. However, basic sizing formulations gathered from patents were discussed by Thomason [40]. A roving sizing is ready for end-use and includes additives such as lubricants and antistatics for ease of handling and weaving, as well as surfactants, film formers and resin adhesion promoters (silanes) for matrix bonding [40].

## 2.2. Methods

### 2.2.1. Film stacking and press consolidation

Prior to film stacking, the matched steel tool used for impregnation was properly treated with a high-temperature-resistant release agent Loctite® Frekote 700-NC (Loctite Deutschland GmbH, Germany). To compensate for the difference in fabric grammage and respective ply thickness, the number of stacked reinforcement plies was adjusted to yield a total grammage of approximately 2400 g/m<sup>2</sup> per film stack. In the case of roving fabrics this corresponded to 4 plies of 600 g/m<sup>2</sup> reinforcement; in the case of filament yarn fabrics, this corresponded to 8 plies of 290 g/m<sup>2</sup> reinforcement or 6 plies of 390 g/m<sup>2</sup> reinforcement. Fabrics and films were cut to dimensions of 350 · 250 mm and stacked alternately, starting and ending the stack with a polymer film. The fabric plies were stacked with the warp strands oriented in the same direction. The number of stacked films amounted to 9 layers in every stack. Fabrics and films were not pre-dried prior to compression moulding.

Laminate manufacture was accomplished by means of hydraulic pressing in a 2-stage process. Heating and impregnation were carried out in a Wickert WLP 80/4/3 hot press (Wickert Maschinenbau GmbH, Germany), whereas cooling down and consolidation were carried out in a separate water cooled Höfer H10 press (Höfer Presstechnik GmbH, Austria). Both presses were interconnected by a tool shuttle system. Temperatures were monitored during every impregnation trial to guarantee equal processing conditions. Thin-film thermocouples of type-K, 402–716 (TC Mess-und Regeltechnik GmbH, Germany) were inserted into the centre of the film stacks and processes were logged by a Testo 176 T4 temperature data logger (Testo SE & Co. KGaA, Germany). The hot press was pre-heated to its maximum possible temperature of 300 °C. A contact pressure of 0.2 MPa was applied to the impregnation tool to ensure proper heat transfer. After reaching the melting point of the thermoplastic material (PA6: 220 °C, PPS: 280 °C), impregnation pressure was slowly raised to 1.5 MPa and maintained until the desired processing temperature was reached in the middle of the stack: 260 °C (PA6), or 295 °C (PPS). Subsequently, the impregnation tool was transported to the cooling press and cooled under 0.5 MPa consolidation pressure to 100 °C. Thereafter, the panels were demoulded by ejector pins.

Fig. 1 shows the representative processing cycles for PA6 and PPS laminates. In the case of PA6 processing, the impregnation tool was loaded with a film stack and inserted at ambient temperature into the pre-heated press. GF-PA6 laminates were ready for demoulding after 30 min of processing time. PPS film stacks required a different approach due to the upper temperature capabilities (300 °C) of the hot press. To reduce thermal stress on the fibre coatings, the impregnation tool was instead pre-heated in an empty state to 300 °C (1 h heating time). A GF-PPS stack was assembled on a 0.5 mm steel sheet and thereafter loaded into the pre-heated impregnation tool. To compensate the “relatively low” PPS processing temperatures, an impregnation time of 15 min was selected to achieve complete wet-out. GF-PPS laminates were ready for demoulding after 40 min (pre-heating of the impregnation tool excluded).

The commercial GF-epoxy prepreg was defrosted prior to cutting. Eight plies of the prepreg were stacked (with the warp strands oriented in the same direction) and press-cured according to the curing cycle

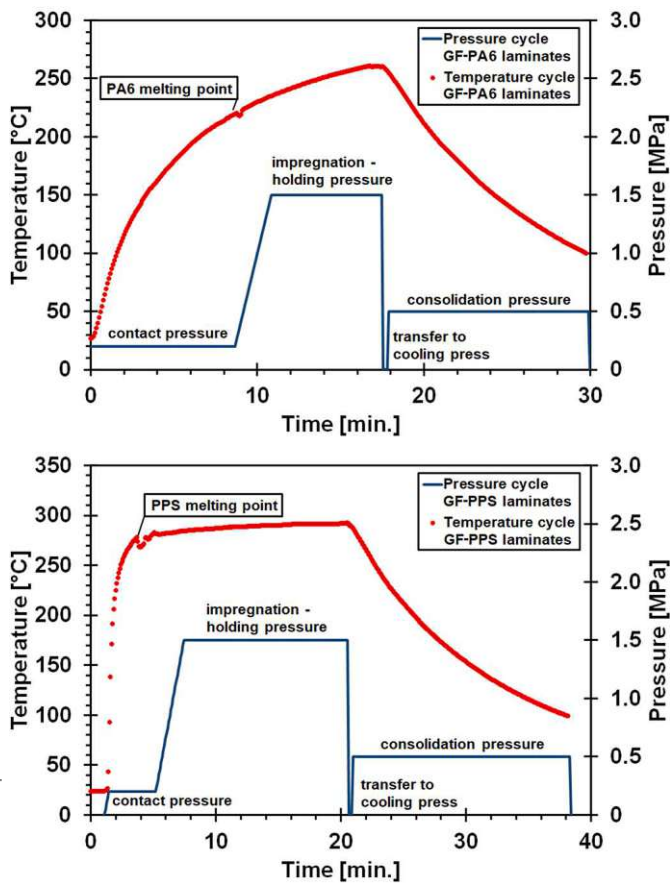


Fig. 1. Laminate processing cycles for GF-PA6 (top) and GF-PPS (bottom) laminates.

recommended by the prepreg manufacturer for 15 min, at 140 °C. Accordingly, the hot press was operated at 145 °C. For comparability with PPS laminates, the moulding pressure during curing was 0.5 MPa (manufacturer recommends 0.4 MPa). According to the manufacturer, it is unnecessary to temper cured laminates with thicknesses below 10 mm.

### 2.2.2. Laminate testing

In order to evaluate the influence of fibre coatings on the mechanical properties, 3-point flexural tests and short-beam-shear tests (apparent interlaminar shear strength, ILSS) were carried out on a Zwick/Roell ZMART. PRO 10 kN universal testing machine. A total of 5 samples was averaged per material combination.

According to EN ISO 14125, a crosshead speed of 1 mm/min and a span-to-thickness ratio of 20 is required for flexural testing woven GF specimens [41]. In conformity with EN ISO 14130, a crosshead speed of 1 mm/min and a span-to-thickness ratio of 5 is required for testing. In flexural and ILSS tests, the radius of the loading nose was 5 mm and the radii of the supports measured 2 mm.

Laminates with dimensions of 100 · 150 mm (150 mm warp direction) were impacted at an energy of 50 J according to EN ISO 18352 [42] by means of a drop tower (constructed in-house according to EN ISO 18352) and a steel impactor with an 8 mm radius. A secondary impact was prevented from further damaging the specimens by means of a locking mechanism. Compression, and compression after impact (CAI) tests were carried out on a 150 kN Zwick Z150 universal testing machine and a CAI fixture at a crosshead speed of 2 mm/min.

Samples were cut on a water-cooled Diadisc 4200 circular saw (Mutronic Präzisionsgerätebau GmbH & Co. KG, Germany) and conditioned according to EN ISO 291 [43]. PA6 composites were conditioned

for 14 days prior to testing in a climate chamber at 23 °C and 50% relative humidity (RH). The reference material Tepex 102 was stored under unregulated environmental conditions and was therefore oven dried (80 °C/24 h) and subsequently conditioned at 23 °C and 50% RH for 14 days prior to testing.

The densities of composite samples  $\rho_{c\_experimental}$  were determined according to EN ISO 1183 by buoyancy method [44]. In addition, the glass fibre mass fraction  $\omega_f$  of the same composite samples was determined via thermogravimetric analysis at 625 °C on a LECO TGA801 macro thermogravimetric analyser (Leco Instrumente GmbH, Germany) according to EN ISO 1172 [45]. Likewise, the exact glass fibre densities  $\rho_f$  of fabric leftovers from macro TGA samples were determined by density measurement. With the knowledge of the composite specimen density  $\rho_{c\_experimental}$ , glass fibre density  $\rho_f$  and glass fibre mass fraction  $\omega_f$ , it was possible to calculate the respective fibre volume fraction  $\nu_f$  according to equation (1):

$$\nu_f = \frac{\omega_f \cdot \rho_{c\_experimental}}{\rho_f} \cdot 100 \quad (1)$$

The laminate void fraction  $\nu_p$  was determined according to equation (2) and equation (3):

$$\nu_p = \frac{\rho_{c\_theoretical} - \rho_{c\_experimental}}{\rho_{c\_theoretical}} \cdot 100 \quad (2)$$

$$\rho_{c\_theoretical} = \frac{1}{\frac{\omega_f}{\rho_f} + \frac{1-\omega_f}{\rho_m}} \quad (3)$$

where the composite density of a theoretical void-free laminate  $\rho_{c\_theoretical}$  is calculated from the glass fibre mass fraction  $\omega_f$  together with the fibre density  $\rho_f$  and matrix densities  $\rho_m$  (PA6: 1.13 g/cm<sup>3</sup>; PPS: 1.35 g/cm<sup>3</sup>; Epoxy-resin: 1.22 g/cm<sup>3</sup>).

### 2.2.3. SEM imaging

Impregnation quality and micromorphologies were analysed by means of SEM imaging. Samples were gold sputtered and inspected via back scattered electron imaging at an accelerating voltage of 20.0 kV on a Vega II LMU SEM (Tescan, Czech Republic) and a FESEM MIRA3 LMH (Tescan, Czech Republic). For detailed impregnation analysis, specimens were polished with 4500-grit SiC discs and water.

## 3. Results and discussion

Several macro-mechanical strength properties influenced by the level of fibre-matrix adhesion, such as longitudinal flexural strength [14], short-beam-shear strength and longitudinal compression strength [19,39] were investigated in this work. These tests are indirect methods to assess changes in the quality of interfacial adhesion and can therefore not be used to make comments on the interfacial shear strength (IFSS). However, these macro-mechanical tests may well be suited for comparative studies or quality screening among the same material class.

### 3.1. Results from GF-PA6 laminate testing and SEM analysis

The results from flexural and ILSS tests of GF-PA6 laminates are displayed in Table 2. In terms of fibre volume fractions, a good correlation was reached among laminates produced in-house and the commercial GF-PA6 reference ( $\nu_f$ : 46.2%). A good basis for comparison was also reflected in similar flexural moduli of coated fabrics in the range of 18–20 GPa.

All coated fabrics led to reasonable laminate strength properties with PA6, the only exception being the desized yarn laminate. The desized yarn laminate exhibited the lowest properties throughout, which indicated that PA6 has relatively low affinity towards uncoated glass fibre surfaces. Comparing the laminate properties further, considerable differences were observed among yarn finishes on mechanical

**Table 2**

Properties of woven GF-PA6 laminates sorted in ascending order by flexural strength. The standard deviation is given by the values between brackets.

Property	desized yarn GF-PA6	epoxysilane yarn finish GF-PA6	thermoset-compatible roving GF-PA6	chromium yarn finish GF-PA6	PA6-compatible roving GF-PA6	thermoplastic multi-compatible roving GF-PA6	aromatic aminosilane yarn finish GF-PA6	aminosilane yarn finish GF-PA6	commercial GF-PA6 reference
Flexural strength	147.4 (11.5)	387.0 (18.2)	434.1 (26.3)	465.5 (23.5)	470.3 (15.4)	476.0 (47.7)	483.4 (8.1)	519.8 (22.4)	460.1 (26.6)
$\sigma_{fMax}$ [MPa] <sup>a</sup>									
Flexural modulus E [GPa] <sup>a</sup>	16.2 (0.6)	19.4 (0.9)	20.1 (1.1)	20.5 (0.4)	19.1 (0.6)	19.7 (1.6)	20.9 (0.7)	20.7 (1.0)	18.6 (0.4)
ILSS $\tau_{Max}$ [MPa] <sup>b</sup>	19.4 (0.4)	32.8 (1.1)	22.7 (1.4)	35.0 (1.6)	44.2 (0.5)	35.4 (1.7)	49.5 (1.2)	50.5 (1.8)	42.6 (0.9)
ILSS dry $\tau_{Max}$ [MPa] <sup>b</sup>	22.3 (0.6)	37.0 (0.5)	24.2 (1.3)	37.3 (0.4)	49.3 (1.4)	40.2 (3.1)	51.1 (1.4)	54.4 (1.2)	50.0 (2.0)
Composite density $\rho_c$ [g/cm <sup>3</sup> ]	1.82 (0.02)	1.84 (0.00)	1.83 (0.02)	1.81 (0.01)	1.81 (0.01)	1.83 (0.01)	1.79 (0.01)	1.81 (0.01)	1.81 (0.00)
Fibre volume fraction $\nu_f$ [%]	48.1 (1.3)	49.3 (0.2)	48.1 (1.4)	47.3 (0.9)	46.6 (0.4)	47.9 (0.7)	45.9 (0.5)	47.2 (0.8)	46.2 (0.3)
Laminate void fraction $\nu_p$ [%]	0.13 (0.03)	0.36 (0.04)	0.67 (0.02)	0.09 (0.02)	0.84 (0.05)	0.94 (0.11)	0.07 (0.02)	0.06 (0.05)	1.08 (0.06)

<sup>a</sup> Flexural test specimen: 60 · 25 mm, span: 40 mm, conditioned at 23 °C 50%RH for 14 days.

<sup>b</sup> ILSS test specimen: 20 · 10 mm, span: 10 mm; conditioned at 23 °C 50%RH for 14 days; ILSS dry: 80 °C/48 h and allowed to cool.

performance. Since the aminosilane, aromatic aminosilane and epoxysilane yarn finishes were applied equimolarly, the differences in strength performance are attributable to a variation in adhesion. Apparently, the epoxysilane yarn finish exhibits inferior compatibility to PA6 than the tested aminosilane and aromatic aminosilane yarn finishes. It is suspected that PA6 undergoes hydrogen-bonding with aminosilanes due to the presence of highly polar amide groups [46]. Moreover, diffusion of the highly polar PA6 polymers into the silane networks could be possible. With reasonable caution, it is conceivable that chemical reactions are involved. Cho et al. [47] have proposed several covalent reactions between different silanes and amino terminal groups of PA6. In their work they found the lowest performance of PA6 with an aminosilane, which is in sharp contrast to the findings of the present paper. However, this discrepancy can be reasoned by the type of aminosilane they used, which was a diaminosilane (Z6020).

It is worth noting that the chromium yarn finish likewise exhibited high compatibility with the PA6 matrix. A similar unexpected finding was documented by Kiss and co-workers [29] of chromium yarn finish and MAH modified PP. The chromium yarn finish either undergoes radical reactions, coordination, or its performance is simply attributable to excellent wettability. More interestingly, the thermoset-compatible roving laminate also demonstrated high flexural performance (434 MPa) in combination with PA6, whereas Kiss and co-workers [29] reported flexural properties of only 60 MPa using the very same fabric combined with MAH modified PP. The low performance of the thermoset-compatible roving with modified PP matrices was attributed to an incompatible film former in the sizing composition [29], which is apparently compatible with PA6.

Overall, the performance of the commercial GF-PA6 reference could be matched or even surpassed. The thermoset-compatible roving laminate had only slightly lower flexural performance compared to commercial GF-PA6 reference, PA6-compatible roving and thermoplastic multi-compatible roving laminates (all with adapted sizings for PA6 usage). In terms of cost efficiency this is an important finding, since thermoset-compatible rovings tend to be considerably cheaper than rovings with designated thermoplastic polymer compatibility. Similar results of thermoset compatible roving fabrics in combination with PA6 were reported by Hildebrandt [48]. The composition of the commercial GF-PA6 reference was unknown, however, due to it performing closer to

PA6-adapted rovings it likely utilises a similar fibre system. Overall, these trials showed that GF-PA6 laminates do not require matrix modification and strength can be most easily tailored by the selection of the fibre coating. Flexural tests of cross-plyed and compression moulded GF-PA6 UD prepregs conducted by Balakrishnan and co-workers [49] resulted in comparable mechanical properties at close to 500 MPa in strength and roughly 25 GPa modulus. Vlasveld and co-workers [50] reported flexural strength values of conditioned GF-PA6 laminates in the region of 450 MPa which were assembled from finished yarn fabrics provided by TenCate Advanced Composites. It appears that the flexural strength values of well-coupled GF-PA6 laminates with bidirectional reinforcement is generally found in the region between 450 and 500 MPa.

It is understood that dry fibre strengths vary between yarn and roving reinforcement (the heat-cleaning of yarns prior to finishing causes fibre strength to deteriorate [51]). However, based on the flexural testing outcomes, the type of reinforcement (yarn or roving) did not manifest itself in a clear performance difference. The yarn fabrics were not consistently outperformed by roving fabrics. Specimen failure was documented and illustrated in Fig. 2. Most laminates exhibited a combined compression-tension failure upon flexural loading. The roving reinforced laminates were indented from the loading nose on the compression side and had slight traces of micro-buckling away from the loading area, whereas the severity of micro-buckling in yarn laminates was strongly dependent on the coating used. The desized yarn laminates exclusively failed due to micro-buckling. Laminates with epoxysilane yarn finish also exhibited strong micro-buckling on the compression side. The ability of a laminate to resist micro-buckling upon compression is an indirect sign of the quality of fibre-matrix adhesion, since a poorly bonded matrix lowers the critical stress for buckling through a reduction of fibre support [52,53]. The ability to resist micro-buckling is especially important in a woven fibre architecture with inherent out-of-plane fibre waviness. As can be seen from the failed specimens, those which resisted micro-buckling more effectively also exhibited higher laminate strengths, for example laminates with aminosilane yarn finish.

To exclude poor impregnation and possible void formation as an influencing factor, specimens were polished and inspected by SEM imaging. Fig. 3 shows the microstructure of the desized yarn laminate and a laminate with aminosilane yarn finish. The polished specimen made

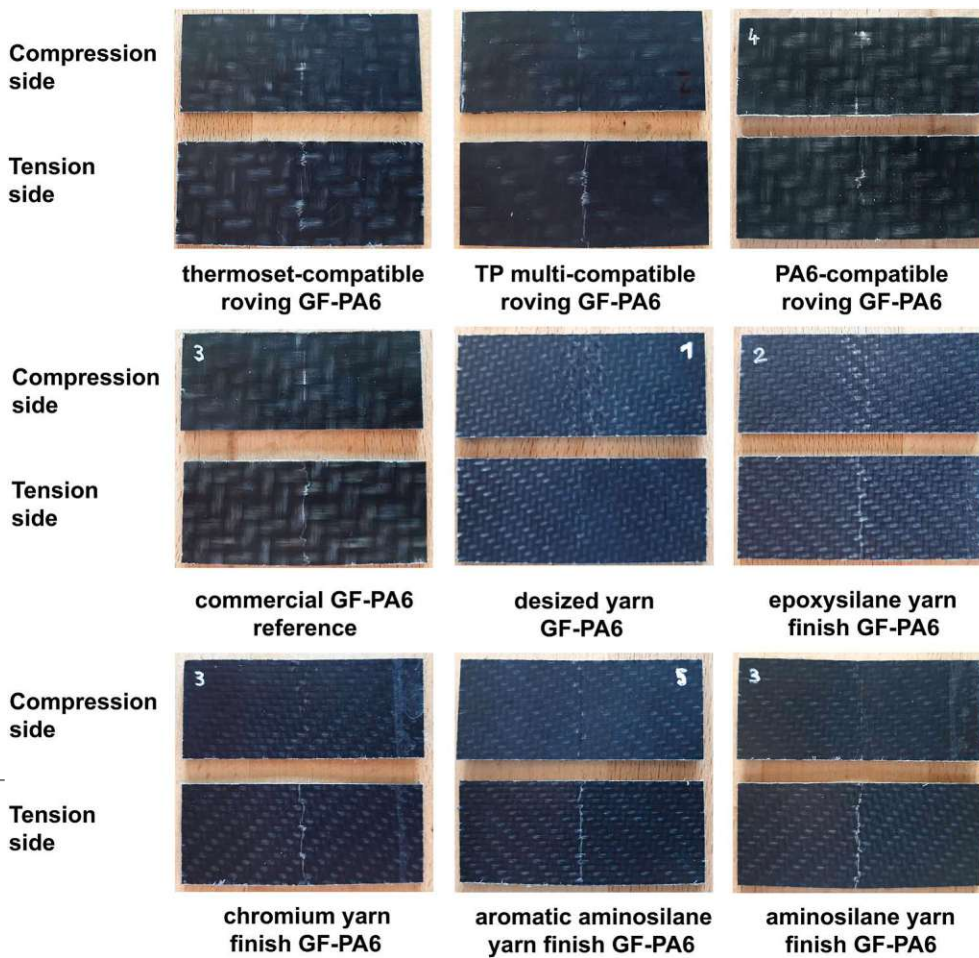


**Fig. 2.** Failure of flexural tested GF-PA6 specimens 60 · 25 · 2 mm, support span 40 mm. Note, some specimens may appear distorted due to permanent deformation from bending. Desized yarn laminate: failure due to micro-buckling on the compression side; laminate with epoxysilane yarn finish: strong micro-buckling alongside tensile fracture; Remaining laminates: combined compression-tension failure.

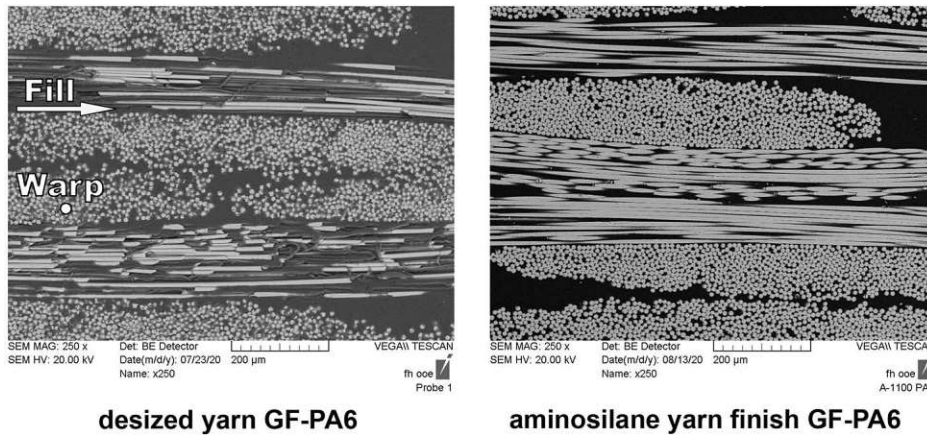


**Fig. 3.** SEM images of polished specimens. Desized yarn GF-PA6 specimen (left) and polished GF-PA6 specimen with aminosilane yarn finish (right), both exhibiting proper impregnation.

from the desized yarn laminate exhibited strong fibre-pull out of the fill (weft) yarns, giving rise to the initial impression of poor impregnation. However, this excessive pull-out upon polishing is rather thought to be a sign of poor fibre-matrix adhesion as the poorly bonded matrix was not able to hold the fibres in place. This was evidenced by the smooth channels left behind in the matrix. Warp fibre bundles of the desized yarn laminate were always fully saturated by the matrix, signalling proper impregnation. In contrast, the excellent polishability of the laminate with aminosilane yarn finish, signalled good fibre-matrix

adhesion without any noticeable fibre pull-out. Based on this observation, the completeness of impregnation (not speaking of adhesion) was comparable between both laminates. Both laminates appeared void-free at 250x magnification. Calculations of the void volume fraction indicated void contents below 1% of in-house manufactured GF-PA6 laminates.

In ILSS tests, none of the PA6 laminates failed due to interlaminar shear, but frequently through combined failure of inelastic deformation, compression failure or compression-tension failure. According to EN ISO

Die approbierte gedruckte Originalversion dieser Dissertation ist an der TU Wien Bibliothek verfügbar. The approved original version of this doctoral thesis is available in print at TU Wien Bibliothek.

14130 [54], if no interlaminar shear failure is provoked, the test values measured do not represent interlaminar shear strength. However, if compression or tension failure is observed, it is permitted to use the values for comparative purposes among test series made of the same materials [54]. To be precise, the values obtained from GF-PA6 laminates have limited significance and in this case, a more suitable term of the measured property would be short-beam strength (without shear). These short-beam strength values were mostly in good agreement with the progression of flexural strength properties across different fabric coating types. However, anomalies were detected in the thermoset-compatible roving and thermoplastic multi-compatible roving laminates. They exhibited “lower than expected” ILSS values in consideration of their flexural strength performance.

To alleviate the influence of moisture content on the ILSS of GF-PA6 specimens, measurements were also conducted in dry specimen state. All GF-PA6 materials exhibited an increase of ILSS in dry state, which verifies that absorbed water acts as a plasticiser and lowers overall strength performance. The effect of moisture content affecting GF-PA6 composite performance is well understood in literature [6]. The cross section of an ILSS specimen with aminosilane yarn finish is depicted in Fig. 4. As mentioned previously, no apparent shear failure was observable within GF-PA6 specimens. Even in dry specimen state the PA6 matrix appeared to be too ductile to induce short-beam-shear failure.

### 3.2. Results from GF-PPS laminate testing and SEM analysis

The moulded GF-PPS laminates were adjusted to yield a fibre volume fraction and thickness similar to the GF-epoxy prepreg in the range of 55% and 1.6 mm, respectively. Since EN ISO 14125 and EN ISO 14130 were complied with, the span for testing was adjusted according to the mean thickness of the composite laminates (flexural testing support span: 30 mm; ILSS testing support span: 7.5 mm). Flexural strength and ILSS values are provided in Table 3.

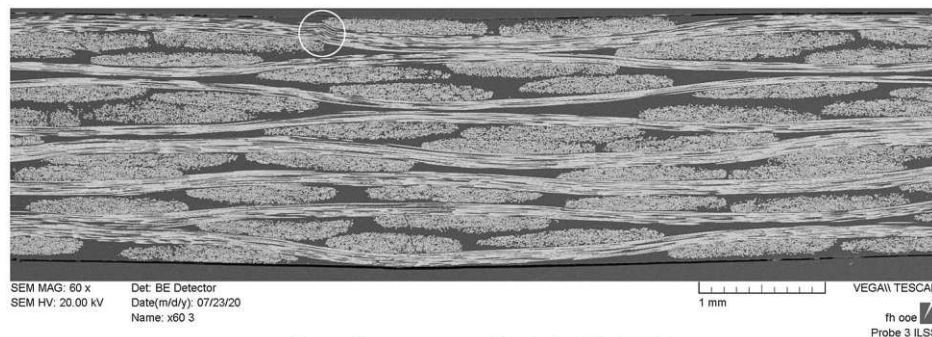
Surprisingly, despite PPS being a less polar polymer than PA6 [55], none of the laminates constructed of coated fabrics exhibited poor strength performance. Flexural strengths of coated fabrics were consistently above 500 MPa, except for the desized yarn laminate in the region of 250 MPa. The overall higher performance of GF-PPS laminates compared to GF-PA6 laminates is also attributable to their higher fibre volume fraction. However, GF-PPS laminates exhibited void contents mostly in a region above 1%. Nonetheless, the observations verified, that with the presence of fibre coatings, PPS most definitely undergoes at least one of the adhesion mechanisms mentioned in the introduction.

The commercial GF-epoxy reference exhibited the highest flexural modulus of all tested laminates (30 GPa at 56% fibre volume fraction). This stiffness reading appears to be exceptionally high for a woven GF composite if the rule of mixtures is taken into account. Yet, similarly high flexural stiffness readings (25–28 GPa at 50% fibre volume

fraction) were reported by Reed et al. for woven GF-epoxy prepregs at a span-to-thickness ratio of 20 [56]. The GF-PPS laminate made from desized yarn exhibited a flexural modulus of 21 GPa, whereas GF-PPS laminates made from coated fabrics demonstrated an increase in mean flexural modulus. Up to 28 GPa modulus was measured depending on the coating (despite relatively constant fibre volume fractions and laminate thicknesses). Similar flexural modulus readings were reported by Wang and co-workers [57] at 27 GPa from woven GF-PPS laminates at 50% fibre volume fraction. Unfortunately, the authors did not disclose the coating used in their composite systems. Fig. 5 shows a comparison of SEM images of both desized yarn and chromium finished yarn GF-PPS laminates. Both laminates exhibited fully impregnated fibre bundles with the difference of weft yarn pull-out (desized yarn laminate) due to a difference in adhesion.

A comparison of micromorphological images is given in Fig. 6, where clear differences were observed in terms of failure mode from cohesive to interfacial debonding, depending on the presence or absence of a fibre coating.

In terms of strength, the commercial GF-epoxy reference performed at the lower end of the flexural strength spectrum (567 MPa) compared to GF-PPS composites made from coated fabrics. However, it should be mentioned that the strength performance of the GF-epoxy reference was likely affected by its mean void content of 2.6%. By comparison, the thermoplastic multi-compatible roving, the aminosilane yarn finish and chromium yarn finish exhibited the highest flexural strength performance in combination with PPS at over 700 MPa. The coatings possibly enhance interfacial wetting of PPS, facilitate IPN formation or chemical bonding. Epoxysilanes are reported to yield good performance in combination with PPS [58]. Liu et al. [59] together with Durmaz and Aytac [60] proposed a coupling reaction between PPS and epoxide groups. In the event that PPS possesses thiol (-SH) terminal groups, chemical bonding with epoxysilanes is thought to occur [59,60]. However, as was established in the course of this research, the aminosilane yarn finishes and chromium yarn finish were far more effective at promoting adhesion between PPS and the glass fibres compared to the epoxysilane yarn finish. If PPS end groups consist of chlorides, reactions with amines are conceivable as Durmaz and Aytac also proposed [60]. This could explain the performance of PPS with the aminosilane yarn finishes used in this work. While there is a possibility that such chemical bonding mechanisms occur, it is unclear why the chromium yarn finish demonstrates even higher mechanical properties. One explanation may be through complexation of terminal phenylene-chloride to chromium. Yet, no clear evidence was found that chloride terminal groups are contained within PPS by means of IR-spectroscopy (determined on Spectrum Two™ FTIR-spectrometer, PerkinElmer), illustrated in Fig. 7. Durmaz and Aytac specified the peaks at 704 and 741  $\text{cm}^{-1}$  as C-Cl stretching [60]. However, according to various literature [61–63], these peaks are rather attributable to ring bending or C-S stretching within the polymer



aminosilane yarn finish GF-PA6

Fig. 4. Cross-section of a GF-PA6 ILSS tested specimen with aminosilane yarn finish. The specimen exhibited plastic deformation and compressive fibre-buckling (indicated by the white circle) with no sign of interlaminar shear.



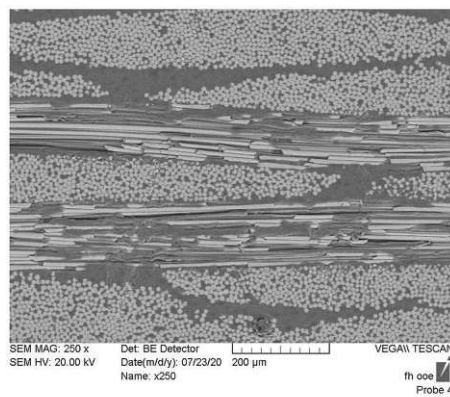
**Table 3**

Properties of woven GF-PPS laminates sorted in ascending order by flexural strength. The standard deviation is given by the values between brackets.

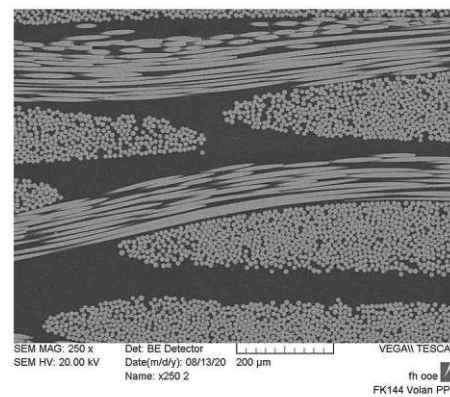
Property	desized yarn GF-PPS	thermoset-compatible roving GF-PPS	epoxysilane yarn finish GF-PPS	aromatic aminosilane yarn finish GF-PPS	thermoplastic multi-compatible roving GF-PPS	aminosilane yarn finish GF-PPS	chromium yarn finish GF-PPS	commercial GF-epoxy reference
Flexural strength $\sigma_{fMax}$ [MPa] <sup>a</sup>	254.1 (15.2)	550.7 (40.6)	559.8 (18.9)	620.0 (56.8)	745.6 (45.1)	748.4 (9.3)	772.5 (26.0)	566.8 (29.8)
Flexural modulus E [GPa] <sup>a</sup>	21.1 (1.8)	24.6 (2.3)	25.1 (0.9)	25.9 (2.5)	25.9 (2.1)	27.5 (1.0)	28.2 (1.3)	30.4 (0.4)
ILSS $\tau_{Max}$ [MPa] <sup>b</sup>	9.7 (2.4)	25.4 (2.1)	32.2 (2.6)	36.0 (5.0)	34.6 (2.4)	43.5 (0.6)	49.8 (1.1)	55.8 (1.2)
Discolouration	none	none	none	minor	minor	minor	none	–
Composite density $\rho_c$ [g/cm <sup>3</sup> ]	2.00 (0.04)	1.98 (0.03)	2.00 (0.02)	2.01 (0.02)	2.03 (0.01)	2.04 (0.05)	2.02 (0.01)	1.97 (0.00)
Fibre volume fraction $v_f$ [%]	57.2 (1.7)	56.0 (2.8)	54.7 (1.5)	58.3 (3.7)	57.1 (0.5)	57.7 (3.4)	56.1 (0.6)	55.9 (0.1)
Laminate void fraction $v_p$ [%]	1.12 (0.26)	1.82 (0.58)	1.17 (0.25)	1.97 (0.30)	0.87 (0.42)	1.20 (0.41)	0.53 (0.17)	2.63 (0.28)

<sup>a</sup> Flexural test specimen: roving: 50 · 25 mm; yarn: 50 · 15 mm; span: 30 mm; conditioned at 23 °C 50%RH for 14 days.

<sup>b</sup> ILSS test specimen: 15 · 7.5 mm; span: 7.5 mm; conditioned at 23 °C 50%RH for 14 days.

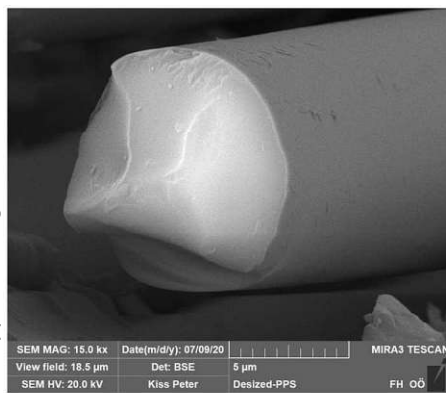


**desized yarn GF-PPS**



**chromium yarn finish GF-PPS**

**Fig. 5.** SEM images of polished GF-PPS laminates composed of desized yarn (left) and chromium finished yarn (right), both exhibiting proper impregnation.



**desized yarn GF-PPS**



**chromium yarn finish GF-PPS**

**Fig. 6.** Fractured fibres showing a difference in microscale matrix adhesion. Different failure modes are observed depending on the presence or absence of a fibre coating.

left: desized yarn GF-PPS laminate showing interfacial debonding and no adherent PPS matrix on the EC9 fibre (matrix is stripped away from the fibre)

right: GF-PPS laminate with chromium yarn finish showing cohesive failure and a fully adhered layer of PPS matrix on the entire EC9 glass fibre.

backbone.

EDX analysis of the interface region of chromium yarn finish GF-PPS showed the presence of C and S (PPS polymer), together with Si, Ca, Al (composition of E-glass) and Au (gold sputtering). However, chlorine could not be detected as depicted in Fig. 8. Furthermore, a Beilstein test of the PPS polymer gave no indication of chlorides being present in the utilised PPS type. Similarly, chromium contained in the glass fibre could not be detected by means of EDX analysis. The concentration of chromium is most possibly below the detection limit of the EDX

detector. Overall, the findings favour wetting and the IPN theory being responsible for adhesion, rather than covalent bonding.

Industrially manufactured woven GF-PPS laminates tend to have flexural strengths in the region of 600–700 MPa according to material datasheets. For example, Cetex® TC1100 GF-PPS laminates by Toray Advanced Composites, which are extensively used in aircraft construction [64], have 50% fibre volume fraction and are specified at 659 MPa flexural strength and 23 GPa modulus (ISO 178) [65]. Based on the observations in the present work, it is likely that the industry uses

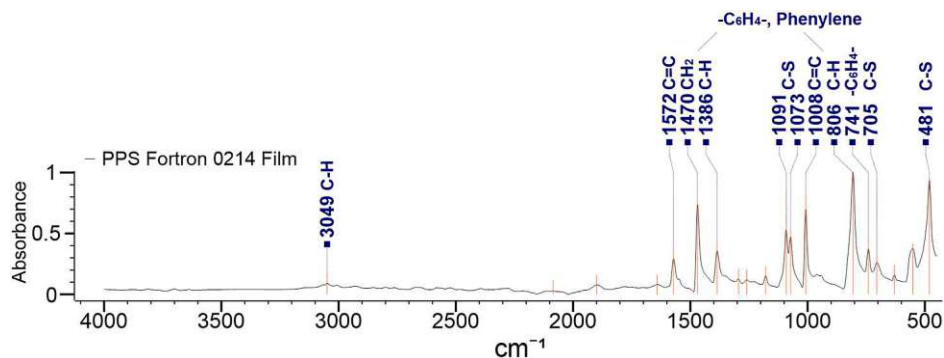


Fig. 7. FTIR absorption spectrum of PPS film.

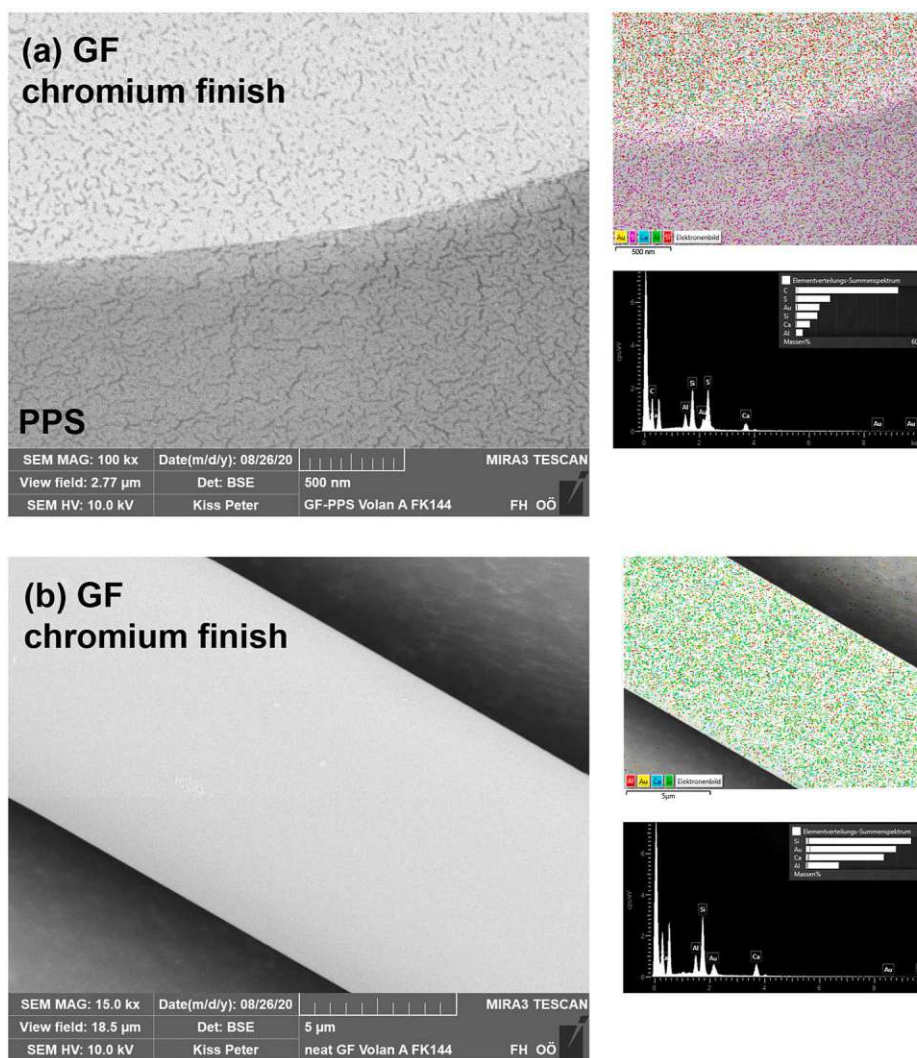


Fig. 8. EDX spectra of GF-PPS laminate and neat glass fibre. (a) Interphase region of a polished GF-PPS sample (cross-section), taken from a chromium finished warp yarn and respective EDX spectrum. (b) neat chromium finished glass fibre with EDX spectrum.

aminosilane coatings, or chromium-based (Volan A) coatings for the manufacture of GF-PPS laminates.

Chromium-based finish being utilised in aerospace grade thermoplastic composite laminates is evidenced by the fact that Shi and co-workers [66] were supplied with Cetex® GF-PEI semipreg containing such finish. Additionally, if the information provided by Roessler [67] still holds true today, Airbus-Industries accepts Volan A finishes exclusively. Even though chromium in its trivalent state constitutes no

immediate hazard, such finishes may nevertheless be substituted by alternative adhesion promoters due to environmental concerns (heavy metals). As witnessed, aminosilane yarn finishes proved to be highly potent adhesion promoters for PPS and a viable replacement for chromium finishes.

Similar to the observations made regarding GF-PA6 laminates, failure of GF-PPS laminates appeared on the compression or compression-tension side of flexural specimens, depending on their fibre treatment.

The most interesting behaviour was identified with chromium yarn finish GF-PPS laminates. They demonstrated no sign of compression micro-buckling upon flexural testing, but rather tensile fracture only. The test series is depicted in Fig. 9. Shi and co-workers [66] made the very same observation of flexural tested GF-PEI laminates made of chromium finished yarns, which exhibited tensile fracture exclusively.

The progression of ILSS values of GF-PPS laminates was in good agreement with the corresponding flexural strength performance. The highest ILSS value of GF-PPS laminates was reached with chromium yarn finish at 50 MPa. However, the overall highest ILSS value was obtained from the commercial GF-epoxy reference at 56 MPa. In contrast to GF-PA6 laminates, the GF-PPS laminates experienced shear failure as shown in Fig. 10, which most possibly resulted from the less ductile and stiffer PPS matrix. Therefore, the obtained ILSS values of GF-PPS laminates represent the apparent interlaminar shear strength as opposed to GF-PA6 laminates, which did not exhibit shear-induced failure.

### 3.3. Compression, and compression after impact tests on GF-PA6 and GF-PPS laminates

Compression, and compression after impact tests were carried out on the commercial GF-PA6 and GF-epoxy reference materials, together with the best-of-best and worst-of-worst in-house manufactured GF-PA6 and GF-PPS laminates from flexural testing. Upon the 50 J impact, the laminates demonstrated substantial differences in inflicted damage, which is depicted in Fig. 11. All laminates tested, were punctured by the impactor, except for the GF-PA6 laminate made from aminosilane yarn finish. It dissipated the energy most effectively by plastic deformation without cracking open. From visual inspection, the second-best performing series in impact tests was the commercial GF-PA6 reference (the same damage behaviour was reported by Dogan and Arman [68]). The commercial GF-epoxy reference and laminates made from desized yarn performed the worst upon impact loading, with the impactor penetrating the laminates fully and becoming wedged. With regard to the desized yarn laminates, their poor impact behaviour was quite contrary to what is reported by some literature sources. Mallick [39] reports that ballistic protection increases with a decrease in fibre-matrix bond strength. Therefore, ballistic composite armour includes glass fibres which are incompatible with the matrix [39]. It was found in our research that laminates with compatible fibre coatings perform better in the impact tests compared to laminates made of an incompatible fibre-matrix combination (desized yarn). In the case of GF-PPS laminates, the chromium yarn finish showed slightly better impact resistance than the desized yarn. Overall, however, the GF-PA6 laminates exhibited better impact resistance compared to GF-PPS laminates.

Table 4 displays the measured compression and compression after

impact strengths. Based on the results, it could be seen that GF-PA6 laminates boast very good strength retention after an impact event. CAI strength decreased only slightly from the compression strength of undamaged laminates. GF-PPS laminates with chromium yarn finish exhibited the largest strength fall-off from a mean compression strength of 92.3 MPa to a mean CAI strength of 66.9 MPa.

## 4. Conclusions

Continuous glass fibre-reinforced PA6 and PPS composite laminates were prepared by film stacking and static press-impregnation. Various fabric- and coating types were analysed to find material combinations which potentially exhibit high-strength performance. Aminosilane yarn finish (A-1100) stood out as a highly potent adhesion promoter for both PA6 and PPS matrices, showing consistently high-performance throughout flexural, ILSS and impact tests. In contrast, laminates made from desized fabrics (no coating) demonstrated significantly inferior mechanical properties. This observation verified that fibre coatings are mandatory for the best possible composite performance. Furthermore, SEM analysis verified that fibre-matrix adhesion clearly occurs in the presence of fibre coatings, whereas desized yarns showed no adherent matrix at the fibre surface after laminate fracture. GF-PPS laminates are applicable as a strong and stiff material. At room temperature conditions, GF-PPS laminates even outperformed a commercial GF-epoxy reference laminate in terms of strength at comparable fibre volume fractions. For a balance between strength, stiffness and greater impact resistance, GF-PA6 laminates are highly applicable.

Chromium yarn finish (Volan A) has a wide variety of possible interaction mechanisms and is known for excellent bonding with several thermosetting resins. However, its high compatibility towards PA6 and PPS matrices has not yet been discussed in the open literature. GF-PPS laminates with chromium yarn finish exhibited a mean flexural strength of 770 MPa and 28 GPa modulus alongside an ILSS of 50 MPa at 56% fibre volume fraction.

Overall, it was found that the strength characteristics of neat PA6 and PPS matrices can be tailored most efficiently by the fibre coating type. Chemical alteration of the polymer backbone (grafting of functional side groups or similar treatment) or matrix modification by intermixable coupling agents is not required for these polymers in combination with continuous glass fibre reinforcement. The fact that virtually any of the coated fabrics used in combination with PA6 and PPS led to high strength composites, strongly favoured wetting and interpenetrating network formation as possible explanations for the adhesion mechanisms involved. A follow-up study shall investigate as to what extent chemical bonding could be involved in GF-PA6 and GF-PPS composites, or if the adhesion observed is purely physical in nature.

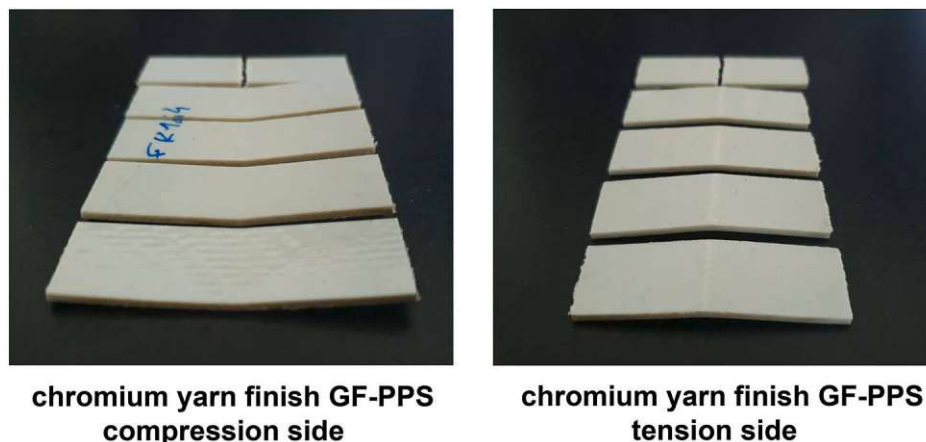


Fig. 9. Flexural tested GF-PPS specimens with chromium yarn finish, exhibiting tensile fracture only and no sign of compression micro-buckling.

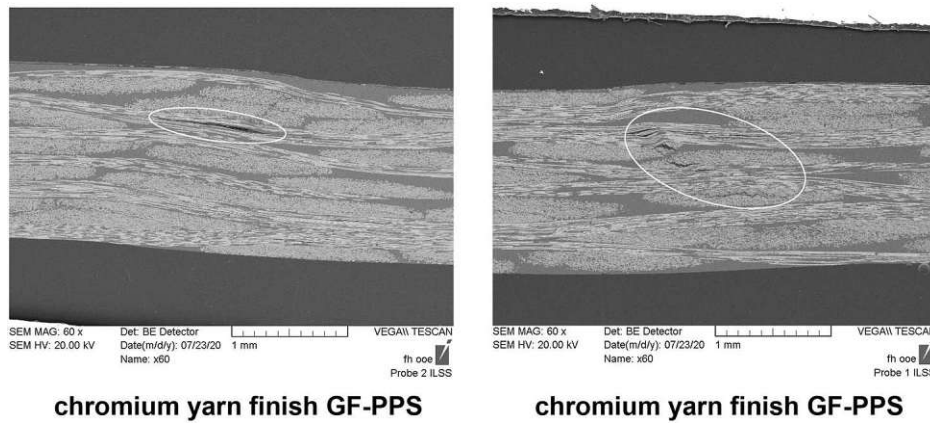


Fig. 10. ILSS tested GF-PPS specimens with chromium yarn finish, exhibiting shear induced delamination (indicated by white circles) in addition to plastic deformation.

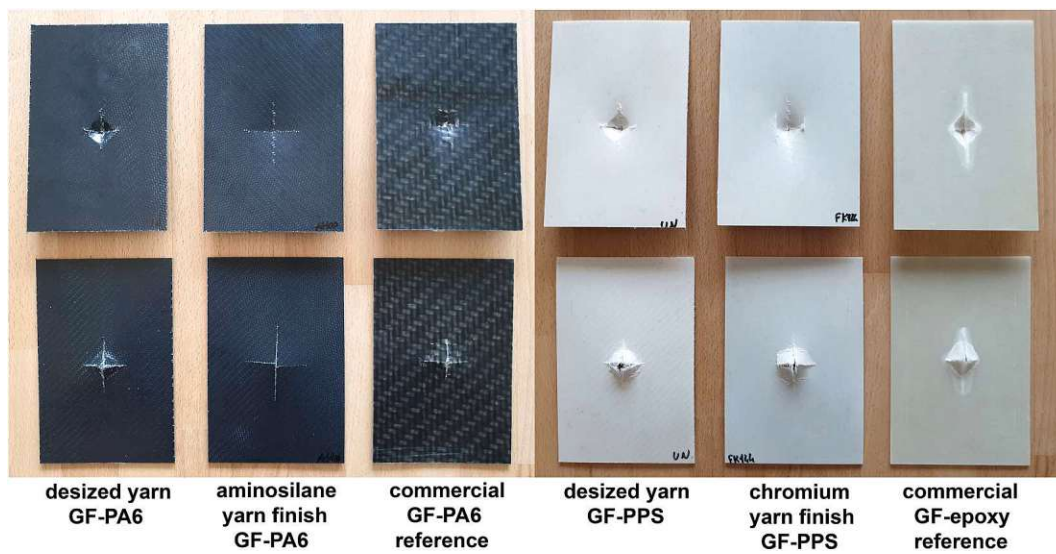


Fig. 11. Laminate damage after 50 J impact; GF-PA6 laminates with 2.0 mm thickness, GF-PPS and commercial GF-epoxy reference laminates with 1.6 mm thickness. top: front striking face, bottom: rear striking face.

Table 4

Compression strength and compression after impact (CAI) strength properties. The standard deviation is given by the values between brackets.

Material	Compression strength [MPa] undamaged laminate <sup>a</sup>	Compression after 50 J impact strength [MPa] <sup>a</sup>
desized yarn GF-PA6	36.1 (2.8)	35.4 (1.1)
aminosilane yarn finish GF-PA6	67.9 (2.4)	65.4 (4.5)
commercial GF-PA6 reference	74.1 (1.5)	68.2 (1.9)
desized yarn GF-PPS	44.9 (1.1)	37.5 (1.2)
chromium yarn finish GF-PPS	92.3 (4.2)	66.9 (6.1)
commercial GF-epoxy reference	65.4 (2.9)	63.8 (1.0)

<sup>a</sup> Compression, and CAI specimens: 100 · 150 mm, conditioned at 23 °C 50% RH for 14 days.

Declaration of competing interest

The authors declare that they have no known competing financial interests or personal relationships that could have appeared to influence the work reported in this paper.

Acknowledgements

We would like to offer our special thanks to GIVIDI Fabrics S.r.l, LITE GmbH, BASF SE and Johns Manville Slovakia a.s. for providing their materials for research purposes. Permission for publishing the mechanical property data is also gratefully acknowledged.

The authors are grateful to the State Government of Upper Austria and the European Regional Development Fund for providing financial support for this research in the programme EFRE-IWB 2020 for the project: “ProFVK”.



References

[1] Kiss P, Stadlbauer W, Burgstaller C, Stadler H, Fehringer S, Haeuserer F, et al. In-house recycling of carbon- and glass fibre-reinforced thermoplastic composite laminate waste into high-performance sheet materials. *Composites Part A Appl Sci Manuf* 2020;139:106110. <https://doi.org/10.1016/j.compositesa.2020.106110>.  
 [2] Vaidya UK, Chawla KK. Processing of fibre reinforced thermoplastic composites. *Int Mater Rev* 2008;53:185–218. <https://doi.org/10.1179/174328008X325223>.



- [56] Reed RP, Madhukar M, Thaicharoenporn B, Martovetsky NN. Low-temperature mechanical properties of glass/epoxy laminates. *AIP Conf. Proc.* 2014;1574:60:109–16. <https://doi.org/10.1063/1.4860612>.
- [57] Wang S, Zhou Z, Zhang J, Fang G, Wang Y. Effect of temperature on bending behavior of woven fabric-reinforced PPS-based composites. *J Mater Sci* 2017;52:13966–76. <https://doi.org/10.1007/s10853-017-1480-0>.
- [58] Zhao L, Yu Y, Huang H, Yin X, Peng J, Sun J, et al. High-performance polyphenylene sulfide composites with ultra-high content of glass fiber fabrics. *Compos B Eng* 2019;174:106790. <https://doi.org/10.1016/j.compositesb.2019.05.001>.
- [59] Liu Z, Wu YQ, Wang XJ, Long SR, Yang J. Effects of the coupling agent on the mechanical properties of long glass fiber reinforced polyphenylene sulfide composites. *Mater Sci Forum* 2015;815:509–14. <https://doi.org/10.4028/www.scientific.net/MSF.815.509>.
- [60] Durmaz BU, Aytac A. Characterization of carbon fiber-reinforced poly(phenylene sulfide) composites prepared with various compatibilizers. *J Compos Mater* 2020;54:89–100. <https://doi.org/10.1177/0021998319859063>.
- [61] Fan Z-Z, He H-W, Yan X, Zhao R-H, Long Y-Z, Ning X. Fabrication of ultrafine PPS fibers with high strength and tenacity via melt electrospinning. *Polymers* 2019;11:530. <https://doi.org/10.3390/polym11030530>.
- [62] Zuo P, Tcharkhtchi A, Shirinbayan M, Fitoussi J, Bakir F. Overall investigation of poly (phenylene sulfide) from synthesis and process to applications—a review. *Macromol Mater Eng* 2019;304:1800686. <https://doi.org/10.1002/mame.201800686>.
- [63] Batista NL, de Faria MCM, Iha K, de Oliveira PC, Botelho EC. Influence of water immersion and ultraviolet weathering on mechanical and viscoelastic properties of polyphenylene sulfide–carbon fiber composites. *J Thermoplast Compos Mater* 2015;28:340–56. <https://doi.org/10.1177/0892705713484747>.
- [64] Wang Y, Zhang J, Zhang J, Zhou Z. Temperature effects on mechanical properties of woven thermoplastic composites for secondary aircraft structure applications. *MATEC Web Conf* 2017;108. <https://doi.org/10.1051/mateconf/201710801009.01009>.
- [65] Toray Advanced Composites. Toray Cetex® TC1100 PPS product data sheet. <https://www.toraytac.com/product-explorer/products/u017/Toray-Cetex-TC1100;2019>.
- [66] Shi H, Villegas IF, Bersee HEN. Strength and failure modes in resistance welded thermoplastic composite joints: effect of fibre–matrix adhesion and fibre orientation. *Compos Part A Appl Sci Manuf* 2013;55:1–10. <https://doi.org/10.1016/j.compositesa.2013.08.008>.
- [67] Rössler M. *Repairs of aircraft composite structures*. Norderstedt: BoD Books on Demand; 2015.
- [68] Dogan A, Arman Y. Effects of temperature and impactor nose diameter on the impact behavior of PA6 and PP thermoplastic composites. *J Elastomers Plastics* 2019;51:64–74. <https://doi.org/10.1177/0095244318780509>.



# The effect of thermally desized carbon fibre reinforcement on the flexural and impact properties of PA6, PPS and PEEK composite laminates: A comparative study

Peter Kiss<sup>a,d,\*</sup>, Jonathan Glinz<sup>b</sup>, Wolfgang Stadlbauer<sup>a</sup>, Christoph Burgstaller<sup>c</sup>, Vasiliki-Maria Archodoulaki<sup>d</sup>

<sup>a</sup> University of Applied Sciences Upper Austria, School of Engineering, Stelzhamerstrasse 23, 4600, Wels, Austria

<sup>b</sup> University of Applied Sciences Upper Austria, Research Group Computed Tomography, Stelzhamerstrasse 23, 4600, Wels, Austria

<sup>c</sup> Transfercenter fuer Kunststofftechnik GmbH, Franz-Fritsch-Strasse 11, 4600, Wels, Austria

<sup>d</sup> TU Wien, Institute of Materials Science and Technology, Getreidemarkt 9, 1060, Vienna, Austria

## ARTICLE INFO

### Keywords:

Carbon fibres  
Thermoplastic resin  
Adhesion  
Mechanical testing

## ABSTRACT

Commercial carbon fibre (CF) fabrics are frequently equipped with an epoxy-based (EP) sizing, which is required for fibre protection during weaving but unsuitable for subsequent thermoplastic processing due to incompatibility. The present study investigates a heat treatment method of CF fabrics in order to remove the incompatible sizing and promote interfacial adhesion with thermoplastic matrices through the oxidised carbon surface. The removal of the EP-sizing from CF fabrics (desizing) was conducted by infrared-irradiation (IR) in air atmosphere at 400 °C. IR-desized CF fabrics were confirmed to be free from sizing residues by SEM imaging and thermogravimetric analysis. Subsequently, CF-PA6, CF-PPS and CF-PEEK thermoplastic composite laminates (TPCL) were manufactured by means of film stacking and hot compression moulding with fibre volume fractions ranging from 45–47%. For comparative purposes, the in-house moulded TPCL were benchmarked against state-of-the-art industrial TPCL in 3-point flexural, short-beam flexural and Charpy impact tests. Overall, very similar performance was attained between IR-desized TPCL and their industrial counterparts. Excellent wet-out and interfacial adhesion of IR-desized CF was observed from SEM imaging of fractured laminates. Conversely, TPCL prepared from EP-sized CF fabrics were found to be neither sufficiently consolidated nor thoroughly wetted out by the thermoplastic matrix, confirming poor interfacial compatibility. The correspondingly poor mechanical performance of EP-sized TPCL emphasised the importance of EP-sizing removal.

## 1. Introduction

Carbon fibre (CF) composites, where applicable, boast extraordinary stiffness and strength properties at low bulk density. Recent efforts in industrial composite material development have focused on substituting thermoset matrices with thermoplastics in continuous fibre-reinforced products. In this newly emerging field, fully impregnated thermoplastic composite laminates (TPCL) of the Cetex® [1], Tenax® [2] and Tepex® [3] brands have become well established and are considered state-of-the-art materials. Yet little is known about such industrial-grade materials concerning fibre-matrix related topics in literature. In general, it can be assumed that the fibre interfaces in these high-performance industrial laminates are prepared such that excellent fibre-matrix

adhesion is promoted.

TPCL made of continuous fibre reinforcements open up new possibilities in high-volume manufacturing processes such as thermoforming and overmoulding [1,4–6]. Furthermore, thermoplastic matrices mitigate many utility problems associated with thermoset resins, such as susceptibility to delamination from impacts [7–9], limited storage lives of prepregs and the complexity of recycling [10]. It cannot be denied that thermoplastic matrices also involve several drawbacks, which limit their scope of application. Most notably, TPCL should not be operated above their glass transition temperature ( $T_g$ ) in demanding thermal applications [4,11]. Should this be the case, the structural integrity may be compromised by matrix softening, which could lead to permanent deformation or buckling under high loads [11]. If service temperatures

\* Corresponding author. University of Applied Sciences Upper Austria, School of Engineering, Stelzhamerstrasse 23, 4600, Wels, Austria.

E-mail address: [peter.kiss@fh-wels.at](mailto:peter.kiss@fh-wels.at) (P. Kiss).

<https://doi.org/10.1016/j.compositesb.2021.108844>

Received 5 January 2021; Received in revised form 19 March 2021; Accepted 23 March 2021

Available online 28 March 2021

1359-8368/© 2021 The Authors. Published by Elsevier Ltd. This is an open access article under the CC BY license (<http://creativecommons.org/licenses/by/4.0/>).

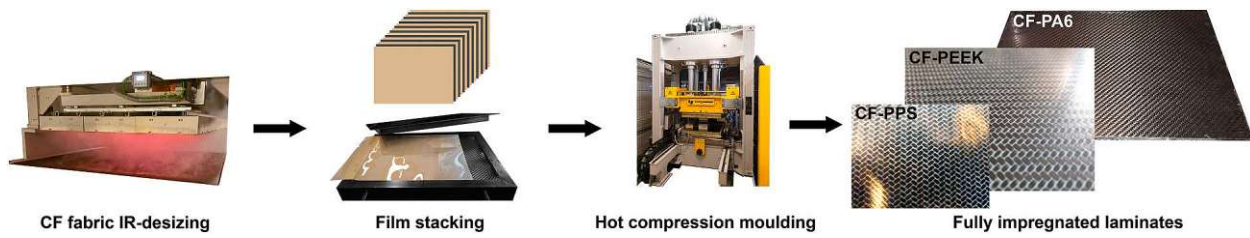


Fig. 1. Processing scheme for TPCL production by film stacking technique.

**Table 1**  
Physical properties of constituent composite materials. The standard deviation is given by the values within brackets.

	IR-desized CF [51]	PA6 cond./dry [58]	PPS [59]	PEEK [60]
Melting temperature [°C]	–	220	280	343
Tensile modulus E [GPa]	240	1.0/3.0	3.8	4.1
Tensile strength [MPa]	4100	40/80	90	105
Elongation at break [%]	1.7	>50/20	3	30
Density ρ [g/cm <sup>3</sup> ]	1.77	1.14	1.35	1.30
Measured density ρ [g/cm <sup>3</sup> ]	1.773 (0.000)	1.117 (0.005)	1.346 (0.007)	1.302 (0.005)

exceed 100 °C, Polyaryletherketones (PAEK) such as Polyetheretherketone (PEEK) are frequently considered for load bearing and chemically resistant composite components [12]. Below 100 °C, Polyphenylene Sulfide (PPS) and Polyamide 6 (PA6) matrices are of particular interest due to their greater cost efficiency [8,13].

Challenges commonly arise when fibres and matrices are brought together. In order to assure adequate fibre-matrix adhesion, the fibre reinforcement must be rendered compatible with the matrix. Throughout numerous studies, the graphitic planes of the bare unoxidised CF surface have been identified as highly inert for proper matrix bonding [14–17]. Therefore, considerable effort has been directed

towards CF surface functionalisation by methods such as plasma treatment, thermal treatment, ozone treatment, oxidation using nitric acid, electrochemical oxidation, or combinations thereof [15–21]. In industrial practice, CF tow is electrochemically oxidised (activated) and subsequently passed through a sizing bath [21], whereby a “sizing” constitutes a thin coating applied by the fibre manufacturer [8,22,23].

CF tow is traditionally coated with modified epoxy-based sizings (EP-sizing) for thermoset applications [24–26]. Importantly, the EP-sizing conveys lubricity and integrity to the CF tow, which protects the material from fibre breakage and fuzzing during subsequent handling, tow-spreading or high-speed weaving operations [25]. However, there is much disagreement over the role of sizings concerning fibre-matrix adhesion in CF composites among researchers. Many scholars find CF sizings important for adhesion [19,27–29], whereas others report improved adhesion of unsized or desized CF over sized CF [30–32]. According to Juska and Puckett, who gathered information directly from a CF manufacturer, CF sizings are mainly applied for fibre protection, not to improve fibre-matrix adhesion [33]. As previously mentioned, a widely held belief is that adhesion is mainly promoted by the electrochemically functionalised and roughened CF surface [33]. By comparison, the application of sizings on glass fibre (GF) reinforcement is considered to be a prerequisite for adequate fibre-matrix adhesion [8,13,22,23]. It should be noted that GF require organosilane based sizings for bonding due to their inherently different surface composition and morphology compared to CF [8,22,34–36].

Since EP-sized tow is the most commonly available form of CF reinforcement, there is a strong necessity for desizing (removal of sizing)

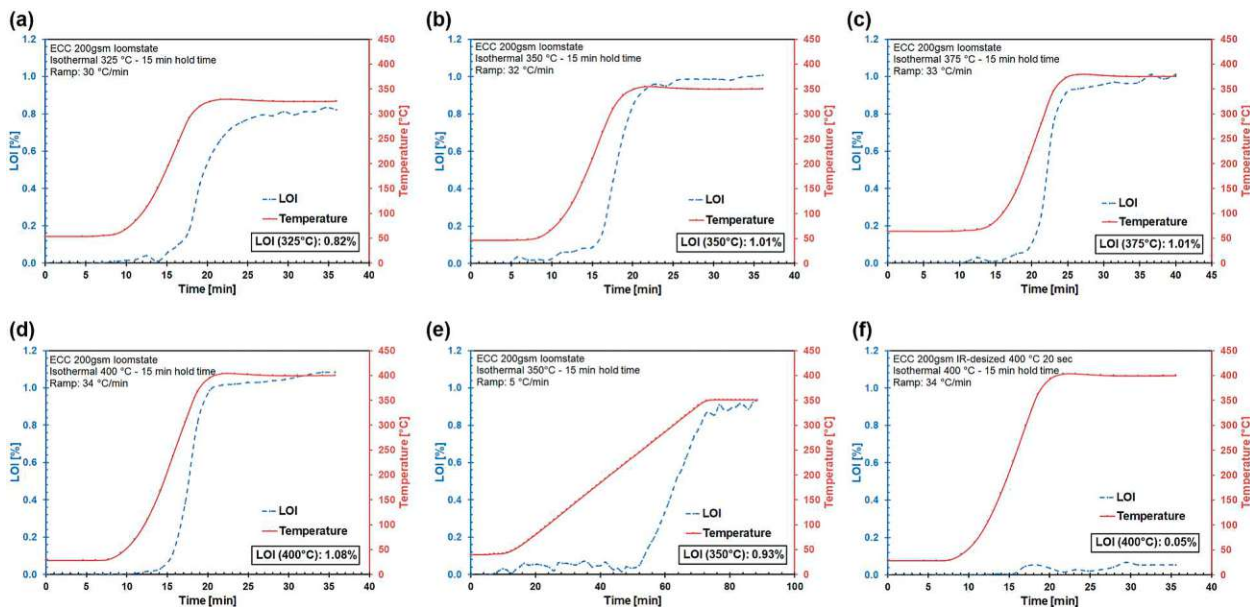
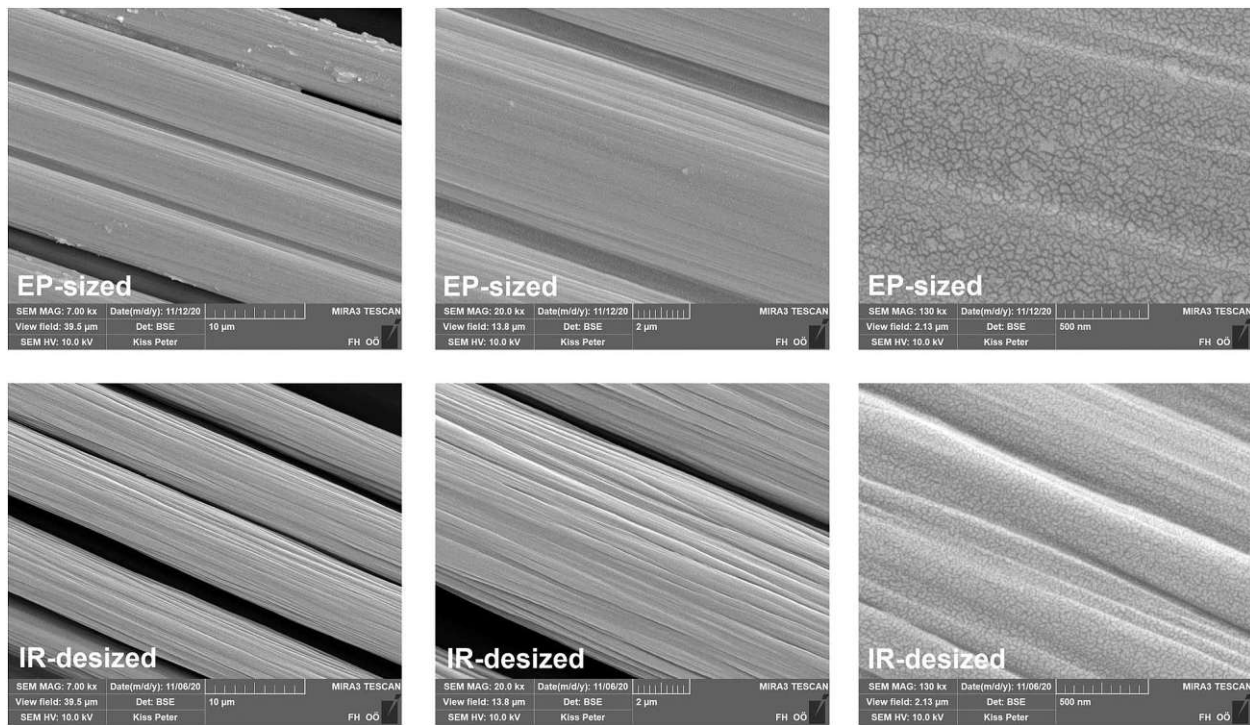


Fig. 2. Desizing parameters determined by measurement of the loss on ignition (LOI) (dashed blue lines) from macro thermogravimetric analyses. The solid red lines represent the temperature program. (a)–(d) LOI of loomstate CF fabric samples with EP-sizing at different temperatures (325–400 °C), (e) slow ramp rate of 5 °C/min, and (f) residual sizing level of IR-desized CF fabric. (For interpretation of the references to colour in this figure legend, the reader is referred to the Web version of this article.)





**Fig. 3.** SEM images of PAN-based CF, EP-sized (top) and IR-desized (bottom) at different magnifications. The IR-desized CF (bottom) have longitudinal ridges on the surface extending parallel to the fibre axes, whereas these ridges are almost fully covered by sizing in the case of EP-sized CF (top).

prior to thermoplastic processing. EP-sizings are strongly limited by their thermo-oxidative stability [15,25], with a decomposition onset in a region of 250 °C [4]. Furthermore, EP-sizings are known to cause adverse effects on interfacial adhesion with thermoplastics which generally renders them unsuitable for thermoplastic processing [4,25]. If the EP-sizing is not removed from the CF reinforcement, decomposition gases would obstruct thermoplastic melt impregnation and result in inconsistent laminate quality with high porosity. As such, an EP-sizing may simply be considered a handling agent, e.g. for weaving in the TPCL processing chain.

According to scientific and patent literature, EP-sizings may be removed by numerous approaches. Most commonly, researchers desize CF by immersion in acetone over a prolonged period of time or by Soxhlet extraction [29,37–40]. However, it has also been reported that solvent extraction may not remove the EP-sizing completely [17,37]. Nevertheless, there are scalability issues with organic solvent desizing due to potentially explosive and harmful atmospheres, and questionable cost-effectiveness. Other investigated procedures involve heat treatment in air atmosphere via muffle furnaces or convection ovens [41], infrared-irradiation [4], or sizing pyrolysis in nitrogen atmosphere at up to 600 °C [19,20,42]. In patent literature, CF desizing via heat treatment in air or nitrogen is generally favoured over other methods [25,43–45]. It should be noted that CF reinforcements would not have to be desized if thermoplastic-compatible sizings were utilised. However, commercially available CF reinforcements with thermoplastic sizings are rare at the moment, or non-existent in the 3K tow range.

Lately, Polyetherimide (PEI) and Polyimide (PI) oligomers have attracted attention as film formers in tailored high-temperature thermoplastic-compatible sizings [40,46–50]. PEI-sized CF are currently offered by Teijin Ltd. as 12K or 24K tows primarily for the purpose of thermoplastic unidirectional (UD)-tape production [48,51–53]. Undoubtedly, the PEI-sizing provides the necessary protection of the tows, without the need for subsequent sizing removal. As of yet it is still somewhat unclear whether PEI-sizings significantly improve adhesion with thermoplastics as claimed by the fibre manufacturer (potential improvement of transverse flexural properties). Several studies found

only minor improvement, or no improvement at all of PEI-sized CF over desized CF. Dilsiz and Wrightman found that neither the work of adhesion, nor the interfacial shear strength (IFSS) were improved by PEI-sized CF compared to unsized CF [31]. Chen et al., together with Liu et al. observed minor improvements in IFSS, interlaminar shear strength (ILSS) and flexural strength of PEEK reinforced with PEI-sized CF over desized CF [39,41,54]. Similar findings on CF-PEEK composites were reported by Yuan et al., where ILSS could be improved by PI-sizing. However, flexural strength remained mostly constant [50]. Unfortunately, none of these studies reported the fibre volume fractions of the TPCL.

As discussed, there are many possibilities for CF surface preparation, and it is unknown precisely which treatment methods are favoured by TPCL manufacturers. Nevertheless, there is some evidence suggesting that thermoplastic sizings are not utilised in industrial woven TPCL. First, industrial woven TPCL are based almost exclusively on 3K tow reinforcement [53,55], while at present 3K tows are not supplied with thermoplastic sizings by CF manufacturers [48,51,52]. Furthermore, the technical datasheets of industrial TPCL designate the type of CF used in some cases, e.g. “Tenax®-E HTA40 E13 3K 200 tex” [56]. In this example, “E13” is an EP-sizing, which is most possibly removed from the fabric for the previously mentioned reasons of poor thermal stability and incompatibility. Continuous desizing of fabrics could be carried out by harnessing the potential of IR-irradiation as presented by Mitschang, Blinzler and Wöginger [4]. Certainly, it cannot be precluded that desized CF fabrics undergo post-treatment (resizing/finishing) for industrial TPCL applications. However, the added expense of CF fabric post-treatment would not be justifiable if the laminate properties were not improved significantly.

To this aim, it seems necessary to investigate a comparison between in-house produced TPCL with known composition and industrial TPCL based on PA6, PPS and PEEK matrices, and to investigate the desizing effects of CF on the mechanical properties of TPCL more in detail. TPCL are compared in 3-point flexural tests, short-beam flexural tests and Charpy impact tests to assess the potential of IR-desized CF reinforcement.

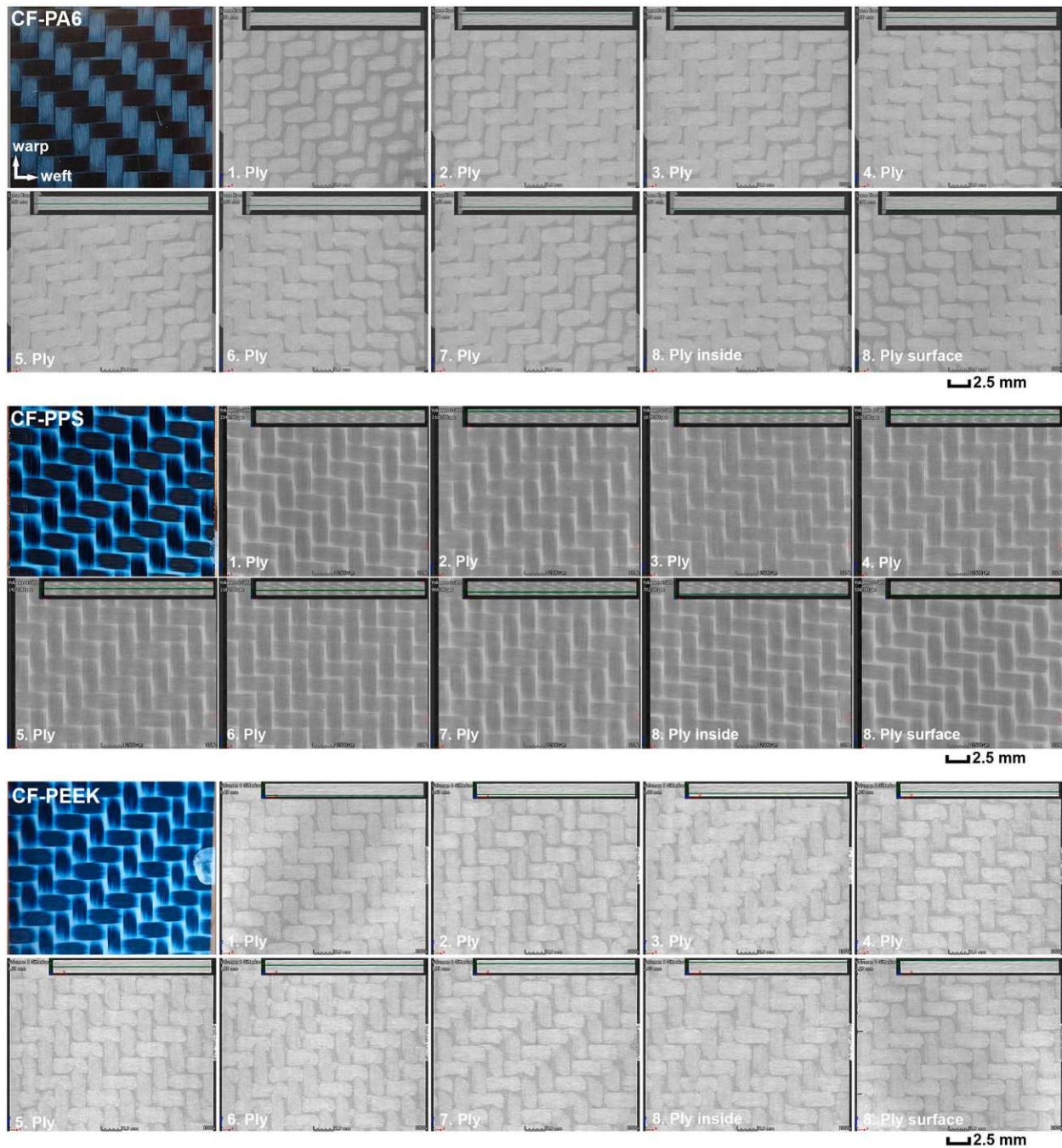


**Fig. 4.** XCT scans of 8-ply IR-sized CF-PA6 (top), CF-PPS (centre) and CF-PEEK (bottom). The TPCL exhibited fully impregnated and void-free layers (voids would appear black due to a large density difference). The plane at which each image was taken is highlighted by a horizontal green line. (For interpretation of the references to colour in this figure legend, the reader is referred to the Web version of this article.)

**Table 2**  
Properties of CF-PA6, CF-PPS and CF-PEEK laminates (IR-sized vs. industrial references). The standard deviation is given by the values within brackets.

Property	IR-sized CF-PA6 cond./dry	Industrial CF-PA6 reference cond./dry	IR-sized CF-PPS	Industrial CF-PPS reference	IR-sized CF-PEEK	Industrial CF-PEEK reference
Flexural strength $\sigma_{fmax}$ [MPa]	599.0 (25.6)/716.3 (12.4)	590.4 (33.8)/705.5 (20.4)	831.5 (24.3)	931.4 (84.3)	845.3 (33.9)	1025.3 (33.7)
Flexural modulus E [GPa]	46.8 (1.3)/48.7 (0.5)	46.2 (0.5)/48.1 (0.7)	52.4 (0.6)	62.7 (0.6)	50.5 (1.2)	61.7 (0.8)
Charpy impact strength (fn) [kJ/m <sup>2</sup> ]	45.0 (2.8)/46.7 (3.4)	45.5 (3.2)/46.4 (2.7)	49.7 (2.0)	63.9 (2.4)	48.6 (2.7)	65.8 (1.9)
Short-beam strength [MPa]	44.4 (2.1)/56.5 (1.5)	45.7 (0.9)/56.3 (2.0)	60.2 (1.6)	72.6 (2.6)	81.1 (2.0)	89.9 (2.9)
Composite density $\rho_c$ [g/cm <sup>3</sup> ]	1.42 (0.01)	1.42 (0.01)	1.54 (0.01)	1.57 (0.00)	1.51 (0.01)	1.55 (0.00)
Fibre volume fraction $\nu_f$ [%]	46.5 (0.7)	45.7 (1.1)	46.8 (0.8)	52.7 (0.6)	45.3 (0.9)	52.1 (0.5)

Die approbierte gedruckte Originalversion dieser Dissertation ist an der TU Wien Bibliothek verfügbar. The approved original version of this doctoral thesis is available in print at TU Wien Bibliothek.

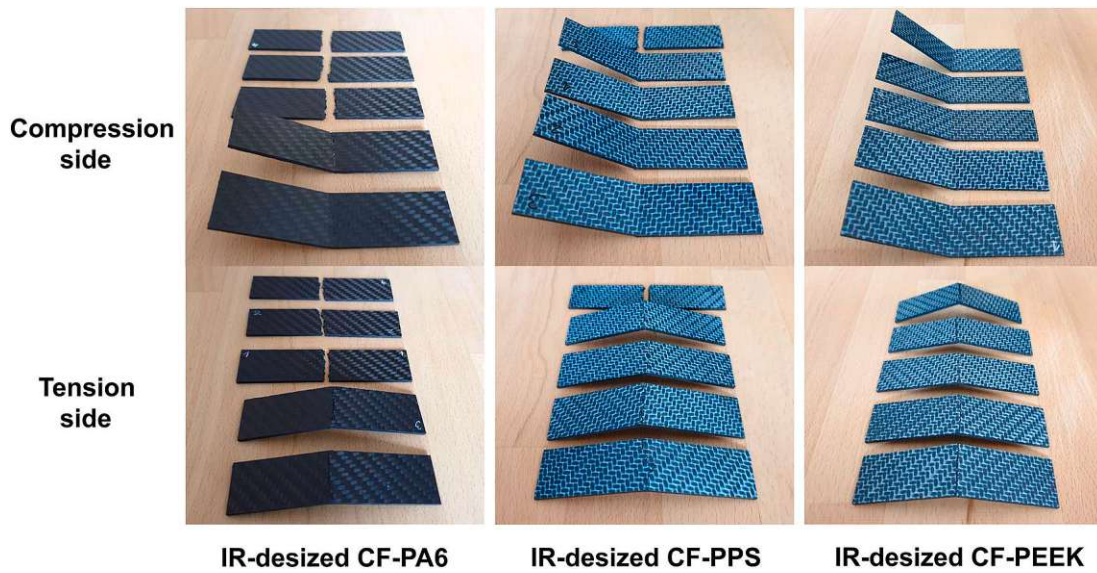


Fig. 5. 3-point flexural tested specimens ( $100 \cdot 25 \cdot 2 \text{ mm}^3$ , support span 80 mm) exhibiting tensile fracture.

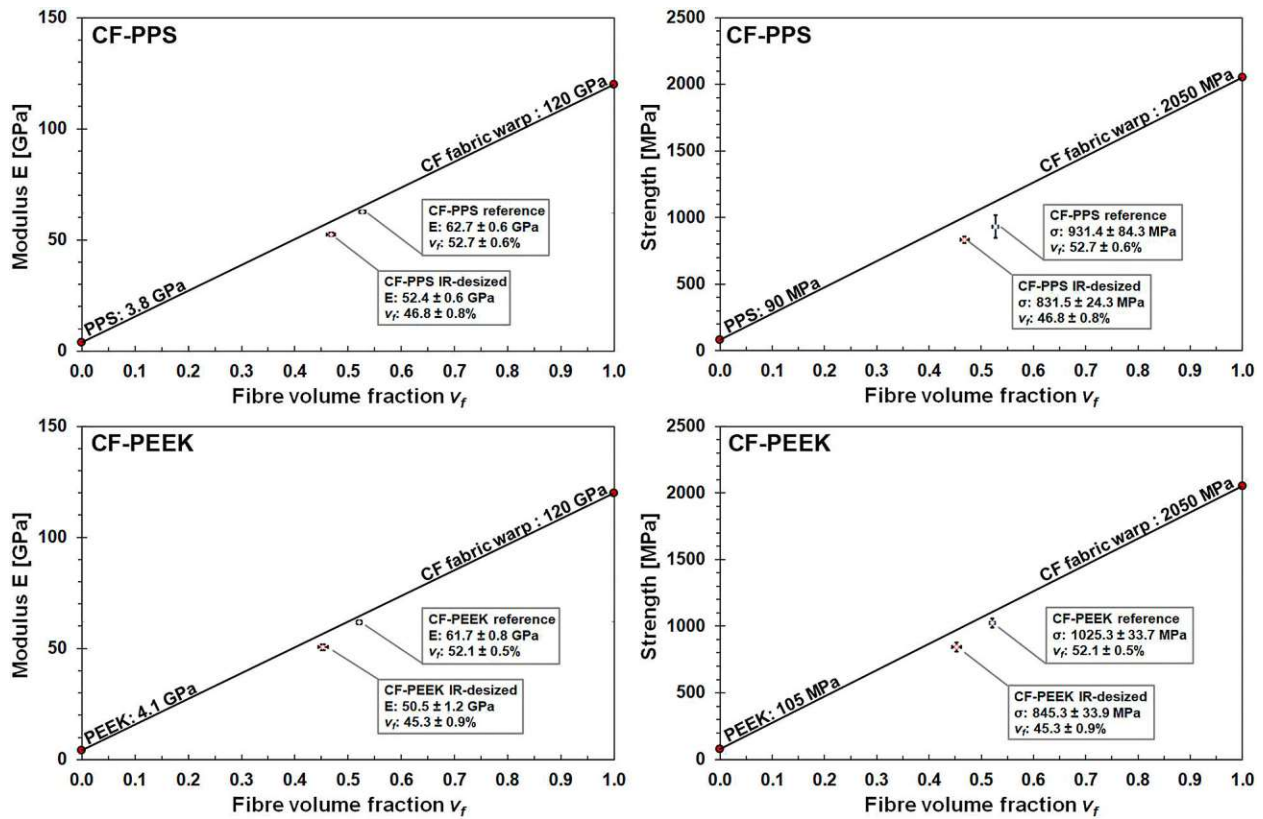


Fig. 6. Rule of mixtures (ROM) of flexural tested CF-PPS and CF-PEEK samples. Moduli (left) and strengths (right) are plotted against the fibre volume fraction. The samples are closely correlated to the theoretical ROM progression, which indicates that the flexural testing outcome of IR-desized samples and the industrial CF references is mainly affected by a difference in fibre volume fraction.

## 2. Materials and methods

### 2.1. Materials

The CF fabric considered for thermoplastic reinforcement was provided by ECC - Engineered Cramer Composites (Germany). Polyacrylonitrile (PAN) derived high tenacity (HT) CF tow based on Teijin Tenax®-E HTA40 E13 (EP-sizing) 3K, 200 tex was woven into a 2/2 twill

fabric (style 452) with  $200 \text{ g/m}^2$  areal weight. The loomstate (as received) fabric was subjected to a thermal desizing process, denoted hereinafter as IR-desized CF. It should be mentioned that testing outcomes are focused on the desized variant of the CF fabric, since the loomstate (EP-sized) fabric was found to be non-processible by thermoplastic film-impregnation (as will be discussed in section 3.4).

PA6 based on Durethan® B30S (supplied by LANXESS Deutschland GmbH, Germany) was extruded in-house to  $120 \mu\text{m}$  films by means of a

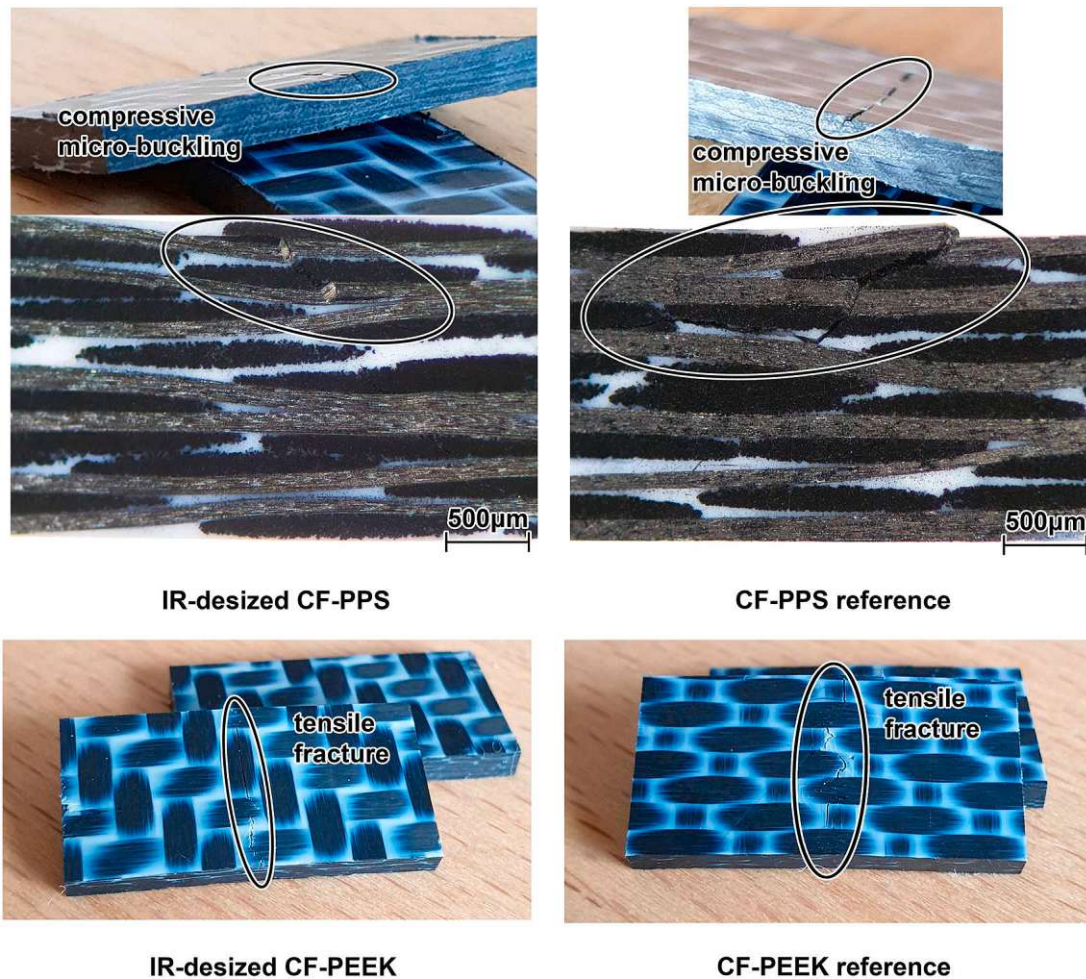


**Fig. 7.** Tested short-beam flexural CF-PPS and CF-PEEK samples showcasing respective failure modes. CF-PPS (top) failed due to compressive micro-buckling, whereas CF-PEEK (bottom) failed due to tensile fracture. None of the specimens exhibited mid-plane shear delamination.

flat-film extrusion line at a barrel and die temperature of 260 °C.

PPS films LITE P were supplied in 120 µm thickness by LITE GmbH (Austria), based on the linear PPS grade Celanese Fortron® 0214.

PEEK films LITE K were supplied in 120 µm thickness by LITE GmbH (Austria), based on Victrex® PEEK 151G.

Industrial reference laminates based on CF-PA6 Tepex® 202 (fibre volume fraction  $\nu_f$ : 46%), CF-PPS Cetex® TC1100 ( $\nu_f$ : 53%) and CF-PEEK Tenax®-E TPCL PEEK-HTA40 ( $\nu_f$ : 52%) were used for a comparison of the mechanical properties. The industrial CF-PA6 reference consisted of 8 plies of 2/2 twill woven HT-CF fabrics (3K) with 200 g/m<sup>2</sup> areal weight and laminate thickness of 2.0 mm. The industrial CF-PPS and CF-PEEK references consisted of 6 plies of 5-harness satin (5HS) woven HT-CF fabrics (3K) with 280 g/m<sup>2</sup> areal weight and laminate thicknesses of 1.8–1.85 mm. All laminates exhibited a consistent ply layup, i.e. warp tows arranged in the same direction across the laminate thickness. The industrial CF-PA6 reference was manufactured by semi-continuous compression moulding (intermittent press), the CF-PPS and CF-PEEK references were manufactured by static compression moulding (static platen press). The exact pressing parameters are unknown to the authors.

## 2.2. Methods

### 2.2.1. Thermal desizing process

Basic desizing parameters were deduced from the loss on ignition (LOI, % wt. loss) of loomstate CF fabrics by MTGA (macro thermogravimetric analysis) on a LECO TGA801 analyser (Leco Instrumente

GmbH, Germany). MTGA analyses were conducted on loomstate CF fabric samples (sample weight of 1–1.5g) ranging from 325–400 °C in 25 °C increments to assess the decomposition behaviour of the EP-sizing without damaging the CF reinforcement. This methodology differed from the CF size content determination according to EN ISO 10548, where sizing is pyrolysed in nitrogen atmosphere [57]. However, the knowledge of decomposition behaviour in air atmosphere was required for subsequent IR-desizing trials. Based on the MTGA results, desizing experiments were upscaled via a double-sided IR-heating system by Krelus (Krelus AG, Switzerland), controlled by IR-pyrometers MI3 (Raytek GmbH, Switzerland). For validation, the remaining sizing level and microstructure of IR-desized CF fabric was determined via LOI measurement and inspected via SEM imaging, respectively.

### 2.2.2. Film stacking and compression moulding

IR-desized CF fabrics and thermoplastic films were cut to size and stacked into a flat panel impregnation tool, which was priorly treated with Zyvac® Composite Shield (supplied by POLYchem Handelsges.m.b.H., Austria) high-temperature release agent. 8 plies of CF fabric with consistent warp tow orientation were stacked with 9 layers of film alternately corresponding to a [(0,90)<sub>4</sub>]<sub>s</sub> ply sequence, whereby (0,90) is used for representation of one fabric layer. Thin-film thermocouples of type-K, 402–716 (TC Mess-und Regeltechnik GmbH, Germany) were positioned at the centre ply of the film stacks to monitor the temperature during compression moulding. The subsequent hot compression moulding cycle was conducted on a LZT-OK-220-L hydraulic press (Langzauner GmbH, Austria) with heated platens capable of operating at



**Fig. 8.** SEM micrographs of EP-sized CF-PA6 laminate (top) and IR-desized CF-PA6 laminate (bottom). The EP-sizing inhibited wet-out of the fibre bundles resulting in a flexural modulus of 8 GPa and flexural strength of 82 MPa of the laminate. Note, both laminates were moulded with the same parameters.

up to 500 °C. For each respective polymer type, the heated platens were operated 50 °C above the melting temperature of the polymer for faster heat transfer (melting temperature PA6: 220 °C [58]; PPS: 280 °C [59]; PEEK: 343 °C [60]). The impregnation tool was inserted into the pre-heated press and closed at a low contact pressure of 0.2–0.3 MPa. Once the stack temperature had reached 20 °C above the melting temperature of the polymer, static impregnation pressure was raised to 1.5 MPa. An impregnation time (dwell time) of 10 min was selected before commencing cooldown under 1.5 MPa static pressure. Laminates were demoulded at 70 °C. A schematic processing route for TPCL production is outlined in Fig. 1.

### 2.2.3. Laminate testing

In order to evaluate the effect of IR-desized CF fabrics on the mechanical properties of TPCL, 3-point flexural-, short-beam flexural- and Charpy impact tests were conducted. Specimens were cut in the fabric warp direction by means of a circular saw Diadisc 5200 (Mutronic Präzisionsgerätebau GmbH & Co.KG, Germany) utilising a saw blade for thermoplastic composites (Mutronic Diatool PKD-blade).

3-point flexural tests were performed on a Zwick/Roell ZMART. PRO 10 kN universal testing machine. According to EN ISO 14125, 100 · 25 · 2 mm<sup>3</sup> flexural test specimens were prepared and tested at a crosshead speed of 5 mm/min and a support span of 80 mm [61]. The radius of the loading nose was 5 mm and the radii of the supports measured 2 mm.

Short-beam flexural tests were performed on a Zwick/Roell ZMART. PRO 10 kN universal testing machine. According to EN ISO 14130, 20 ·

10 · 2 mm<sup>3</sup> short-beam flexural test specimens were prepared and tested at a crosshead speed of 1 mm/min and a support span of 10 mm [62]. The radius of the loading nose was 5 mm and the radii of the supports measured 2 mm.

Charpy impact tests were performed on a Zwick 5113.300 pendulum impact tester. In accordance with EN ISO 179, 50 · 15 · 2 mm<sup>3</sup> Charpy impact specimens were prepared and impacted in flatwise normal (fn) manner by means of a 7.5 J impactor and an impact speed of 3.85 m/s [63]. A support span of 40 mm was chosen for impact testing according to EN ISO 179 [63].

A total of 5 specimens (Charpy: 10 specimens) were averaged per material combination. Specimens were conditioned at 23 °C and 50% relative humidity (RH) for 14 days (equilibrium moisture content according to EN ISO 62 [64]) in a climate chamber prior to testing. It is well known that the properties of PA6 and its composites are influenced by conditioning [10]. Depending on the fibre volume fraction, CF-PA6 composites typically demonstrate a moisture uptake of 2–5 wt% [65], whereas CF-PPS and CF-PEEK exhibit a moisture uptake of 0.2–0.4 wt% [66,67]. High moisture contents in CF-PA6 decrease the matrix (shear) modulus and (shear) strength, which adversely affect composite static strength [68]. Therefore, the CF-PA6 materials were also tested in dry state (specimens dried at 70 °C for 48h and left to cool prior to testing) which represents a “dry-as-moulded condition”. Testing was conducted at 23 °C according to EN ISO 291 [69].

### 2.2.4. XCT analysis – impregnation quality and void-content

The impregnation quality and void-content of the composite samples

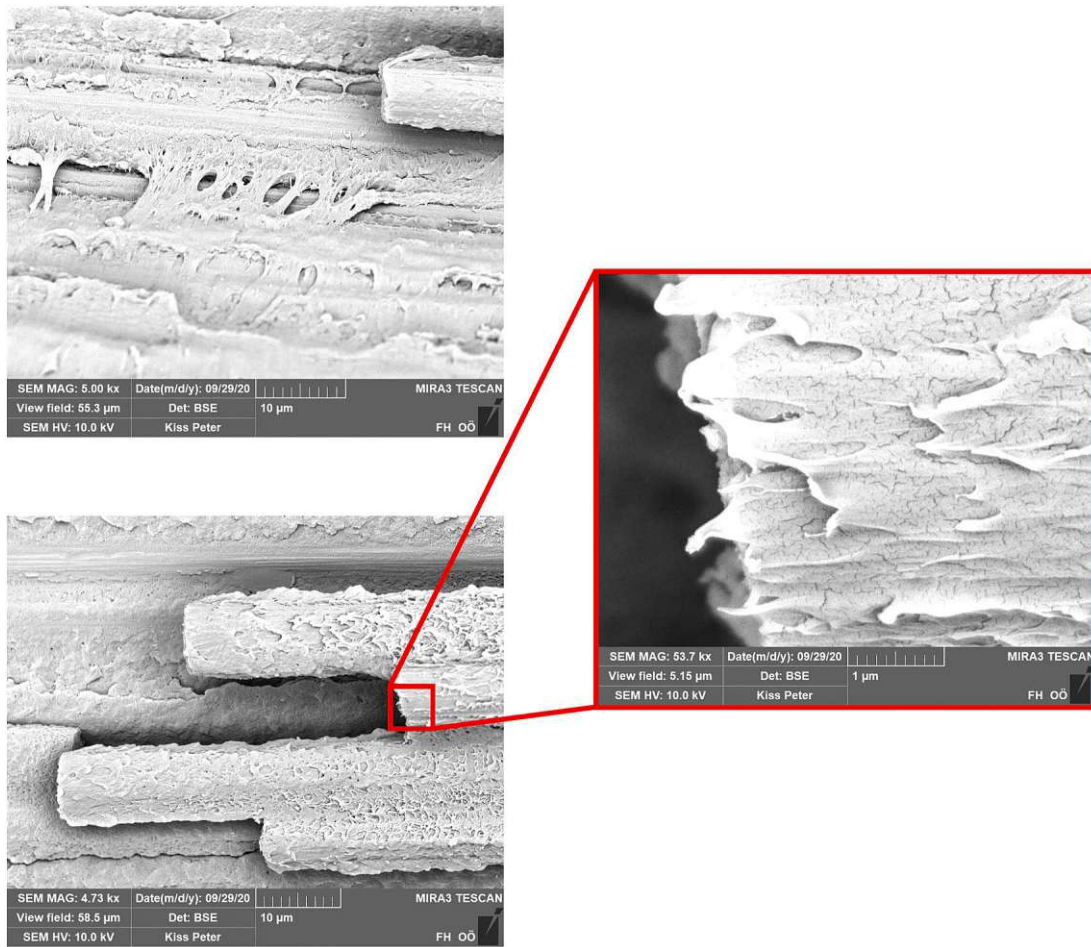


**Fig. 9.** SEM images of fractured IR-desized CF-PA6 laminate showing full wetting of the CF reinforcement. The composite exhibited matrix cracks running parallel to the fibres (cohesive failure) and fibre fractures rather than interfacial debonding (adhesive failure). At the microscale ductile features of the matrix are apparent.

was analysed via X-ray micro-computed tomography (XCT) on a Phoenix/X-Ray Nanotom 180NF (General Electric, USA), equipped with a tungsten coated diamond target. Specimens were scanned at a voxel size of  $(14 \mu\text{m})^3$ , 80 kV tube voltage, 230  $\mu\text{A}$  current and 500 ms exposure time with no pre-filter applied. 1400 projections were captured during a full rotation with an averaging over 4 images per projection, resulting in a total scan time of 60 min. Standard beam hardening correction, implemented in the reconstruction software was applied as correction for cupping artefacts. Subsequently, the digital volume data was analysed in Volume Graphics Studio (Volume Graphics GmbH, Germany) by means of a porosity/inclusion analysis.

### 2.2.5. Density and fibre volume fraction

Since the decomposition temperatures of PPS and PEEK lie within a region where CF degradation simultaneously occurs in air (500 °C), correctly determining the fibre mass fraction using resin-burn off methods on macroscopic samples is very difficult [70,71]. However, combined with the XCT analysis, which provides information about the sample porosity, it is possible to calculate the fibre volume fraction by measuring the density of the composite and its constituent components. Provided that the sample porosity is negligible, the respective fibre volume fraction  $\nu_f$  can be calculated according to equation (1):

$$\nu_f = \frac{\rho_c - \rho_m}{\rho_f - \rho_m} \cdot 100 \quad (1)$$

where  $\rho_c$ ,  $\rho_f$ , and  $\rho_m$  represent the composite sample density, IR-desized CF fabric density and crystallized matrix film density, respectively.

Densities were determined according to EN ISO 1183 by buoyancy method [72]. Samples of IR-desized CF fabric  $\rho_f$  were immersed in the test liquid for several minutes for an accurate density reading. The densities determined, alongside datasheet properties of the constituent materials, are provided in Table 1.

### 2.2.6. SEM imaging

CF fabrics and fractured specimens were inspected via back scattered electron imaging on an FESEM MIRA3 LMH (Tescan, Czech Republic), at an accelerating voltage of 10.0 kV.

## 3. Results and discussion

### 3.1. Results from fabric desizing experiments

The CF fabric in the present study consisted of 3K tows with an EP-sizing level of 1.3 wt% according to the manufacturer data sheet [51]. Loomstate fabric desizing parameters were varied from 325–400 °C in MTGA experiments as shown in Fig. 2.

It was observed that a desizing temperature of 325 °C did not suffice to fully desize the sample within a dwell-time of 15 min (LOI was roughly 0.8%). However, at 350–400 °C the LOI reached 1.1%. Ultimately, the desizing temperature appeared to be more important than the dwell time. This observation corresponded well to desizing experiments conducted by Mitschang, Blinzler and Wöginger [4], who already observed that an extension in dwell time does not influence the desizing result significantly. This temperature dependency could be linked to the Arrhenius equation, where an increase in 10 °C would roughly double

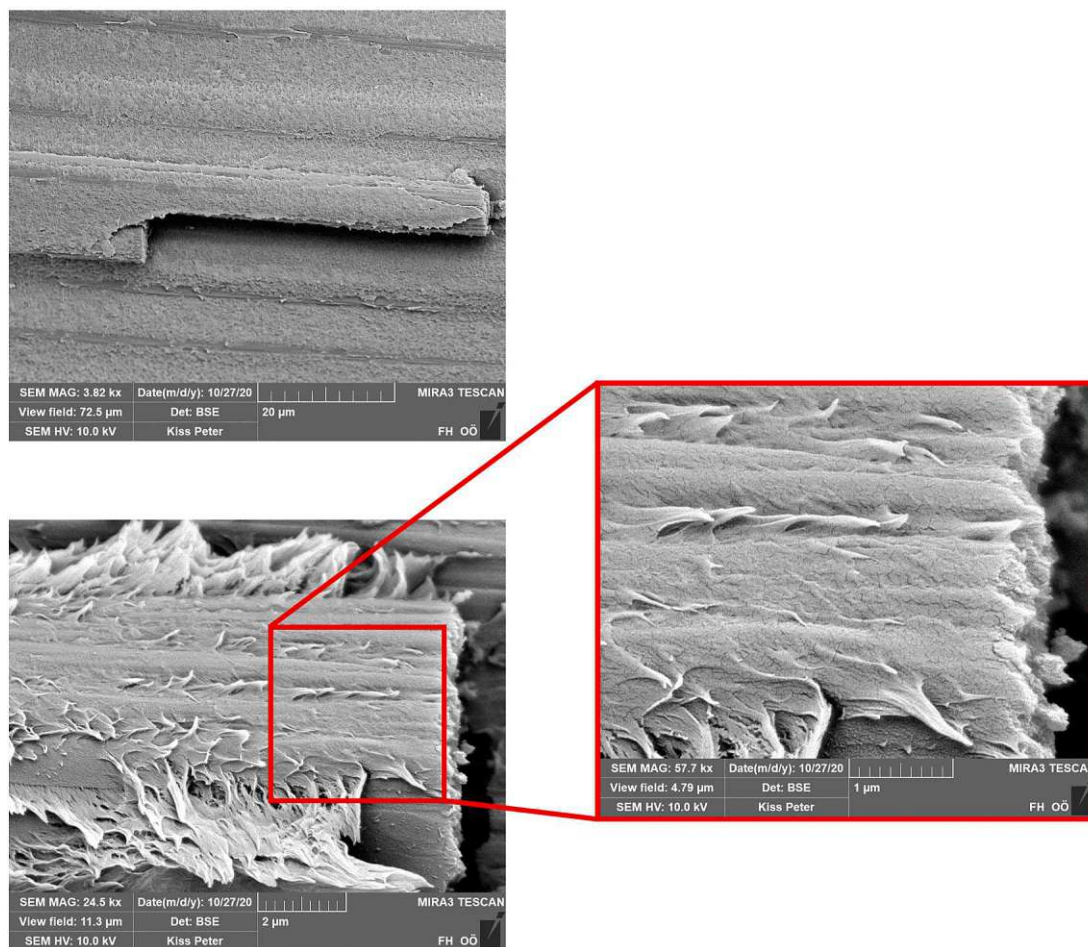


**Fig. 10.** SEM images of fractured IR-desized CF-PPS laminate showing full wetting of the CF reinforcement. The PPS matrix exhibited cohesive failure rather than interfacial debonding. At the microscale ductile features of the matrix are apparent.

the reaction rate of sizing decomposition. A LOI of 1.3 wt% (sizing level stated by the fibre manufacturer [51]) was never observed in the desizing experiments. This could be attributable to several factors: variations within the sizing process, sizing rub-off from the weaving process, formation of indecomposable sizing residues during heating, or minor weight gain of CF due to oxidation counteracting weight loss during heating. Nonetheless, the EP-sizing appeared to be readily decomposable by thermal treatment.

The observations from the MTGA experiments were subsequently upscaled for IR-desizing. IR-desizing of the fabrics was performed at 400 °C and a dwell time of 20 s to decompose the EP-sizing as quickly as possible, without damaging the fibres. A dwell time of 20 s appeared sufficient, since no more visible decomposition gases from the sizing were generated thereafter. The LOI of IR-desized fabric was 0.05%, which confirmed that the fabric was fully desized. SEM inspections depicted in Fig. 3, further verified the IR-desizing result. Here, the difference between EP-sized (loomstate) and IR-desized fibres became clearly apparent. The EP-sized filaments appeared smooth and bonded together, whereas the IR-desized filaments revealed a clean and ridged surface, resembling their factory state prior to sizing application. Judging by the SEM images, the CF surfaces remained undamaged following IR-exposure at 400 °C.

It was noticed that the IR-desized CF fabric became significantly more compliant as the individual tows tended to disintegrate very easily. Therefore, special care was taken during further handling in order to prevent fibre-fibre friction, breakage and fuzzing.

### 3.2. Results from XCT analysis

The laminate plies were fully impregnated by the thermoplastic melts and appeared void-free when examined by XCT analysis, as presented in Fig. 4. Furthermore, the warp tows showed no signs of misalignment or wash-out following film stack impregnation. This guaranteed an ideal basis for mechanical property comparisons. The slight misalignment of weft tows is attributable to some variation within the provided fabric.

### 3.3. Results from laminate testing

The results of 3-point flexural, short-beam flexural and Charpy impact tests with corresponding laminate fibre volume fractions are displayed in Table 2.

The flexural strength in the longitudinal fibre direction is frequently considered a fibre-matrix sensitive property [8,22,33,36,68,73], even though the interfaces are subjected to a very complex stress state upon bending. If the fibres are wetted poorly by the matrix or exhibit low interfacial adhesion, premature compressive micro-buckling is the predominant failure mode due a reduction of fibre support by debonding mechanisms [8]. Yet, all 3-point flexural test specimens failed in tension as depicted in Fig. 5, which indicated good fibre support in compression and therefore good fibre wet-out [8].

Since the IR-desized CF-PA6 and industrial CF-PA6 reference demonstrated very similar fibre volume fractions of 45–46%, a direct comparison between the two could be drawn. In fact, their performance level was equal in all mechanical tests. Dry CF-PA6 samples generally exhibited higher flexural moduli and flexural strengths compared to

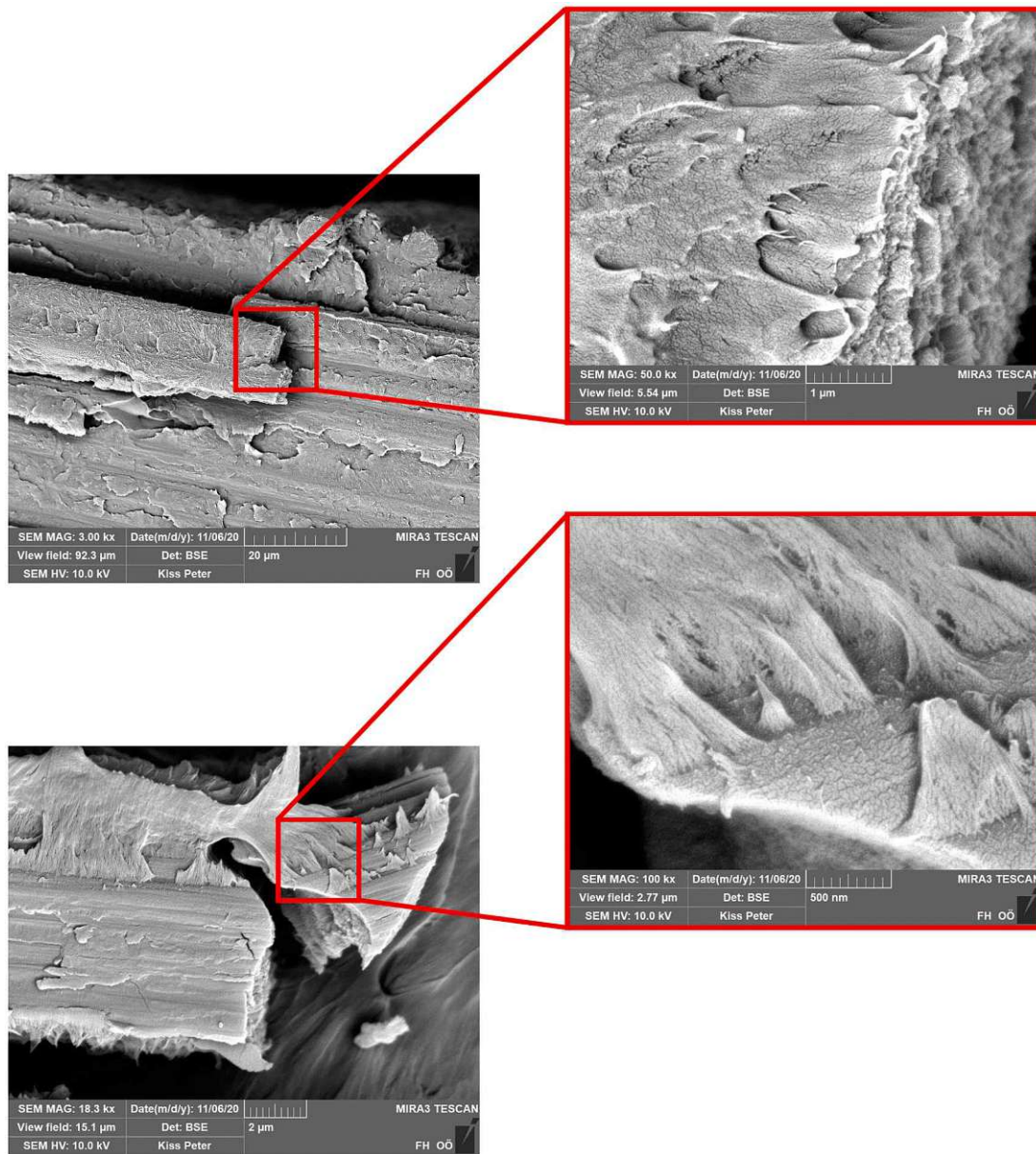


Fig. 11. SEM images of fractured IR-desized CF-PEEK laminate showing full wetting of the CF reinforcement. The PEEK matrix exhibited cohesive failure rather than interfacial debonding. At the microscale ductile features of the matrix are apparent.

conditioned samples, which is conceivable due to moisture acting as a plasticiser [10]. More noticeable differences were observed between CF-PPS and CF-PEEK samples, where the industrial references boasted higher performance in the mechanical tests compared to IR-desized samples. Due to the tensile fracture of the specimens, the rule of mixtures (ROM) was applied to provide an estimate on the influence of fibre volume fraction on the measured material performance. Margem and co-workers demonstrated that the ROM calculated from the tensile properties of the composite constituents correlates relatively well to the flexural properties [74]. The ROM is depicted in Fig. 6 using the example of CF-PPS and CF-PEEK properties.

The theoretical values of the CF filament tensile strength (4100 MPa) and tensile modulus (240 GPa) from Table 1 were divided by half to roughly account for a woven fabric structure. A good approximation was established in this manner. The sample strengths and moduli scaled almost linearly along the theoretical ROM-line, which evinced that especially the strength potential of the fibres has been effectively utilised by strong matrix adhesion for the given fibre volume fraction. Thus, the major difference between the

laminates was mostly attributable to a variation in fibre volume fraction rather than a difference in fibre-matrix adhesion. Another factor, which could have influenced the testing outcomes, was a difference in the weaving pattern of the fabrics [75]. In aerospace-grade TPCL (PPS and PEEK) the 5HS weave is relatively popular, having lower crimp and fewer yarn intersections compared to the 2/2 twill weave. Furthermore, the 5HS fabrics in industrial CF-PPS and CF-PEEK references were stacked such that the surface plies were warp-faced. Nonetheless, in consideration of the higher fibre volume fractions and different weave pattern of industrial CF-PPS and CF-PEEK references, it can be inferred from the 3-point flexural tests that IR-desized TPCL and their industrial references were almost equal in performance.

In Charpy impact tests ( $f_n$ ) of CF-PA6 no difference was discernible between conditioned (more ductile matrix) and dry (more brittle matrix) samples. The impacted samples consistently failed in catastrophic brittle manner with straight crack paths, resulting in hinge breaks or complete breaks without notable inelastic deformation. Moreover, the impact strength of CF-PA6 samples was only slightly below that of IR-desized CF-PPS and IR-desized CF-PEEK laminates in a region close to 50 kJ/



m<sup>2</sup>. These observations suggest that the Charpy impact tests were mostly fibre-dominated and affected by the low elongation at break of CF rather than being matrix type dominated [76,77]. Similar behaviour was already observed by Kiss et al. in a comparison between CF and GF composites [10]. Impact strength is reported to increase steadily up to a fibre volume fraction of about 60% before decreasing again in continuous fibre-reinforced laminates [78–80]. The higher impact strength of industrial CF-PPS and CF-PEEK references (which also failed in catastrophic brittle manner) is therefore attributable to the higher fibre volume fractions. It should be mentioned that the Charpy pendulum impact test is not comparable with drop tower impact tests where sample panels are secured in a clamping fixture and delamination behaviour can be studied [7–9].

Determination of ILSS by means of the short-beam flexural test is frequently regarded as a fibre-matrix sensitive property [81]. However, specimen failure mode must be considered for correct interpretation. Consequently, unless mid-plane interlaminar failure has been clearly observed, the values determined from this test method cannot be attributed to a shear property and are invalid according to EN ISO 14130 [62]. Indeed, none of the specimens failed due to mid-plane shear delamination, but rather in compression, tension, or combined failure which was rather unexpected. Since the measured properties did not represent ILSS, the strength values were designated as “short-beam strength”. Nevertheless, for comparative purposes it is permitted to use the short-beam strength data of specimens exhibiting the same failure mode [62].

CF-PA6 samples failed due to compressive micro-buckling coupled with inelastic deformation in conditioned state. In dry state, CF-PA6 samples failed due to compressive micro-buckling combined with tensile fracture. CF-PPS samples predominantly failed due to compressive micro-buckling in the outer plies, whereas CF-PEEK samples failed due to tensile fracture only as presented in Fig. 7.

IR-desized CF-PA6 and the industrial CF-PA6 reference boasted the same short-beam strength, whereas in the case of CF-PPS and CF-PEEK samples, the industrial references boasted higher short-beam strengths compared to the IR-desized samples. However, due to failure occurring in vicinity of the surface (tension or compression), it is highly likely that the measured strength values were once again influenced by the fibre volume fraction and the weave structure as discussed previously. As demonstrated, correct ILSS determination of thermoplastic composites is not a trivial task. PPS, which is comparable to epoxy matrices in terms of modulus and elongation at break [59], evinced no sign of mid-plane delamination. Therefore, it remains questionable whether ILSS testing of woven TPCL is reliable for an assessment of the quality of interfacial adhesion. Nonetheless, the test may be suitable for quality control in continuous production.

### 3.4. Fibre-matrix adhesion of IR-desized CF fabrics

In Fig. 8, transverse tensile fracture surfaces of CF-PA6 laminates (EP-sized vs. IR-desized) are depicted which shall demonstrate the difference in fibre wet-out and fibre-matrix adhesion of the materials. The EP-sizing inhibited fibre wet-out and the resulting laminate exhibited poor mechanical performance in a region of 8.0 GPa flexural modulus and 82 MPa flexural strength. The importance of removing the incompatible EP-sizing layer is apparent.

The fundamental science of the adhesion mechanisms between thermoplastics and reinforcing fibres are still not fully understood today [34]. A thermal desizing process of the CF reinforcement, as presented in this work may facilitate several adhesion mechanisms such as wetting, non-covalent interactions, covalent bonding, mechanical interlocking, and increased interfacial friction. Since the backbones of thermoplastic polymers are relatively inert, covalent bonding is usually not considered to be among their primary adhesion mechanisms [8], unless the thermoplastic polymer is modified with a reactive additive [22]. The thermoplastics under discussion (PA6, PPS and PEEK) were unmodified homopolymers, and yet interfacial adhesion with the IR-desized CF reinforcement appeared sufficiently high for each type of polymer. This was clearly demonstrated by the flexural strength

results and further verified by the following fractographic SEM images in Fig. 9, Fig. 10 and Fig. 11.

Given that the polymers differed considerably from one another chemically, adhesion by covalent bonding only appears to be an insufficient explanation. While covalent bonds could theoretically form due to the high temperatures prevailing during laminate manufacture, this would imply that all thermoplastics tested would undergo the same kind of chemical reaction, which clearly cannot be the case. Therefore, non-covalent interactions and mechanical phenomena such as interlocking were suspected to be the main cause of the high material performance. The ridged surface of the desized CF reinforcement seemed to contribute largely to the overall adhesion by anchoring the thermoplastic matrices. This can be observed from the localised ductile features shown in the SEM images.

EP-sizing removal by heat treatment in air could alter the CF surface in many ways. It is possible that the former oxidised CF surface (from the factory electrochemical treatment) could be exposed again. Furthermore, additional functional groups may be introduced to the CF surface by air oxidation as experimentally validated by several researchers [14, 82]. These surface oxides could facilitate wetting with many thermoplastics as suggested by Hexcel Corporation [83]. Overall, the large surface area of CF, polar and dispersive interactions from wetting (non-covalent interactions), together with mechanical interlocking could suffice to result in adequate adhesion. Additionally, aromatic polymers such as PPS and PEEK could be able to display interactions by  $\pi$ - $\pi$  stacking with the graphitic carbon fibre structure [84].

Summarizing the experiments, the EP-sizing was found to be well suited to the desizing process. The IR-desized CF facilitated interfacial wetting with thermoplastics and it appeared that industrial TPCL manufacture also favours the use of desized CF fabrics. At the present time, special thermoplastic-compatible sizings such as PEI-sizings are unavailable in combination with 3K tows. However, as TPCL are gaining interest and making their way out of the niche market, it is conceivable that thermoplastic-compatible sized 3K tow may be available “off-the-shelf” in the near future which would render a desizing process redundant. In the meantime, it appears that thermal desizing of readily available EP-sized CF fabrics is the main approach taken for high-performance TPCL production in industrial practice.

## 4. Conclusions

The present study investigated the manufacture of TPCL from commercial EP-sized high tenacity CF fabrics. Since the EP-sizing inhibited wet-out by thermoplastic melts in preliminary tests, this highly incompatible sizing layer had to be removed from the CF reinforcement. Thermal treatment by infrared-irradiation was chosen as a quick and efficient means to remove the EP-sizing layer from the CF fabrics. SEM images verified that the EP-sizing had decomposed fully, by exposure of clean and ridged CF surfaces. Compression moulded CF-PA6, CF-PPS and CF-PEEK TPCL prepared from the IR-desized fabrics revealed complete wet-out of the laminates and proper fibre-matrix adhesion as characterised by XCT scans and SEM fractography, respectively. When compared to industrial materials, similar mechanical properties and laminate failure modes were observed.

If price is the main concern, CF-PA6 provides a very good balance between cost and performance. However, moisture uptake impairs modulus slightly and has a particularly adverse effect on static strength. CF-PPS and CF-PEEK are more predictable in terms of mechanical behaviour in practical applications since these polymers demonstrate significantly lower moisture uptake and therefore consistent material performance. CF-PEEK offers a slight advantage over CF-PPS in static strength. Ultimately, the desized CF surface provided sufficient compatibility with the neat (unmodified) thermoplastic matrices examined which was ascribed to non-covalent interactions and mechanical interlocking.

## Declaration of competing interest

The authors declare that they have no known competing financial interests or personal relationships that could have appeared to influence the work reported in this paper.



Europäische Union Investitionen in Wachstum & Beschäftigung. Österreich.

## Acknowledgements

The authors would like to offer their special thanks to ECC - Engineered Cramer Composites and LITE GmbH for providing their materials for research purposes. Permission for publishing the mechanical property data is also gratefully acknowledged.

The authors are grateful to the State Government of Upper Austria and the European Regional Development Fund for providing financial support for this research in the EFRE-IWB 2020 programme for the project: "ProFVK".

## References

- Mathijssen D. Leading the way in thermoplastic composites. *Reinforc Plast* 2016;60:405–7. <https://doi.org/10.1016/j.repl.2015.08.067>.
- Fisher M, Hampe H. Interview with hinrich hampe. Toho Tenax. *Reinf Plast* 2017;61:330–1. <https://doi.org/10.1016/j.repl.2017.04.055>.
- Dittmar H, Plaggenborg H. Lightweight vehicle underbody design. *Reinforc Plast* 2019;63:29–32. <https://doi.org/10.1016/j.repl.2017.11.014>.
- Mitschang P, Blinzler M, Wöginger A. Processing technologies for continuous fibre reinforced thermoplastics with novel polymer blends. *Compos Sci Technol* 2003;63:2099–110. [https://doi.org/10.1016/S0266-3538\(03\)00107-6](https://doi.org/10.1016/S0266-3538(03)00107-6).
- Han P, Butterfield J, Price M, Buchanan S, Murphy A. Experimental investigation of thermoforming carbon fibre-reinforced polyphenylene sulphide composites. *J Thermoplast Compos Mater* 2015;28:529–47. <https://doi.org/10.1177/0892705713486133>.
- Akkerman R, Bouwman M, Wijskamp S. Analysis of the thermoplastic composite overmolding process: interface strength. *Front Mater* 2020;7:1–16. <https://doi.org/10.3389/fmats.2020.00027>.
- Vieille B, Casado VM, Bouvet C. About the impact behavior of woven-ply carbon fiber-reinforced thermoplastic- and thermosetting-composites: a comparative study. *Compos Struct* 2013;101:9–21. <https://doi.org/10.1016/j.compstruct.2013.01.025>.
- Kiss P, Schoefer J, Stadlbauer W, Burgstaller C, Archodoulaki V-M. An experimental study of glass fibre roving sizings and yarn finishes in high-performance GF-PA6 and GF-PPS composite laminates. *Compos B Eng* 2021;204:108487. <https://doi.org/10.1016/j.compositesb.2020.108487>.
- Liu H, Liu J, Ding Y, Zheng J, Kong X, Zhou J, et al. The behaviour of thermoplastic and thermoset carbon fibre composites subjected to low-velocity and high-velocity impact. *J Mater Sci* 2020;55:15741–68. <https://doi.org/10.1007/s10853-020-05133-0>.
- Kiss P, Stadlbauer W, Burgstaller C, Stadler H, Fehringer S, Haeuserer F, et al. In-house recycling of carbon- and glass fibre-reinforced thermoplastic composite laminate waste into high-performance sheet materials. *Compos Part A Appl Sci Manuf* 2020;139:106110. <https://doi.org/10.1016/j.compositesa.2020.106110>.
- Wang S, Zhou Z, Zhang J, Fang G, Wang Y. Effect of temperature on bending behavior of woven fabric-reinforced PPS-based composites. *J Mater Sci* 2017;52:13966–76. <https://doi.org/10.1007/s10853-017-1480-0>.
- Veazey D, Hsu T, Gomez ED. Next generation high-performance carbon fiber thermoplastic composites based on polyaryletherketones. *J Appl Polym Sci* 2017;134:19–21. <https://doi.org/10.1002/app.44441>.
- Mallik PK. *Composites engineering handbook*. CRC Press; 1997. <https://doi.org/10.1201/9781482277739>.
- Chukov D, Nematulloev S, Torokhov V, Stepashkin A, Sherif I, Tcherdyntsev V. Effect of carbon fiber surface modification on their interfacial interaction with polysulfone. *Res. Phys* 2019;15:102634. <https://doi.org/10.1016/j.rinp.2019.102634>.
- Duchoslav J, Unterweger C, Steinberger R, Fürst C, Stifter D. Investigation on the thermo-oxidative stability of carbon fiber sizings for application in thermoplastic composites. *Polym Degrad Stab* 2016;125:33–42. <https://doi.org/10.1016/j.polydegradstab.2015.12.016>.
- Li J. The effect of surface modification with nitric acid on the mechanical and tribological properties of carbon fiber-reinforced thermoplastic polyimide composite. *Surf Interface Anal* 2009;41:759–63. <https://doi.org/10.1002/sia.3089>.
- Servinis L, Henderson LC, Gengenbach TR, Kafi AA, Huson MG, Fox BL. Surface functionalization of unsized carbon fiber using nitrenes derived from organic azides. *Carbon N Y* 2013;54:378–88. <https://doi.org/10.1016/j.carbon.2012.11.051>.
- Sharma M, Gao S, Mäder E, Sharma H, Wei LY, Bijwe J. Carbon fiber surfaces and composite interphases. *Compos Sci Technol* 2014;102:35–50. <https://doi.org/10.1016/j.compscitech.2014.07.005>.
- Hu J, Li F, Wang B, Zhang H, Ji C, Wang S, et al. A two-step combination strategy for significantly enhancing the interfacial adhesion of CF/PPS composites: the liquid-phase oxidation followed by grafting of silane coupling agent. *Compos B Eng* 2020;191:107966. <https://doi.org/10.1016/j.compositesb.2020.107966>.
- Koissin V, Kotanjac Ž, Warnet LL, Lefferts L, Akkerman R. Deformability of a woven fabric modified with in-situ grown nanofibres. *Int J Material Form* 2018;11:705–15. <https://doi.org/10.1007/s12289-017-1384-1>.
- Gulyás J, Földes E, Lázár A, Pukánszky B. Electrochemical oxidation of carbon fibres: surface chemistry and adhesion. *Compos Part A Appl Sci Manuf* 2001;32:353–60. [https://doi.org/10.1016/S1359-835X\(00\)00123-8](https://doi.org/10.1016/S1359-835X(00)00123-8).
- Kiss P, Stadlbauer W, Burgstaller C, Archodoulaki V-M. Development of high-performance glass fibre-polypropylene composite laminates: effect of fibre sizing type and coupling agent concentration on mechanical properties. *Compos Part A Appl Sci Manuf* 2020;138:106056. <https://doi.org/10.1016/j.compositesa.2020.106056>.
- McMican R. Sizing stability is a key element for glass fibre manufacturing. *Reinforc Plast* 2012;56:29–32. [https://doi.org/10.1016/S0034-3617\(12\)70110-8](https://doi.org/10.1016/S0034-3617(12)70110-8).
- Aoki R, Yamaguchi A, Hashimoto T, Urushisaki M, Sakaguchi T, Kawabe K, et al. Preparation of carbon fibers coated with epoxy sizing agents containing degradable acetal linkages and synthesis of carbon fiber-reinforced plastics (CFRPs) for chemical recycling. *Polym J* 2019;51:909–20. <https://doi.org/10.1038/s41428-019-0202-7>.
- Lenferink RG, Van Dreumel WHM. Method for preparing a fabric substantially consisting of carbon fibers United States Patent US7252726B2. 2007.
- Chukov Nematulloev, Zadorozhnyy Tcherdyntsev, Stepashkin Zheretsov. Structure, mechanical and thermal properties of polyphenylene Sulfide and polysulfone impregnated carbon fiber composites. *Polymers* 2019;11:684. <https://doi.org/10.3390/polym11040684>.
- Zhang Q, Liu L, Jiang D, Yan X, Huang Y, Guo Z. Home-made epoxy emulsion sizing agent for treating carbon fibers: thermal stability and mechanical properties. *J Compos Mater* 2015;49:2877–86. <https://doi.org/10.1177/0021998314557298>.
- Liu F, Shi Z, Dong Y. Improved wettability and interfacial adhesion in carbon fibre/epoxy composites via an aqueous epoxy sizing agent. *Compos Part A Appl Sci Manuf* 2018;112:337–45. <https://doi.org/10.1016/j.compositesa.2018.06.026>.
- Eyckens DJ, Arnold CL, Simon Ž, Gengenbach TR, Pinson J, Wickramasingha YA, et al. Covalent sizing surface modification as a route to improved interfacial adhesion in carbon fibre-epoxy composites. *Compos Part A Appl Sci Manuf* 2021;140:106147. <https://doi.org/10.1016/j.compositesa.2020.106147>.
- Dai Z, Shi F, Zhang B, Li M, Zhang Z. Effect of sizing on carbon fiber surface properties and fibers/epoxy interfacial adhesion. *Appl Surf Sci* 2011;257:6980–5. <https://doi.org/10.1016/j.apsusc.2011.03.047>.
- Dilsiz N, Wightman J. Effect of acid-base properties of unsized and sized carbon fibers on fiber/epoxy matrix adhesion. *Colloids Surfaces A Physicochem Eng Asp* 2000;164:325–36. [https://doi.org/10.1016/S0927-7757\(99\)00400-8](https://doi.org/10.1016/S0927-7757(99)00400-8).
- Luo Y, Zhao Y, Duan Y, Du S. Surface and wettability property analysis of CCF300 carbon fibers with different sizing or without sizing. *Mater Des* 2011;32:941–6. <https://doi.org/10.1016/j.matdes.2010.08.004>.
- Juska TD, Puckett PM. In: Mallik PK, editor. "Matrix resins and fiber/matrix adhesion" in composites engineering handbook. New York, USA: Marcel-Dekker, Inc.; 1997.

- [34] Thomason JL. Glass fibre sizing: a review of size formulation patents. Glasgow, Scotland: Blurb; 2015.
- [35] Thomason JL. Glass fibre sizing: a review. *Compos Part A Appl Sci Manuf* 2019; 127:105619. <https://doi.org/10.1016/j.compositesa.2019.105619>.
- [36] Plueddemann EP. Silane coupling agents. Boston, MA: Springer US; 1991. <https://doi.org/10.1007/978-1-4899-2070-6>.
- [37] Wu Q, Li M, Gu Y, Wang S, Yao L, Zhang Z. Effect of sizing on interfacial adhesion of commercial high strength carbon fiber-reinforced resin composites. *Polym Compos* 2016;37:254–61. <https://doi.org/10.1002/pc.23176>.
- [38] Pillay S, Vaidya UK, Janowski GM. Liquid molding of carbon fabric-reinforced nylon matrix composite laminates. *J Thermoplast Compos Mater* 2005;18:509–27. <https://doi.org/10.1177/0892705705054412>.
- [39] Liu H, Zhao Y, Li N, Zhao X, Han X, Li S, et al. Enhanced interfacial strength of carbon fiber/PEEK composites using a facile approach via PEI&ZIF-67 synergistic modification. *J Mater Res Technol* 2019;8:6289–300. <https://doi.org/10.1016/j.jmrt.2019.10.022>.
- [40] Hassan EAM, Yang L, Elagib THH, Ge D, Lv X, Zhou J, et al. Synergistic effect of hydrogen bonding and  $\pi$ - $\pi$  stacking in interface of CF/PEEK composites. *Compos B Eng* 2019;171:70–7. <https://doi.org/10.1016/j.compositesb.2019.04.015>.
- [41] Liu H, Zhao Y, Li N, Li S, Li X, Liu Z, et al. Effect of polyetherimide sizing on surface properties of carbon fiber and interfacial strength of carbon fiber/polyetheretherketone composites. *Polym Compos* 2020. <https://doi.org/10.1002/pc.25876>. pc.25876.
- [42] Koissin V, Bor T, Kotanjac Ž, Lefferts L, Warnet L, Akkerman R. Carbon nanofibers grown on large woven cloths: morphology and properties of growth. *Chimia* 2016; 2:19. <https://doi.org/10.3390/c2030019>.
- [43] Kafi A-A. Method of sizing carbon fibers, sized carbon fibers, and carbon fiber composites WO2016193927A1. 2016.
- [44] Kibayashi M, Seike S, Pranger L. Carbon fiber US20130253096A1. 2013.
- [45] Pegna J, Schneitner J, Williams K, Goduguchinta R. High strength ceramic fibers and methods of fabrication US10047015B2. 2018.
- [46] Giraud I, Franceschi S, Perez E, Lacabanne C, Dantras E. Influence of new thermoplastic sizing agents on the mechanical behavior of poly(ether ketone)/carbon fiber composites. *J Appl Polym Sci* 2015;132. <https://doi.org/10.1002/app.42550>. n/a-n/a.
- [47] Giraud I, Franceschi-Messant S, Perez E, Lacabanne C, Dantras E. Preparation of aqueous dispersion of thermoplastic sizing agent for carbon fiber by emulsion/solvent evaporation. *Appl Surf Sci* 2013;266:94–9. <https://doi.org/10.1016/j.apsusc.2012.11.098>.
- [48] Teijin Carbon Europe GmbH. Tenax® carbon fiber HTS45/IMS65 P12/P22 product information on safe handling. 2018. [https://www.tejincarbon.com/fileadmin/user\\_upload/PISH\\_Tenax\\_Carbon\\_Fiber\\_P-Size\\_v02\\_en\\_2018-07-15\\_EN.pdf](https://www.tejincarbon.com/fileadmin/user_upload/PISH_Tenax_Carbon_Fiber_P-Size_v02_en_2018-07-15_EN.pdf). [Accessed 10 November 2020].
- [49] Howell E, Bassetti S. Interview with steven bassetti. *Reinforc Plast* 2017;61:326–9. <https://doi.org/10.1016/j.repl.2017.09.001>.
- [50] Yuan C, Li D, Yuan X, Liu L, Huang Y. Preparation of semi-aliphatic polyimide for organic-solvent-free sizing agent in CF/PEEK composites. *Compos Sci Technol* 2021;201:108490. <https://doi.org/10.1016/j.compscitech.2020.108490>.
- [51] Teijin Carbon Europe GmbH. Product data sheet Tenax® filament yarn. 2020. [https://www.tejincarbon.com/fileadmin/PDF/Datenblätter\\_en/Product\\_Data\\_Sheet\\_TSG01en\\_EU\\_Filament\\_.pdf](https://www.tejincarbon.com/fileadmin/PDF/Datenblätter_en/Product_Data_Sheet_TSG01en_EU_Filament_.pdf). [Accessed 10 November 2020].
- [52] SGL Carbon. SIGRAFIL® continuous carbon fiber tows. 2020. <https://www.sglcarbon.com/pdf/SGL-Broschure-The-Enablers-EN.pdf>. [Accessed 10 November 2020].
- [53] EL-Dessouky HM, Lawrence CA. Ultra-lightweight carbon fibre/thermoplastic composite material using spread tow technology. *Compos B Eng* 2013;50:91–7. <https://doi.org/10.1016/j.compositesb.2013.01.026>.
- [54] Chen J, Wang K, Zhao Y. Enhanced interfacial interactions of carbon fiber reinforced PEEK composites by regulating PEI and graphene oxide complex sizing at the interface. *Compos Sci Technol* 2018;154:175–86. <https://doi.org/10.1016/j.compscitech.2017.11.005>.
- [55] EL-Dessouky HM. 6 spread tow technology for ultra lightweight CFRP composites: potential and possibilities. *Adv. Compos. Mater. Prop. Appl. De Gruyter Open Poland*; 2017. p. 323–48. <https://doi.org/10.1515/9783110574432-006>.
- [56] Teijin Carbon Europe GmbH. Tenax® -E TPCL PEEK-HTA40. 2018. [https://www.tejincarbon.com/fileadmin/PDF/Datenblätter\\_en/PDS\\_Tenax-E\\_TPCL-PEEK-HTA40\\_v11\\_2018-06-08\\_en.pdf](https://www.tejincarbon.com/fileadmin/PDF/Datenblätter_en/PDS_Tenax-E_TPCL-PEEK-HTA40_v11_2018-06-08_en.pdf). [Accessed 14 November 2020].
- [57] DIN EN ISO 10548:2003-12 Carbon fibre - determination of size content (ISO 10548:2002); German version EN ISO 10548:2003. 2003. <https://doi.org/10.31030/9508682>.
- [58] LANXESS Deutschland GmbH. Datasheet DURETHAN® B30S 2020. [https://techcenter.lanxess.com/scp/americas/en/products/datasheet/LANXESS\\_Durethan\\_B30S\\_000000\\_ISO\\_EN.pdf?docId=31442939](https://techcenter.lanxess.com/scp/americas/en/products/datasheet/LANXESS_Durethan_B30S_000000_ISO_EN.pdf?docId=31442939). [Accessed 12 October 2020].
- [59] Celanese Corporation. Datasheet FORTRON® 0214 2020. <https://tools.celanese.com/products/datasheet/SL/FORTRON®0214>. [Accessed 12 October 2020].
- [60] Victrex plc. Datasheet VICTREX® PEEK 150G/151G 2020. <https://www.victrex.com/~/media/datasheets/victrextids150g-151g.pdf>. [Accessed 12 October 2020].
- [61] DIN EN ISO 14125:2011-05. Fibre-reinforced plastic composites - determination of flexural properties (ISO 14125:1998 + Cor.1:2001 + Amd.1:2011); German version EN ISO 14125:1998 + AC:2002 + A1:2011. 2011. <https://doi.org/10.31030/1753441>.
- [62] DIN EN ISO 14130:1998-02. Fibre reinforced plastic composites - determination of apparent interlaminar shear strength by short beam-method (ISO 14130:1997); German version EN ISO 14130:1997. 1998. <https://doi.org/10.31030/7433990>.
- [63] Plastics - determination of Charpy impact properties - Part 1: non-instrumented impact test (ISO 179-1:2010); German version EN ISO 179-1:2010. 2010. <https://doi.org/10.31030/1625765>.
- [64] DIN EN ISO 62:2008-05 Plastics - determination of water absorption (ISO 62:2008); German version EN ISO 62:2008. 2008. <https://doi.org/10.31030/1407167Amendments>.
- [65] Sang L, Wang Y, Wang C, Peng X, Hou W, Tong L. Moisture diffusion and damage characteristics of carbon fabric reinforced polyamide 6 laminates under hydrothermal aging. *Compos Part A Appl Sci Manuf* 2019;123:242–52. <https://doi.org/10.1016/j.compositesa.2019.05.023>.
- [66] Wang Qiuling, Springer GS. Moisture absorption and fracture toughness of PEEK polymer and graphite fiber reinforced PEEK. *J Compos Mater* 1989;23:434–47. <https://doi.org/10.1177/002199838902300501>.
- [67] Ma C-CM, Yur S-W. Environmental effect on the water absorption and mechanical properties of carbon fiber reinforced PPS and PEEK composites. *J Thermoplast Compos Mater* 1989;2:281–92. <https://doi.org/10.1177/089270578900200403>.
- [68] Beland S. High performance thermoplastic resins and their composites. Park Ridge, USA: Noyes Publications; 1990.
- [69] DIN EN ISO 291:2008-08, Plastics - standard atmospheres for conditioning and testing (ISO 291:2008); German version EN ISO 291:2008. 2008. <https://doi.org/10.31030/1441132>.
- [70] Giżyński M, Romelczyk-Baishya B. Investigation of carbon fiber-reinforced thermoplastic polymers using thermogravimetric analysis. *J Thermoplast Compos Mater* 2019. <https://doi.org/10.1177/0892705719839450>. 0892705719839450.
- [71] Mohsin MAA, Iannucci L, Greenhalgh ES. Fibre-volume-fraction measurement of carbon fiber reinforced thermoplastic composites using thermogravimetric analysis. *Heliyon* 2019;5:e01132. <https://doi.org/10.1016/j.heliyon.2019.e01132>.
- [72] DIN EN ISO 1183-1:2019-09. Plastics - methods for determining the density of non-cellular plastics - Part 1: immersion method, liquid pycnometer method and titration method (ISO 1183-1:2019. Corrected version 2019-05); German version EN ISO 1183-1:2019. 2019. <https://doi.org/10.31030/3023324>.
- [73] Tran LQN, Fuentes CA, Dupont-Gillain C, Van Vuure AW, Verpoet I. Understanding the interfacial compatibility and adhesion of natural coil fibre thermoplastic composites. *Compos Sci Technol* 2013;80:23–30. <https://doi.org/10.1016/j.compscitech.2013.03.004>.
- [74] Margem JI, Gomes VA, Margem FM, Ribeiro CGD, Braga FO, Monteiro SN. Flexural behavior of epoxy matrix composites reinforced with malva fiber. *Mater Res* 2015; 18:114–20. <https://doi.org/10.1590/1516-1439.359514>.
- [75] De Almeida O, Ferrero J-F, Escalé L, Bernhart G. Charpy test investigation of the influence of fabric weave and fibre nature on impact properties of PEEK-reinforced composites. *J Thermoplast Compos Mater* 2019;32:729–45. <https://doi.org/10.1177/0892705718778744>.
- [76] Cantwell WJ, Morton J. The impact resistance of composite materials — a review. *Composites* 1991;22:347–62. [https://doi.org/10.1016/0010-4361\(91\)90549-V](https://doi.org/10.1016/0010-4361(91)90549-V).
- [77] Jogur B, Nawaz Khan A, Das A, Mahajan P, Alagirusamy R. Impact properties of thermoplastic composites. *Textil Prog* 2018;50:109–83. <https://doi.org/10.1080/00405167.2018.1563369>.
- [78] Barbosa A de P, Oliveira MP, Altoé GR, Margem FM, Monteiro SN. Charpy impact test of epoxy matrix composites reinforced with buriti fibers. *Mater Sci Forum* 2014;775–776:296–301. <https://doi.org/10.4028/www.scientific.net/MSF.775-776.296>.
- [79] Nascimento LFC, Monteiro SN, Louro LHL, Luz FS Da, Santos JL Dos, Braga FDO, et al. Charpy impact test of epoxy composites reinforced with untreated and mercerized mallow fibers. *J Mater Res Technol* 2018;7:520–7. <https://doi.org/10.1016/j.jmrt.2018.03.008>.
- [80] Cheon SS, Lee DG. Impact properties of glass fiber composites with respect to surface treatment and fiber volume fraction. *ICCM Int Comm Compos Mater* 2012; 372.
- [81] d'Hooghe EL, Edwards CM. Thermoplastic composite technology; tougher than you think. *Adv Mater* 2000;12:1865–8. [https://doi.org/10.1002/1521-4095\(200012\)12:23<1865::AID-ADMA1865>3.0.CO;2-N](https://doi.org/10.1002/1521-4095(200012)12:23<1865::AID-ADMA1865>3.0.CO;2-N).
- [82] Lee J-S, Kang T-J. Changes in physico-chemical and morphological properties of carbon fiber by surface treatment. *Carbon N Y* 1997;35:209–16. [https://doi.org/10.1016/S0008-6223\(96\)00138-8](https://doi.org/10.1016/S0008-6223(96)00138-8).
- [83] HexTow® continuous carbon fiber, sizings available with HexTow® continuous carbon fiber products. 2020. <https://www.hexcel.com/Products/Carbon-Fiber/HexTow-Continuous-Carbon-Fiber>. [Accessed 11 October 2020].
- [84] Yu B, Fu S, Wu Z, Bai H, Ning N, Fu Q. Molecular dynamics simulations of orientation induced interfacial enhancement between single walled carbon nanotube and aromatic polymers chains. *Compos Part A Appl Sci Manuf* 2015;73: 155–65. <https://doi.org/10.1016/j.compositesa.2015.02.027>.



# Dipl.-Ing. Peter Kiss

## Berufserfahrung

**Wissenschaftlicher Mitarbeiter und Doktorand F&E Composites** 2018 - 2021

FH Wels F&E GmbH, Wels

Materialentwicklung und Prozessentwicklung CFK und GFK

Thermoplastische Imprägnierung

Thermoformen und Tapelegen

Mechanische und morphologische Charakterisierung von Laminaten

Dissertation in Kooperation mit TU-Wien Fakultät für Maschinenbau

**Wissenschaftlicher Mitarbeiter Bachelor und Master F&E Composites** 2016 - 2018

Transfercenter für Kunststofftechnik GmbH, Wels

Organoblechentwicklung

Konsolidierung und Prozessüberwachung bei der

Aushärtung von duroplastischen Verbunden im Autoklav-Verfahren und Infusionsverfahren

## Bildungsweg

Doktorat TU-Wien Seit 10/2018

Maschinenbau

FH-Wels Master

Kunststofftechnik

2016 - 2018

FH-Wels Bachelor

Metall und Kunststofftechnik

2013 - 2016

HTL Rosensteingasse

Kolleg für chemische Industrie

Universität Wien

Chemie

2009 - 2010

Universität Wien

Ernährungswissenschaften

2008 - 2009

BRG/BORG Oberpullendorf

2000 - 2008

Volksschule Oberpullendorf

1997 - 2000

Volksschule Bad Hofgastein

1996 - 1997

## Kontakt und persönliche Daten

Adresse

[Redacted]

[Redacted]

Mobil

[Redacted]

E-Mail

[Redacted]

Geburtsdatum

[Redacted]

Geburtsort

[Redacted]

Nationalität

[Redacted]

## Persönlichkeit

**Forscherdrang**

Entwicklung/Optimierung neuartiger Materialien und Methoden

**Selbständigkeit**

in Recherche und Entwicklung

**Problemlösungsdenken**

Ursachenfindung bei komplexen Problemen

**Zusammenhänge erkennen**

bei materialtechnischen und wissenschaftlichen Fragen

**Teamfähigkeit**

Problemlösungen im Team und große Hilfsbereitschaft

## Fremdsprachen

Englisch

[Progress bar]

Ungarisch

[Progress bar]

## Kenntnisse

MS-Office

[Progress bar]

CAD

[Progress bar]

Composite-  
verarbeitung

[Progress bar]

## Interessen

**Freizeit**

Mountainbiken, Wandern, Motorsport und Automobile

**Beruf**

Materialentwicklung, Prozessoptimierung, Werkstofftechnik, Kunststoffe, Verbundwerkstoffe, Polymerchemie, 3D-Druck

Die approbierte gedruckte Originalversion dieser Dissertation ist an der TU Wien Bibliothek verfügbar.  
The approved original version of this doctoral thesis is available in print at the TU Wien Bibliothek.



# Dipl.-Ing. Peter Kiss

## Wissenschaftliche Publikationen

Kiss P, Glinz J, Stadlbauer W, Burgstaller C, Archodoulaki V-M.

“The effect of thermally desized carbon fibre reinforcement on the flexural and impact properties of PA6, PPS and PEEK composite laminates: A comparative study”. Composites Part B: Engineering 2021:108844.

[doi.org/10.1016/j.compositesb.2021.108844](https://doi.org/10.1016/j.compositesb.2021.108844).

Kiss P, Schoefer J, Stadlbauer W, Burgstaller C, Archodoulaki V-M.

“An experimental study of glass fibre roving sizings and yarn finishes in high-performance GF-PA6 and GF-PPS composite laminates”. Composites Part B: Engineering 2021;204:108487.

[doi.org/10.1016/j.compositesb.2020.108487](https://doi.org/10.1016/j.compositesb.2020.108487).

Kiss P, Stadlbauer W, Burgstaller C, Stadler H, Fehringer S, Haeuserer F, Archodoulaki V-M.

“In-house recycling of carbon- and glass fibre-reinforced thermoplastic composite laminate waste into high-performance sheet materials”. Composites Part A: Applied Science and Manufacturing 2020;139:106110.

[doi.org/10.1016/j.compositesa.2020.106110](https://doi.org/10.1016/j.compositesa.2020.106110).

Kiss P, Stadlbauer W, Burgstaller C, Archodoulaki V-M.

“Development of high-performance glass fibre-polypropylene composite laminates: Effect of fibre sizing type and coupling agent concentration on mechanical properties”. Composites Part A: Applied Science and Manufacturing 2020;138:106056. [doi.org/10.1016/j.compositesa.2020.106056](https://doi.org/10.1016/j.compositesa.2020.106056).

## Fachvorträge

Kiss P

„Development of high-performance thermoplastic composite laminates“  
materialsTUDay 13.10.2020, TU-Wien, Wien

Thor M, Kiss P, Sause MGR, Hinterhölzl R

„[Strategies for the manufacturing of wrinkle-free composite parts](#)“  
SAMPE Europe 1-4.Okt.2020, Amsterdam

Kiss P, Burgstaller C

„[Von der Thermoplast-Tapeherstellung zum Bauteil](#)“  
Composites United (CU) Forum 06.02.2020, ENGEL AUSTRIA GmbH, Schwertberg

## Laborpraktika

### **Greiner Bio-One BioScience GmbH September 2015 und 2016**

Chemikalienherstellung für die Produktion

Herstellung von chemischen Lösungen für OEM Kunden

Dokumentation nach GMP-Richtlinien

### **Baxter Innovations GmbH Juli 2012**

Biochemische Durchführung von Analysen per Polyacrylamid-Gelelektrophorese (SDS-PAGE)

Durchführung photometrischer Analysen

Herstellung von Reagenzien, Puffern und Standards für die Durchführung von Analysen

Steriles Arbeiten nach GLP-Richtlinien

Protokollierung und Auswertung der Ergebnisse nach GMP-Richtlinien